UNIVERSITY OF LONDON THESIS

Degree PhD Year 2008 Name of Author COGRAM, Patricia

Inositol and Protein Kinase C in the prevention of Neural Tube Defects

Patricia Cogram

A thesis submitted for the degree of Doctor of Philosophy in the University of London

July 2007

Neural Development Unit
Institute of Child Health
University College London
30 Guilford Street
London
WC1N 1EH

ProQuest LLC
789 East Eisenhower Parkway
P.O. Box 1346
Ann Arbor, MI 48106-1346

DEDICATION

I would like to dedicate this thesis to my son Blas,

To mum and dad,

Juan Manuel Perez de Cogram

Norna Behm Silverman

To my brothers,

Juan Eduardo Perez de Cogram

Facundo Perez de Cogram

Lucas Perez de Cogram

And to five good friends,

Daniel Gluschankof, Eduardo Weisz, Lucy Widman
Joe Pelluchi and Pablo Armelin

ABSTRACT

A number of mouse genetic mutants develop neural tube defects (NTDs). In some cases, defects can be prevented by administration of folic acid during pregnancy, whereas in other mutants there is no response. This parallels the human situation in which a proportion of NTDs appear resistant to folic acid therapy. *Curly tail* is the best characterised mouse model of folic acid-resistant NTDs. Previously it was shown that the incidence of spina bifida in curly tail mice can be reduced by administration of inositol during embryonic development. In this thesis, I compared the effectiveness of two isomers, myo- and D-chiro-inositol, with administration either directly to embryos in vitro, or to pregnant females by subcutaneous or oral routes. Although both inositols exerted a preventive effect on spina bifida, by all routes of administration, D-chiro-inositol consistently exhibited greater potency than myo-inositol. The protective effect of inositol has been shown previously to be mediated through the activity of the inositol/lipid cycle and to depend on downstream activation of protein kinase C (PKC). In the studies decscribed in this thesis, I examined the role of PKC in more detail. The expression of PKC isoforms was first examined by immunohistochemistry. Broad spectrum chemical inhibitors were then used in whole embryo culture to confirm that one or more PKC isoforms are indispensable for normalisation of neural tube closure by inositol. Specific peptide inhibitors were then applied, and revealed that PKC beta I, gamma and zeta are most important in the protective pathway. Finally, I demonstrated that inositol stimulates cell proliferation in the hindgut of *curly tail* embryos, reversing the imbalance of cell proliferation that is known to lead, via enhanced ventral curvature of the caudal region, to delay or failure of neural tube closure.

ACKNOWLEDGEMENTS

I would like to thank all members of the Copp lab, past and present, for their support and friendships all these years.

Special gratitude goes to my mentor, Professor Andrew Copp for the chance to work in such a stimulating environment with his continual support and infectious optimism, for his guidance and invaluable advice. I have always cherished his constant promotion of new ideas and fruitful scientific discussions. In summary, he has given me an invaluable example and preparation to one day become an independent scientist.

In particular I would like to thank my second supervisor Dr Nicholas Greene for his time and patience, encouragement and valuable supervision. For being a friend as well as an excellent guide all these years, for his tenacious optimism for inositol; without his help and inspiration this thesis would not be written.

Also for their supervision I would like to thank Dr. Jennifer Murdoch and Dr. Deborah Henderson, they have always been there to answer my questions and introduced me to the techniques used throughout this thesis.

A very special thank you go to Dr Carlos Gaston for his inspiring scientific discussions during our coffee breaks, for his contagious enthusiasm and passion for science, for teaching me how to ski and the brain storming we shared at the Protein Phosphorylation meeting in New Mexico. Above all for being that good friend I will always remember.

To all the adventurers in the Copp group for including me in the team which madly tried to row across the English Channel, more than once!

A big thank you to Dr Patricia Ybot-Gonzalez, for her supervision, advice and companionship all these years.

Thank you to Drs Adam Rutherford, Iain Mc Kinnan and John Chilton for babysitting Blas while I was implanting osmotic mini pumps on *curly tail* mice.

A warm and special thanks goes to Mrs Katie Gardener for teaching me the masteries of gavaging mice and surgically implanting osmotic mini pumps, and also for sharing with me her experience on how to combine good parenting with having a career.

Thanks also to John and Sheila Tesh for analysing the *curly tail* embryos. To Dr Angie Wade, for doing and explaining so well all the statistical tests used in this thesis.

To Brenda Gilliver for her capacity for multitasking has allowed me to be able to finish writing up this thesis providing me with a working computer and the office space, for her support, good humour and companionship all these months. To Stella Fusco and Lynne Mason for making me feel part of the office team with their every day smiles, lattes and cappuccinos. A big thank you to every one in the ICH 6th floor office who integrated me with huge kindness; special thank you goes to Naomi Leatham for her courtesy and support when I have to stay late hours.

Thanks to the Developmental Biology Unit for sharing reagents and advice especially to Dr Fang Zhang for her 'deluxe' immunohistochemistry protocols, and expert advice.

Out of the laboratory I would like to mention my friends, Fluffy, Tommy and Darren who have genuinely supported me during my thesis, believing in what I do and making the writing up a realisable possibility.

Wellbeing and the Wellcome Trust funded the work in this thesis, which has allowed me a very privileged entry into scientific research, and last, I thank the Institute of Child Health for this opportunity.

TABLE OF CONTENTS

LIST OF FIGURES

LIST OF TABLES

ABBREVIATIONS

3AT	3-amino-1,2,4-triazole
AA	Amino acid
Bis I	Bisindolylmaleimide I
Bis V	Bisindolylmaleimide V
BSA	Bovine serum albumin
C1/C2	Catalytic domain
CI	Cubitus Interruptus
CT	Curly tail
DAG	Diacylglycerol
DAPI	4'-6-diamidino-2-phenylindole
ddH_20	distilled deionised water
DEPC	Diethyl pyrocarbonate
DIC	Differential interference contrast (Nomarski)
DLHP	Dorsolateral hinge point
DMEM	Dulbecco's Modified Eagle's Medium
DMSO	Dimethyl sulfoxide
DNA	Deoxyribosenucleic acid
dNTP	deoxynucleoside triphosphate
E	Embryonic day
EDTA	Ethylenediaminetetraacetic acid
EMSA	Electrophoresis mobility shift assay
ENU	Ethylnitrosourea mutagenesis

EST	Expressed sequence tag
Ex	Excencephaly
FCS	Fetal calf serum
GAG	Glycosaminoglycan
gL	Granular layer
H	Hindgut
Go6976	Godecke 6976
GPI	Glycosylphosphatidylinositol
GST	Glutathione-S-transferase
HBDDE	2,2',3,3',4,4'-hexahydroxy-1,1'-biphenyl-6,6'-dimethanol dimethyl ether
HH	Hedgehog
H3	Phospho histone 3
IP-3K	Phosphatidylinositol-3-kinase
Kb	Kilo base
LB	L-broth
LMP	Low melting point
Lp	*Loop-tail*
M	Mitosis
M	Presomitic mesoderm
MHP	Median hinge point
N	Notochord
NLS	Nuclear localisation signal
Np	Neural plate
NTD	Neural tube defects
NTMT	Sodium chloride/Tris/magnesium chloride/Tween buffer
OD	Optic density

PBS	Phosphate buffered saline
PCD	Programmed cell death
PCP	Planar cell polarity
PI	Phosphoinositol monophosphate
PIP2	Phosphoinositol diphosphate
PKC	Protein kinase C
PKCα	Protein kinase C alpha
PKCβI	Protein kinase C beta I
PKCβII	Protein kinase C beta II
PKCγ	Protein kinase C gamma
PKCζ	Protein kinase C zeta
PCNA	Proliferating Cellular Nuclear Antigen
PFA	Paraformaldehyde
pcL	Purkinje cell layer
PLC	Phospholipase C
PMA	Phorbol myristate acetate
PNP	Posterior neuropore
RACK	Receptor for activated C-kinase
RPM	rotation per minute
RT	Reverse transcription
S	S-phase
Sb	Spina bifida
SBA	Spina bifida aperta
SBO	Spina bifida oculta
SD	Synthetic defined medium
SDS	Sodium dodecyl sulphate

SDS-PAGE	Sodium dodecyl sulfate polyacrylamide gel electrophoresis
SF	Split face
Shh	Sonic hedgehog
Smo	Smoothened
SSC	Sodium chloride
TPA	Phorbol ester 12-*O*-tetradecanoylphorbol-13-acetate

CHAPTER 1

GENERAL INTRODUCTION

1.1 INTRODUCTION

The formation of the vertebrate nervous system begins at gastrulation when, during neural induction, a subset of ectodermal cells segregates and thickens to form the neural plate. Soon afterwards, the neural plate undergoes a series of morphogenetic events that ends with the formation of a hollow neural tube characteristic of the chordate phylum, this process being known as neurulation. Impairment of neurulation leads to a range of anomalies known as neural tube defects (NTDs) that are among the commonest congenital malformations in humans.

The embryonic process of neurulation has been well characterised morphologically in different animal systems (Schoenwolf, 1985;Shum and Copp, 1996;Colas and Schoenwolf, 2001). Some of the genetic pathways controlling this programme have been identified from the large number of mouse mutants that display NTDs (Juriloff and Harris, 2000;Copp et al., 2003). However, the underlying molecular mechanisms are still largely unknown.

1.2 THE NORMAL PROCESS OF NEURULATION

Neurulation is divided into two parts: primary and secondary neurulation. Primary neurulation results in the formation of the cranial neural tube and the upper spinal cord rostral to the mid-sacral region, through a process that involves the specification and shaping of the neural plate, followed by the elevation and fusion of the neural folds (Criley, 1969). Initially, the neural plate becomes specified by the underlying mesoderm and is transformed into a pseudo-stratified columnar epithelium that thickens apicobasally. The edges of the columnar epithelium elevate to form the neural folds that

converge in the dorsal midline and fuse, forming the neural tube. Once primary neurulation has occurred and the neural tube has closed, secondary neurulation takes place caudally to the mid-sacral region. At this axial level, the neural tube forms by condensation of mesenchymal cells within the tail bud region which forms an epithelium that subsequently cavitates, forming the secondary neural tube (Schoenwolf, 1984;Copp and Brook, 1989). Secondary neurulation is a separate autonomous process in relation to primary neurulation, at least in the chick embryo, where if primary neurulation is disrupted experimentally secondary neurulation still occurs normally (Costanzo *et al.*, 1982).

1.2.1 Primary neurulation occurs in a cranio-caudal sequence

During primary neurulation in the mouse embryo, closure of the neural tube starts at three different initiation sites, in a cranio-caudal sequence along the body axis (Fig 1.1) (MacDonald *et al.*, 1989;Copp *et al.*, 1990;Golden and Chernoff, 1993). The first initiation site, Closure 1, occurs in the mouse embryo at the 4-6 somite stage with closure occurring at the cervical/hindbrain region and continuing in a zippering-like fashion caudally along the future spine and rostrally into the hindbrain. By the 12 somite stage, a second site of closure, Closure 2, occurs at the forebrain/midbrain boundary and proceeds caudally into the midbrain and rostrally into the forebrain. At about the same somite stage, a third site of closure, Closure 3, occurs at the rostral extremity of the prosencephalon, and proceeds caudally towards the midbrain. As a result of these three *de novo* sites of closure, three neuropores become apparent. The anterior neuropore (within the forebrain, formed by closure progression from Closures 2 and 3) closes at approximately the 17 somite stage. Soon afterwards, the hindbrain neuropore (formed by progression from Closures 1 and 2) closes, and the zippering mechanism initiated at

Closure 1 spreads caudally, resulting in the closure of the posterior neuropore at the 29 somite stage.

The developmental stage and exact position in which the events of neurulation take place vary between mouse strains (Juriloff *et al.*, 1991). Hence, the site of Closure 2 is polymorphic between mouse strains and its position confers susceptibility to cranial neural tube defects (Fleming and Copp, 2000).

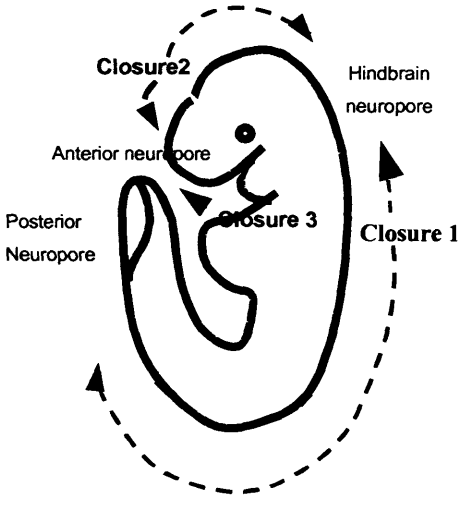

Figure1.1 Initiation sites of neural tube closure

Diagram to illustrate the three sites of the neural tube closure and the three neuropores during primary neurulation. From Copp (1994)

1.2.2 The spectrum of NTDs depends on which of the events of neurulation fail to be completed

The spectrum of NTDs depends on which of the *de novo* closure sites or neuropore closures fail to be completed (Fig. 1.2)(Copp and Bernfield, 1994). Hence, failure of initiation of Closures 2 and 3 or incomplete closure of the anterior or hindbrain neuropores leads to an open cranial neural tube termed exencephaly. The second type of NTD, lumbosacral spina bifida results from failure of the posterior neuropore to complete closure. The size and severity of the lesion depends upon the axial level where closure failed. Hence if closure stops at a more rostral level these results in a more severe phenotype. Cranial NTDs and spina bifida can occur independently or in combination, in humans and in mouse. Failure of initiation of Closure 1 causes craniorachischisis, the most severe form of NTD, in which the hindbrain and spinal neural tube remain open (Fig. 1.2). In the mouse models that display craniorachischisis, Closures 2 and 3 occur, and development of the forebrain and rostral midbrain appear normal (Greene *et al.*, 1998;Murdoch *et al.*, 2001). These observations indicate that the genetic regulation of Closure 1 differs from that of Closures 2 and 3.

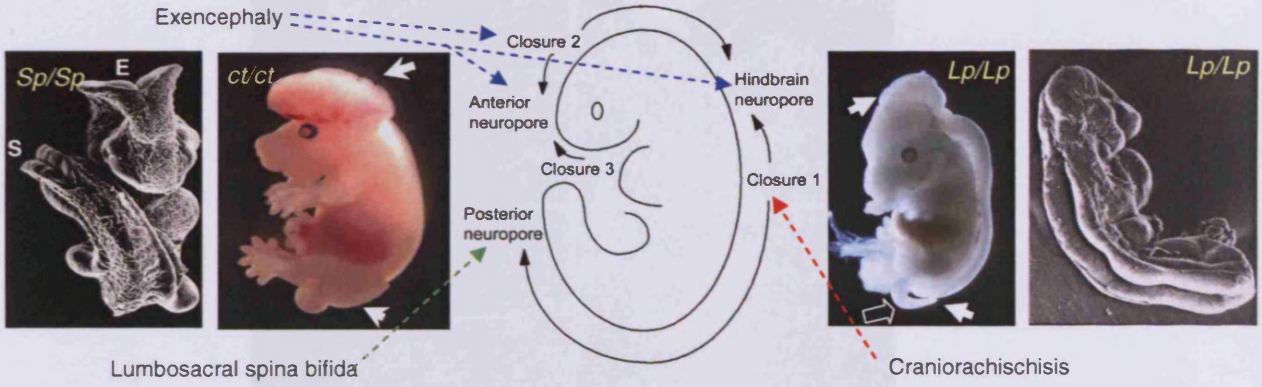

Figure 1.2 The three main subtypes of NTDs

Diagram to illustrate exencephaly, craniorachischisis and lumbosacral spina bifida, which result from failure of closure initiation events or from failure of each neuropore to complete closure (arrows). The embryo on the left shows exencephaly (**E**) and lumbosacral spina bifida (**S**) whilst the embryo on the right shows craniorachischisis (diagram modified from A. (Copp and Bernfield, 1994)).

The neural folds form by elevation and bending of the lateral edges of the neural plate at either side of the midline. The morphology that the neural plate acquires during closure differs in the cranial and spinal neural tube. In the midbrain region of the cranial neural tube, the neural folds initially adopt a biconvex shape as they elevate. Subsequently, the lateral edges bend inwards to form the dorsolateral hinge points (DLHPs), which bring the apices of the neural folds into apposition at the dorsal midline (Morriss-Kay, 1981;Morriss-Kay et al., 1994).

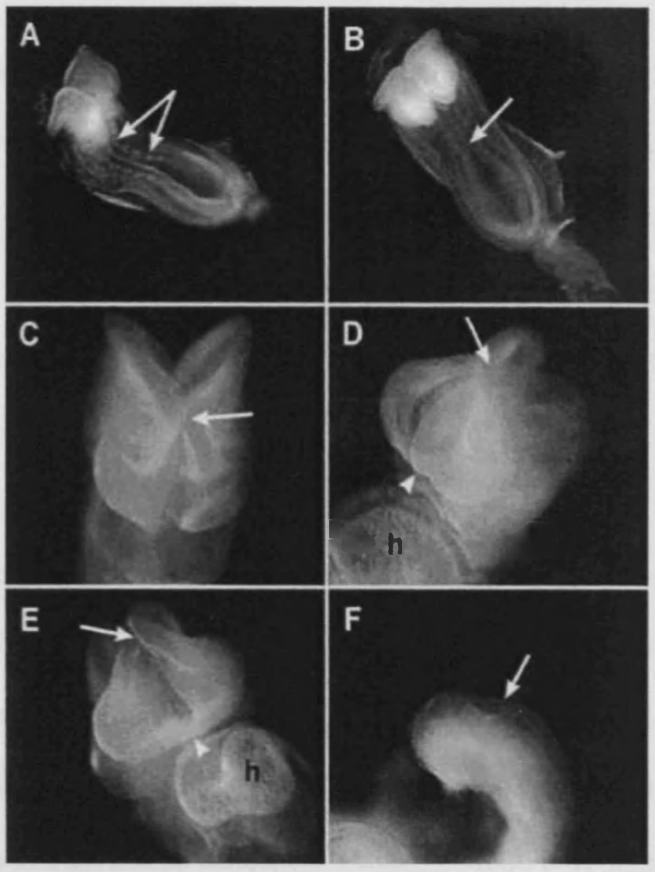

1.3 Morphological changes during primary neurulation: convergent-extension, elevation, bending and apposition

(**A-B**) Oblique and dorsal images of a 6-8-somite-stage embryo showing the initiation neural tube closure (Closure 1) at the level of the future hindbrain-cervical junction (arrows). (**C-E**) Three views of the head of a 12 to 16-somite-stage embryo showing the second point of closure (Closure 2) at the level of the forebrain-midbrain junction (arrow) and a third point of closure (Closure 3) at the rostral end of the neural tube (arrowhead). (**F**) The posterior neuropore at the caudal extremity of the neural tube. Closure of the spinal neural tube proceeds from the hindbrain-cervical junction caudally and eventually closes the posterior neuropore at the 29 somite-pair stage. (h) heart. (Photography by Dr K Tosney)

As the wave of spinal neural tube closure spreads down the body axis, the morphology of the neural plate at the spinal cord region changes in a stereotypic fashion (Shum and Copp, 1996). Three distinct morphologies (named Modes of neurulation) have been

reported, from the cross-sectional appearance of the neural plate at different axial levels (Fig.1.3; 1.4). In Mode 1 spinal neurulation, which is seen in the closing posterior neuropore at the 7-15 somite stage, the neural plate bends medially forming the median hinge point (MHP), whilst the lateral edges elevate with straight sides and the neural folds approach each other in the dorsal midline, closing the neural tube to form a slit-like lumen.

At the 16-24 somite stage, when Mode 2 spinal neurulation occurs, the neural plate bends not only at the midline, forming the MHP, as in Mode 1, but the dorsal region of each neural fold also bends forming the dorso-lateral hinge points (DLHPs). DLHPs cause the tips of the neural folds to appose in the dorsal midline yielding a closed neural tube with a diamond shaped lumen. At the 25-30 somite stage, in Mode 3 of spinal neurulation, the neural plate does not form a MHP, whereas DLHPs are prominent, closing the neural tube to form a circular shaped lumen. These stereotypical changes in morphology of the spinal neuroepithelium as it closes to form the neural tube have been observed in mouse neurulation. In other systems, such as the chick, DLHP formation occurs in the hindbrain region, but apparently not in the caudal neural tube, demonstrating differences between these species (Schoenwolf, 1985)

1.3 NTDS IN HUMANS

1.3.1Types of NTDs in humans

NTDs are among the commonest congenital malformation in humans with an average prevalence of 1:1000 live births worldwide (Edmonds and James, 1993). Human NTDs can be divided into open and closed defects. Open NTDs result from failure of the neural tube to close during primary neurulation, whilst closed NTDs result from aberrant

secondary neurulation and abnormal axial skeleton development (Lemire, 1988). As in mouse, open NTDs can be grouped depending on which event of closure fails to occur (Van Allen *et al.*, 1993). Exencephaly, open neural tube in the cranial region, can be sub-grouped into three classes. Rostrally, failure of closure 3 at the forebrain region with facial clefting leads to anencephaly. Failure of Closure 2, results in an open midbrain-hindbrain and is named holocrania, whilst failure of closure of the hindbrain neuropore results in merocrania.

As in mouse, spina bifida results from failure of closure of the PNP resulting in an open caudal neural tube that can be exposed (myelocele) or covered by meninges (myelomeningocele). Craniorachischisis is the most severe NTD, and the neural tube remains open along almost the entire rostro-caudal axis.

Neurulation in humans starts at 17-18 days post fertilisation and ends by 26-28 days after fertilisation with closure of the PNP (Campbell *et al.*, 1986). In humans, as in mouse, the initiation of neural tube closure is discontinuous (Van Allen *et al.*, 1993), and sites of initiation equivalent to Closure 1 and Closure 3 have been described (Golden and Chernoff, 1995;Juriloff and Harris, 2000), although some studies do not identify Closure 2 (O'Rahilly and Müller, 2002). Humans undergo secondary neurulation in the low sacral and coccygeal regions. Despite failure in neural tube closure, neural differentiation and nerve connections can occur (Campbell *et al.*, 1986). However tissue exposure to the amniotic fluid results in degeneration of the open neural tube leading to musculoskeletal, gastrointestinal and urinary dysfunction often associated with NTDs in patients (Stark, 1977).

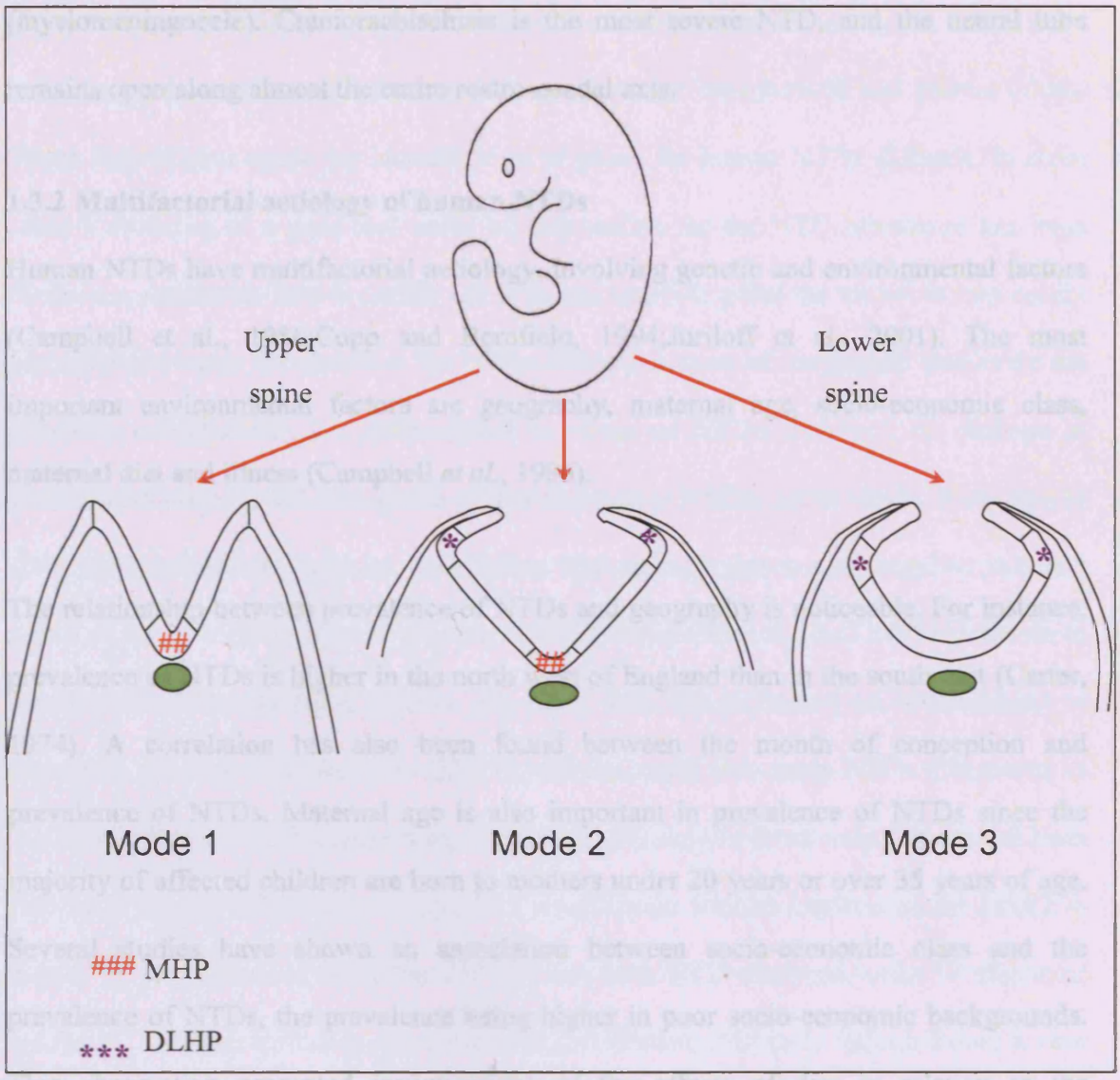

Figure 1.4 Diagram to illustrate the morphology of the neural plate during progressive closure of the posterior neuropore

Mode 1 is characterised by formation of a MHP with straight neural folds apposing each other. In Mode 2 of neurulation the neural plate bends medially to form the MHP and, dorsally, the neural folds bend bilaterally to form the DLHPs. In Mode 3 of neurulation, closure is solely dependent on DLHPs. Diagram modified from Ybot-Gonzalez (2001)

As in mouse, spina bifida results from failure of closure of the PNP resulting in an open caudal neural tube that can be exposed (myelocele) or covered by meninges

(myelomeningocele). Craniorachischisis is the most severe NTD, and the neural tube remains open along almost the entire rostro-caudal axis.

1.3.2 Multifactorial aetiology of human NTDs

Human NTDs have multifactorial aetiology, involving genetic and environmental factors (Campbell et al., 1986;Copp and Bernfield, 1994;Juriloff et al., 2001). The most important environmental factors are geography, maternal age, socio-economic class, maternal diet and illness (Campbell *et al.*, 1986).

The relationship between prevalence of NTDs and geography is noticeable. For instance, prevalence of NTDs is higher in the north west of England than in the south east (Carter, 1974). A correlation has also been found between the month of conception and prevalence of NTDs. Maternal age is also important in prevalence of NTDs since the majority of affected children are born to mothers under 20 years or over 35 years of age. Several studies have shown an association between socio-economic class and the prevalence of NTDs, the prevalence being higher in poor socio-economic backgrounds. This observation prompted investigations of the effects of diet in relation to the prevalence of NTDs. Indeed, supplementing mothers with folic acid or multivitamins has been shown to lead to a reduction in the prevalence of NTDs (Wald *et al.*, 1991;Czeizel and Dudás, 1992). A correlation has also been found between maternal illness, including higher fever, during the first month of pregnancy and an increase in the risk of NTDs.

The genetic component of NTDs is supported by family studies showing that siblings of affected individuals have a ten times greater risk of NTDs than the background prevalence (Campbell *et al.*, 1986). In addition, an increased risk is observed in offspring of affected parents (Blatter *et al.*, 1997). However, the inheritance of NTDs does not

follow a pattern of single-gene inheritance, but rather suggests multigenic inheritance with strong environmental influence (Campbell et al., 1984;Juriloff and Harris, 2000). These factors have made the identification of genes for human NTDs difficult. In some cases a mutation in a gene that could be responsible for the NTD phenotype has been found in a patient but also in unaffected relatives, indicating that the mutation may confer susceptibility but is not causative for NTDs. Moreover some of the genetic studies do not take into consideration the phenotypical spectrum of NTDs, and look for linkage or causative mutations within a group of heterogeneous NTDs: spina bifida, exencephaly and craniorachischisis, without considering that specific genes may regulate just one aspect of neural tube closure. For instance, targeted disruption of *Msx2* has been shown to cause exencephaly in mice (Liu *et al.*, 1995) and this prompted an investigation to determine whether mutations in *MSX2* in humans could also cause NTDs (Stegmann et al., 2001). The study concluded that, despite identifying one deletion in one patient from 204 NTD cases, there was no statistical significance for the implication of *MSX2* in human NTDs. However from the 204 patients with NTD analysed, only 13 displayed cranial NTDs (also including craniorachischisis). Hence, this study included only a very small cranial NTD sample (Stegmann et al., 2001), despite this phenotype being most likely *Msx2*-related based on the mouse studies.

Mutations in the *PAX3* gene have been found in patients with NTDs (Hol *et al.*, 1995). However, a second population study using 194 people including 50 NTD cases failed to find an association between the *PAX3* and NTDs (Chatkupt *et al.*, 1995). A mutation in *SLUG*, a zinc finger transcription factor involved in neural crest development, was found in a patient with NTD. Moreover, the mutation was not present in unaffected individuals raising the possibility that *SLUG* could be causative of the NTD observed in this patient

(Stegmann *et al.*, 1999). A mutation in *PAX1* was detected in a single patient with spina bifida, suggesting that this gene can also act as a susceptibility factor (Joosten *et al.*, 1998).

Further genetic studies have centred on identifying mutations in enzymes that act in the folic acid pathway. The importance of folic acid in NTDs comes from studies indicating a protective effect of folic acid administration during the periconceptional period (Wald *et al.*, 1991). This prompted studies to identify mutations in genes that participate in the biochemical pathways involving folic acid, which may confer susceptibility to NTDs. A polymorphism in the 5,10-methylene-tetrahydrofolate reductase gene (*MTHFR*) has been found to confer a two-fold increased risk of NTDs in some populations (Van der Put et al., 1995) (Botto and Mastroiacovo, 1998), although there is no association with NTDs in other populations. *MTHFR* encodes an enzyme that catalyses the conversion of 5,10-methyl-tetrahydrofolate to 5-methylene-tetrahydrofolate. Homozygous individuals for the C677T polymorphism are predisposed to mild hyperhomocysteinemia when their folate status is low. The precise mechanism that confers susceptibility to NTDs in individuals homozygous for C677T is unknown.

1.4 THE EMBRYONIC PROCESS OF SPINAL NEURULATION

After Closure 1 has occurred at the cervical-hindbrain region, closure of the spinal neural tube continues caudally forming the posterior neuropore. Failure of the posterior neuropore to complete closure leads to spina bifida. The embryonic mechanism that controls closure of the posterior neuropore can be autonomous to the neural plate (intrinsic forces) or non-autonomous to the neural plate (extrinsic forces) (Smith and Schoenwolf, 1997;Colas and Schoenwolf, 2001;Copp et al., 2003).

1.4.1 Intrinsic forces control morphogenesis of the neural plate

As spinal neurulation progresses along the body axis the neural plate bends at specific dorsoventral locations (Fig. 1.4). The MHP forms in contact with the notochord and the DLHPs form bilaterally in contact with the surface ectoderm (Shum and Copp, 1996;Ybot-Gonzalez et al., 2002). Bending in these regions has been suggested to be mediated by intrinsic forces so that the behaviour of neuroepithelial cells changes compared to those in the non-bending regions. Indeed, morphological studies in the chick revealed that the neuroepithelial cells can adopt one of three types of morphology: spindle-shape, wedge-shape and inverted wedge-shape (Smith *et al.*, 1994). In the MHP and DLHP, the majority of cells acquire a wedge-shape morphology which results from an expansion of the basal surface of the cell compared to its apical surface. In contrast, in the non-bending regions, spindle-shape cells and inverse-wedge (apically expanded)cells are in the majority (Smith *et al.*, 1994). Two different mechanisms have been proposed that result in cell wedging: constriction of apical microfilaments and changes in the cell cycle.

1.4.1.1 Constriction of apical microfilaments

A pseudostratified epithelium will bend if its apical surface area is reduced with respect to its basal surface area. The reduction in apical surface area has been proposed to be mediated through the constriction of apical containing microfilaments in a purse-string fashion (see Fig. 1.5)(Karfunkel, 1974;Nagele and Lee, 1980;Sadler *et al.*, 1982). Indeed, microfilaments and cytoskeleton-associated proteins, such as actin, MARCKS, vinculin, spectrin and Shroom are localised apically during neural plate morphogenesis (Nagele and Lee, 1980;Sadler et al., 1982;Stumpo et al., 1995b;Xu et al., 1998;Ybot-Gonzalez and Copp, 1999;Hildebrand and Soriano, 1999;Haigo et al., 2003).

To test experimentally the function of the cytoskeleton in neurulation, actin microfilament polymerisation was disrupted in embryo culture using cytochalasins and calcium chelating agents (Morriss-Kay and Tuckett, 1985;Ybot-Gonzalez and Copp, 1999). In these experiments cranial neural tube closure was inhibited, whilst spinal neural tube closure occurred relatively normally, indicating that cytoskeletal integrity is required for cranial neurulation whilst its loss is not prohibitive for spinal neural tube closure (Ybot-Gonzalez and Copp, 1999). However treatment of embryos with cytochalasin D prior to Closure 1 inhibited this closure site, resulting in a craniorachischisis-like phenotype (Ybot-Gonzalez and Copp, 1999). It appears then that initiation of closure is dependent on the actin cytoskeleton but once Closure 1 has occurred, disruption of the actin cytoskeleton does not affect the continuation and completion of spinal neural tube closure.

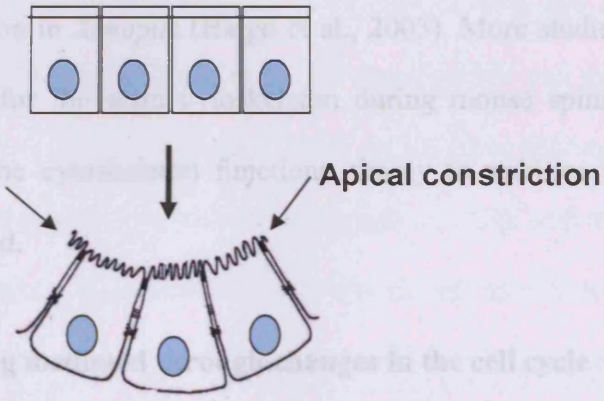

Figure 1.5 Constriction of apical filaments and bending of neural plate

Diagram to illustrate how constriction of apical microfilaments could generate bending of the neuroepithelium by constricting the apical surface area with respect to the basal surface area.

This observation is partially supported by the finding that mouse mutants for cystokeletal or putative cytoskeletal dynamics proteins exhibit exencephaly but generally not spina bifida (Copp et al., 2003). For instance, null embryos for MARCKS, the actin-binding protein vinculin, compound mutants for the Abl and Arg tyrosine kinases or for the protein kinase a subunits Cα/Cβ1 all display exencephaly but not spina bifida (Stumpo et al., 1995b;Koleske et al., 1998;Xu et al., 1998;Huang et al., 2002). This supports the idea that cytoskeletal integrity is more important for cranial neurulation than spinal neurulation. However, it could also indicate that these genes are not expressed in the lower spinal regions, which would explain the lack of spina bifida in these mutants. Indeed, two mutants for cytoskeleton-related proteins, Shroom and MARKS-related (also called MacMARCKS) protein, develop spina bifida at low frequency (Wu et al., 1996;Hildebrand and Soriano, 1999). Interestingly, Shroom has been shown to be required for apical microfilament constriction in polarised epithelial cells and to regulate hinge point formation in *Xenopus* (Haigo et al., 2003). More studies are required to rule out a critical role for the actin cytoskeleton during mouse spinal neurulation and to establish whether the cytoskeleton functions simply to stabilise the neural plate once bending has occurred.

1.4.1.2 Cell wedging mediated through changes in the cell cycle

The neuroepithelium consist of a single pseudostratified cell layer in which the nucleus of each cell migrates from the basal surface to the apical surface and back to the basal surface, a phenomenon known as interkinetic nuclear cell migration (Langman *et al.*, 1967). Studies in chick embryos have shown that the positioning of the nucleus, from basal to apical, is linked to the cell cycle (Smith and Schoenwolf, 1987). Hence, during mitosis, nuclei are localised at the apical surface generating inverse wedge-shape cells,

during G1 and G2 phases they are located between the apical and basal surfaces, creating a spindle-shape, and in S phase, they are located basally, generating wedge-shape cells. If a sizeable subset of cells have their nuclei in a basal position, this can potentially generate a neuroepithelial bend, by increasing the basal surface area respective to the apical surface area. Indeed, cells that form the MHP are mostly wedge-shaped and have a longer cell cycle S phase and a shorter M phase than cells outside the MHP (Smith and Schoenwolf, 1987;Smith and Schoenwolf, 1988). Hence, localised changes in the neuroepithelial cell cycle can generate specific sites of bending of the neural plate (see Fig. 1.6). These observations have been shown for the MHP in chick and mouse embryos. A similar mechanism could account for bending at the DLHP, although this has not been proven yet.

1.4.2 Extrinsic forces drive spinal neurulation

During neurulation the neuroepithelium is in contact with the surface ectoderm, the endoderm and the mesoderm. Changes in cell shape and/or cell number in these tissues could provide extrinsic forces that might assist neural plate folding (Schoenwolf, 1985). To test this hypothesis tissue isolation experiments in chick and mouse embryos, where the lateral mesoderm and endoderm tissues are removed, have been performed and result in normal folding of the spinal neural plate (Alvarez and Schoenwolf, 1992;Van Straaten *et al.*, 1993;Ybot-Gonzalez *et al.*, 2002). However, if the surface ectoderm is removed, the neural plate fails to bend dorsolaterally in both chick and mouse resulting in an open neural tube (Alvarez and Schoenwolf, 1992;Ybot-Gonzalez et al., 2002). This indicates that, of all the lateral tissues, only the surface ectoderm is necessary for formation of DLHPs. One hypothesis to explain the extrinsic role of the surface ectoderm has been formulated from experiments in chick embryos, which suggested that medial expansion of

the surface ectoderm through convergent extension movements could potentially provide the force that brings the paired neural folds together (Alvarez and Schoenwolf, 1992).

However, if the neural folds are dissected from the mesoderm and endoderm and only a small fragment of the surface ectoderm is left intact in contact with the neural fold, closure of the neural tube still occurs with the presence of DLHPs (Ybot-Gonzalez *et al.*, 2002). Therefore, whilst the surface ectoderm could mediate a pushing force at early stages, it seems unlikely that this process functions during Mode 2 and Mode 3 of neurulation, and rather the surface ectoderm may be required to signal to the underlying neural folds to form the DLHPs.

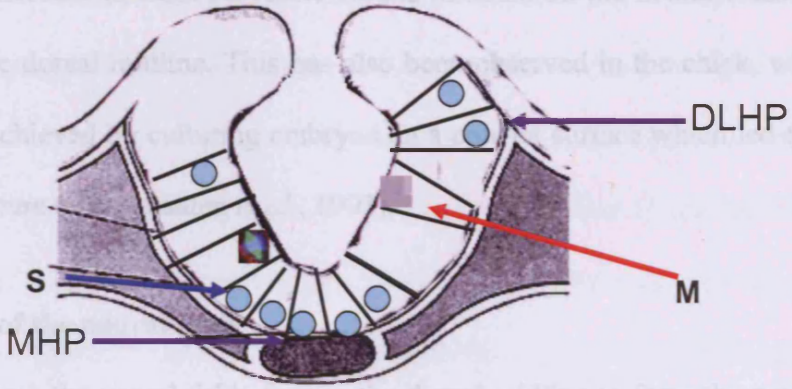

Figure 1.6. Diagram to illustrate the cell cycle-dependent position of the nucleus in formation of bending regions in a transverse section through the PNP

In the neural plate, cells undergo interkinetic nuclear migration, such that the nucleus is located apically during mitosis (M) and basally during S-phase (S). When the nucleus is in a basal or apical position the cell acquires a wedge or inverted wedge shape respectively. In the median hinge point (MHP), an increased proportion of cells is in S-phase with basally located nuclei. The increase in number of wedge shaped cells in the

ventral midline of the neural plate appears to create the MHP. Cell cycle variations resulting in cell wedging could also regulate DLHPs, although this has not studied in detail.

Whilst the mesoderm and endoderm are not required for DLHP formation, these tissues are nevertheless important for neurulation, since an imbalance of cell proliferation within these tissues can affect spinal neural tube closure. For example, an increase in axial curvature is seen in affected *curly tail* mutant embryos due to an imbalance in cell proliferation in the hindgut endoderm and notochord, which results in increased axial curvature and delay or failure of posterior neuropore closure (Brook et al., 1991c;Van Straaten et al., 1993). In *curly tail,* bending at the DLHPs and MHP occurs normally, whereas the increase in axial curvature results in strain on the neural folds that impedes meeting at the dorsal midline. This has also been observed in the chick, where delay in closure was achieved by culturing embryos on a convex surface which led to an increase in axial curvature (Van Straaten *et al.*, 1993).

1.4.3 Fusion of the neural folds

After apposition, the neural folds fuse in the dorsal midline to form the neural tube. The surface ectoderm of each neural fold loses its continuity with the neuroepithelium, and closes over the top of the neural tube to form the epidermis. Fusion of the neural folds has been proposed to be mediated by cell protrusions, lamelipodia, extending from the apposing cells (Geelen and Langman, 1979). Lamelipodia structures have been observed by scanning electron microscopy on the luminal surface of the neural plate and at the edges of the surface ectoderm (Geelen and Langman, 1979). However, the molecules involved in cell to cell recognition have not been studied during closure of the spinal neural tube. Carbohydrate-rich material localised at the tips of the neural folds has been

suggested to assist fusion by increasing the adhesiveness of the neural folds (Moran and Rice, 1975) (Sadler, 1978). Indeed, embryos cultured with phospholipase C to remove carbohydrate material exhibit delayed neural tube closure (O'Shea and Kaufman, 1980). However, the observed phenotype could be due to enzymatic removal of glycosylphophatidylinositol-anchored (GPI) proteins, including cell adhesion molecules. More studies are needed to understand the role of adhesion molecules in spinal neurulation.

1.5 MOUSE GENETIC MODELS OF NEURAL TUBE DEFECTS

To date more than 80 genes that cause NTDs in mice have been identified by positional cloning, gene targeting or gene trap screens (Juriloff and Harris, 2000;Copp et al., 2003;Harris and Juriloff, 2007a). Despite the identification of a large number of genes required for neurulation, in most cases the embryonic mechanisms leading to NTDs in each individual mutant are not well characterised. The number of mouse mutants that display exencephaly is greater than the number with spina bifida, perhaps indicating greater complexity of genetic regulation of cranial neural tube closure. The identification of these "NTDs genes" provides a tool to determine the molecular pathways that regulate neurulation. For instance, the planar cell polarity pathway is now known to regulate Closure 1 (review). In this section I will explain the importance of using mouse models for the study of NTDs and I will concentrate on some pathways for which information is available from mouse mutants that display spina bifida. The wide range of defects seen in the NTD mutants is also found in humans; it is possible, therefore, that each phenotypic category of mutants mimics a subtype of human NTDs. Today a large number of mouse mutants that produce NTDs have been identified (Juriloff and Harris, 2000;Harris and Juriloff, 2007b).

1.5.1 Use of mouse models to investigate NTDs

Mouse models offer an alternative to direct study of human NTDs, which is hampered by several factors. Human NTDs appear to have a multigenic complex aetiology, with strong influence of environmental factors, such as lifestyle and diet (Campbell et al., 1986;Copp and Bernfield, 1994). Moreover, the identification of causative genes for NTDs by linkage analysis requires large families, and this represents a difficulty since families with large numbers of NTDs are rare. In addition to this, embryological studies using human embryos can raise serious ethical issues.

The use of the mouse represents an excellent model to elucidate the genetic programmes controlling NTDs. With the sequence of the mouse genome completed and the availability of microsatellite markers for genetic mapping, the identification of the mutated genes responsible for NTD phenotypes has become quicker. Moreover, several mutagenesis strategies, particularly using chemical mutagenesis, gene trap strategies or gene targeting, have begun to make a major contribution to the list of known NTDs genes. Phenotype-driven mutagenesis programmes using chemical mutagens such as ethylnitrosourea (ENU) or chlorambucil are available to the scientific community (Justice et al., 1999;Nolan et al., 2000;Justice, 2000). This approach, allows the identification of new mouse mutations that have a particular phenotype, for instance NTDs. The mutated gene must then be identified by positional cloning.

Another type of mutagenesis is the "gene-trap" strategy, where genes are disrupted by vector insertion in ES cells, generating ES-cell clones containing a disrupted gene. This strategy has the advantages that large numbers of genes can be disrupted and then identified by a forward-genetic strategy, prior to implantation of ES cells to generate the

mouse mutant (Skarnes et al., 1992;Mitchell et al., 2001). The disadvantages of this technique include the unpredictable nature of the phenotype caused by the gene trap and the necessity for germ-line transmission of the mutated gene in order to generate a mouse mutant line.

A further mutagenesis approach is gene targeting that allows precision design of the type of mutation. Hence, deletions, point mutations or insertions can all be achieved. The advantage of gene targeting is that mapping of the mutated gene is not required. However the resulting phenotype is unpredictable and knowledge of the gene structure is required to generate the targeted mutant mouse.

The mouse also represents a good experimental tool to investigate the cellular and embryological bases of neurulation. Mouse embryos are easily accessible and can be cultured for up to 48 hours *in vitro* (Copp *et al.*, 1999). Neurulation in mouse takes place from the 5 to 29 somite stage during a 48 hour period. Therefore, mouse embryos can be cultured throughout the entire neurulation process, allowing experimental manipulation. This is important in the study of the effects of teratogenic substances on closure of the neural tube as well as the analysis of vitamin supplementation to prevent NTDs.

1.5.2 Genes in the planar cell polarity pathway regulate Closure 1

Recently, mutations in the planar cell polarity (PCP) pathway genes have been found to be responsible for the craniorachischisis phenotype observed in three different mouse mutants, *loop tail*, *circletail* and *crash* (Kibar et al., 2001;Murdoch et al., 2001;Curtin et al., 2003;Murdoch et al., 2003). Embryos that are homozygous for mutation in *Vangl2* (*loop-tail*), *Scribble* (*circletail*) and *Celsr1* (*crash*) display failure of Closure 1 leading to craniorachischisis. The other mouse mutants known to display craniorachischisis is the

Dishevelled 1/2 double knockout (*Dsh1/2*) (Hamblet *et al.*, 2002) and the *frizzled* 3,6 double knockout. Embryonic examination shows that at least three of these mutants, *loop-tail, circletail* and *Dsh1/2* have a similar phenotype to that of *Xenopus* embryos where convergent-extension has been disrupted (Wallingford *et al.*, 2000;Wallingford and Harland, 2002). Embryos display shorter body axis, with a broad floor plate and failure of the neural tube to close.

Convergent extension movements occur during gastrulation and consist of the migration of cells from a lateral position towards the midline, where they intercalate, resulting in lengthening of the anterior-posterior axis and extension of midline cells anteriorly (Keller et al., 1992;Davidson and Keller, 1999). Disruption of convergent-extension movements has not yet been reported in mouse mutants with craniorachischisis but initial studies using DiI labelling suggest that convergent extension is disrupted in homozygous *loop-tail* (*Lp)* embryos ((Ybot-Gonzalez et al., 2007b)). The embryonic mechanism of convergent-extension has been studied in *Xenopus,* where disruption in the PCP pathway in the midline results in a broader floor plate or MHP, with formation of the neural folds far apart that prevent fusion (Wallingford and Harland, 2002).

Genes that control the PCP pathway, a non canonical-Wnt pathway, have been identified in *Drosophila* to control the polarisation of cells in the plane of the epithelium. This is required for example, for the unidirectional array of bristles on the wing and for the arrangement of ommatidia in the compound eye (Kühl et al., 2000;Mlodzik, 2002). The PCP pathway shares components of the Wnt pathway, such as the transmembrane receptor Frizzled and the downstream effector Dishevelled. However, unlike the Wnt pathway, the PCP pathway does not result in stabilisation and nuclear translocation of β-

catenin by Dishevelled to control cell proliferation and cell fate decisions. Rather, Dishevelled is thought to signal through small GTPases such as RhoA and Rac to regulate cytoskeleton assembly and cell motility (Mlodzik, 2002) (Keller, 2002). In support of this idea are the experiments in which mouse embryos treated with cytochalasin D before the onset of Closure 1 resulted in failure of this closure site, indicating that cell rearrangements that control Closure 1 are cytoskeleton-dependent. It is unknown how *Vangl2*, *Scribble* and *Celsr1* are related to each other within the PCP pathway.

1.5.3 Sonic hedgehog (Shh) pathway and neural tube closure

The Shh pathway has been implicated in neural tube closure, specifically in regulating the formation of DLHPs (Ybot-Gonzalez *et al.*, 2002). Shh is an extracellular signalling protein that regulates a number of embryological processes, such as patterning of the neural tube and limbs, cell proliferation and cell-fate determination. Postnatally, aberrant Shh signalling pathway has been linked to basal cell carcinomas and medulloblastoma tumours (Chiang et al., 1996;Goodrich et al., 1997;Fan et al., 1997;Wechsler-Reya and Scott, 1999). The molecular mechanisms underlying the Shh signalling pathway have been principally determined by studies in *Drosophila* (Ruiz i Altaba, 1999). The preliminary pathway involves binding of HH to its transmembrane receptor Patched (Ptc), which prevents the inhibition of Smoothened (Smo), a transmembrane protein that forms part of the HH receptor complex. De-inhibtion of Smo allows signalling to a cytoplasmatic protein complex formed by Fused, Costal-2 and Cubitus Interruptus (CI) (Tabin and McMahon, 1997). When Shh is not present, proteolytic processing of CI results in the generation of the shorter CI N-terminal form that functions as a transcriptional repressor of HH downstream genes. Binding of HH to its receptor inhibits the CI proteolysis resulting in the stable full length CI that functions as a transcriptional activator of HH downstream genes. In mouse, Shh, Patched and Gli are the vertebrate

homologues of *Drosophila* HH, Patched and CI. In mouse three Gli proteins have been identified, Gli1, Gli2 and Gli3 that code for zinc finger domain (ZFD) transcription factors. In mouse Gli1 and Gli2 displays a similar function to the full length CI, and acts as a transcriptional activator of Shh downstream genes. However, Gli3 has a repressive function similar to that of the N-terminal CI (Marigo *et al.*, 1996).

During neurulation, Shh emanating from the notochord functions as a morphogen, to pattern the neural tube so that progenitor cells in the ventral region acquire ventral fates and become ventral neural types including motor neurons. Mice that are null for Shh display a dorsalised neural tube, and dorsal markers such as *Pax3* become expressed in ventral regions (Chiang *et al.*, 1996). In contrast over-expression of Shh results in loss of dorsal fates and a ventralised neural tube.

Several mice that carry mutations in Shh pathway genes display NTDs, for example two mutant alleles of *Open brain* (*opb*), one spontaneous and the second ENU-induced. Embryos homozygous for either mutant allele display exencephaly, spina bifida, polydactyly and poorly developed eyes (Sporle *et al.*, 1996). Analysis of $opb^{-/-}$ mutant embryos shows a lack of dorsal neuronal cell types, a phenotype that resembles mice with partial loss of function of Patched or over-expression of Shh (Milenkovic *et al.*, 1999). The gene mutated in *opb* was identified as *Rab23,* encoding a member of the Rab family of GTPases, which controls vesicle transport. How this protein participates in Shh signalling remains unknown but, since *opb* phenocopies *Gli3* and *Patched1* mutant embryos, Rab23 may antagonistically regulate the Shh pathway.

Interestingly, null embryos for Patched1 (*Ptch1*) and double homozygotes for protein kinase a subunit Cα/Cβ1 (*Prkaca, Prkacb*), display cranial NTDs that may also be caused by excessive Shh signalling. In *Drosophila,* protein kinase A phosphorylates CI, a process that is required for protein cleavage to yield the N-terminal transcriptional repressor form of CI (Chen *et al.*, 1999). In vertebrates, a similar mechanism has been proposed (Ruiz i Altaba, 1999). Double homozygote embryos for *Prkaca* and *Prkacb* have excess Shh signalling, possibly because pKA cannot phosphorylate Gli proteins (Huang et al., 2002).

Further evidence for the importance of regulation of the Shh pathway in neurulation comes from the *Extra-toes*^{J} mouse (*Xt*^{J}), that carries a deletion in *Gli3*, and also displays cranial NTDs (Hui and Joyner, 1993). Lack of Gli3, which acts as a repressor of Shh downstream targets, results in excessive Shh signalling and exencephaly.

The information obtained from mouse mutants indicates that the Shh pathway is necessary for cranial and spinal neurulation. However, the embryonic mechanisms leading to NTDs in these mutants have not been characterised. One hypothesis to explain the exencephalic phenotype could be the loss of dorsal structures due to excessive Shh signalling resulting in a ventralised neural tube. In the spinal neural tube, the role of Shh has been studied in more detail (Ybot-Gonzalez *et al.*, 2002). Shh signalling was found to inhibit DLHP formation. Indeed, homozygous null embryos for Shh develop DLHPs at an earlier stage of neurulation, during Mode 1, compared to the wild type embryos. DLHP formation can also be inhibited by local release of Shh peptide using implanted beads next to the neural folds, resulting in straight neural folds. In normal development, the inhibitory action of Shh on DLHPs formation declines at more caudal levels. Shh is expressed in the notochord at progressively lower intensity as spinal neurulation

progresses, allowing DLHPs to appear and so enabling the transition to Mode 2 and Mode 3. Therefore, Shh controls the timing of DLHP development by inhibiting its formation.

A hypothetical model of DLHP regulation has been postulated (see Fig. 1.6)(Ybot-Gonzalez *et al.*, 2002). In this model, the balance between positive (inducing) and negative (inhibiting) signals regulates DLHP formation. An unknown inducing signal from the surface ectoderm stimulates bending of the neural plate, perhaps through regulation of the cell cycle of the adjacent tissue. Early in neurulation, at Mode 1, Shh is expressed at high levels in the notochord and antagonises the positive signal from the surface ectoderm resulting in straight neural folds. However, as neurulation progresses (Mode 2 and Mode 3 of neurulation) the expression of Shh decreases, reducing the inhibitory effect and resulting in bending of the neural folds that are under the influence of the inducing signal.

This model is supported by experimental observations and the analysis of mouse mutants. Once Closure 1 has occurred, the MHP is not required for closure of the neural tube. Thus, mouse mutants for *HNF3β*, *Gli2*, *Shh* and *Gli1/Gli2* double mutants do not form a floor plate (MHP) and yet close their neural tube successfully in a Mode 3 morphology (Ang and Rossant, 1994;Chiang et al., 1996;Motoyama et al., 1998;Matise et al., 1998;Park et al., 2000).

Removal of the surface ectoderm abolishes DLHPs formation (Ybot-Gonzalez *et al.*, 2002) showing that the surface ectoderm must signal to the underlying neural folds to induce the formation of DHLPs. Initially, *BMP2* expressed from the surface ectoderm, was thought to be a good candidate molecule to induce DLHP. However recent

examination of embryos that lack BMP2 revealed that DLHP are actually formed prematurely in these embryos, as in *Shh*$^{-/-}$ embryos ((Ybot-Gonzalez et al., 2007a)). Recently, it was found that *BMP2* from the surface ectoderm induces noggin expression in the dorsal neural fold.

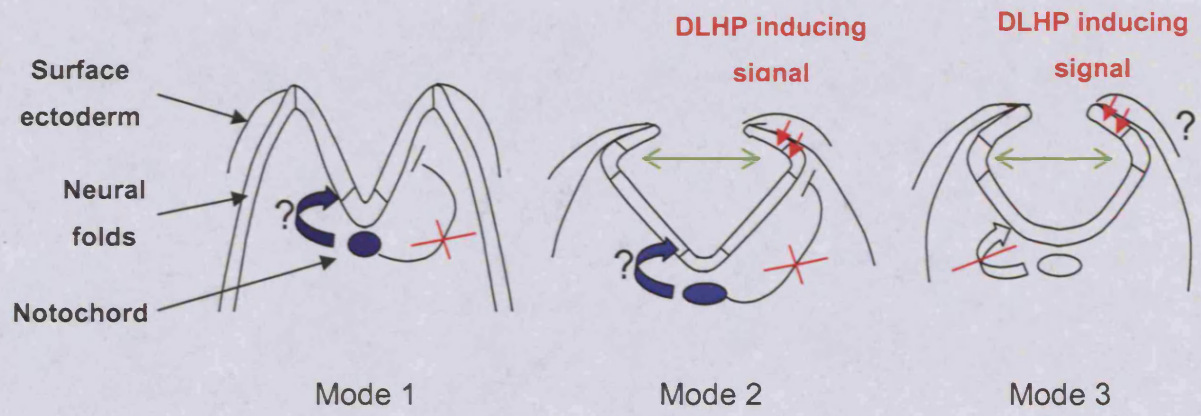

Figure 1.7 Diagram to illustrate the proposed regulation of DLHPs in three progressive stages of mouse neurulation

Strong expression of Shh from the notochord in Mode 1 of neurulation inhibits DLHPs, whilst an unknown signal from the notochord induces the MHP (blue arrow). In Mode 2, Shh expression declines and its inhibitory action is lost. An unknown inducing signal from the surface ectoderm (red arrows) induces bending of the underlying neural fold (green arrows). In Mode 3, the MHP inducing signal is lost and closure of the neural tube depends only on DLHPs. Diagram modified from Ybot-Gonzales (2002).

Bending of the neural plate at the DLHPs regions ensures apposition of the neural folds prior to their fusion in the dorsal midline. However, determining how DLHPs are regulated has been hampered by the lack of mouse mutants that fail to develop DLHPs. A mouse mutant that lacked DLHPs would provide an opportunity to understand the

molecular mechanisms required for DLPHs formation and neural tube closure in the low spinal region (Ybot-Gonzalez et al., 2007a).

1.5.4 Wnt signalling pathway

The Wnts are a family of secreted proteins that regulate many biological processes (Cadigan and Nusse, 1997). Functional analyses in *Xenopus* suggest that the Wnt family can be divided into two functionally distinct groups. The first group of Wnts induces a secondary axis when ectopically expressed in embryos. They activate the canonical Wnt/β-catenin pathway and induce the transcription of target genes such as *siamois* and *Xnr3* ((Brannon and Kimelman, 1996); (Carnac et al., 1996); McKendry et al. 1997). The second group of Wnts, which includes Xwnt5a and Xwnt11, activates the noncanonical Wnt signaling pathway that controls morphogenetic cell movements (Kuhl 2002; Tada et al. 2002). It was shown in zebrafish that mutations in *Wnt11/silberblick* and *Wnt5a/pipetail* inhibit normal gastrulation movements (Rauch et al., 1997); (Heisenberg et al., 2000). The noncanonical Wnt pathway branches into two cascades. One is the Wnt/JNK pathway, which involves c-Jun N-terminal kinase (JNK); (Boutros et al., 1998); (Yamanaka et al., 2002). The other is the Wnt/Ca^{2+} pathway (Kuhl et al. 2000). In *Drosophila*, the Wnt/JNK pathway is called the planer cell polarity (PCP) pathway, and it specifies cell polarities in epithelial cells and other types of cells (Adler, 2002).

The Wnt signaling pathway is mediated by a seven-transmembrane Wnt receptor, Frizzled, and the signal is transmitted through a cytoplasmic protein, Dishevelled (Dsh), which plays pivotal roles in both the canonical and noncanonical Wnt pathways (Boutros and Mlodzik, 1999); (Rousset et al., 2002). In *Drosophila*, Dsh localizes to the membrane, and this localization is required for Dsh function (Axelrod, 2001). *Xenopus* Dsh (Xdsh) is also translocated from the cytoplasm to the plasma membrane in response to a signal

generated by Frizzled receptors (Yang-Snyder et al., 1996); (Axelrod et al., 1998). One such receptor is *Xenopus* Frizzled7 (Xfz7), which is involved in the noncanonical Wnt pathway (Djiane et al., 2000); (Medina and Steinbeisser, 2000); (Medina et al., 2000). However, the mechanism of this translocation and the activation of Dishevelled are not known. The signal transduction of the canonical pathway seems to be different from that of the noncanonical pathway, because the membrane translocation of Xdsh is not required for the activation of the canonical Wnt pathway (Rothbacher et al. 2000).

Protein kinase C (PKC) is thought to be involved in the noncanonical Wnt signaling pathway, particularly in the Wnt/Ca^{2+} pathway, for several reasons. Xwnt5a and rat Frizzled2 activate the phosphatidylinositol pathway and increase the intracellular Ca^{2+} levels in zebrafish embryos (Slusarski et al., 1997). The phosphatidylinositol pathway and Ca^{2+} levels are closely related to PKC activation. In fact, overexpression of *Frizzled* causes the translocation of epitope-tagged PKCα from the cytoplasm to the plasma membrane in *Xenopus* embryos (Sheldahl et al., 1999); (Medina et al., 2000). Kuhl et al., (2001) showed that PKCα phosphorylated Dsh in vitro. In addition, the loss of *Xfz7* function leads to a defect in tissue separation during *Xenopus* gastrulation, which is rescued by the overexpression of PKCα (Winkbauer et al., 2001). PKC is also implicated in the Xwnt11 signaling pathway for *Xenopus* cardiogenesis (Pandur et al., 2002) and in the Dwnt4 pathway for *Drosophila* ovarian morphogenesis (Cohen, Jr. and Shiota, 2002).

Although much evidence suggests that PKC is involved in the Wnt signaling pathway, the molecular roles of PKC in this pathway are not well understood.

1.5.5 MARCKS signalling pathway

As previously described the neural tube is formed by morphogenetic movements largely dependent on cytoskeletal dynamics. Actin and many of its associated proteins have been proposed as important mediators of neurulation. For instance, mice deficient in Myristoylated Alanine-Rich C Kinase Substrate (MARCKS), an actin cross-linking membrane-associated protein that is regulated by PKC and other kinases, present severe developmental defects, including failure of cranial neural tube closure. MARCKS is a ubiquitous protein substrate for different PKC family kinases and proline directed kinases such as MAPK and Cdks (Aderem, 1992b).Its PKC-phosphorylation domain or PSD (Phosphorylation Site Domain) is highly conserved and it is also the site for interaction with other molecules, such as calcium-calmodulin, negatively charged membrane phospholipids and F-actin (Aderem, 1992a). Binding to calcium-calmodulin and the plasma membrane, as well as actin filament cross-linking activity, are antagonized by PSD phosphorylation (Laux, 2000). Conversely, calcium-calmodulin binding inhibits PSD phosphorylation and actin crosslinking. In addition to neural tube closure, MARCKS and MacMARCKS have been implicated in several other events related to the actin cytoskeleton, such as cell motility, cell spreading, membrane ruffling, phagocytosis, exocytosis and neurite outgrowth (Laux, 200).

1.6 DIETARY DEFICIENCY AND NTDs

The role of dietary deficiency during pregnancy has been studied in various animal models including the hamster (Mooij et al., 1993), rat (Miller et al., 1994) and mouse (Heid et al., 1992). No association has been found in any of these models between folate deficiency and increased incidence of offspring affected by NTDs. The question of dietary deficiency has also been addressed using the *in vitro* whole embryo culture system. Cockcroft (1988)

showed that specifically omitting folate from dialysed serum cultures reduces embryonic growth but does not yield NTDs, in contrast to *myo*-inositol whose omission leads to the development of cranial NTDs. In other studies, embryos have been cultured under sub-optimal conditions to produce NTDs in non-mutant strains. Such conditions produce a range of defects that can be ameliorated by various supplements. Rat embryos cultured in cow serum (Coelho et al., 1989) or canine serum (Flynn et al., 1987) develop cranial NTDs which can be prevented by supplementation with methionine. Culturing rodent embryos in human serum produces NTDs which can be prevented by supplementation with L-homocysteine (VanAerts et al., 1994). However, these studies do not provide a satisfactory model for the human condition for a number of reasons. Firstly, the original culture conditions are sub-optimal since embryos exhibited growth retardation as well as NTDs, which does not appear to mirror the human situation where pregnancies resulting in NTDs have not been shown to be sub-optimal. Secondly, the administration of methionine or homocysteine, but not folic acid, prevents NTDs whereas homocysteine is a risk factor for human NTDs. Moreover, although these agents are related to folate metabolism, a model for the human condition would have to be preventable by folic acid itself.

1.7 THE *curly tail* MUTANT MOUSE

Figure 1.8 *curly tail* mouse. (Photograph from (Catherine Chalmers, 2007)

1.7.1 The *curly tail* mutant as a model for NTDs in humans

Although no animal model has been convincingly established as the equivalent of human NTDs, many aspects of the *curly tail* mouse mutant appear to parallel the malformations in humans (Embury et al., 1979). Lesions occur at both ends of the central nervous system, resulting in exencephaly and spina bifida. Exencephaly occurs in 1-2 % of embryos, spina bifida in around 15 % and tail flexion defects in around 50 % (Anatomy and Embryology review). There is a marked female excess both in exencephalic mice and anencephalic humans where the female:male ratios are 4:1 and 3:1 respectively (Carter, 1974); (Embury et al., 1979). Polyhydramnios, which usually occurs in human anencephalic pregnancies, is also found in association with *curly tail* mouse fetuses with open lesions and is especially significant in the exencephalics. Large numbers of rapidly adherent cells, with distinctive morphology, in the amniotic fluid is another common characteristic in humans (Wald et al., 1977); (Brock and Sutcliffe, 1972), and *curly tail* (Embury et al., 1979) NTD pregnancies. Hydrocephaly sometimes occurs in conjunction with NTDs in both the *curly tail* mouse and humans. Furthermore, raised alphafetolprotein levels in the amniotic fluid can be detected in affected fetuses of both mouse and human (Adinolfi et al., 1976); (Brock and Sutcliffe, 1972).

1.7.2 The *curly tail* defect at the genetic level

The *curly tail* mouse arose as a spontaneous mutation in 1950 in the inbred GFF stock at the Glaxo Laboratories. The founder female was subsequently mated to a CBA/Gr male and then the mice were bred as a closed colony (Grünberg, 1954). As described above, around 60 % of *curly tail* mice exhibit NTDs which have variable expression: exencephaly, lumbo-sacral spina bifida, a coiled or kinked tail. These mice are referred to as 'affected' and symbolized by CT. The rest of the mice are morphologically normal and

are referred to as 'unaffected', symbolized by ST. Whatever their phenotype, it is believed that all *curly tail* mice are homozygous for a recessive genetic mutation (*ct/ct*), the expression of which is modified by the genetic background (Grüneberg 1954); (Seller et al., 1979); (Estibeiro and Copp, 1990). Evidence for recessivity came from out-crossing CT mice to BALB/c, A/Strong, C57BL/6 and DBA/2 strains which produced no offspring with neurovertebral abnormalities in the F1 generation; NTDs reappeared in the back-cross generation. However, there was a significant deviation from the expected 50 % CT in the backcross offspring, and the actual expression differed according to the inbred strain used: 24 % of offspring were CT in the BALB/c cross, 8 % in the A/Strong cross, 22.5 % in the C57BL/6 cross and 0.4 % in the DBA/2 cross, suggesting that genetic background has a modifying effect on the expression of the gene (Embury et al., 1979). Selective breeding experiments provided further evidence that all mice, irrespective of their phenotype, are homozygous recessive with the gene having variable penetrance and expressivity (Embury et al., 1979).

1.7.2.1 Grainyhead (*Grhl-3*)

The Grainyhead, drosophila, Homolog of, or 3 sister of mammalian grainyhead (sister of MGR); SOM or Grainyhead like 3 (*Grhl3*) belongs to a family of transcription factors related to the Drosophila *grainyhead* (*grh*) protein. The Drosophila gene *grainyhead* is the founding member of a large family of genes that are highly conserved from fly to human. The family consists of two main branches, with *grainyhead* as the ancestral gene for one branch and the recently cloned Drosophila CP2 (Gemini) as the ancestral gene for the other. Functionally, *Grainyhead*, the best-studied protein in its subfamily, is mainly a regulator of developmental control genes in *D.melanogaster*, such as *Ultrabithorax*, *dopa decarboxylase*, *tailless* and *decapentaplegic* (Ting et al., 2003). Fruit flies carrying

grainyhead mutations display an embryonic lethal phenotype. Like *grainyhead*, the human *Grhl3* gene produces several distinct isoforms with differing functional properties through alternative splicing.

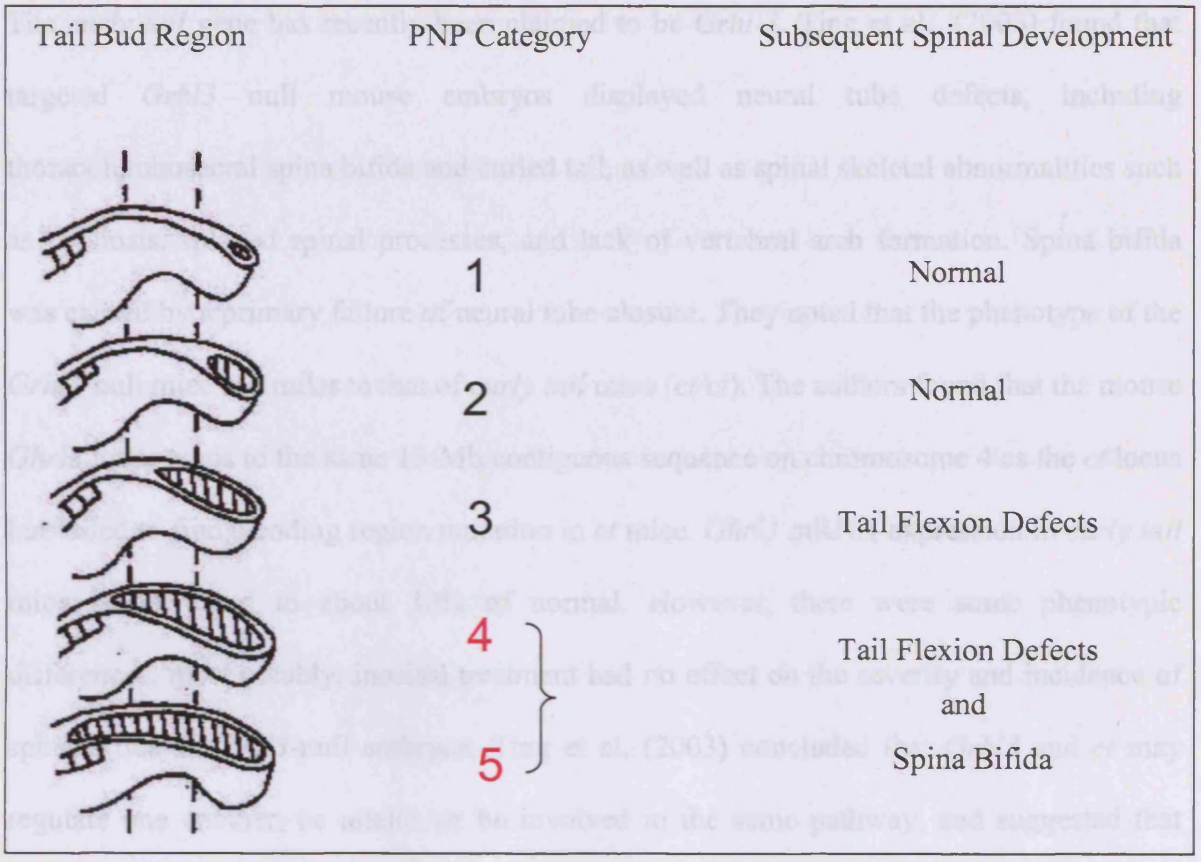

Figure 1.9 Diagrams of tail bud regions of *curly tail* embryos. The diagram illustrates the five PNP categories and subsequent spinal development. Modified from Copp, 1985

The tissue distributions of these isoforms differ and all display highly restricted expression patterns. These findings indicate that *Grhl3*, like its family members, may play important roles in mammalian development. By database analysis, Ting et al. (2003) mapped the mouse *Grhl3* gene to chromosome 4 and, by *in situ* hybridization, they detected *Grhl3* expression at mouse embryonic day (E) 8.5 in the non neural ectoderm immediately adjacent to the neural plate, which was undergoing folding to form the neural tube. At later

time points, more widespread expression was observed in the surface ectoderm, as well as in other tissues lined by squamous epithelium, including the oral cavity, urogenital sinus, and anal canal. Expression progressively increased until E15.5.

The *curly tail* gene has recently been claimed to be *Grhl-3*. Ting et al., (2003) found that targeted *Grhl3* null mouse embryos displayed neural tube defects, including thoracolumbosacral spina bifida and curled tail, as well as spinal skeletal abnormalities such as kyphosis, splayed spinal processes, and lack of vertebral arch formation. Spina bifida was caused by a primary failure of neural tube closure. They noted that the phenotype of the *Grhl3*-null mice is similar to that of *curly tail* mice (*ct/ct*). The authors found that the mouse *Ghrl3* locus maps to the same 13-Mb contiguous sequence on chromosome 4 as the *ct* locus but failed to find a coding region mutation in *ct* mice. *Ghrl3* mRNA expression in *curly tail* mice is decreased to about 30% of normal. However, there were some phenotypic differences; most notably, inositol treatment had no effect on the severity and incidence of spina bifida in *Grhl3*-null embryos. Ting et al. (2003) concluded that *Grhl3* and *ct* may regulate one another, be allelic, or be involved in the same pathway, and suggested that *Grhl3* is a good candidate for the gene underlying the *curly tail* phenotype.

Mace and colleagues found that *grainyhead* activates wound repair genes in cells surrounding injuries in the outer layer of fly embryos (Mace et al., 2005). They created wounds in flies and analyzed that *grainyhead* initiates repair. They also found that in flies lacking *grainyhead*, wounds failed to heal. Moreover, mice lacking *grainyhead* proved to have more permeable skin than normal mice and had deficient wound repair (Ting et al., 2005). Such a conserved genetic mechanism for wound repair is considered an important finding, given that little is known about how wound repair is halted when injuries are

healed. Nor is it understood how cancer cells evade this stop program. The discovery that *grainyhead-like* factors are required for the response to injury opens up new avenues of research in the field of wound healing as well as cancer research and development, since many cancer cells and developmental processes activate genes normally involved in wound healing in order to kick start processes such as cell division and cell migration

1.7.3 The *curly tail* defect at the morphological level

In 1954, Grüneberg suggested, from morphological observations, that spinal neural tube malformations in *curly tail* embryos were the result of delayed closure of the posterior neuropore (PNP). Further evidence was provided by Copp (1985) who followed the *in vitro* development of individual curly tail embryos that exhibited varying extents of delay in PNP closure. He classified the axial length of the PNP, at the stage of 25-29 somites, into five categories (Fig. 1.9). In categories 1 and 2, the PNP is restricted to the expanded distal region of the tail bud. In category 3, the PNP extends beyond the distal region of the tail bud, but does not reach the level of the hindlimb bud rudiment. In category 4, the PNP extends into the region of the hindlimb bud but does not encroach upon the rows of somites. In category 5, the PNP overlaps, in its cranial extent, with the somite rows. It was found that when the PNP was restricted to the expanded distal region of the tail bud the majority of *curly tail* embryos (63 %) were unaffected and developed a straight tail *in vitro* while the rest of the embryos had tail flexion defects. When the PNP extends beyond the distal expansion, but does not reach the level of the hindlimb bud rudiment, significantly more embryos (71 %) developed tail flexion defects with a few (8 %) having spina bifida as well. On the other hand when the PNP extends into the region of the hindlimb bud or when the PNP overlaps, in its cranial extent, with the somite rows, only 8 % of the embryos were normal, and the proportion of embryos that developed spina bifida

increased to 34 % (Copp, 1985). This understanding of different development of embryos according to the length of unclosed neural folds at the PNP allows comparison between prospective normal and affected *curly tail* embryos at a stage that precedes the development of fully formed spinal NTDs (Copp, 1985).

During the course of other experiments with *curly tail* mice, it was noticed that embryos which have a large PNP often exhibit excessive ventral curvature of the caudal region (Copp et al., 1988a). To determine whether there is a true relationship between the size of the PNP and the angle of curvature, these two parameters were measured in individual embryos. The angle of ventral curvature of the caudal region was found to vary significantly with neuropore size, such that the curvature is greatest in embryos with a large PNP and least in embryos with a small neuropore (Brook et al., 1991a). This was an interesting observation in view of previous suggestions that curvature of the body axis can affect the rate of neurulation in the cranial region of the mouse embryo (Jacobson and Tam, 1982); (van Straaten et al., 1992). Moreover, splitting of the caudal region to prevent development of curvature was effective in reducing PNP length in *curly tail* embryos, strongly supporting the idea that ventral curvature is the cause of delayed PNP closure (Brook et al., 1991a), (van Straaten and Copp, 2001)

1.7.4 The *curly tail* defect at the cellular level

Regional variations in the rate of cell proliferation have been suggested to be an important factor determining the success or failure of normal neurulation in higher vertebrates (Kauffman, 1968); Wilson, 1982). In studies of mouse mutants with neural tube defects, a prolonged neuroepithelial cell cycle was found in regions of open cranial neural tube of homozygous *splotch* mutant mouse embryos (Wilson, 1974); (Wilson and Center, 1974). The increased ventral curvature in *curly tail* embryos appears to result from a growth

imbalance in the caudal tissues of the embryos. When the different cell types in the PNP region of normal and affected *curly tail* embryos were compared, a reduced proliferation rate, equivalent to a 25% increase in cell cycle time, was found in gut endoderm and notochord. Other cell types, including neuroepithelium, surface ectoderm and mesoderm, showed no difference between normal and abnormal embryos (Copp et al., 1988c).

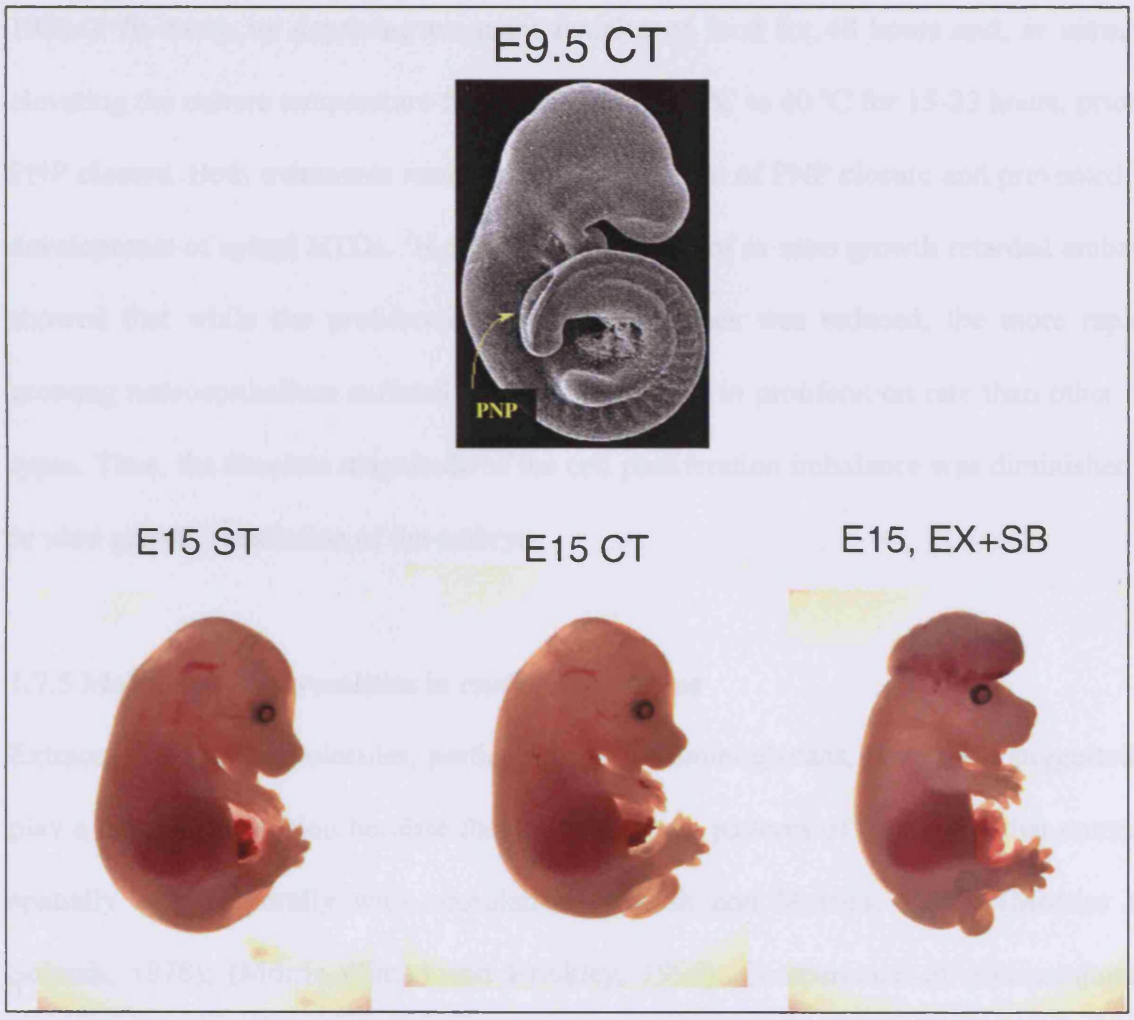

Figure 1.10 Neural tube malformations in *curly tail* embryos. (ST) straight tail; (CT) curly tail; (EX) excencephaly; (SB) spina bifida. Arrow poins to the open PNP. (E) embryonic day.

This imbalance of growth between the dorsally situated neuroepithelium and the ventrally situated notochord and gut endoderm, in the PNP region, has been shown to be responsible for the development of spinal NTDs in affected *curly tail* embryos. Evidence comes from experiments in which NTDs were prevented by re-establishing a balance of proliferation between the slowly growing notochord/gut endoderm and the unaffected neuroepithelium. This was achieved by retarding the growth of the embryo in two ways (Copp et al., 1988c): *In utero*, by depriving pregnant females of food for 48 hours and, *in vitro*, by elevating the culture temperature from the optimal 38 °C to 40 °C for 15-23 hours, prior to PNP closure. Both treatments resulted in normalization of PNP closure and prevented the development of spinal NTDs. ^{3}H-thymidine labelling of *in vitro* growth retarded embryos showed that while the proliferation rate of all tissues was reduced, the more rapidly growing neuroepithelium suffered a greater reduction in proliferation rate than other cell types. Thus, the absolute magnitude of the cell proliferation imbalance was diminished by *in vitro* growth retardation of the embryo.

1.7.5 Molecular abnormalities in *curly tail* embryos

Extracellular matrix molecules, particularly glycosaminoglycans, have been suggested to play a role in neurulation because they show specific patterns of deposition that correlate spatially and temporally with neurulation (Solursh and Morriss, 1977); (Morriss and Solursh, 1978); (Morris-Wiman and Brinkley, 1990). Comparisons of glycoconjugates were made prior to the completion of neurulation, between normally developing curly *tail* embryos and those developing spinal NTDs. Newly synthesized hyaluronan, which accumulates in large quantities in the posterior neuropore of normal embryos, was found to be significantly reduced in amount in the developing basement membranes beneath the medial aspect of the neuroepithelium and around the notochord in the PNP region of

affected *curly tail* embryos (Copp and Bernfield, 1988b). Other embryonic regions and other glycoconjugates showed no differences between normal and affected *curly tail* embryos, and their accumulation pattern was similar to non-mutant embryos (Copp and Bernfield, 1988a).

Affected *curly tail* embryos also exhibit abnormal binding of the iron-binding growth factor, transferrin, which is taken up and localised in the hindgut of neurulation stage mouse embryos (Copp et al., 1992). Reduced binding was observed in the hindgut of affected *curly tail* embryos compared with their unaffected littermates, although the level and sites of expression of the transferrin receptor are not altered (Hoyle et al., 1996).

Several studies have demonstrated an interaction between retinoic acid and the frequency of NTDs in *curly tail* embryos (Chen et al., 1994) and this has been correlated at the molecular level with altered expression of nuclear retinoic acid receptors (Greene and Copp, 1997a).

1.7.6 *Curly tail*, a mouse model of folate-insensitive NTDs

Although some cases of human NTDs can be prevented by folic acid, there is increasing evidence that many cases do not respond. For instance, there was no reduction in NTD frequency in the U.K. during the first ten years after folic acid supplementation was introduced (Abramsky et al., 1999). In 1994 Seller provided preliminary evidence that exogenous *myo-inositol* reduces NTD frequency in *curly tail* mice. Greene and Copp (1997) repeated and extended this study using the curly tail mouse as a model of folate-resistant NTDs. They found that intraperitoneal injection of pregnant female mice with *myo-inositol* at various times during the critical phase of neural tube closure significantly

decreased the frequency of spina bifida in developing embryos. A single injection on embryonic day 9.5 reduced NTDs frequency by 70% in *ct* embryos.

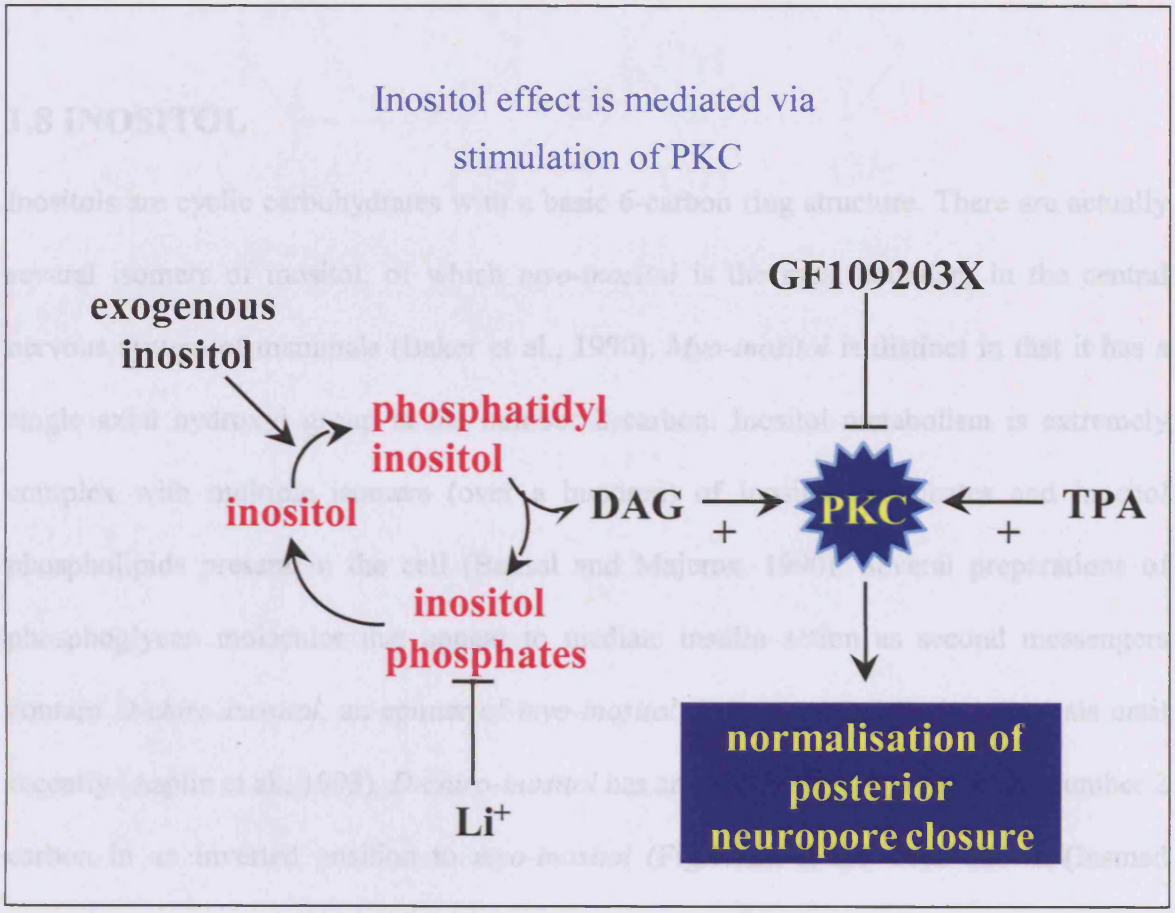

Figure 1.11 Diagram representing what was known prior to this thesis about the possible inositol mechanism in normalising PNP closure in *curly tail* embryos.

Greene and Copp (1997) demonstrated further that inositol prevents spinal NTDs *in vitro* and showed that inositol increases the flux through the inositol/lipid cycle, stimulates protein kinase C activity, and up-regulates the expression of retinoic acid receptor beta. They concluded that their findings in the *curly tail* mutant reveal a molecular pathway of NTD prevention and suggest possible efficacy of combined treatment with folate and

inositol in overcoming the majority of human NTDs (Greene and Copp, 1997a). This hypothesis is currently being tested in a clinical trial.

1.8 INOSITOL

Inositols are cyclic carbohydrates with a basic 6-carbon ring structure. There are actually sevaral isomers of inositol, of which *myo-inositol* is the most abundant in the central nervous system of mammals (Baker et al., 1990). *Myo-inositol* is distinct in that it has a single axial hydroxyl group at the number 2 carbon. Inositol metabolism is extremely complex with multiple isomers (over a hundred) of inositol phosphates and inositol phospholipids present in the cell (Bansal and Majerus, 1990). Several preparations of phosphoglycan molecules that appear to mediate insulin action as second messengers contain *D-chiro-inositol*, an epimer of *myo-inositol* that was unknown in mammals until recently (Asplin et al., 1993). *D-chiro-inositol* has an axial hydroxyl group at the number 2 carbon in an inverted position to *myo-inositol* (Fig.1.12). It has been shown (Insmed Incorporated, unpublished data) that diabetic subjects excrete 5-40 times as much *D-chiro-inositol* in the urine as normal subjects and that the rate of excretion depends critically on the degree of diabetic control. Plasma *D-chiro-inositol* levels are influenced by insulin treatment and are a strong predictor of hypertriglyceridemia, the most common lipid abnormality in diabetic patients (Larner, 2001). *D-chiro-inositol* can be obtained from the diet in the form of pinitol, a methyl inositol found in legumes. The effects of *D-chiro-inositol* on diabetic subjects are being studied (Insmed Incorporated, unpublished data). The exact structure of the *D-chiro-inositol*-containing molecules thought to be responsible for these effects at the biochemical level has not been reported (Larner, 2001).

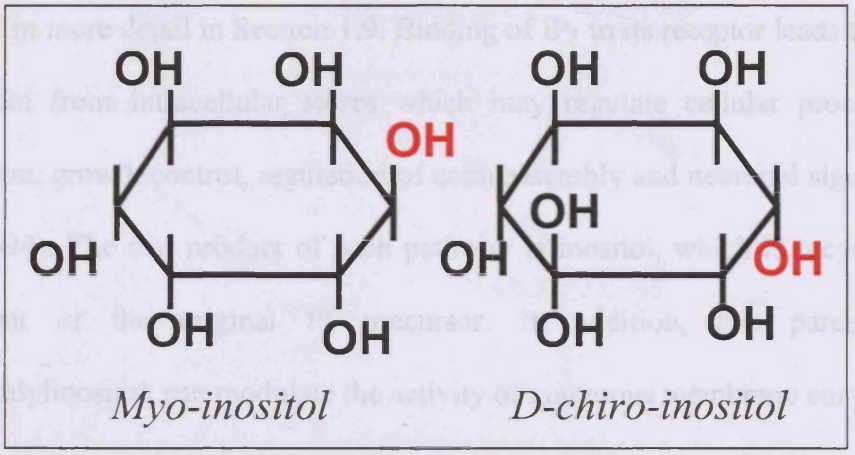

Figure 1.12 Diagram illustrating *myo-inositol* and *D-chiro-inositol* (structural differences are enhanced in red colour).

1.8.1 Mechanisms of inositol signalling

The inositol/lipid cycle plays a central role in inositol metabolism and is involved in signal transduction leading to the regulation of many cellular functions (Berridge, 1995). Cellular uptake of inositol occurs via a sodium-coupled transporter, which is a member of the sugar transporter superfamily (Nikawa et al., 1991). Inositol is utilised in synthesis of the membrane lipid, phosphatidylinositol (PI), in which it constitutes the polar head group. Subsequent phosphorylation steps lead to generation of phosphatidylinositol diphosphate (PIP_2) which is the major substrate for receptor activated phospholipase C (Figure 1.13). The major two pathways for activation of isoforms of PLC involve G-protein linked receptors which activate PLCβ via GTP-binding proteins and receptor tyrosine kinases which activate PLCγ (Berridge, 1993). Hydrolysis of PIP_2 generates inositol 1,4,5-triphosphate (IP_3) and diacylglycerol (DAG) which are major downstream effectors of the cycle. DAG is physiological activator of protein kinase C (PKC), an important family of regulatory enzymes (Hinchliffe and Irvine, 1997). The potential function of PKC in prevention of NTDs is one focus of this study and is, therefore,

reviewed in more detail in Section 1.9. Binding of IP_3 to its receptor leads to mobilisation of calcium from intracellular stores which may regulate cellular processes such as fertilisation, growth control, regulation of actin assembly and neuronal signalling (Martin et al., 1994). The end product of each pathway is inositol, which is recycled back as a component of the original PI precursor. In addition, this parent compound, phosphatidylinositol, can modulate the activity of numerous membrane enzymes.

1.8.2 Phosphatidylinositol 3-kinase

Aside from the inositol/lipid cycle, phosphoinositides have an additional role in signal transduction involving the enzyme, phosphatidylinositol 3-kinase (PI 3-Kinase) which is recruited and concomitantly activated following stimulation of various receptor tyrosine kinases (Divecha and Irvine, 1995). Following auto-phosphorylation and dimerisation, the activated receptors for ligands such as platelet-derived growth factor α and β, colony stimulating factor-1, c-kit and hepatocyte growth factor, are able to interact directly with PI 3-Kinase (Rodgers and Theibert, 2002). An alternative mechanism is also utilised in which the activated receptor interacts with PI 3-Kinase via an adapter molecule such as insulin receptor substrate-1 and erb/B_3 in the case of the insulin and epidermal growth factor receptors respectively (Banker, 2003).

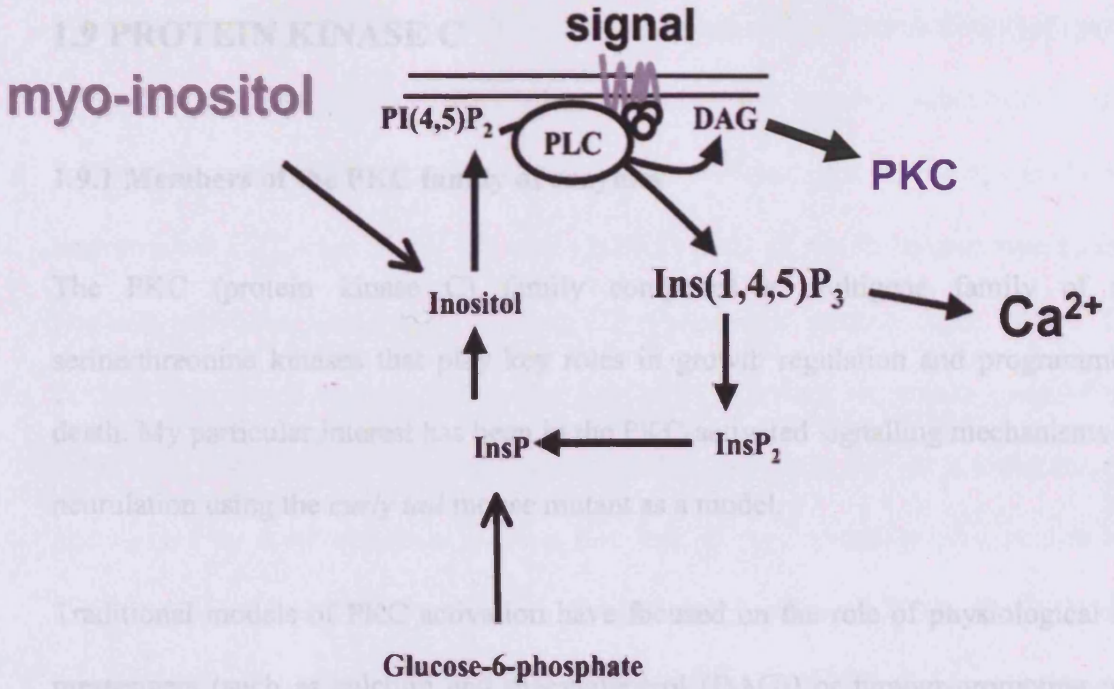

Figure 1.13 The inositol phosphate signalling pathway. When the G-protein coupled receptor B is activated, it activates a 'G protein' which in turn stimulates phospholipase C (PLC). PLC cleaves phosphoinositol diphosphate (PIP_2) into inositol 1,4,5 triphosphate (IP_3) and diacylglycerol (DAG). DAG is a physiological activator of PKC. The second messenger, IP_3 releases Ca^{2+} from the endoplasmic reticulum into the cytoplasm which triggers further biochemical reactions. Diagram from Martin, 2001.

The active PI3-Kinase enzyme, a heterodimer of regulatory (85 kDa) and catalytic (110 kDa) subunits, phosphorylates the D-3 position of PI, PIP and PIP_2, the later probably being the major substrate in vivo (Chou et al., 1998). Functions for the lipid products of PI 3-Kinase have been proposed in activation of Ca^{2+}-atypical PKC (PKC ζ), vesicular trafficking, organisation of actin and planar cell polarity (reviewed by (Cantley, 2002). The downstream function appears to be mediated through Rac, a member of the Rho class GTP-binding proteins, which is activated by exchange of bound GDP for GTP (Parker, 1995).

1.9 PROTEIN KINASE C

1.9.1 Members of the PKC family of enzymes

The PKC (protein kinase C) family comprises a multigene family of related serine/threonine kinases that play key roles in growth regulation and programmed cell death. My particular interest has been in the PKC-activated signalling mechanisms during neurulation using the *curly tail* mouse mutant as a model.

Traditional models of PKC activation have focused on the role of physiological second messengers (such as calcium and diacylglycerol (DAG)) or tumour-promoting phorbol esters (such as PMA) to anchor PKCs in their active conformations on membranes (Berridge, 1987). However, most cells co-express multiple PKC isoforms that have distinct (and occasionally functionally opposing) cellular responses. PKC isoform specificity has been attributed to distinctive compartmentalization patterns for individual PKC isoforms (Abeliovich et al., 1993a;Bareggi et al., 1995). The prevailing model holds that protein–protein interactions between a particular PKC isoform and its unique membrane-associated anchoring protein (itself localized to a specific membrane sub-domain) serve to recruit the PKC isoform to a distinct sub-cellular compartment, in close proximity with its unique target substrates (Dekker and Parker, 1994;Nakhost et al., 2002).

1.9.2 PKC structure and regulation

PKC isoforms are single polypeptide chains with N-terminal regulatory domains that contain an autoinhibitory pseudosubstrate domain, two membrane-targeting modules (termed C1 and C2) and a highly conserved C-terminal catalytic domain (that contains the

C3 and C4 motifs required for ATP/substrate binding and catalytic activity) (Figure 1.14) (Parker and Murray-Rust, 2004). PKC isoforms are broadly subdivided into three subfamilies based upon their structurally distinct N-terminal regulatory domains. The conventional PKCs are α, βI, βII and γ (cPKCs), all of which contain two membrane-targeting modules, designated C1 and C2 (Parker and Murray-Rust, 2004). The C1 domain consists of tandem ~50-residue DAG/PMA-binding sequences termed C1A and C1B; each adopts a globular conformation and co-ordinates Zn^{2+} at a metal ion-binding site formed by three cysteines and one histidine. X-ray crystallographic studies identify C1 domains as hydrophobic switches (Parker and Parkinson, 2001). Each C1 domain consists of two β-sheets and a short C-terminal α-helix. PMA (or endogenously generated DAG) binds to a hydrophilic cleft situated in an otherwise hydrophobic surface at the tip of the C1 domain (between two 'unzipped' β-strands) (Mochly-Rosen and Kauvar, 2000). By capping this polar groove, PMA (or DAG) forms a contiguous hydrophobic surface that promotes PKC binding to membranes (Balogh et al., 1995). The second cPKC membrane targeting motif is the C2 domain, a motif that is found in many proteins that participate in membrane trafficking and signal transduction. C2 domains characteristically consist of eight β-strands connected by loops of variable lengths. C2 domains of cPKC isoforms bind anionic phospholipids in a calcium-dependent manner due to the presence of several invariant calcium-binding residues in three loops at one end of the structure (Asaoka et al., 1992).

Novel PKCs (nPKCs: δ, ε, η and θ) also have twin C1 domains and a C2 domain. However, C2 domain-like sequences of nPKCs lack calcium-co-ordinating acidic residue side chains. Hence nPKCs are maximally activated by DAG/PMA, without requiring

calcium (Parker and Murray-Rust, 2004); (Dekker and Parker, 1994); (Mochly-Rosen and Kauvar, 2000)).

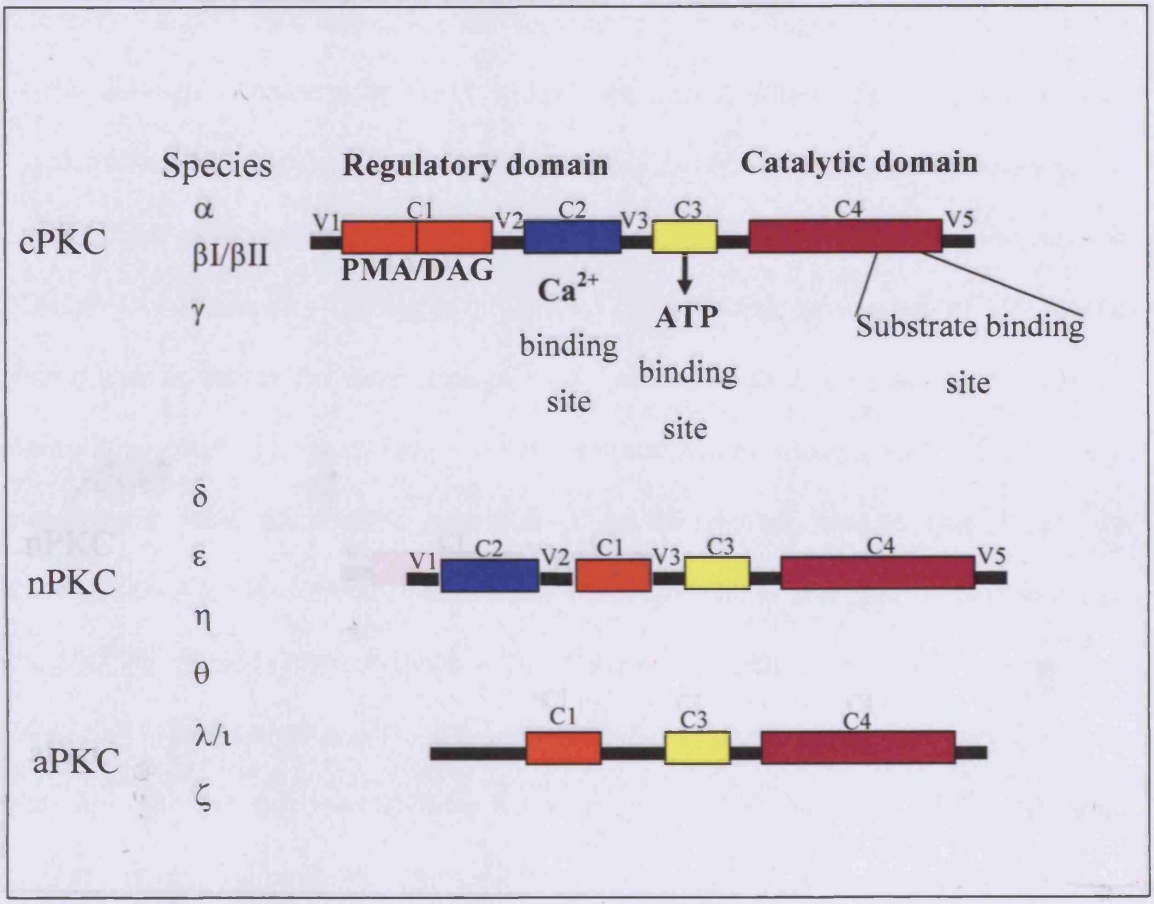

Figure 1.14 Protein Kinase C Isoforms. Scheme depicting the sequence homology between PKC isoforms and their subfamilies. (Diagram adapted from (Disatnik et al., 2002). c: classical; n: novel; a: atypical.

Atypical PKCs (aPKCs: ζ and ι/λ) are the third PKC isoform subfamily. aPKCs lack a calcium-sensitive C2 domain and contain only a single cysteine-rich zinc finger structure that does not bind DAG or PMA. As a result, aPKC isoforms are not allosterically regulated by calcium or DAG/PMA (Parker and Murray-Rust, 2004). Rather, aPKCs are activated by a distinct set of phospholipid cofactors, as well as by stimulus-induced

phosphorylation events (a topic that is beyond the scope of this thesis (see (Hirai and Chida, 2003); (Standaert et al., 1997).

Current models of PKC activation are based largely on studies of cPKC isoforms which, in the absence of calcium or DAG, interact only weakly/transiently with membranes. Agonists that promote phosphoinositide hydrolysis and Ins(1,4,5)P_3 generation lead to the mobilization of intracellular calcium, which binds to the C2 domain and increases its affinity for membranes (Blobe et al., 1996). This initial association of cPKC with membranes facilitates the interaction of the C1 domain with DAG (the other product of phosphoinositide hydrolysis) (Fig.1.14) (Parker and Murray-Rust, 2004). C1/C2 domain engagement with membranes promotes a conformational change that expels the autoinhibitory pseudosubstrate domain from the substrate-binding pocket and facilitates the PKC-mediated phosphorylation of membrane substrates (Parker and Murray-Rust, 2004). With the exception of the C2 domain-mediated effects of calcium, nPKC isoform activation for the most part follows a similar mechanism. For both cPKC and nPKC isoforms, translocation to membranes generally is considered an indication of activation (Mochly-Rosen and Kauvar, 2000).

1.9.3 Importance of PKC interaction with scaffolding proteins

Most cells co-express multiple PKC isoforms that display only limited substrate specificity *in vitro* and yet elicit distinct cellular responses in intact cells. PKC isoform specificity *in vivo* has been attributed to isoform-specific interactions with various anchoring proteins that localize individual PKC isoforms to specific membrane microdomains (in close proximity with their allosteric activators and/or substrates) (Mochly-Rosen and Kauvar, 2000). To date, a relatively large number of PKC-binding partners have been identified, including STICKs (substrates that interact with C-kinase),

various cytoskeletal proteins (such as actin or tubulin), true scaffolding proteins such as caveolin isoforms and AKAPs (A-kinase anchoring proteins), and RACKs (receptors for activated C-kinase) (Jaken and Parker, 2000). The RACK family of membrane-associated PKC-anchoring proteins has figured particularly prominently in the recent literature, since peptides designed to block or promote PKC isoform-selective interactions with their cognate RACKs are currently being evaluated for various cardiovascular indications in humans (Buensuceso et al., 2001). RACK proteins consist of a seven-WD40-motif repeat structure. The current model holds that cells express a unique RACK, with a distinct subcellular localization, for each PKC isoform (Stebbins and Mochly-Rosen, 2001). By selectively/saturably binding only the activated conformation of a PKC, each RACK protein recruits its cognate PKC isoform (in an active conformation) to a specific membrane compartment (Mackay and Mochly-Rosen, 2001) (Fig.1.15). To date, proteins with characteristics of RACKs for PKCβ (RACK1), PKCε (RACK2 or b-COP) and PKCδ (p32/gC1qBP) have been identified (Chen et al., 2001). However, it is important to note that RACK proteins can also fulfil functions unrelated to PKC. For example, RACK1 is reported to act as a scaffold to organize signalling complexes containing SFKs, heterotrimeric G-protein βγ subunits, STAT1 (signal transducer and activator of transcription 1) and the receptor protein tyrosine phosphatase PTPm (Chen et al., 2001). RACK2 (or β-COP, a coated-vesicle protein that participates in intracellular transport and vesicular release) was identified as a binding partner for certain RGS (regulators of G-protein signalling) proteins (Mackay and Mochly-Rosen, 2001).

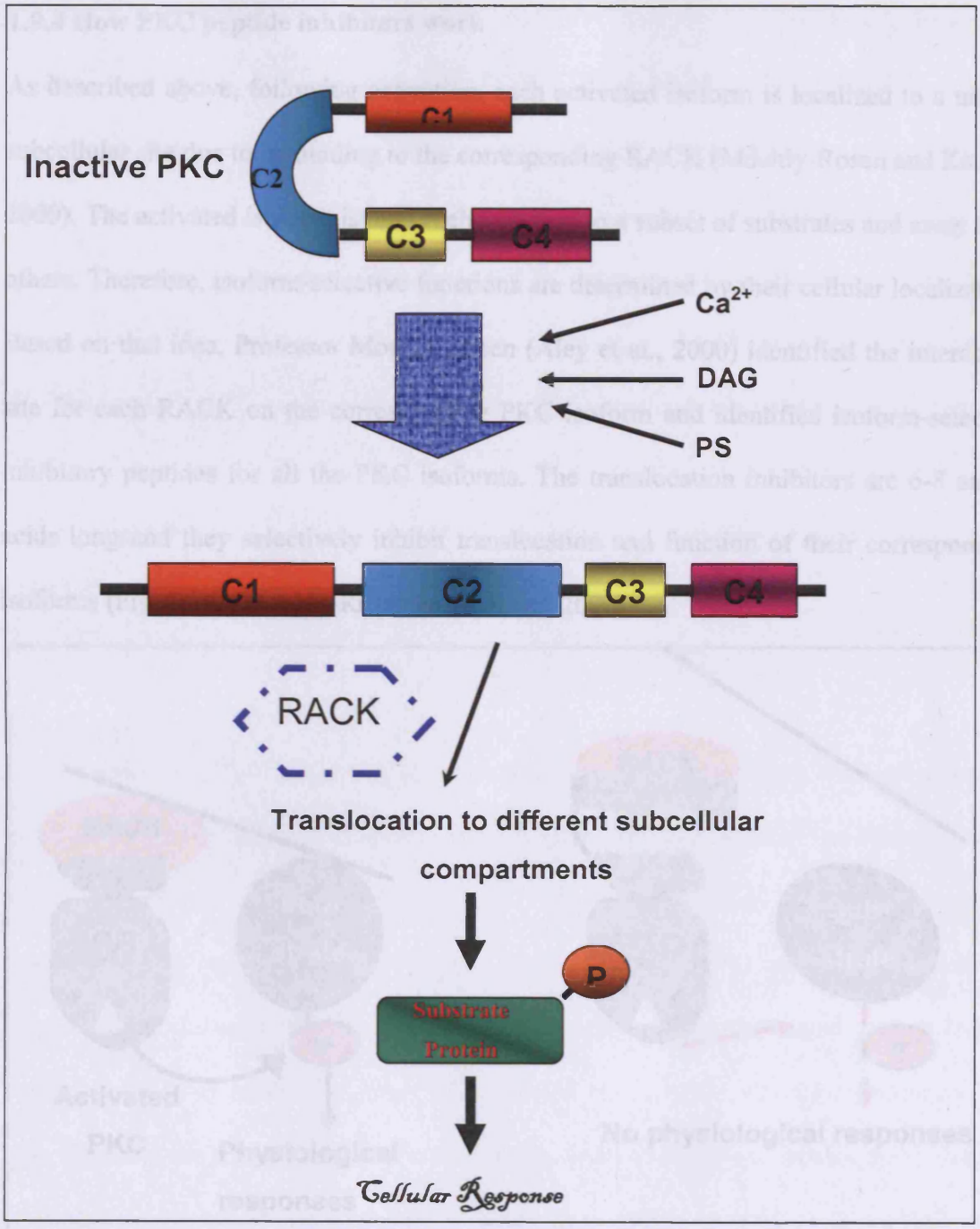

Figure 1.15 Signal transduction PKC cascades: the interaction of calcium-dependent PKCs with selective activators diacylglycerol (DAG), phosphatidylserine (PS) and calcium (Ca^{2+}) reduces the affinity of the pseudosubtrate domain for the catalytic site, thus opening the folded conformation and allowing the activation of the enzyme. The activated PKC can be directed to specific cellular compartments via anchoring proteins such as RACKs. (Diagram adapted from Amadio, 2006).

1.9.4 How PKC peptide inhibitors work

As described above, following activation, each activated isoform is localized to a unique subcellular site due to its binding to the corresponding RACK (Mochly-Rosen and Kauvar, 2000). The activated isoform is thus anchored next to a subset of substrates and away from others. Therefore, isoform-selective functions are determined by their cellular localization. Based on that idea, Professor Mochly Rosen (Aley et al., 2000) identified the interaction site for each RACK on the corresponding PKC isoform and identified isoform-selective inhibitory peptides for all the PKC isoforms. The translocation inhibitors are 6-8 amino acids long and they selectively inhibit translocation and function of their corresponding isoforms (Fig. 1.16) (Mochly-Rosen and Kauvar, 2000)

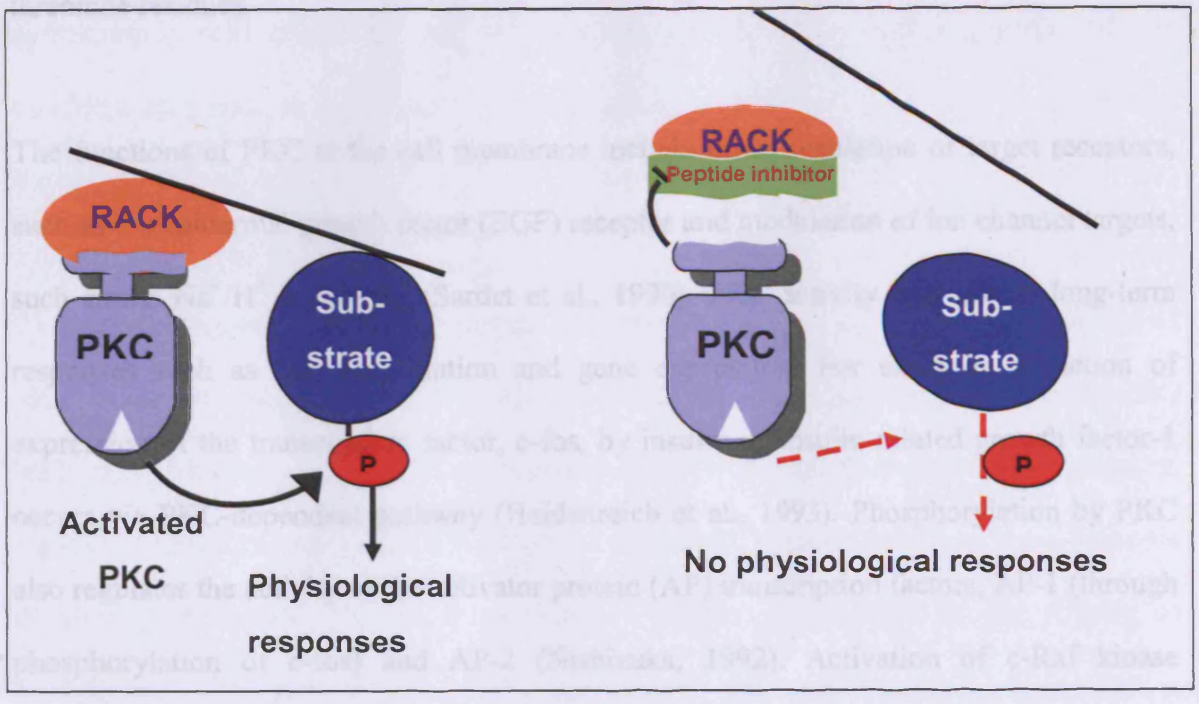

Figure 1.16 Translocation inhibitors. On the left, PKC (lilac) binding to its RACK (Orange) results in anchoring of the activated isoform near its substrate (blue). Phosphorylation (P) of that substrate leads to the physiological responses of that isoform. On the right, a peptide corresponding to the RACK-binding site on PKC (green) inhibits the translocation and function of its corresponding isoform. The translocation inhibitor,

derived from the RACK-binding site on the PKC, binds to the RACK and blocks the binding of the activated isoform to that RACK. Hence, the physiological response mediated by that PKC isoform is not observed. (Diagram adapted from (Mochly-Rosen and Kauvar, 2000)

1.9.5 Function of PKC

Roles for PKC have been proposed in regulation of a variety of cellular processes including function of membrane proteins, cell cycle control and transcription of various genes (reviewed by (Nishizuka, 1986); Mochly Rosen 2004). At the molecular level, the effect of PKC is mediated through phosphorylation of protein substrates on serine or threonine residues.

The functions of PKC at the cell membrane include down regulation of target receptors, such as the epidermal growth factor (EGF) receptor and modulation of ion channel targets, such as the Na^+/H^+ exchanger (Sardet et al., 1990). PKC activity also affects long-term responses such as cell proliferation and gene expression. For example, induction of expression of the transcription factor, c-fos, by insulin or insulin related growth factor-1 occurs via PKC-dependent pathway (Heidenreich et al., 1993). Phosphorylation by PKC also regulates the activity of the activator protein (AP) transcription factors, AP-1 (through phosphorylation of c-fos) and AP-2 (Nishizuka, 1992). Activation of c-Raf kinase following phosphorylation by PKC may also be involved in regulation of AP-1 (Hug and Sarre, 1993).

The major PKC substrate MARCKS may be of particular interest in relation to neural tube closure as the null mutant mouse displays exencephaly (Stumpo et al., 1995a). Moreover, knockout of the MARCKS family protein, MRP also causes NTD (Chen et al., 1996).

1.10 EXPERIMENTAL APPROACH

This thesis provides a study of both the development and prevention of NTDs in the mouse embryo. The events of posterior neural tube closure are studied using the whole embryo culture system, which allows a detailed analysis of neurulation as a dynamic, ongoing process.

In *Chapter 3,* the previously demonstrated prevention of spina bifida in the *curly tail* mutant by inositol (Greene & Copp) is investigated further by analysis of two different isomers of inositol, with comparison of their relative efficacy. Both *myo-* and D-*chiro*-inositol, were found to prevent spinal NTDs but with greater potency observed for D-*chiro*-inositol. The possibility that inositol therapy might cause fetal malformations was carefully analyzed, as a "pre-clinical" evaluation, prior to using inositol as an adjunct therapy to folic acid for prevention of NTDs in a human clinical trial.

The aim of *Chapter 4* was to investigate the possible involvement of specific isoforms of PKC in the mechanism of the *curly tail* defect and/or in the biochemical and molecular basis of the inositol protective effect. In this chapter I examined neurulation-stage embryos for PKC expression and applied chemical and peptide PKC inhibitors to *curly tail* embryos developing in culture. This study revealed an absolute dependence on the activity of PKCβ1 and γ for prevention of NTDs by inositol, and partial dependence on PKCζ, whereas other PKCs were found dispensable for the protective effect of inositol. Interestingly, inhibition of PKCs does not appear detrimental to normal development during neurulation.

The *curly tail* cell proliferation defect was investigated in *Chapter 5* in order to determine whether the protective effect of inositol may work via stimulating cell proliferation in *curly tail* embryos. Defective proliferation of hindgut cells is a key component of the pathogenic sequence leading to NTDs in *curly tail*. Hindgut cell proliferation was found to be stimulated specifically by inositol, as judged by PCNA and phospho-histone H3 immunohistochemistry, an effect that required activation of PKCβI. This final chapter, reveals the cellular basis by which specific PKC isoforms function during the prevention of mouse spinal NTDs by inositol.

CHAPTER 2

MATERIAL AND METHODS

All the reagents used in this thesis were obtained from Sigma unless otherwise specified. The components of individual solutions are described in the text except for certain general solutions, which are listed in section 2.8.

2.1 MICE

2.1.1 Generation of experimental litters

Experimental litters were generated by timed matings in which females were paired with males overnight and checked for copulation plugs the following morning. The day of finding a plug was designated embryonic day (E) 0.5.

2.1.2 *Curly tail* mice

The *curly tail* mutation is maintained in our laboratory as a closed, random-bred stock of homozygous (*ct/ct*) individuals (Van Straaten and Copp, 2001). The background of the stock, although not inbred, appears homogeneous with respect to genes that influence the incidence of NTDs. The background is probably a mixture of the GFF and CBA/Gr inbred strains that comprised the original breeding pair (Grüneberg, 1954). The mice are fed with R&M Diet (Quest Nutrition) and tap water. They are maintained in a ventilated room at 22°C on a light/dark cycle with the dark period from 1 a.m. to 9 a.m. About two-thirds of the *curly tail* mice are affected with spinal NTDs (10-15 % spina bifida, 40-50 % curly tails), whereas the rest are unaffected and have no morphological abnormality. To obtain experimental litters, affected males (tail flexion defect) were mated with females that were either unaffected (straight tail) or had tail flexion defects. Both affected and unaffected females were used as a source of experimental embryos, since the incidence of NTDs has been shown to be the same in both types of litter (Copp et al., 1982). In order to allow accurate estimation of gestational age, for certain experiments timed matings

were performed by pairing two females with one male, at approximately 8:30 a.m. and checking for copulation plugs 3-4 hours later.

2.1.3 CD1 mice

The CD1 stock was used as a non-mutant control in all experiments. It is maintained as a random bred colony with males obtained from Charles River U.K. Ltd. (Margate, U.K.).

2.2 EMBRYO CULTURE

2.2.1 Embryo dissection

Pregnant mice were killed by cervical dislocation at the appropriate day of gestation, 9 days 5 hours for *curly tail* mice. Conceptuses were explanted using watchmaker's forceps into pre-warmed (37°C) Dulbecco's Modified Eagles Medium (Gibco) containing 10% fetal calf serum (Advance Protein Products). Using fine watchmaker's forceps, embryos were dissected free from the decidua, trophoblast and Reichert's membrane leaving the yolk sac and ectoplacental cone intact (Fig. 2.1). Embryos were then either:

1) Cultured intact (Section 2.2.2)

2) Dissected immediately from the yolk sac and amnion and fixed in 4% PFA. The yolk sac in same studies was rinsed in PBS and frozen for PCR genotyping (Section 2.7.1).

3) Dissected and the caudal region dissociated to prepare primary cell cultures (Section 2.6.2)

2.2.2 Embryo culture

Groups of three embryos were cultured in 30 ml disposable plastic tubes (Nunc, Universal) containing 3 ml immediately-centrifuged heat-inactivated rat serum (the culture method was modified from (Cockroft, 1990). In general there was a delay of 2

hours between killing the female mouse and putting the embryos into culture. Cultures started at 9 days 6 hours (*curly tail*) or 9 days 14 hours (CD1) of gestation, were gassed for 1 minute with 20% O_2, 5% CO_2, 75% N_2 (all gases from Cryoservice Ltd.) and incubated at 38°C in a roller bottle incubator (Cockroft, 1990). After approximately 17 hours, the cultures were again gassed for 1 minute with 40% O_2, 5% CO_2, 55% N_2 and incubated for a further 7 hours.

2.2.3 Preparation of rat serum

Rat blood was collected from the abdominal aorta of rats anaesthetized with diethyl ether. The blood was collected in a 20 ml plastic syringe and immediately centrifuged for 5 minutes at 3,500 rpm to pellet the red cells. The fibrin clot that formed in the upper plasma layer was squeezed to release the serum. The blood was re-centrifuged for 5 minutes at 3,500 rpm for 5 minutes and then the clear supernatant serum was drawn off with a Pasteur pipette. The serum was centrifuged again for 5 minutes at 3,500 rpm to pellet any remaining red cells and then the supernatant was drawn off and divided into 5 ml aliquots. The serum was heat inactivated in a water bath at 56 °C for 30 minutes and then stored at -20 °C.

2.2.4 Analysis of embryo cultures

At the end of the culture period, embryos were first assessed for viability: any embryos that did not exhibit a vigorous yolk sac blood circulation (grade 1 or 2) and heart beat were eliminated from subsequent analysis (see Table 2.1). Extraembryonic membranes were then removed and embryos were scored for: (i) posterior neuropore length (the distance between the rostral end of the posterior neuropore and the tip of the tail bud), (ii)

crown-rump length (Figure 2.2.4.2) and (iii) somite number. Length measurements were made using an eyepiece graticule on a Zeiss SV6 stereomicroscope (Table 2.2).

Yolk sac circulation	category	Description
Very good	+++ (1)	Blood circulation vigorous and affecting whole yolk sac
Good	++ (2)	Blood circulation slow and /or in only part of the yolk sac
Bad/no circulation	+ (3)	No blood circulation visible

Table 2.1 Assessment of yolk sac circulation

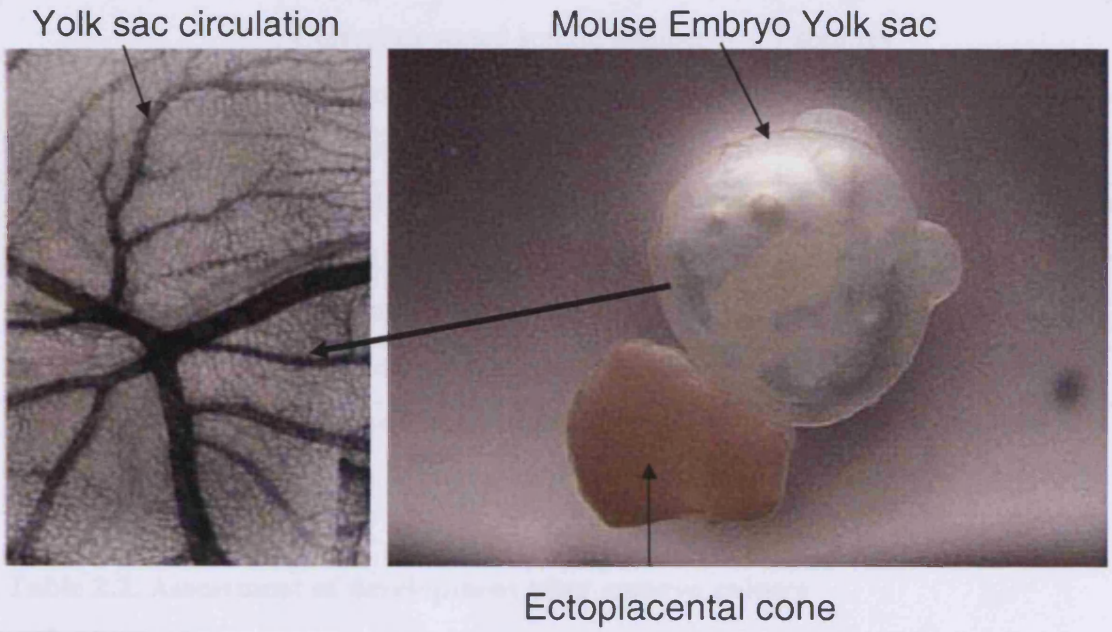

Figure 2.1 Yolk sac circulation. Yolk sac circulation was here used as a measurement of development. On the left panel the yolk sac vessels were injected with black ink with the sole purpose to enhance the view of the yolk sac circulation on the photograph.

Feature assessed	Expected appearance after culture (normal development)	Potential abnormalities
Yolk sac circulation	Category 1 or 2 (see Table 2.2.1)	No yolk sac circulation
Crown rump length	Normal when compared to littermates with all other developmental criteria normal	Significantly reduced size when compared to normal litter mates
Somites	Clearly defined somite boundaries Correct expected somite number = Time of culture/2 + original somite number	Irregular or unaligned somites Fewer somites than expected for time in culture
Neural tube	Closed head region and caudal neural tube or small PNP at E10.5 (approx. 30 somites)	Regions of open neural tube Wavy or distorted neural tube
Heart	Looped heart and beating	No heart beat
Axial rotation	Embryo fully turned by E9.5 (approx. 20 somites)	Turning incomplete

Table 2.2. Assessment of development after embryo culture

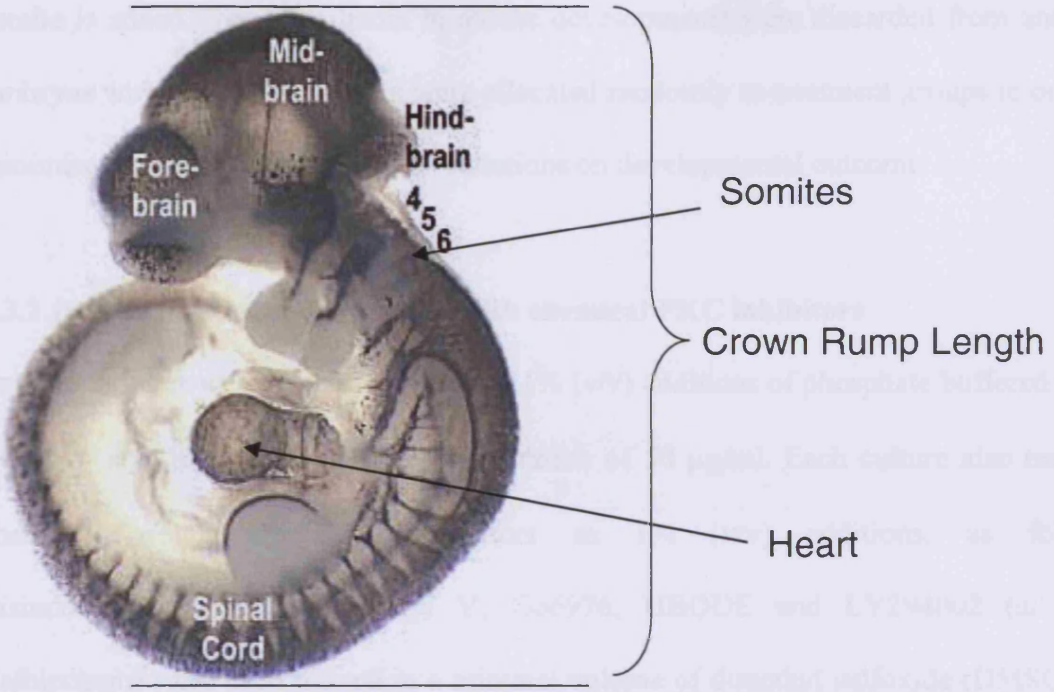

Figure 2.2.Assessment of development after embryo culture. Physiological parameters such as the developing circulatory system (Heart), crown rump length and somite numbers were used as a measurement of development after embryo culture.

2.3 *IN VITRO* TREATMENT OF EMBRYOS

2.3.1 Administration of inositol

Thirty minutes after the start of culture, *myo*-inositol (Sigma, UK) or D-*chiro*-inositol (InsMed, Virginia, USA) was added to the medium (62.5 µl of inositol stock per ml rat serum) to achieve a final concentration of 5, 10, 20 or 50 µg/ml inositol in the cultures. Control cultures received an equal volume of phosphate buffered saline (PBS). In order to avoid variations in outcome as a result of differences in developmental stage among the cultured embryos, cultures were initiated using only embryos with approximately 17-19 somites (assessed by dissection and somite counting of specimen embryos from each litter). Following 24 hours culture, embryos that fell outside the 29-31 somite range (one

somite is added every two hours in mouse development) were discarded from analysis. Embryos within individual litters were allocated randomly to treatment groups in order to minimise the effect of litter-to-litter variations on developmental outcome.

2.3.2 *In vitro* treatment of embryos with chemical PKC inhibitors

Embryo cultures were supplemented with 1% (v/v) additions of phosphate buffered saline (PBS) or *myo*-inositol, to a final concentration of 50 μg/ml. Each culture also received chemical or peptide PKC inhibitors as 1% (v/v) additions, as follows. Bisindolylmaleimide (Bis) I and V, Go6976, HBDDE and LY294002 (all from Calbiochem) were each diluted in a minimal volume of dimethyl sulfoxide (DMSO) and further diluted in PBS to give 1 mM stock solutions, which were added to embryo cultures to a final concentration of 10 μM. DMSO diluted in PBS was added to control cultures.

Inhibitor	Concentration used*	PKC isoform inhibited
Bis I	10 μM	α, βI, βII, γ, ε
Bis V	10 μM	Inactive form of BisI
Gö 6976	10 μM	α, βI, βII, γ
HBDDE	50 μM	α, γ
LY294002	1.4 μM	PI3K

Table 2.3 Concentration information for chemical PKC inhibitors

* Concentrations chosen to reflect IC_{50} values for each PKC isoform

2.3.3 *In vitro* treatment of embryos with peptide PKC inhibitors

Peptide PKC inhibitors coupled to carrier peptide were provided by Professor Daria Mochly-Rosen (Stanford University), and 100 μM solutions in PBS were added to embryo cultures to a final concentration of 1 μM.

Peptide inhibitor code number	**Region against which peptide was designed**	**Isoform inhibited**
pp109	(C2-4)	α
pp 97	(V5-3)	βI
pp 96	(V5-3)	βII
pp 110	(C2-4)	γ
pp 101	(δV1-1/carrier)	δ
pp 106	epsilon agonist	ε
pp 98	Pseudosubstrate inhibitor of zeta	ζ
pp 94	(carrier-carrier)	Control peptide

Table 2.4 Peptide translocation-inhibitors of PKC isoforms coupled to an *Antennapedia* carrier peptide, as used in this study

2.4 ADMINISTRATION OF INOSITOL *IN UTERO*

2.4.1 Methods for *in utero* administration

Inositol was administered to embryos *in utero* by two methods. Osmotic mini-pumps (capacity 100 µl, delivery rate 1 µl/hour, for 72 hr; Model 1003D, Alzet) were filled with solutions of 30, 75 or 150 mg/ml inositol (which delivered inositol at 29, 72 and 144 µg/g body weight/day respectively, for an average 25 g mouse). Control mice received mini-pumps containing PBS. Mini-pumps were incubated in sterile PBS at 37°C for 4 hours and then implanted subcutaneously on the back of pregnant mice at E8.5 (Fig. 2.3). General anaesthesia was induced by an intra-peritoneal injection of 0.01 ml/g body weight of a solution comprising 10% Hypnovel® (Midazolam 5 mg/ml) and 25% Hypnorm® (fentanyl citrate 0.315 mg/ml, fluanisone 10 mg/ml) in sterile distilled water. In a separate experiment, pregnant mice were gavaged with 0.5 ml inositol solution in PBS (400 µg inositol/g body weight) at 12 hourly intervals from E8.5 to E10.5 (six doses in total). Hence, the dose of inositol delivered orally was 800 µg/g body weight/day.

Figure 2.3 Osmotic mini pumps were subcutaneously implanted in the upper body of *ct* mice

2.4.2 Analysis of fetuses following inositol treatment *in utero*

Pregnant females were killed at E18.5, the uterus was opened and the total number of implantations, classified as viable fetuses or resorptions, was recorded. Fetuses were dissected from the uterus and inspected immediately for the presence of open lumbo-sacral spina bifida and tail flexion defects, which are the primary manifestations of the *curly tail* genetic defect (Van Straaten and Copp, 2001). A randomly selected sample of fetuses was fixed in Bouin's fluid and subjected to detailed internal pathological analysis (performed by Dr Sheila Tesh) by free-hand serial sectioning, using the method of Wilson (1965). A further sample of fetuses was fixed in 95% ethanol and processed for skeletal examination (performed by Dr John Tesh), by the method of Whittaker and Dix (1979). Fetuses and skeletal preparations were photographed using a Zeiss SV11 stereomicroscope.

2.5 IMMUNOHISTOCHEMISTRY

2.5.1 Preparation of routine histological sections

2.5.1.1 Dehydration and embedding

Embryos were fixed in 4% paraformadehyde (PFA) in PBS at 5 °C overnight. Before embedding in paraffin wax, the tissue was dehydrated by passage through a series of ethanol solutions of increasing concentration: 30%, 50%, 70% and 100%. Twenty-minute changes at each step were employed. Since alcohol is not miscible with molten paraffin, the alcohol in the tissue was removed by a 15 minute exposure to a mixture of equal parts of absolute ethanol and Histoclear (National Diagnostics) followed by two 15 minute changes in pure Histoclear. The tissue was transferred using a pipette to a glass-embedding dish containing molten paraffin wax (melting point 56 °C) in an embedding oven. After 30 minutes, the paraffin wax was poured out, and was replaced by fresh wax.

After another 30 minutes, when the tissue was thoroughly infiltrated with paraffin wax, the tissue was embedded as follows. While observing with a dissecting microscope, the dish containing the embryo was allowed to cool until the bottom layer of wax started to solidify. The tissue was properly orientated, in order to yield transverse sections when cut parallel to the bottom surface of the dish, using two pairs of heated blunt forceps. The paraffin wax was left at room temperature for several hours and then the dish was stored at -20 °C overnight. This enabled the paraffin block to be removed from the dish, after which it was then stored at 4 °C until required for sectioning.

2.5.1.2 Sectioning

The paraffin block was roughly trimmed using a razor blade and the base of the block was slightly melted and attached to a wooden block, which was clamped to the microtome chuck. Ribbons of sections were cut at a thickness of 6 μm using a *Leitz* microtome. The ribbons were cut into short lengths and transferred to TESPA-coated slides (TESPA, 3-aminopropyl-triethoxy-silane glass slides, Sigma). Water, at 40 °C, was pipetted onto the surface of the slides, the sections were placed on top of the water and then the slides were placed on a slide dryer at 37°C in order to allow the sections to float and spread. Excess water was then removed from the slides, which were left to dry overnight. Slides were stored at 4°C until used for staining.

2.5.2 Immunodetection of PKC isoforms

Sections were re-fixed in 4% paraformaldehyde in PBS for 5 minutes at room temperature and subsequently washed twice in PBS, 1% BSA, 0.25% Triton X-100 for 15 minutes. Antibodies were diluted prior to application as determined by prior titration studies. A range of dilutions for each antibody was tested initially, based on information

provided in data sheets from commercial suppliers, or from previous usage by other groups. The dilution providing optimal signal with minimal background was selected for all subsequent experiments. Typically 100 µl of primary antibody was prepared for each section. Antiserum was diluted in the same solution utilised for non-specific protein blocking (10% fetal calf serum in PBS containing 1% TWEEN 20 (PBS-T)). Primary antibodies were diluted as shown in Table 2.5, and applied immediately following blocking, without washing. The blocking solution was carefully poured from the slide onto a folded tissue; and replaced with antibody solution. In the case of negative control tissue sections, the blocking solution was not replaced. Primary antibodies were applied overnight at 4 °C. Next day, any excess antibody was rinsed from the sections by immersion in a Coplin jar containing PBS-T for 10 minutes with gently shaking. This was repeated 3 times to ensure all unbound antibody had been washed off, to minimise background staining. The selection of secondary antibody varied with the species from which the primary was obtained, and with the desired choice of detection method. The secondary antibodies were raised in goat and directed against either rabbit or mouse immunoglobulin, and conjugated to FITC. Secondary antibodies were diluted (1:40) in PBS, 10% FCS, 0.25% Triton X-100, and incubated for 1 hour at room temperature in a humid chamber. The humid chamber was covered with aluminium foil to prevent the fluorescence from becoming 'bleached' by exposure to light. Unbound secondary antibody was then rinsed from the sections by three 10 minute washes in PBS-T. Slides were dried and mounted in Citifluor (anti-photobleaching mounting medium for immunofluorescence, Citifluor Ltd.). Controls for immunohistochemistry were: 1) Omission of primary antibody (to test non-specific staining of secondary antibody); 2) Substitution of primary antibody by non-specific IgG; 3) Pre-absorption of primary antibody with the specific peptide against which antibody was raised. Peptide sources are

shown in Table 2.5. In addition, when fluorescence immunodetection was used, Hoechst nuclear dye was also added to the secondary antibody mixture. This resulted in all nuclei staining blue in colour under fluorescent illumination.

2.5.3 Immunochemical Reagents

PKC isotype hyphen-specific affinity purified rabbit IgG primary antibodies were obtained from Santa Cruz Biotechnology (Santa Cruz, CA) (See Table 2.3 for details). The secondary antibody was a FITC-conjugated goat anti-rabbit IgG (Jackson Immuno Research).

2.5.4 PCNA

The Proliferating Cellular Nuclear Antigen (PCNA) was detected using a mouse monoclonal IgG_{2a} antibody derived by fusion of spleen cells from a BALB/c mouse immunised with recombinant PCNA with Sp2/0-Ag 14 myeloma cells (Santa Cruz Biotechnology). It reacts against the PCNA p36 protein expressed at high levels in proliferating cells of human, murine, insect and yeast origin.

2.5.5 H3

Anti-phospho-Histone H3 (Upstate Biotechnology, Buckingham, UK) specifically recognises the phosphorylated 17 kDa histone H3 that is found only in mitotic cells. The antibody was raised in the rabbit, using amino acids 7-20 of the human H3 as immunogen.

2.5.6 Hoechst Dye

Staining of cell nuclei was performed using Hoechst 33258 at 1.2 mg/ml dilution in water. This stock was further diluted 1 in 500 prior to use.

Antigen detected	*Primary antibody code	Concentration used
PKC α	Sc208	1:200
PKC βI	Sc209	1:100
PKC βII	Sc210	1:100
PKC γ	Sc211	1:200
PKC ε	Sc214	1:200
PCNA	PC10	1:100
Phospho Histone H3	(Upstate Biotech, Buckingham, UK)	1:100
Hoechst	33258	1:1000

Table 2.5 Immunochemical reagents

*Unless stated, all primary antibodies were obtained from Santa Cruz Biotechnology (Santa Cruz, CA)

2.6 MOUSE CELL CULTURE

2.6.1 Generation of *curly tail* primary cell lines

Embryos at the 27 somite stage were removed from the uterus and placed in PBS in a plastic dish. The posterior neuropore region was excised from around the level of somite

20 and cut into small pieces, minced, and transferred into a 15 ml centrifuge tube containing 10 ml dissociation buffer (GIBCO™ Cell Dissociation Buffer, enzyme free, Hanks'-based) (roughly enough for 15 tails) and incubated for 20 minutes at room temperature with gentle shaking. The large tissue clumps were dissociated by repeated pipetting using a 10 ml serological pipette and by passage through a Nitex filter. The supernatant was transferred into a fresh centrifuge tube and spun for 5 minutes at 1,000 rpm at room temperature. The supernatant was discarded and the cells were resuspended in 5 ml growth medium. Cells were counted using a haemocytometer and the final volume was adjusted to 2x 10^6 cells/ml. The cells were seeded directly on plastic dishes and cultured at 37°C in 5% CO_2 for 5 passages.

2.6.2 Culture methods

Cells were cultured on glass cover slips coated for 30 minutes with poly-L-lysine and 30 minutes with fibronectin (to allow attachment of cells to the glass substrate). The cover slips were transferred to a 24-well culture dish, seeded with approximately 1x10^4 cells and cultured for 5 hours in Dulbecco's Modified Eagle's Medium (DMEM) containing 10% v/v heat inactivated fetal bovine serum and 1% v/v penicillin-streptomycin solution (10,000 units penicillin and 10 mg streptomycin per ml).

2.6.2.1 Culture splitting

All solutions were pre-warmed to 37°C. The cells were briefly washed with PBS (without $CaCl_2$ and $MgCl_2$) and then detached by adding a few drops of trypsin-EDTA solution (0.05% porcine trypsin and 0.02% EDTA.4Na) and incubating at room temperature as necessary. Adding 2 ml of growth medium inactivated the trypsin. The cells were centrifuged for 5 minutes at 1,000 rpm, at room temperature, and the supernatant was

discarded. The cells were then resuspended in the desired amount of fresh growth medium and seeded in plastic dishes.

2.6.2.2 Immortalised cells used in control cultures

3T3 mouse cell line used was obtained from the Dunn School Cell Bank (Department of Pathology, University of Oxford). They were grown in DMEM in a humidified 37°C incubator, with 5% CO_2.

2.6.3 Treatment of cells with TPA and PKC peptide inhibitors

In all experiments, cells were serum starved by culture in DMEM containing 1% fetal calf serum for 18 hours. Some samples were then treated with 100 mM TPA for 10 minutes and then for 20 minutes with 100 mM PKC isoform-specific peptide-bound inhibitors.

2.6.4 Immunocytochemical analysis

Cells grown on cover slips were stained with anti-PKC antibodies (Table 2.2.5). All solutions were applied in 100 µl volumes, which were sufficient to entirely coat the coverslip. Coverslips were placed on top of small pedestals (lids from screw-capped eppendorf tubes). This allowed the coverslips to be manipulated easily. Cells were fixed in 4% PFA solution for 8 minutes. After fixation, coverslips were lifted using forceps and excess solution was removed by touching the side of the coverslip on some folded tissue paper. The coverslip was then washed by dipping successively in three 30 ml tubes containing PBS. Each dip lasted around 4 seconds. The primary antibody (diluted 1:200 in 10% fetal calf serum in PBS) was then applied and left for 1 hour at room temperature. Following this, the primary antibody was blotted off, and the coverslip was washed three times in PBS as before. The secondary antibody (diluted 1:40 in 10% fetal calf serum in

PBS) was then applied and left for 1 hour at room temperature. The coverslip was then washed a further 3 times in PBS, followed by a brief wash in distilled water. Finally, Citifluor was used to mount the coverslips on clean glass slides. Translocation of specific PKC isoforms was assessed using PKC isoform-specific antibodies (Santa Cruz Biotechnology) in immunofluorescence studies and the percentage of cells showing translocation was determined by counting labeled cells, in a blinded fashion. Each isoform experiment was performed in triplicate. The slides were visualised using a Zeiss fluorescence microscope fitted with a digital camera, and images were recorded using Northern Eclipse computer software and scanned directly into OpenLab.

2.6.5 Labelling indices

The labelling indices (total number of labelled cells divided by the total cell number, multiplied by hundred) were obtained from alternate transverse sections through the rostral end of the PNP stained for PCNA or histone H3. Experiments were carried out in triplicate by an observer blinded for treatment type.

CHAPTER 3

PREVENTION OF FOLATE-RESISTANT NTDs

3.1 INTRODUCTION

Folic acid supplementation during early pregnancy can prevent a proportion of NTDs, as indicated by several clinical trials and other observational studies (Abramsky et al., 1999);(Wald et al., 2001); (Antony and Hansen, 2000). Nevertheless, NTDs may occur even following maternal folic acid supplementation. For example, in the randomized controlled trial conducted by the Medical Research Council Vitamin Research group, UK (Wald et al., 1991), the recurrence rate of NTDs was reduced by approximately 72%. Thus, NTDs still occurred despite maternal supplementation with 4 mg folic acid per day. Interestingly, the recurrence rate in folic acid-treated pregnancies in this MRC trial (1 %) was ten times higher than the usual occurrence rate in the population (0.1 %, or 1 per 1000). Furthermore, the recent introduction of folic acid fortification of bread flour in the USA has resulted in only a 26% decline in the prevalence of NTDs (Honein et al., 2001). While these findings may indicate the need for increased levels of folic acid supplementation, they are also consistent with a proportion of NTDs exhibiting resistance to prevention by exogenous folic acid.

Mouse genetic models of NTDs provide further evidence for the existence of folate-resistant NTDs types Wald, 2001;(Carmichael et al., 2003). Mutant strains including *Cart1*, *crooked tail* and *splotch* exhibit NTD that can be prevented by folic acid administered during early pregnancy (Zhao et al., 1996), whereas folic acid is ineffective in preventing NTDs in the mutant strains *curly tail*, *Axial defects* and *ephrin-A5* (Glanville and Cook, 1992;Tran et al., 2002). Of these 'folate-resistant' strains, *curly tail* provides a particularly useful model for human NTDs both in terms of its etiology and pathogenesis (van Straaten and Copp, 2001).

3.1.1 Inositol as a preventive therapy for folic acid-resistant NTDs in mice

Previous work has shown that a proportion of the folate-resistant NTDs in *curly tail* mice can be prevented by treating pregnant females, or embryos *in vitro*, with *myo*-inositol (Greene and Copp, 1997a). This work was prompted by the earlier finding that deficiency of *myo*-inositol in the culture medium of rat and mouse embryos causes a high incidence of cranial NTDs (Akashi et al., 1991). Moreover, NTDs that develop in rat embryos cultured under hyperglycemic or diabetic conditions are associated with depletion of inositol (Kubow et al., 1993) and can be ameliorated by supplementation with *myo*-inositol (Baker et al., 1990). These findings raised the possibility that inositol may offer a potential alternative therapeutic option for prevention of folate-resistant NTD. Although the effect of inositol on human NTD recurrence, in cases of suspected folate-resistance, has not yet been rigorously evaluated, a recent case study has highlighted a possible beneficial effect. *Myo*-inositol therapy was associated with a normal third pregnancy outcome, in a family with two previous consecutive NTD pregnancies despite full folic acid supplementation (Cavalli and Copp, 2002).

The purpose of this chapter is to evaluate in detail the potential of inositol as a primary therapeutic agent in preventing mouse NTDs using the *curly tail* mouse as a model. The aims were to test different routes of administration and to investigate any possible harmful effects of inositol on the developing embryo. In addition, I compared the efficacy of two enantiomers of inositol, *myo*-inositol and *chiro-inositol.*

3.2 RESULTS

Embryos were exposed to inositol either by direct treatment in whole embryo culture, or by dosing pregnant females via subcutaneous and oral routes.

3.2.1 D-*chiro*-inositol has greater potency than *myo*-inositol in normalising neural tube closure

Curly tail embryos were cultured in the presence of inositol for 24 hours from E9.5, the period during which the neural tube is closing in the low spinal region of the mouse embryo. In normal embryos, primary neurulation is completed by closure of the posterior neuropore at E10.5 (at the 29-30 somite stage) (Copp et al., 1999), whereas in *curly tail* embryos neuropore closure is delayed, or fails to be completed, leading to the development of tail flexion defects and spina bifida, respectively(Copp et al., 1988c). Posterior neuropore length at E10-10.5 (Fig. 3.1) is positively correlated with the likelihood that an embryo will progress to develop a spinal NTD (Copp et al., 1988b).

Both *myo*- and D-*chiro*-inositol showed a dose-dependent normalisation of posterior neuropore length in embryo culture, as judged by the statistically significant reduction in neuropore length observed in embryos treated with higher inositol doses (Table 3.1). Strikingly, however, D-*chiro*-inositol reduced neuropore length significantly at both 20 and 50 μg/ml whereas a comparable effect was seen only with 50 μg/ml *myo*-inositol. In fact, embryos exposed to 20 μg/ml *myo*-inositol (and 5-10 μg/ml D-*chiro*-inositol) exhibited neuropore lengths that were not significantly different from PBS-treated controls (Table 3.1). Therefore, it appears that D-*chiro*-inositol has increased potency compared with *myo*-inositol in normalizing neurulation, an effect that is detectable *in vitro*, outside the maternal environment.

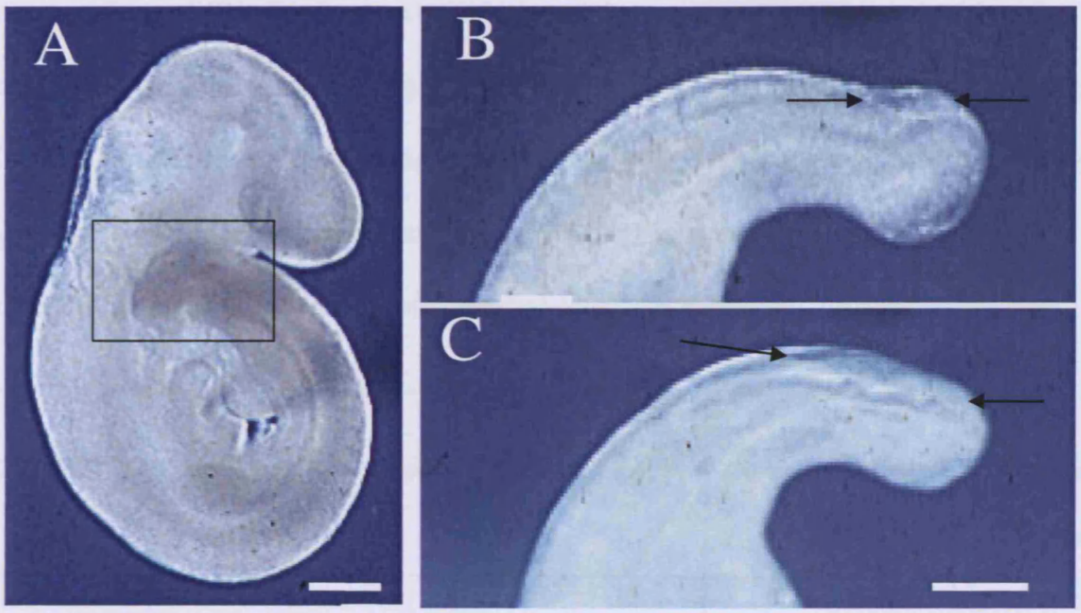

Figure 3.1 PNP closure in *curly tail* mouse embryo. A. *Curly tail* embryo after 24 hours culture from E8.5 to E9.5. Box indicates the posterior neuropore region. **B, C.** Higher magnification views of the caudal end of cultured *curly tail* embryos showing posterior neuropores of varying length. The region of open neural folds occupies the dorsal part of the caudal region, between the arrows in (B) and (C). Embryos with a large neuropore (C) progress to develop spina bifida and/or a tail flexion defect, whereas embryos with a small neuropore (B) complete neural tube closure normally. Scale bars: **A** = 0.5 mm; **B**,**C** = 0.2 mm.

3.2.2 Neither *myo*- nor D-*chiro*-inositol affects the rate of embryonic growth in embryo culture

In the experimental design, embryos in the different treatment groups were matched for somite number, both before and following the culture period (see section 2.3.1). The aim was to avoid differences in developmental outcome (PNP length) that might arise from comparing embryos of different stages. As expected, therefore, mean somite number following culture was closely similar in all the treatment groups (Table 3.1). There was

no significant difference in crown-rump length between embryos treated with either *myo*- or D-*chiro*-inositol and PBS-treated controls (Table 3.1), suggesting that the effect of inositol is specific to the closing posterior neuropore, and not mediated via embryonic growth acceleration or retardation. In particular, the greater potency of D-*chiro*-inositol does not appear to result from a differential effect on embryonic growth.

TREATMENT	Conc. (μg/ml)	No. embryos	Somite number [1]	Crown-rump length (mm)	PNP length [1] (mm)
PBS	0	16	30.3 ± 0.15	3.56 ± 0.10	0.59 ± 0.13
myo	20	16	30.5 ± 0.12	3.50 ± 0.12	0.62 ± 0.06
	50	16	30.5 ± 0.14	3.57 ± 0.07	0.06 ± 0.03*
D-*chiro*	5	15	30.6 ± 0.13	3.50 ± 0.10	0.62 ± 0.11
	10	15	30.5 ± 0.13	3.39 ± 0.10	0.55 ± 0.11
	20	18	30.6 ± 0.16	3.55 ± 0.10	0.09 ± 0.11*
	50	15	30.3 ± 0.16	3.49 ± 0.08	0.07 ± 0.03*

Table 3.1. Comparison of growth and developmental parameters in *curly tail* embryos cultured in the presence of *myo*- and D-*chiro*-inositol

[1] Values presented are: mean ± SEM. Statistical analysis: somite number and crown-rump length do not differ significantly between treatment groups (Analysis of variance on ranks: $p = 0.72$ and 0.54 respectively), whereas posterior neuropore (PNP) length varies significantly between treatment groups ($p < 0.0001$).

Ordinal regression analysis shows that PNP length is significantly reduced (marked with asterisk) in embryos treated with *myo*-inositol (50 μg/ml) and D-*chiro*-inositol (20 and 50 μg/ml) compared with those exposed to PBS alone ($p < 0.05$), whereas PNP length in other inositol-treated groups does not differ significantly from the PBS control group.

3.2.3 D-*chiro*-inositol reduces the frequency of spinal neural tube defects to a greater extent that *myo*-inositol following *in utero* administration

I next evaluated the possibility of using subcutaneous and oral routes of inositol administration to prevent NTDs in the fetuses of pregnant *curly tail* females. In order to administer inositol at a constant rate over a period of 72 hours of pregnancy, to encompass the stages of neural tube closure, osmotic mini-pumps were surgically implanted. These delivered inositol by subcutaneous infusion at a rate of 1 μl/hour. Using this approach a dose-dependent effect of both *myo*- and D-*chiro*-inositol was observed.

At a dose of 29 μg/g body weight/day, neither *myo*- nor D-*chiro*-inositol produced a significant reduction in the frequency of fetuses developing spina bifida nor was the distribution of fetuses between the three phenotype categories (spina bifida, tail defect and normal) altered significantly (Table 3.2.). In contrast, dosing levels of 72 and 144 μg/g body weight/day both produced a significant reduction in the frequency of spina bifida compared with PBS-treated pregnancies and caused a significant shift in the distribution of fetuses towards the mild end of the phenotype spectrum (Table 3.2.). D-*chiro*-inositol appeared most effective at both 72 and 144 μg/g body weight/day, causing a 73-83% decrease in spina bifida frequency relative to PBS controls. *Myo*-inositol produced a consistent 54-56% reduction in spina bifida frequency, but this did not reach statistical significance (see below).

Statistical comparisons between the PBS, D-*chiro*- and *myo*-inositol treatment groups, separately at each dose level (3 x 2 chi-square tests), reveals significant variation in frequency of spina bifida at 72 and 144 μg/g body weight/day (p = 0.014 and 0.006 respectively) but not at 29 μg/g body weight/day (p = 0.494 respectively). Pairwise

testing reveals a significantly lower frequency of spina bifida among fetuses treated with D-*chiro*-inositol compared with PBS at 72,144 μg/g body weight/day (p = 0.006, and 0.013 respectively) but not at 29 μg/g body weight/day (p = 0.291). Frequency of spina bifida among fetuses treated with *myo*-inositol is consistently intermediate between the values for D-*chiro*-inositol and PBS, and does not differ from either treatment group at any dose level ($p > 0.05$). Hence, D-*chiro*-inositol exerts a significantly more potent preventive effect against spina bifida than *myo*-inositol when delivered sub-cutaneously.

As an alternative route of treatment, inositol was administered to pregnant females by gavage, using a twice-daily dosing regime, from E8.5 to E10.5 that delivered 800 μg/g body weight/day (equivalent to the intraperitoneal dose used in the previous study (Greene and Copp, 1997a). As with sub-cutaneous administration, there was a marked reduction in the frequency of spina bifida among the offspring of mice treated with either *myo*- or D-*chiro*-inositol. There was also observed a significant shift in the distribution of fetuses between the three phenotype categories (Table 3.2). D-*chiro*-inositol was most effective, causing a statistically significant 86% reduction in the frequency of spina bifida (p = 0.032), while the 53% reduction observed for *myo*-inositol was not statistically significant (p = 0.059).

I investigated whether clustering of fetuses of particular phenotypes within litters may have affected the outcome of the comparison between *myo*-inositol, D-*chiro*-inositol and PBS. An ordinal multilevel regression model (which took into account the potential non-independence of fetuses within litters) was fitted to the data. This confirmed that fetuses treated subcutaneously with D-*chiro*-inositol are significantly more likely to be normal than those treated with PBS ($p < 0.0005$). The comparison between *myo*-inositol and PBS

also reached statistical significance in this analysis ($p < 0.002$). In the oral dosing study, fetuses were more likely to be normal when treated with D-*chiro*-inositol than PBS ($p = 0.0097$), whereas the values for *myo*-inositol and PBS did not differ significantly ($p = 0.13$).

Importantly, the multilevel analysis indicated that the difference between treatment groups is unaffected when possible litter effects are taken into account. Hence, it appears that the reduction in NTD frequency following treatment with *myo*- and D-*chiro*-inositol is unlikely to arise from litter-to-litter variations.

3.2.4 No evidence of an adverse effect of inositol on pregnancy success or fetal outcome

One possible explanation for a decrease in spina bifida frequency following maternal inositol administration could be an increase in loss of affected fetuses during pregnancy. Therefore, resorption rate and litter size were examined in pregnancies receiving either subcutaneous mini-pumps or twice-daily gavage. No significant differences were found between pregnancies treated with inositol and those receiving PBS alone (Table 3.3). This strongly suggests that there is no adverse effect of inositol dosing on the overall success of mouse pregnancy. A noticeable reduction was found, however, in the litter size of mice subjected to oral inositol administration, where litters contained fewer fetuses than those receiving inositol subcutaneously (Table 3.3). As litter size did not vary between treatments this difference is thought to reflect the increased maternal stress caused by daily gavage (without anaesthesia) compared to a single surgical operation, under general anaesthesia, to insert a subcutaneous miniosmotic pump. To identify any adverse effects of inositol treatment on fetal outcome, an extensive pathological analysis of treated

Table 3.2 Frequency of neural tube and tail defects among *curly tail* fetuses treated *in utero* with *myo-* and D-*chiro*-inositol

[1] Inositol dose is expressed as: μg inositol/g body weight/day.

[2] Phenotype frequencies are expressed as number of fetuses with % of total for treatment group.

[3] Statistical analysis: distribution of embryos among the three phenotype categories varies significantly with treatment group at 72, 144 and 800 μg inositol/g body weight/day (Chi-square tests, p = 0.0005, 0.0051 and 0.026 respectively) but not at 29 μg inositol/g body weight/day (p = 0.34).

Table 3.2

			Phenotype of fetuses [2,3]		
Route of administration	Treatment	Inositol dose [1]	Spina bifida ± *curly tail*	*Curly tail*	Normal
Sub-cutaneous	PBS	-	6 (24.0)	14 (56.0)	5 (20.0)
	myo	29	6 (20.7)	12 (41.4)	11 (37.9)
	D-*chiro*	29	3 (11.5)	17 (65.4)	6 (23.1)
	PBS	-	14 (13.5)	63 (60.6)	27 (25.9)
	myo	72	4 (6.0)	37 (55.2)	26 (38.8)
	D-*chiro*	72	2 (2.3)	39 (45.4)	45 (52.3)
	PBS	-	19 (18.6)	49 (48.0)	34 (33.3)
	myo	144	8 (8.5)	52 (55.3)	34 (36.2)
	D-*chiro*	144	5 (5.0)	46 (46.5)	48 (48.5)
Oral	PBS	-	8 (18.2)	21 (47.7)	15 (34.1)
	myo	800	3 (8.6)	15 (42.9)	17 (48.6)
	D-*chiro*	800	1 (2.6)	12 (30.8)	26 (66.7)

fetuses was performed, using both free-hand serial sectioning and skeletal preparation (carried out by our collaborator, Ms Sheila Tesh). This analysis confirmed the occurrence of spina bifida and tail defects in a proportion of fetuses (Figure 3.3), as also scored by external fetal inspection.

Additionally, exencephaly, a failure of cranial neural tube closure, was observed in a small proportion of fetuses (Tables 3.4 and 3.5). Exencephaly is a recognised defect in *curly tail* homozygotes (Casey et al., 1997). In the present study, no overall increase or decrease in this defect in inositol-treated fetuses was observed compared with PBS controls, although the low frequency of affected fetuses may have obscured any treatment effect.

Internal and skeletal examination of control and inositol treated fetuses revealed almost no major structural defects, apart from NTDs (Tables 3.4 and 3.5). For instance, no major malformations of the heart, lungs, kidney, gut or limbs were identified. Among the morphological changes observed in the analysis, most were minor (e.g. small additional liver lobe) and the great majority occurred as frequently in PBS controls as in fetuses treated with *myo-* or D-*chiro*-inositol (Tables 3.4 and 3.5). D-*chiro*-inositol (144 μg/g body weight/day) was associated with a somewhat elevated frequency of enlargement of the renal pelvis/ureter (Table 3.4), and occurrence of anomalous cervical vertebrae and rudimentary ribs on the 7th cervical vertebra (Table 3.5). However these associations were not statistically significant.

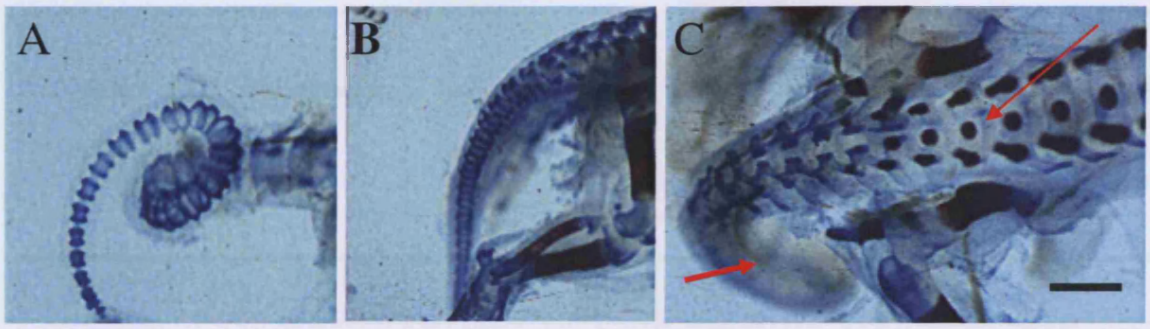

Figure 3.2 Skeletal preparations of E18.5 *curly tail* fetuses.. The tail flexion defect (**A**) comprises 360° curl of the tail, compared with the normal fetus which exhibits a straight tail (B).Compared with a normal fetus in (B), the fetus with spina bifida (C) exhibits vertebral pedicles widely spaced apart and absent neural arches in the low lumbar/sacral region (long arrow in C). The tail (short arrow in C) is enclosed in a skin sac and appears reduced in length owing to deformation and fusion of caudal vertebrae. Scale bars = 2 mm.

Interestingly, anomalous cervical vertebrae appear to be especially associated with exencephaly: both defects were found in a fetus treated with *myo*-inositol (144 µg/g body weight/day) and in a second fetus treated with D-*chiro*-inositol (144 µg/kg body weight/day), which also exhibited thoracic rib anomalies. A further two fetuses from the same D-*chiro*-inositol treated litter had cervical vertebral anomalies and a third had thoracic vertebral and rib anomalies, while a single fetus from a different litter had cervical vertebral anomalies. It seems likely that these cervical anomalies may form part of the spectrum of vertebral column defects present in the *curly tail* mouse, often in association with exencephaly.

Route of administration	Treatment	Inositol dose [1]	No. litters	No. viable fetuses	No. uterine resorptions[2]	Mean litter size ± SEM [3]
Sub-cutaneous	PBS	-	4	25	3 (10.7)	6.25 ± 1.03
	myo	29	4	29	2 (6.5)	7.25 ± 1.80
	D-CHIRO	29	3	26	1 (3.7)	8.67 ± 1.76
	PBS	-	12	104	10 (8.8)	8.67 ± 0.50
	myo	72	8	67	7 (9.5)	8.38 ± 0.78
	D-CHIRO	72	12	86	8 (8.5)	7.17 ± 0.89
	PBS	-	12	102	9 (8.1)	8.50 ± 0.79
	myo	144	12	94	9 (8.7)	7.83 ± 0.44
	D-CHIRO	144	14	99	6 (5.7)	7.07 ± 0.75
Oral	PBS	-	7	44	5 (10.2)	6.29 ± 0.36
	myo	800	6	35	3 (7.9)	5.83 ± 0.48
	D-CHIRO	800	6	39	3 (7.1)	6.50 ± 1.09

Table 3.3 Survival of embryos and fetuses among *curly tail* litters treated *in utero* with *myo-* and D-*chiro*-inositol

[1] Inositol dose is expressed as: μg inositol/g body weight/day.

[2] Values in parentheses indicate resorptions as a % of total number of implantations (i.e. viable fetuses + resorptions). Logistic regression analysis: the proportion of resorptions does not differ significantly between *myo*-inositol and PBS litters ($p = 0.87$), between D-*chiro*-inositol and PBS litters ($p = 0.33$), or between inositol dose levels ($p = 0.88$).

[3] Litter size (viable fetuses per litter) does not vary significantly with treatment group or inositol dose level (two-way analysis of variance: treatments, $p = 0.987$; inositol dose level, $p = 0.054$).

Litters treated with oral inositol contain an average of 1.6 (95% confidence intervals: 0.4, 2.8) fewer animals than litters treated with sub-cutaneous inositol.

Table 3.4 Internal pathological analysis, by freehand serial sectioning, of *curly tail* fetuses treated *in utero* with *myo-* and *D-chiro*-inositol

[1] A single fetus may have more than one morphological finding.

[2] Values are number of fetuses with defect (% of total for treatment group is indicated in parentheses).

[3] Proportion of fetuses with renal pelvis/ureter defect does not differ significantly between fetuses treated with D-*chiro*-inositol (144 μg/g body weight/day) and PBS controls (Fisher's exact test; $p = 0.231$).

[4] Calculation of % based on number of male fetuses.

Table 3.4

			myo		*D-chiro*	
Inositol dose (μg/g body weight/day)	72	144	72	144	72	144
No. fetuses examined [1]	27	17	11	21	24	19
No. males : females	13 : 14	6 : 11	5 : 6	9 : 12	15 : 9	7 : 12
Head:						
Exencephaly ± open eye [2]	1 (3.7)	2 (11.8)	-	2 (9.5)	-	1 (5.3)
Hydrocephaly	1 (3.7)	-	-	1 (4.8)	-	1 (5.3)
Haemorrhage in/around brain	-	2 (11.8)	-	2 (9.5)	-	1 (5.3)
Microphthalmia	-	1 (5.9)	-	-	-	-
Macrophthalmia	1 (3.7)	-	-	-	-	-
Blood in nasopharynx	-	2 (11.8)	-	-	-	1 (5.3)
Thorax and abdomen:						
Bleeding in thorax/abdomen	6 (22.2)	4 (23.6)	2 (18.2)	-	2 (8.4)	1 (5.3)
Thyroid lobe reduction	1 (3.7)	-	-	1 (4.8)	-	-
Carotid artery displaced laterally	-	-	-	-	-	1 (5.3)
Intrahepatic bleeding	-	1 (5.9)	1 (9.1)	1 (4.8)	-	-
Small additional liver lobe	9 (33.3)	4 (23.5)	6 (54.5)	4 (19.0)	6 (25.0)	4 (21.1)
Fissure in liver lobe	-	2 (11.8)	1 (9.1)	-	-	1 (5.3)
Umbilical hernia	1 (3.7)	-	-	-	-	-
Kidney elongated	-	-	-	-	1 (4.2)	-
Renal papilla absent bilaterally	-	1 (5.9)	-	-	-	-
Renal pelvis/ureter enlarged [3]	1 (3.7)	-	-	-	1 (4.2)	3 (15.8)
Testis displaced cranially [4]	1 (7.7)	-	-	-	1 (6.7)	-
Anal opening reduced in size	2 (7.4)	-	-	-	-	-
Subcutaneous oedema	1 (3.7)	-	-	-	-	-

Table 3.5 Skeletal analysis of *curly tail* fetuses treated *in utero* with *myo-* and *D-chiro*-inositol

[1] A single fetus may have more than one morphological finding.

[2]. Values are number of fetuses with defect (% of total for treatment group).

[3] Three fetuses were from the same litter, one of which exhibited exencephaly. The proportion of fetuses with anomalous cervical vertebrae does not differ significantly between fetuses treated with D-*chiro*-inositol (144 μg/g body weight/day) and PBS controls (Fisher exact test; $p = 0.11$).

[4] Proportion of fetuses with rudimentary ribs on 7th cervical vertebra does not differ significantly between fetuses treated with D-*chiro*-inositol (144 μg/g body weight/day) and PBS controls (Fisher exact test; $p = 0.14$).

[5] Both affected fetuses are from the same litter, one also exhibited with exencephaly and cervical vertebral anomalies.

A dash (–) indicates that no fetuses exhibited that finding.

Table 3.5

	PBS control		*myo*		*D-chiro*	
Inositol dose (μg/g body weight/day)	72	144	72	144	72	144
No. fetuses examined [1]	29	18	16	18	22	21
Exencephaly	-	-	-	2 (11.1)	-	2 (9.5)
Bony plaque in frontonasal suture	1 (3.4)	-	1 (6.3)	-	-	1 (4.8)
Anomalous cervical vertebra(e)	-	-	-	-	1 (5.6) [2]	4 (19.0) [3]
Rudimentary ribs on 7th cervical vertebra [4]	4 (13.8)	2 (11.1)	1 (6.3)	3 (16.7)	1 (4.5)	7 (33.3)
Anomalous thoracic vertebrae and/or ribs	-	-	-	-	-	2 (2.5) [5]
Rudimentary 14th ribs	-	1 (5.6)	-	1 (5.6)	-	1 (4.8)
Sternal fusions	1 (3.4)	-	-	-	-	2 (9.5)

3.3 DISCUSSION

This chapter describes studies to evaluate the ability of exogenous inositol to prevent spina bifida in a mouse genetic model of folate-resistant NTDs. Maternal inositol administration significantly reduced the frequency of spina bifida in *curly tail* mice and normalized closure of the PNP in whole cultured embryos. A striking finding was the increased potency of D-*chiro*- compared with *myo*-inositol. At identical dosage levels, subcutaneously administered D-*chiro*-inositol caused a consistently greater reduction in frequency of spina bifida than *myo*-inositol. Moreover, *in vitro*, D-*chiro*-inositol was effective in normalizing neural tube closure at a concentration at which *myo*-inositol had no effect.

3.3.1 Possible reasons for the greater potency of D-chiro-inositol in preventing NTDs

Previous work suggested that the protective effect of *myo*-inositol is mediated via the phosphoinositide cycle (Greene and Copp, 1997a). Briefly, this cycle involves hydrolysis of phosphatidylinositol diphosphate by receptor-activated phospholipase C, to generate the second messengers inositol triphosphate and diacylglycerol (DAG) (Majerus, 1992). Among the downstream events of this signalling pathway, activation of protein kinase C (PKC) by DAG appears to be critical for normalisation of neuropore closure in *curly tail* embryos. For instance, activation of PKC by phorbol esters mimics the effect of inositol supplementation, whereas PKC inhibitors abrogate the protective effect (Greene and Copp, 1997a).

Although the role of PKC in mediating the effect of D-*chiro*-inositol has not yet been investigated, one possibility is that both inositol enantiomers act through the same PKC-dependent pathway. In this case, the greater potency of D-*chiro*-inositol may result from

its differential incorporation and metabolism within the phosphoinositide cycle. Such increased potency of D-*chiro*- compared to *myo*-inositol has been demonstrated in other systems. Thus, insulin stimulation of rat fibroblasts

expressing the human insulin receptor leads to a significant increase in the incorporation of D-*chiro*-inositol into phospholipids whereas the effect on *myo*-inositol incorporation is only marginal (Pak et al., 1993). Moreover, D-*chiro*-inositol induces a much larger reduction in plasma glucose level in rats rendered diabetic by streptozotocin administration compared with exogenous *myo*-inositol (Ortmeyer et al., 1993). These findings suggest an inherently greater potency or bioactivity of D-*chiro*-inositol than *myo*-inositol, perhaps as a result of incorporation into different phosphatidylinositol species (Pak and Larner, 1992). I suggest that the greater potency of D-*chiro*-inositol in preventing NTD in *curly tail* mice, may reflect a relatively greater production of second messengers and/or downstream stimulation of PKC by D-*chiro*-inositol. It is striking, however, that these differences of *in vivo* potency are maintained in the face of the demonstrated interconversion of the two inositol isomers. Pak et al. (1992) showed that [^{3}H]*myo*-inositol is converted to [^{3}H]D-*chiro*-inositol in rat tissues. Perhaps the rate of interconversion is too low to obscure the inherently greater potency of D-*chiro*-inositol in short-term effects on embryonic development.

3.3.2 Relevance of the findings for clinical application of inositol therapy

In order for these experimental findings to be translated into a clinical application, inositol supplementation must be demonstrated to be both effective in preventing NTDs and safe for use during human pregnancy. In terms of efficacy, this study has demonstrated a protective effect of inositol in a mouse NTD model, using subcutaneous

and oral routes of administration, and these findings are supported by previous work in which *myo*-inositol was injected intraperitoneally (Greene and Copp, 1997a). Oral dosing is most likely to be useful in humans, and further support for the effectiveness of oral supplementation with *myo*-inositol comes from the finding of a reduction in the incidence of diabetes-induced abnormalities in rats by oral administration of *myo*-inositol (Khandelwal et al., 1998). The efficacy of inositol in preventing human NTDs has not yet been tested in a clinical trial. However, in a recent case study, inositol supplementation was associated with a normal pregnancy outcome in a woman who had experienced two consecutive NTD pregnancies while taking 4 mg folic acid throughout the peri-conceptional period (Cavalli and Copp, 2002). The empirical recurrence risk of NTD following two previous affected fetuses is approximately 1 in 9 (Seller, 1981) so, clearly, the association of inositol therapy with normal pregnancy outcome in this case may have been a chance association. A larger study of pregnancies at risk of 'folate-resistant' NTDs is needed to test the idea that inositol may be effective in humans, as in mice.

With regard to the safety of inositol therapy during pregnancy, the pathological survey of fetuses from inositol-treated mice revealed no major defects, apart from NTDs, and no increase in the frequency of embryonic or fetal loss *in utero*. These findings are indicative of the relative safety of inositol usage during pregnancy, although direct information from use in human pregnancy is also urgently needed. In the case of the mother who took inositol in a third pregnancy, following two apparently 'folate-resistant' NTD pregnancies, a dose of 0.5 g inositol per day was used, with no apparent side effects for mother or baby (Cavalli and Copp, 2002). In particular, there was no evidence of abnormal uterine contractions, such as have been suggested as a possible adverse effect of inositol therapy (Limpach et al., 2000). The reproductive toxicology of D-*chiro*-inositol

has been the subject of several studies in both rats and rabbits at doses up to 2000 mg/kg/day. In these studies, there were no adverse effects on mating, fertility or embryo/fetal development (Dr G. Allan, Insmed Inc., personal communication). Other lines of evidence also suggest that inositol supplements may be used clinically without adverse side effects. For instance, *myo*-inositol has been previously tested in adults for prevention of depression, panic disorder and obsessive compulsive disorder (Belmaker et al., 1996;Atack, 1996)} and in children for treatment of autism (Levine et al., 1997). No significant side effects were reported in these studies which employed relatively high inositol doses: up to 18 g per day in adults and 200 mg/kg in children. D-*chiro*-inositol has recently been demonstrated to increase the action of insulin in patients with polycystic ovary syndrome, thereby improving ovulatory function and decreasing serum androgen concentrations, blood pressure and plasma triglyceride concentrations (Nestler et al., 1999).

CHAPTER 4

PKC INVOLVEMENT IN NEURAL TUBE CLOSURE

4.1 Introduction

In *Chapter 3*, it was shown that NTDs in the curly *tail* mouse can be prevented by administration of not only *myo*-inositol but also D-*chiro*-inositol. This effect of inositol was previously shown to be mediated through the activity of the inositol/lipid cycle ({Greene, 1997 13402 /id}). Of particular relevance to the present studies, DAG which is produced during inositol phospholipid signalling binds to and activates PKC, and this process appears essential for the action of inositol in preventing NTDs (Greene and Copp, 1997a).

The purpose of the studies in the present chapter was to further investigate the role of PKC in mediating the protective effect of inositol. I first performed an immunohistochemical analysis to verify the relationship between PKC isoform distribution and posterior neuropore closure in the *curly tail* mouse. Second, the requirement for the various isoforms of PKC was investigated using chemical and peptide inhibitors of PKC in embryo culture. The specificity of the peptide inhibitors was also verified using primary cell cultures from *curly tail* mouse embryos.

Embryonic development requires that a wide variety of information be relayed via intracellular signalling pathways. A number of these signals are transduced into a cell through cell surface receptors, which by binding to their ligands, initiate one or more signal transduction cascades and alter the state of phosphorylation of several cellular components through the action of both kinases and phosphatases.

One of these signal transducers is protein kinase C (PKC), which functions during embryo development. The serine/threonine protein kinase C plays a major role in

transmembrane signal transduction (Mochly-Rosen and Kauvar, 2000). It is activated by diacylglycerol originated from membrane phospholipids upon cell stimulation by various ligands, i.e. hormones or growth factors (Dorn et al., 1999). The existence of a wide range of PKC isoenzymes in mammalian tissues has been shown following the first identification of PKC by Nishizuka (Nishizuka, 1988). PKC heterogeneity poses the question as to why so many isoenzymes exist, and suggests that each of them could have a specific relevance in the regulation of various cellular functions (Braun and Mochly-Rosen, 2003). Moreover, a major distinguishing feature of PKC isoforms is their distinct and selective organ and tissue distribution. Several different techniques have been used to examine the expression of PKC isoforms in post-natal and adult tissues (Nishizuka, 1988); (Wetsel et al., 1992); (Bareggi et al., 1995); (Hunter, 1995) Most of the PKC isoenzymes (α, βI, βII, δ, ε and ζ) have been found to be ubiquitously distributed, e. g. in brain, lung, spleen, thymus and skin, whereas PKC γ has been found in the central nervous system (Wu et al., 2000); (Harris and Juriloff, 2007c). PKC isoforms appear to be expressed at low levels during the late stages of gestation and early in the postnatal period and to increase during the first 2 to 3 weeks after birth. However, expression data for PKC during embryonic development were not available prior to day 15 of gestation, preceding the work described in this thesis.

4.1.1 Possible requirement for PKC isoforms in mediating the preventive effect of inositol

Greene and Copp (1997) found that brief treatment with TPA, a PKC activator that mimics DAG, caused a reduction in PNP length of *curly tail* embryos following culture. This effect of TPA was comparable to that observed following inositol supplementation. The protective effect of TPA suggested that PKC activation is crucial in preventing spinal

NTDs in *curly tail* embryos and, since only the conventional and novel PKC isoforms are DAG and TPA-responsive, this focussed attention on these classes of PKC isoforms as likely mediators of the inositol effect. Use of the PKC inhibitor Bisindolylmaleimide I (BisI; GF 109203x) provided support for this idea as addition of Bis I prior to, and during, inositol treatment reversed the protective effect of TPA on closure of PNP (Greene and Copp, 1997a). This inhibitor study indicated that the mechanism of action of inositol involves activation of PKC, and suggested, furthermore, that the critical PKC isoforms might include PKC α, β, γ and ε. These isoforms are reportedly to be selectively inhibited by Bis I at 10 μM, the concentration used by Greene and Copp (1997). To extend this analysis, the present study used a series of additional PKC inhibitors, both chemical and peptide, in order to identify the specific PKC isoforms required for the inositol effect.

4.1.2 PKC chemical inhibitors

The aminoalkyl bisindolylmaleimide I (Bis I; GF109203x; Go6850) is a staurosporine analogue with selective inhibitory activity against PKC (IC_{50} = 10 nM). Importantly, studies of diverse effects of Bis I in intact cells provide evidence for selective recognition of cellular PKC by the inhibitor and therefore suggest the usefulness of Bis I as a probe of PKC function in cell culture. Bis I is known to inhibit cPKCs (α, βI, βII and γ) and PKC ε ((Parker and Parkinson, 2001)). Another staurosporine analogue used in this study is the indole carbazole, Godecke 6976 (Go6976) [12-(2-cyanoethyl)-6,7,12,13-tetrahydro-13-methyl-5-oxo-5H-indolo(2,3-a)pyrrolo (3,4-c)-carbazole] which inhibits PKC α, βI and βII. It has been found that this PKC inhibitor also inhibits DNA synthesis suggesting a pro-proliferative role for the Go6976-inhibited PKC isoforms (Iankov, 2002). Go6976 inhibition of DNA synthesis could be rescued by subsequent incubation with vehicle suggesting that the action of the inhibitor is not irreversibly toxic (Beltman et al., 1996).

Pre-incubation of cells with Go6976 leads to enhancement of IL-6-induced p44/p42 MAPK activity (Martiny-Baron et al., 1993). These findings suggest that in addition to a role in proliferation, PKC is also required for negative regulation of the MAPK pathway. Another selective PKC inhibitor used was 2,2',3,3',4,4'-hexahydroxy-1,1'-biphenyl-6,6'-dimethanol dimethyl ether, (HBDDE) which inhibits PKC α and γ but not PKC βII, δ or ε (Mathur and Vallano, 2000). In order to identify a possible involvement of the atypical PKC isoform ζ, LY294002 was used at a concentration of 2 μM. At this concentration, this inhibitor also blocks the phosphatidylinositol-3-kinase pathway (Vlahos et al., 1994), something to be taken into account when analysing these results. Bisindolylmaleimide V (Bis V; an inactive analogue of GF109203X) was used as a negative control compound, as it does not inhibit PKC (Asakai et al., 2002).

4.1.3 PKC peptide inhibitors

Chemical inhibitors may be specific for sub-classes of PKC isoforms, at certain concentrations, but do not allow the role of single PKC isoforms to be evaluated. For example, the cell-permeable, inhibitor HBDDE is reported to be a selective inhibitor of PKC α and γ with IC_{50} values of 43 and 50 mM, respectively, using an *in vitro* assay. However, data examining the potency and selectivity of HBDDE in intact cells are lacking. Moreover, the concentrations of chemical inhibitors found to block certain groups of PKC isoforms in cultured cell lines, or in cell-free systems, may not apply to biological systems, especially complex multicellular organisms such as mouse embryos. Hence, it is dangerous to assume that use of a chemical inhibitor at a particular concentration in embryo culture will block the same group of PKC isoforms as in cell culture. For this reason, the experiments with chemical inhibitors were extended by the use of peptide PKC inhibitors, which offer isoform-specificity of PKC inhibition.

4.1.3.1 Molecular basis of PKC isoform inhibition by the peptides

Receptor for Activated C-Kinase (RACK) is responsible for the binding of active forms of PKCs. There are different RACKs for different isoforms of PKC (Section 1.3.4), which thus mediate differential subcellular targetting of the isoforms. Inactive forms of PKC occlude the RACK binding site with a pseudo-RACK peptide sequence (Dorn et al., 1999). Peptides that mimic the PKC binding site on RACK proteins are able to inhibit the translocation and thus the activity of PKC. This property results from the fact that anchoring is necessary for the function of individual PKC isoforms, such that inhibition of anchoring inhibits their kinase activity. The peptide sequences bind in a competitive manner to the PKC isoform RACK binding site, blocking its translocation (Dorn et al., 1999). *See Chapter 1.*

4.1.3.2 Use of antennapedia pepetide to carry peptides into the cell

To facilitate transfer of peptides into the cell, they were coupled to a sequence from the homeodomain protein antennapedia. Homeoproteins are a class of transcription factors that bind DNA through a structure of 60 amino acids length, called the homeodomain. The idea that transcription factors could traverse from cell to cell results from the observed internalisation of the homeodomain of the *Drosophila* protein antennapedia (Joliot, 1991). The antennapedia third helix (amino acids 43-58) is necessary for translocation (Derossi et al., 1994); (Theodore et al., 1995). Therefore, to ensure penetration into the cell, peptides are bound to the antennapedia third α helix peptide, which will deliver a 'cargo' into the cell. Internalisation occurs at both 4°C and 37°C, implying that it does not involve classical receptor-mediated endocytosis. Derossi, 1994 has proposed a model in which the positively charged peptide interacts with negatively charged phospholipids on the outer layer of the plasma membrane. Due to the interactions

between tryptophan residues in the peptide and the lipids, the planar form of the outer phospholipid monolayer is distorted, encouraging the formation of inverted micelles, which will contain the peptide (Derossi et al., 1994).

4.2 Results

4.2.1 Specificity of PKC antibodies

The specificity of anti-PKC antibodies was first tested using sections of adult mouse cerebellum (Figure 4.1) as a positive control in which staining patterns have been previously reported. As expected, anti-PKC α, γ and ε stain only Purkinje cells, whereas anti-PKC ßI and ßII stain only granule cells (Figure 4.1 and Table 4.1). These results correlate with those previously described for the rat cerebellum (Bareggi et al., 1995).

4.2.2 PKC isoform expression during mouse embryogenesis

In order to identify the isoforms that might play a role in prevention of NTDs, it was imperative to determine which PKC isoforms are expressed in mouse embryos undergoing spinal neurulation (E9.5 to E10.5). A member of our laboratory performed western blot analysis, which detected expression of all PKC isoforms in whole E 9.5 and E 10.5 embryos. However, this approach was insufficiently sensitive to detect PKC isoform expression in specific embryonic regions, such as the posterior neuropore (PNP), the site of spinal neurulation. I thus performed immunohistochemical staining on histological sections throughout the PNP region. Expression of PKCs was detected in the closing neural tube, hindgut, notochord and presomitic mesoderm, at both E9.5 and E10.5 in *curly tail* embryos (Figure 4.2). A control was run with each experiment to test for non-specific staining of the primary antibody (Figure 4.1). In this control, affinity purified rabbit IgG from pre-immune serum (Sigma) was used instead of isozyme specific primary antibody. Additional controls received only primary antibody or secondary antibody. In all cases, the negative controls gave a complete lack of staining.

Figure 4.1 Distribution of Protein Kinase C isoforms in cerebellum

Immunohistochemistry was used to detect isoforms of protein kinase C within the adult cerebellum. Sagittal sections were immunostained for PKC α (A-B), PKC β (C-D), PKC γ (E-F). Cells in the purkinje cell layer (pcL) are immunoreactive to the antisera to PKC α (A-B) and γ, whereas cells in the granular layer (gL) are negative. In contrast, granule cells are immunoreactive to the antiserum to PKC β, whereas purkinje cells are negative (C-D). A control section that was not incubated in any primary antiserum is also shown (G). B, D and F are high magnifications of A, C and E respectively. For A, C, E and G, scale bar = 20 μm; from B, D and F, scale bar = 250 μm.

Figure 4.1

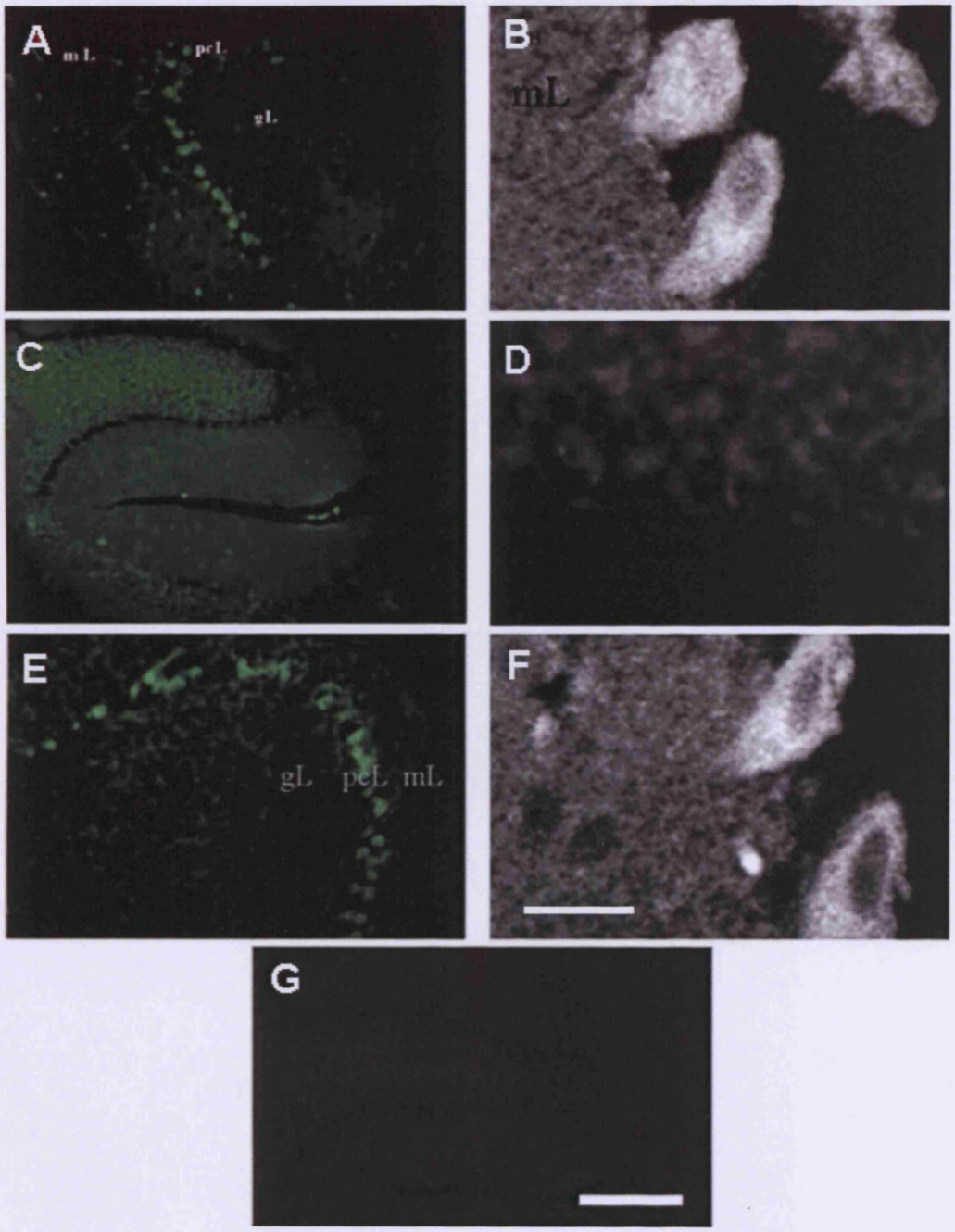

Figure 4.2 Expression of PKC isoforms during mouse spinal neurulation

Immunohistochemistry reveals ubiquitous expression of PKC isoforms during mouse spinal neurulation. Transverse sections through the posterior neuropore region of *curly tail* mouse embryos at E9.5 (**A, C, E, G, I**) and E10.5 (**B, D, F, H, J**) were stained with antibodies specific for PKC α, ßI, ßII, and γ. All PKCs exhibit ubiquitous expression in the neural plate (Np), notochord (N), hindgut (H) and presomitic mesoderm (M) of the posterior neuropore region. Scale bar represents 20 μm.

Figure 4.2

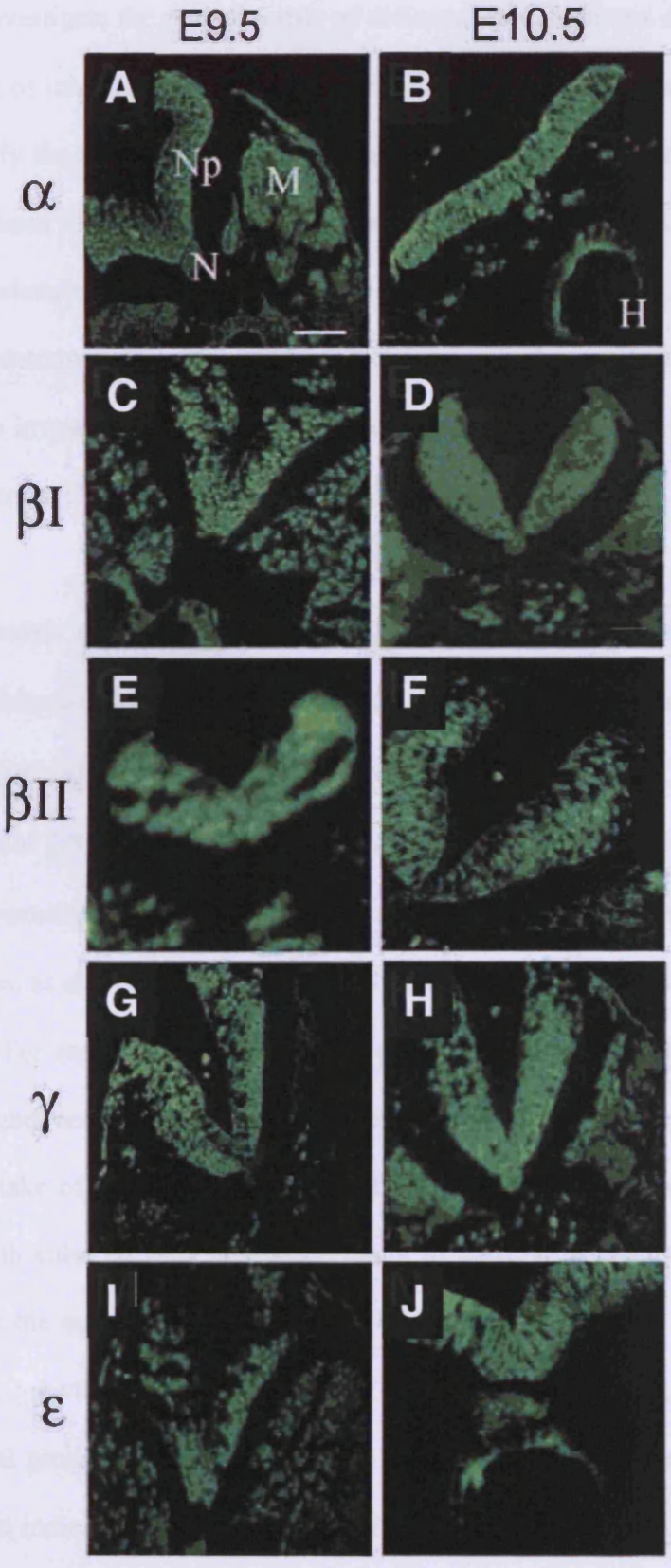

4.2.3 Evaluation of possible effects of chemical inhibitors on growth and development of cultured embryos

In order to investigate the potential role of different PKC isoforms during closure of the PNP, a series of inhibitors was applied to *curly tail* embryos in culture. It was important to first identify the most appropriate concentration to use for each inhibitor, so as not to cause generalised toxicity or growth retardation. Growth retardation is known to reduce the delay of closure of the PNP in *curly tail* embryos (Copp et al., 1988c)) and it was important to determine whether PKC inhibitors alone had any effect on growth, prior to using them to investigate the protective effect of inositol. Inhibitors were first tested in a non-mutant strain, CD1, and then in *curly tail* embryos.

In cellular models of phosphorylation, PKC activity is inhibited with IC_{50} values (half maximal inhibitory concentration) of 0.2 to 10 μM. For example, in an assay of vimentin phosphorylation in Swiss 3T3 cells maximal inhibition of PKC was obtained at a concentration of 2.5-5 μM Bis I, with no inhibition of cAMP-dependent PKA even at the highest concentration. Based on cell culture data, each inhibitor was used at two concentrations, as shown in Tables 4.2 and 4.3 in cultures of CD1 and *curly tail* embryos respectively. For each inhibitor, the lower concentration was typical of that used in cell culture. A higher concentration was also tested, in case it was necessary to overcome any decreased uptake of the inhibitor due to the intact yolk sac surrounding the embryo, as compared with cultured cells which are likely to be more accessible to cell-permeable inhibitors. At the end of the culture period, the crown rump length was measured as an indicator of growth and the number of somites was counted as a measure of developmental progression. In addition, any malformations or abnormalities were noted as these could indicate teratogenic effects of the inhibitors. The yolk sac circulation was recorded as a measure of overall health of the embryo.

4.2.3.1 Chemical inhibitors of PKC do not affect growth or developmental progression of embryos *in vitro*

In CD1 embryos (Table 4.1), there was no difference in mean somite number or mean CR length between PBS/DMSO controls and either low or high concentrations of BisI, or the inactive BisV. Yolk sac circulation was also unaffected and no teratogenic effects, such as irregular somites, under-developed branchial arches, enlarged pericardium or failure of embryonic turning were observed. In contrast, cultures of *curly tail* embryos gave a somewhat different result (Table 4.2). In cultures exposed to the lower concentration of each PKC inhibitor, all treatment groups were comparable in terms of developmental progression and growth, with no significantly difference from PBS/DMSO controls. However, at the higher PKC inhibitor concentrations, *curly tail* embryos showed retardation of developmental progression, as judged by a significant lower somite number at the higher concentration compared to the lower concentration for each inhibitor ($p < 0.05$). Despite this effect, yolk sac circulation was normal in all embryos and malformations were not observed. Moreover, while crown-rump length varied significantly between treatment groups overall (ANOVA; $p< 0.05$), pair-wise comparisons failed to detect significant differences between high or low concentrations of each inhibitor (after correction for multiple comparisons; Holm-Sidak method). Hence, this preliminary culture analysis reveals a greater susceptibility of mutant *curly tail* embryos than wild type CD1 embryos to PKC inhibitor, and indicated the need to use the lower inhibitor concentrations in subsequent curly tail culture studies.

4.2.4 Investigating the effect of chemical PKC inhibitors on PNP closure

PNP length was measured after culture as an indicator of risk of developing spina bifida. In CD1 embryos cultured in the presence of BisI for 24 hours to the 30-32 somite stage,

all the embryos had completed closure of the PNP suggesting that the inhibitors did not have a major deleterious effect.

Treatment	Conc.	No. embryos	Mean somite no. ± SEM [1]	Mean CR length (mm) ± SEM[2]	Yolk sac circulation
PBS/DMSO	_	10	31.0 ± 0.09	3.02 ± 0.03	3
Inositol	50 μg/ml	10	31.6 ± 0.20	3.19 ± 0.11	3
BisI	10 μM	10	30.3 ± 0.11	3.37 ± 0.09	2.9
Bis I	30 μM	10	31.2 ± 0.32	2.97 ± 0.12	3
BisV[3]	10 μM	10	31.6 ± 0.10	2.90 ± 0.21	2.8
BisV	30 μM	10	30.3 ± 0.08	3.42 ± 0.13	2.9

Table 4.1 CD1 embryos cultured for 24 hours from E9.5 to E10.5 in the presence of the PKC chemical inhibitor BisI

PKC inhibitors were diluted in DMSO and further diluted in PBS. A DMSO-PBS solution was used as a control. Inhibitors do not adversely affect developmental progression or growth in CD1 embryos after 24 hr *in vitro* culture.

[1]No significant difference in somite number by analysis of variance between treatments, $P > 0.05$

[2]No significant difference in crown rump (CR) length by analysis of variance between treatments, $P > 0.05$

[3]BisV is an inactive variant of BisI

Table 4.2 *Curly tail* embryos cultured for 24 hours from E 9.5 to E 10.5 in the presence of PKC chemical inhibitors

[1]One way ANOVA shows significant difference in somite number. Pairwise multiple comparisons by the Holm-Sidak method show that for each inhibitor the higher dose tested caused a significant reduction in somite number compared to the PBS/DMSO control and to the lower dose of the same inhibitor, ($p< 0.001$). There was no significant difference in somite number between PBS/DMSO control and lower dose of any inhibitor.

[2]One way ANOVA ($p<0.017$) shows significant variation overall in crown rump length. However, pairwise multiple comparisons by the Holm-Sidak method show that for each inhibitor there is no difference between high and low concentration of each inhibitor, nor between high inhibitor dose and PBS/DMSO control.

Table 4.2

Treatment	Conc.	No. embryos	Mean somite no. ± SEM [1]	Mean CR length (mm) ± SEM[2]	Yolk sac circulation
PBS/DMSO	_	10	30.09 ± 0.06	3.04 ± 0.07	2.9
BisI	10 μM	10	30.3 ± 0.15	3.56 ± 0.10	3
	30 μM	10	23.2 ± 0.70	2.50 ± 0.50	3
BisV	10 μM	10	30.6 ± 0.13	3.50 ± 0.10	3
	30 μM	10	25.5 ± 0.55	1.80 ± 0.64	2.8
Go6976	10 μM	10	30.5 ± 0.13	3.39 ± 0.10	2.9
	30 μM	10	22.3 ± 0.82	2.00 ± 0.21	2.7
HBDDE	50 mM	10	30.6 ± 0.16	3.55 ± 0.10	3
	150 mM	10	25.8 ± 0.54	2.70 ± 0.80	2.8
LY294002	1.4 μM	10	30.3 ± 0.16	3.49 ± 0.08	2.8
	42 μM	10	24.6 ± 0.67	2.60 ± 0.76	3

Curly tail embryos were exposed to each inhibitor alone to determine whether there was an effect on PNP closure. Embryos were also treated with inhibitor and inositol to determine whether suppressing PKC activity reduced the effect of inositol. The mean PNP length of embryos exposed to PBS alone was 0.6 mm (Figure 4.3A), reflecting the *in vivo* situation in which *curly tail* embryos exhibit delayed closure of the PNP, leading to development of NTDs or tail flexion defects in 60% of embryos (Van Straaten and Copp, 2001). When added alone, none of the inhibitors significantly altered PNP length in cultured *curly tail* embryos after twenty four hours ($p > 0.05$; yellow bars, Figure 4.3). Treatment of *curly tail* embryos with 50 μg/ml of *myo*-inositol (first red bar, Figure 4.3) resulted in a significant decrease in PNP length after culture, to a mean value of 0.08 mm, which is characteristic of normally developing embryos. Thus, as demonstrated in *Chapter 3*, inositol normalises PNP closure *in vitro* as well as *in vivo.*

PNP length in the presence of inositol plus inhibitor was 60-90% of that in the presence of inhibitor alone (blue bars, Figure 4.3). Embryos cultured in the presence of inositol and Bis I, exhibit a PNP length that is significantly larger than the PNP length of embryos cultured in the presence of inositol alone, suggesting that the protective effect has been blocked. Similarly when embryos were cultured in the presence of Go6976 and inositol or in HBDDE and inositol, the PNP length of embryos after cultured was significantly larger than the embryos cultured in the presence of inositol alone. In the case of LY294002 the effect of inositol was partially blocked suggesting a role for PKC ζ and/or PI3-kinase. In contrast, the inactive analogue BisV did not prevent the reduction in PNP length caused by co-administration of inositol (second red bar in Figure 4.3). Therefore, the use of chemical inhibitors highlights the potential importance of PKCα, β, γ, ε and ζ(i.e. those isoforms acted upon by the chemical inhibitor) in mediating the effect of inositol although

the chemical inhibitors do not give sufficient specificity to narrow down the effect to individual isoforms.

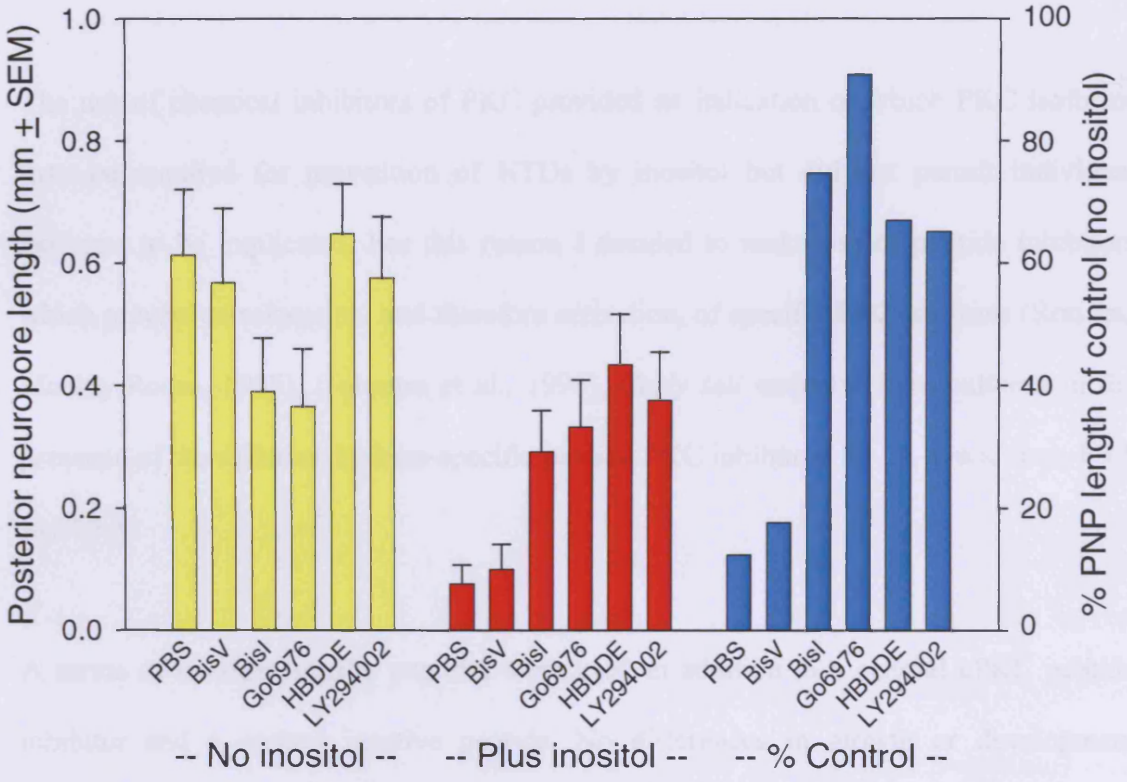

Figure 4.3 Normalization of spinal neural tube closure by inositol in *curly tail* embryos is abrogated by inhibition of specific PKC isoforms.

Chemical inhibitors of PKC were applied to *curly tail* mouse embryos cultured from E9.5 for 24 h, and the posterior neuropore (PNP) length was measured as an indicator of predisposition to spinal NTD. Yellow bars: PNP length of embryos exposed to PKC inhibitors in the absence of inositol; red bars: PNP length of embryos exposed to PKC inhibitors in the presence of inositol; blue bars: PNP length in the presence of PKC inhibitor plus inositol as a % of the value in the presence of PKC inhibitor alone (right axis). Inositol significantly reduces PNP length in the absence of inhibitor (PBS;

$P<0.001$) and in the presence of inactive BisV ($P<0.002$), whereas the inositol effect is abrogated in the presence of chemical inhibitors BisI, Go6976, HBDDE and LY294002 ($P>0.05$).4.2.5 Use of peptide inhibitors to identify the specific PKC isoforms required for protection of PNP closure by inositol.

The use of chemical inhibitors of PKC provided an indication of which PKC isoforms may be required for prevention of NTDs by inositol but did not permit individual isoforms to be implicated. For this reason I decided to make use of peptide inhibitors which prevent translocation, and therefore activation, of specific PKC isoforms (Ron and Mochly-Rosen, 1995), (Johnson et al., 1996). *Curly tail* embryos were cultured in the presence of the different isoform-specific peptide PKC inhibitors for 24 hours, from E9.5 to E10.5.

A series of isoform-specific peptides were used in addition to a general cPKC peptide inhibitor and a control inactive peptide. No differences in growth or development progression, as indicated by crown-rump length and number of somites, were detected between treatment groups (Table 4.4). Moreover, no teratogenic effects were observed. These data suggest that any effect on PNP closure results from specific inhibition of PKC as opposed to generalised toxicity of inhibitors. As shown in *Chapter 3*, embryos cultured in the presence of inositol show a significant reduction in PNP length compared with PBS treated controls and this effect of inositol was maintained in the presence of specific inhibitors for PKCα, βII, δ, and ε, as well as the inactive peptide used as a negative control (Figure 4.4). In contrast, when inositol was added in the presence of inhibitors specific for PKCβI, γ or ζ the therapeutic effect of inositol was largely abolished (red bars in Figure 4.6). Mean PNP lengths were 74%, 81% and 56% respectively of the values

observed in the absence of inositol (blue bars in Figure 4.4). These findings correlate well with the results of the chemical inhibitor study, and indicate the need for βI and γ among the conventional PKCs, and additionally PKCζ among the atypical PKCs, in order for inositol to mediate its enhancing effect on PNP closure in *curly tail* embryos.

4.2.6 Evaluation of peptide inhibitors of PKC in cultured cells

At the outset of this experiment the efficacy of isoform-specific PKC inhibitory peptides had not been verified in embryonic mouse cells. In order to check the effect of the peptide inhibitors on PKC activity, I generated primary fibroblastic cell lines from *curly tail* embryos and used antibody staining to localise PKC isoforms following addition of the DAG analogue TPA to activate PKC.

After culture of primary fibroblasts in medium containing 1% fetal calf serum, immunohistochemistry showed that PKC α, βI, βII, γ and ε were all localised in a diffuse pattern throughout the cytoplasm (Figure 4.4). A parallel set of cultures was treated with TPA, and in each case PKC was seen to have translocated the nucleus (Figure 4.4). Another set of cultures was treated with TPA and one of the isoform-specific peptide inhibitors. Staining for the corresponding PKC isoform showed that the presence of inhibitor prevented translocation of that isoform to the nucleus (Figure 4.4).

Table 4.3 Development of *curly tail* embryos following culture from E 9.5 to E10.5 in the presence of inositol and/or PKC pepetide inhibitors

[1]No significant difference in somite number by analysis of variance between treatments, $P > 0.05$

[2]No significant difference in crown rump (CR) length by analysis of variance between treatments, $P > 0.05$

Table 4.3

	Number of embryos		Mean somite number ± SEM[1]		Mean CR length (mm) ± SEM[2]		Yolk sac circulation	
	+ PBS	+ Inositol	+ PBS	+ Inositol	+ PBS	+ Inositol	+ PBS	+Inositol
No inhibitor	10	10	31.7 ± 0.05	30.5 ± 0.10	3.5 ± 0.21	4.45 ± 0.01	2.8	3
cPKC	10	10	30.4 ± 0.11	31.2 ± 0.8	3.6 ± 0.09	3.60 ± 0.33	2.7	2.7
Control-peptide	10	10	31.2 ± 0.49	30.8 ± 0.19	3.5 ± 0.72	3.8 ± 0.22	2.8	3
PKC α	10	10	31.7 ± 0.05	30.2 ± 0.12	3.8 ± 0.09	3.93 ± 0.10	3	2.8
PKC βI	10	10	30.5 ± 0.02	31.6 ± 0.81	3.9 ± 0.73	3.44 ± 0.32	2.9	3
PKC βII	10	10	30.3 ± 0.10	30.2 ± 0.15	3.5 ± 0.09	3.52 ± 0.19	3	2.8
PKC γ	10	10	30.8 ± 0.21	31.5 ± 0.73	3.9 ± 0.74	3.6 ± 0.41	3	3
PKC ε	10	10	31.7 ± 0.30	31.1 ± 0.10	3.7 ± 0.68	3.8 ± 0.65	3	2.7
PKC δ	10	10	30.5 ± 0.08	30.8 ± 0.66	3.7 ± 0.55	3.45 ± 0.34	2.8	2.9
PKC ζ	10	10	31.1 ± 0.05	31.6 ± 0.25	3.5 ± 0.43	4.3 ± 0.09	2.9	3

Figure 4.4 Inhibition of specific PKC isoforms in cultured *curly tail* embryos –effect on PNP length

Peptide inhibitors of PKC were applied to *curly tail* mouse embryos cultured from E9.5 for 24 h, and the posterior neuropore (PNP) length was measured as an indicator of predisposition to spinal NTDs. Yellow bars: PNP length of embryos exposed to PKC inhibitors in the absence of inositol; red bars: PNP length of embryos exposed to PKC inhibitors in the presence of inositol; blue bars: PNP length in the presence of PKC inhibitor plus inositol as a % of the value in the presence of PKC inhibitor alone (right axis). Normalization of spinal neural tube closure by inositol in *curly tail* embryos is abrogated by inhibition of specific PKC isoforms. Inositol significantly reduces PNP length in the absence of inhibitor (PBS; $P<0.001$) and in the presence of inactive peptide (Pept) or peptide inhibitors to PKC α, ßII, δ ($P<0.005$) and ε ($P<0.05$), whereas the inositol effect is abrogated by inhibitors to PKCßI, γ and ζ ($P>0.05$). There is no effect on PNP length of either chemical or peptide inhibitors in the absence of inositol (analysis of variance, $P>0.05$).

Figure 4.4

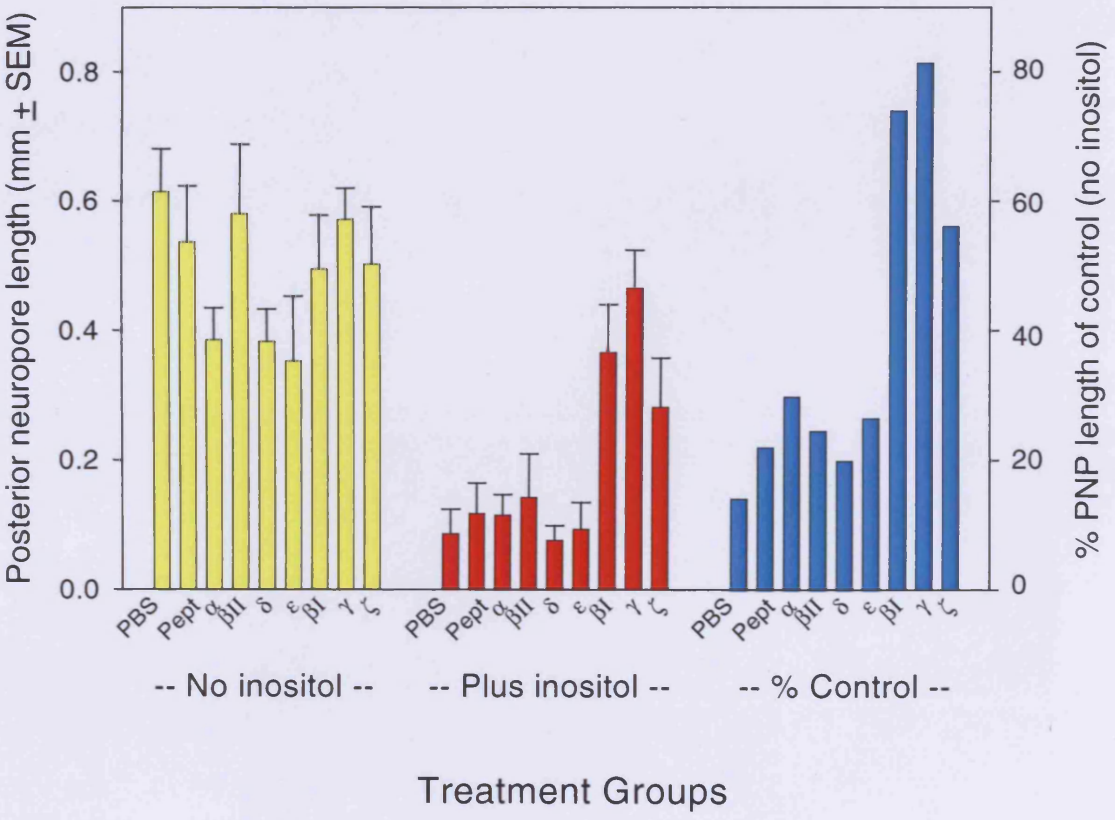
Posterior neuropore length (mm ± SEM)
0.0
0.2
0.4
0.6
0.8
% PNP length of control (no inositol)
0
20
40
60
80
PBS
Pept
α
βII
δ
ε
βI
γ
ζ
-- No inositol --
-- Plus inositol --
-- % Control --
Treatment Groups

Figure 4.5 Inhibition of PKC isoform translocation

Isoform-specific antibodies were used to detect PKC isoforms (as in Figure 4.1 and 4.2) in *curly tail* primary embryonic cell cultures. Cells cultured for 18 h in growth medium containing 1% FCS were either fixed with no additional treatment ('serum starved'; **A, D, G, J, M**), exposed to 100 μM TPA for 10 min prior to fixation (+TPA; **B, E, H, K, N**), or exposed to 1 mM isoform-specific PKC inhibitor for 20 min and to TPA for 10 min prior to fixation (TPA+Inhib; **C, F, I, L, O**). PKCs are uniformly located in the cytoplasm of serum starved cells whereas a 10 min treatment with TPA induces translocation to the nucleus in all cases. Pre-treatment with isoform-specific PKC inhibitors prevents TPA-induced translocation and all PKC isoforms exhibit cytoplasmic staining. Inset in (O) shows same field stained with DAPI to demonstrate nuclei. Scale bar represents 20 μm.

Figure 4.5

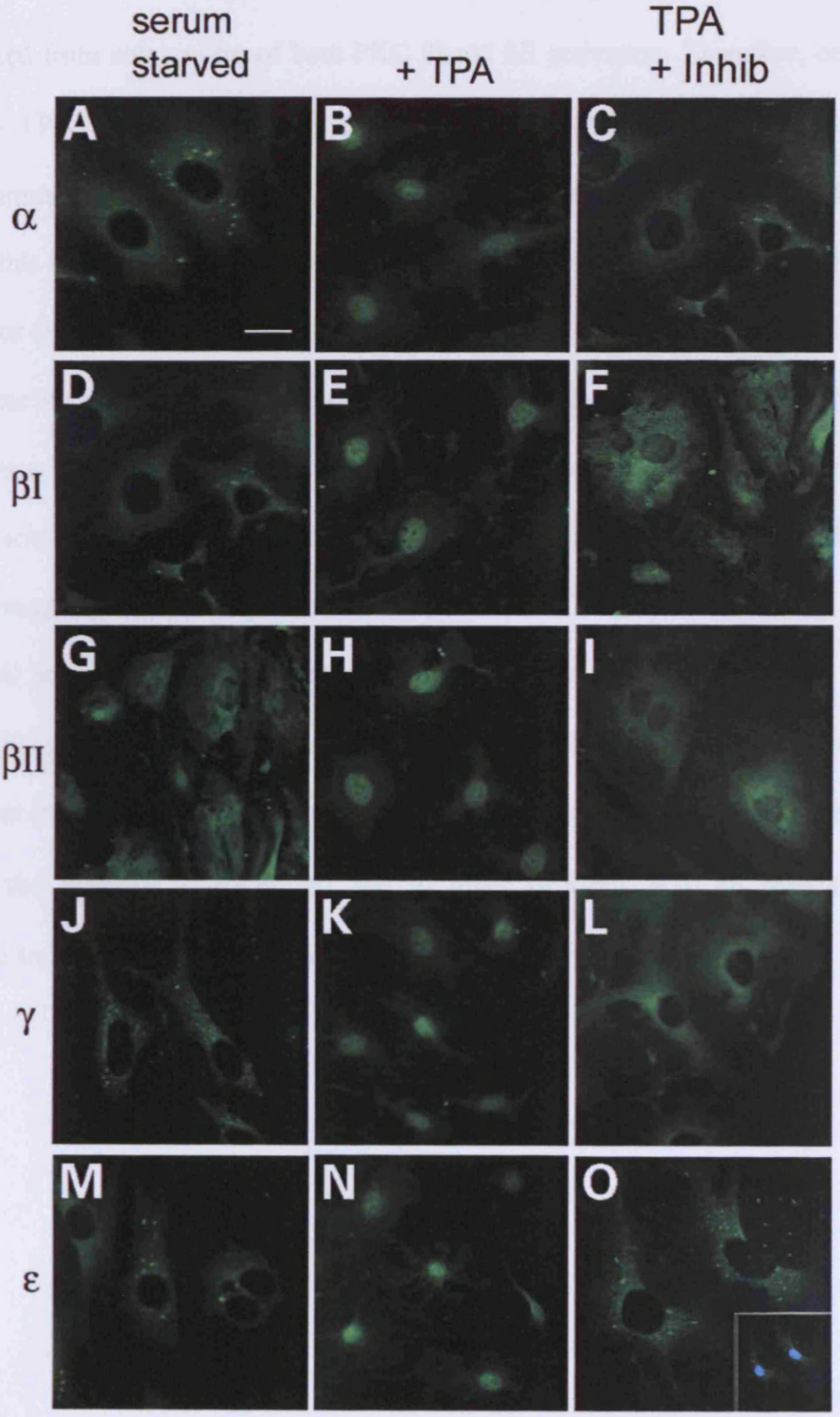

4.2.7 Specificity of inhibitors for PKC βI and βII

Due to the close relationship between PKC ßI and its alternatively spliced variant PKC ßII, I decided to test whether abrogation of the inositol effect by the PKC ßI inhibitor might have resulted from antagonism of both PKC ßI and ßII activation. Therefore, cells were exposed to TPA in culture and the effect on both βI and βII inhibitors were determined by immunohistochemistry. PKC ßI translocated to the nucleus following TPA stimulation, and this translocation to the nucleus was blocked by the ßI inhibitor, but not by the ßII inhibitor (Figure 4.5 A–C). Conversely, translocation of PKC ßII was blocked by the ßII inhibitor but not the ßI inhibitor (Figure 4.5 D–F). This finding confirms that the peptide inhibitors of PKC ßI and ßII are isoform-specific and suggests separate roles for these splice variants in the protective effect of inositol in *curly tail* PNP closure. This finding strongly suggests that the requirement for specific PKC isoforms is unlikely to reflect differential activity of the peptide inhibitors, but may reflect a difference in participation of PKC isoforms in the action of inositol in preventing mouse NTDs. Figure 4.5 also shows that inositol induces translocation of PKC α to the nucleus, demonstrating that apart from the essential isoforms (βI and γ) other isoforms may be activated following inositol treatment. However, their activity is not essential for the prevention of NTDs.

Figure 4.6 Inhibitors of PKCßI and ßII exhibit isoform-specificity

Inositol stimulates PKC translocation, whereas peptide inhibitors to PKCßI and ßII exhibit isoform-specificity in blocking translocation. PKC isoforms were localized by immunocytochemistry on primary cell cultures established from *curly tail* mouse embryos. Serum starved cells exhibit PKCßI and ßII immunoreactivity in the cytoplasm. TPA-induced translocation to the nucleus of PKCßI can be blocked by the ßI inhibitor (**C**) but not by the ßII inhibitor (**B**). Conversely, translocation to the nucleus of PKCßII can be blocked by the inhibitor to ßII (**E**) but not by the inhibitor to ßI (**F**). Addition of 50 μg/ml *myo*-inositol to serum starved cells 6 h prior to fixation induces translocation of PKC α to the nucleus (**H**) whereas PKC α is cytoplasmic in untreated cells (**G**). This effect of inositol is not unique to *curly tail* cells as similar results were obtained in 3T3 cells. Scale bar represents 20 μm.

Figure 4.6

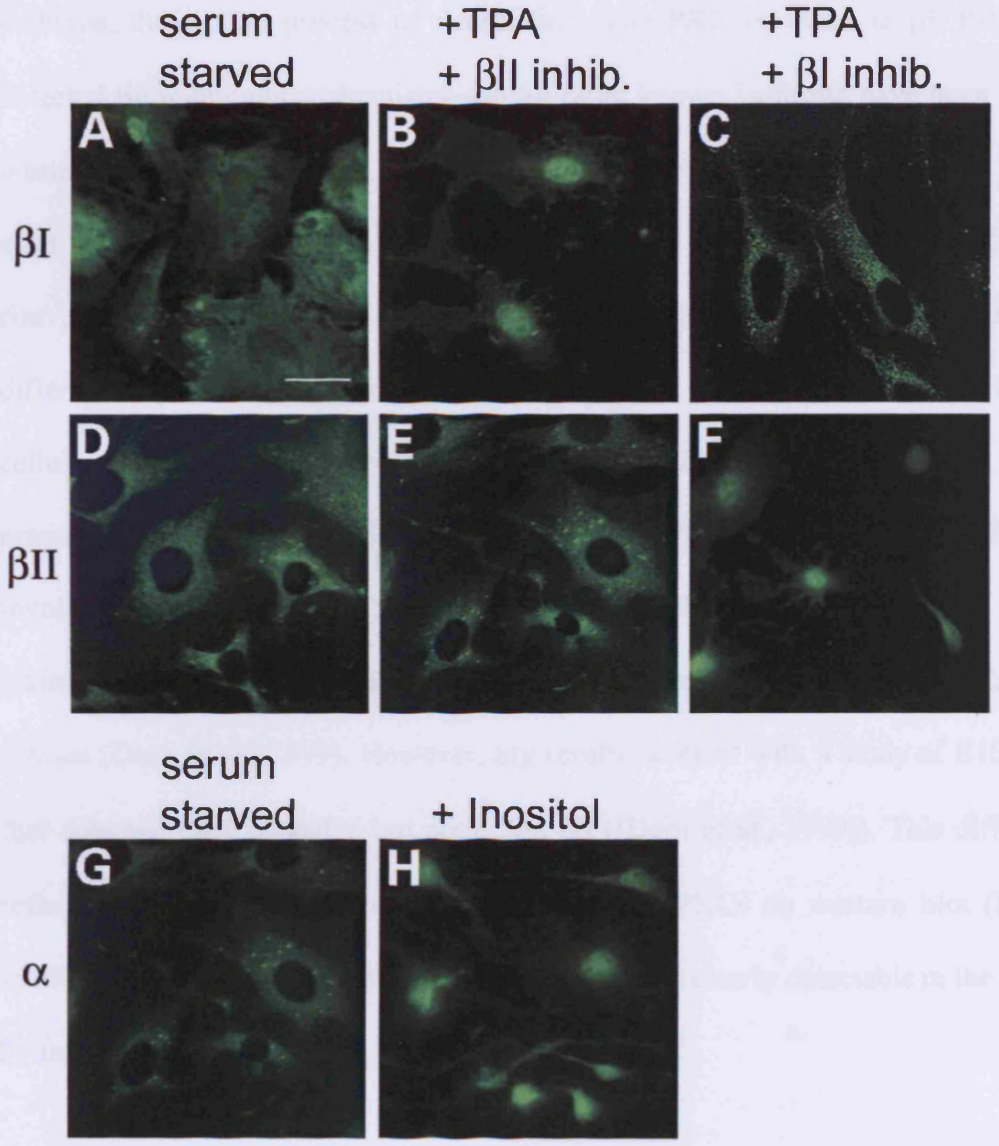
serum
starved
+TPA
+ βII inhib.
+TPA
+ βI inhib.
A
B
C
βI
D
E
F
βII
serum
starved
+ Inositol
G
H
α

4.3 Discussion

4.3.1 Distribution of PKC isoforms

This *Chapter* demonstrates that several different isoforms of PKC are present in *curly tail* embryos, during the process of neurulation. The PKC isoforms α, βI, βII and γ were detected by immunohistochemistry and all other known isoforms have been detected by western blot (Cogram et al., 2004a). Together these results show that the neurulation stage mouse embryo contains representatives from all three categories of PKCs, the conventional, atypical and novel forms. These three categories of PKC isoforms have different requirements for activation of the kinase and are enriched in different sub-cellular localizations in a developmental stage specific fashion (Dorn et al., 1999). This presents the possibility that different isoforms of PKC are differentially activated and involved in different events during embryonic development. The detection of all PKC isoforms from E9.5 to E 17.5 is in agreement with previous analysis of PKCs in E15–17 fetuses (Dorn et al., 1999). However, my results contrast with a study of E10.5 embryos that detected PKC α, and γ, but not ζ and ßII ((Dorn et al., 1999)). This difference may reflect the previously reported low abundance of cPKCs on western blot (Dorn et al., 1999), whereas in the present study all isoforms were clearly detectable in the PNP region by immunohistochemistry.

The published observations that individual isoforms are found in different sub cellular compartments suggest that they are regulated differently (Courage, 1995); (Dorn et al., 1999). For instance, cPKCs are confined to the cytoplasm, suggesting minimal activation during undisturbed development. This finding is consistent with a role for the cPKCs γ and ßI, in mediating the preventive effect of inositol, since activation of these isoforms may be limited in the absence of inositol, providing capacity for activation after treatment.

The results presented in this chapter demonstrate that activation of PKC by inositol treatment of *curly tail* embryos in vitro has a protective effect on closure of the PNP which like inositol supplementation would *in vivo* lead to reduction in spinal NTDs. This suggests a possible mechanism for the prevention of spinal NTDs by inositol supplementation in which there is increase in flux through the inositol/lipid cycle leading to activation of PKC.

Abrogation of the protective effect of inositol by Bis I, a broad spectrum chemical inhibitor of PKCs strongly suggests that the activity of one or more of the classical PKC isoforms is indispensable for normalisation of neural tube closure. Moreover, the chemical inhibitors Go 6976 and HBDDE also inhibited the inositol effect arguing for the requirenment for specific PKC isoforms. The high degree of specificity of the inhibitor Bis I for PKC (Toullec et al., 1991) shows that the effect of inositol (or TPA) on closure of PNP is due to activation of PKC rather than activation of another enzyme. The inhibitor studies also suggest that the mechanism of action of inositol (or TPA) involves activation of PKC rather than secondary negative feedback caused by depletion of PKC as in conditions of sustained treatment (Heidenreich et al., 1993). In the later case, the inhibitor would be expected to mimic the effect of TPA since both inhibition and depletion resulting from chronic TPA treatment reduces cellular PKC activity. Subsequent exposure of embryos to inhibitors of individual isoforms indicates a requirement for PKC βI, γ and possibly ζ in prevention of spinal NTDs by inositol.

In this study use was made of the fact that phorbol esters such as 12-O-tetradecanoyl-phorbol-13-acetate (TPA) can substitute for DAG in activation of PKC, by binding to the same region of the C_1 structural motif (Section 1.5.5). Unlike DAG which is rapidly metabolised, TPA is metabolically stable and can thus cause sustained activation of PKC

(Castagna et al., 1982). PKC activation is probably responsible for the tumor promoting activity of phorbol esters which disturb both proliferation and differentiation events. Prolonged activation of PKC by TPA causes alterations in enzyme activity, in addition to those elicited by transient generation of DAG. Extended exposure to TPA initiates degradation of activated membrane-associated PKC by proteolytic cleavage which leads to depletion of cellular PKC (Nishizuka, 1988). TPA thus has a dual action on PKC, with transient positive activation followed by negative regulation owing to degradation of the enzyme. This complex regulation must be considered when interpreting the effects of TPA treatment on mouse embryos.

4.3.2 Differential requirement for PKC βI and βII

The two most closely related isoforms, PKC βI and βII, are distinct but highly homologous with 96% identity at the amino acid level. They are identical for the first 621 amino acids and differ only in their carboxy-terminal 50-52 amino acids, in which they are 45% homologous (*Chapter 1*, Figure 1.3). The PKCβ gene, and its products βI and βII have well defined structural differences between the two isoforms which presumably account for the isoform specific functions. For example, PKC βII has been found as an actin-binding protein that translocates to the actin cytoskeleton in cells, while antibodies to PKC βII, but not to PKC βI, co-immunoprecipitate actin, (Blobe et al., 1996)). Thus, βII can be distinguished from βI through its interaction with F-actin, perhaps suggesting that the protective effect of inositol in *curly tail* embryos is not due to an effect of PKC on actin function.

Another important difference between the two isoforms comes from a difference in carboxy terminal phosphorylation, which has been indicated in regulating their function and sub-cellular localization. Biochemical and immunolocalization studies of

phosphorylation site mutant proteins reveal that negative charge at this position is require for cytosolic localization of PKC and phorbol ester dependent translocation (Mochly-Rosen and Kauvar, 2000). PKC βI is phosphorylated at T642 whereas PKC βII is phosphorylated at T646, which may contribute to difference in function and localization of the two isoforms (Banan et al., 2004).

Interestingly it has been shown previously that βI and βII play a very important role in cell proliferation but at distinct check points during the cell cycle. PKC βI appears to play a role in control of G1-S progression while βII is implicated in the G2/M transition. The differential role of PKC β isoforms in cell cycle regulation is notable as the underlying defect in *curly tail* embryos involves a cell proliferation defect (see *Chapter 6*)

4.3.3 Requirement for conventional and atypical PKCs

It was previously reported that treatment of *curly tail* embryos with phorbol ester, which acts as a DAG analogue, can mimic the effect of inositol (Greene and Copp, 1997a). This action was proposed to be mediated through activation of conventional or novel PKC isoforms as atypical isoforms are not DAG-responsive. Recent evidence suggests that in some cell types phorbol ester treatment also leads to activation of PI3-kinase and PKCζ (Kim et al., 2001). The data in the present study do indeed suggest some requirement for atypical PKCs, as also indicated by the ability of LY294002 and the PKCζ inhibitor to abrogate the effect of inositol in this study.

It is possible that the PKC ζ isoform could augment the effect of PKC βI and PKC γ on neural tube closure, either through activation of PDK-1 or phosphorylation of additional substrates.

The phosphoinositide cycle involving diacylglycerol and PKCζ is activated downstream of PI3-kinase (Standaert et al., 1997); (Kim et al., 2001). PKCζ may phosphorylate substrates that are directly involved in normalisation of neural tube closure or alternatively could play an indirect role through phosphorylation and regulation of other PKC isoforms {(Ziegler et al., 1999)}. Two obvious possibilities could explain the reduction in inositol efficacy following inhibition of PI3-kinase. First, the effect could be simply due to reduced activation of PKCζ as described for the specific PKCζ inhibitor. Second, activity of all groups of PKCs, like other members of the AGC kinase family, depends on phosphorylation of the T-loop in the kinase domain {(Parekh et al., 2000)}. This phosphorylation is catalysed by 3-phosphoinositide-dependent protein kinase-1 (PDK1) {(Chou et al., 1998), (Dutil et al., 1998)}, in a reaction that, as the name suggests, requires activity of PI3-kinase. PDK1 provides a functional link between activity of PI3-kinase and regulation of PKC signalling that could explain how inhibition of PI3-kinase reduces the magnitude of the PKC-dependent response to inositol in *curly tail* embryos.

4.3.4 Requirement for PKC isoforms during neural tube closure

The results in this chapter show that PKC isoforms are required for prevention of *curly tail* NTDs by inositol. However, in the absence of inositol, inhibition of PKC either by chemical or peptide inhibitors did not worsen the delay in PNP closure in cultured embryos. Nor did it have any adverse effect on neural tube closure in wild type embryos. Thus, it appears that inositol stimulates a novel action of PKC as opposed to an underlying function of PKC in normal neural tube closure. This hypothesis is supported by the lack of an NTD phenotype in null mutant mice for any of the PKC isoforms that are essential for prevention of NTDs. PKC γ null mice exhibit mild defects in learning tasks associated with function of the hippocampus (Abeliovich et al., 1993b), while PKC

β null mice display low alcohol tolerance but no apparent developmental disturbance (Harris et al., 1995). However, as compound mutant mice for these PKC isoforms have not been generated it remains possible that inhibition of both PKC β and γ in the same embryo might have detrimental effects on neurulation.

4.3.5 Which proteins are downstream of PKC activation?

The link between PKC activity and correction of PNP closure in *curly tail* embryos presumably involves phosphorylation of one or more target proteins. There are a number of potentially important PKC substrates that are proteins with direct cellular activity or transcription factors that regulate expression of further downstream proteins. Roles for PKC have been proposed in regulation of a variety of cellular processes including function of membrane proteins, cell cycle control and transcription of various genes (reviewed by (Nishizuka, 1986); (Hug and Sarre, 1993).

The major PKC substrate myristoylated alanine-rich C kinase (MARCKS) may be of particular interest in relation to neural tube closure as the null mutant mouse displays excencephaly (Blackshear et al., 1996b); (Chen et al., 1996). Moreover, knockout of a MARCKS family protein, known as MARCKS-related protein (MacMARCKS or F52) also causes NTDs, inducing both spina bifida and excencephaly (Arbuzova et al., 2002). In future work the identification of substrates for specific PKC isoforms might contribute towards understanding the function of PKC in prevention of NTDs by inositol.

CHAPTER 5

INOSITOL AND CELL PROLIFERATION

5.1 INTRODUCTION

5.1.1 Analysis of proliferation in the posterior neuropore region of developing *curly tail* embryos

As described in *Chapter 1*, NTDs in *ct/ct* embryos are associated with delay and failure of posterior neuropore (PNP) closure between the 24- and 32-somite stages (Copp, 1985; van Straaten et al. 1992). Copp et al. (1988) analysed cell proliferation in the developing caudal region of *ct/ct* embryos and observed decreased cell proliferation in the hindgut endoderm and notochord of embryos with severely enlarged PNP compared to those with normal or near-normal phenotypes. In contrast, neuroepithelial cell proliferation was the same in both groups. Recently, Ting et al (2003) also demonstrated reduced proliferation around the hindgut in embryos lacking *Grhl3* expression, a strong candidate for the *ct* gene. It is proposed that the resulting proliferation imbalance between dorsal and ventral tissues causes increased ventral curvature of the caudal region as the normal neuroepithelium is tethered via extracellular matrix to the underlying defective notochord and gut endoderm. Indeed, enhanced axial curvature was observed in affected *ct/ct* embryos in association with delayed PNP closure and spina bifida development (Brook et al., 1991b).

Further support for the general role of axial curvature in regulating neurulation comes from experiments in which the angle of axial curvature of the chick embryo was experimentally altered by culturing the embryo on curved (either concave or convex) substrates in vitro (van Straaten et al., 1992). Either increasing or decreasing the curvature led to delay in PNP closure and there was a direct correlation between the extent of delay and the degree of curvature. Thus, it seems possible to conclude that excessive curvature, both convex and concave, can oppose neurulation movements in vertebrate embryos. Any factor that alters the angle of curvature can be expected, therefore, to affect the rate of progression of neural fold closure.

It has been proposed that the NTDs in *curly tail* result from reduced expression of *Grhl3* (Auden et al., 2006). Thus, if reduced proliferation is indeed responsible for the failure of PNP closure in *curly tail* embryos it would also be predicted to be present in *Grhl3* mutant embryos. Indeed, when *in vivo* bromodeoxyuridine (BrdU) incorporation was used to examine cellular proliferation in the caudal regions of $Grhl3^{+/+}$ and $Grhl3^{-/-}$ embryos, Ting et al (2003) found that $Grhl3^{-/-}$ embryos at the 21-25-somite stage exhibited a consistent reduction in the number of proliferating cells in the ventral, but not the dorsal, half of this region, compared to wild-type controls. This reduction in BrdU incorporation was particularly evident around the hindgut endoderm, comparable to the findings in the *ct/ct* mice.

Two additional studies have detected abnormalities that may be related to proliferation defects in a subset of *ct/ct* embryos prior to the phenotypic divergence of embryos with normal and enlarged posterior neuropores (21-25-somite stages). Peeters et al. (Peeters et al., 1998) reported a greater proportion of S-phase nuclei in dorsal compared to ventral tissues of the caudal region, and Gofflot et al. (Gofflot et al., 1998) reported reduced expression of *Wnt5a*, a cell proliferation-related gene (Christian et al., 1991), in ventral mesoderm.

5.1.2 Protein Kinase C: a possible role in regulation of cell proliferation

A key outstanding question regarding the mechanism of action of inositol relates to whether the underlying proliferation defect is corrected, or whether inositol enhances closure through an alternative mechanism. Activation of PKC by TPA treatment of *curly tail* embryos *in vitro* has a protective effect on closure of the PNP which, like inositol supplementation, would lead to a reduction in frequency of spinal NTDs (Greene and Copp, 1997b). This suggests a possible mechanism for the prevention of spinal NTDs by inositol supplementation in which there is increased flux through the inositol/lipid cycle

leading to production of diacylglycerol (DAG) and activation of PKC. Moreover, the influence of PKC inhibitors in reversing the protective effect of inositol on closure of the PNP in *curly tail* embryos provides support for this idea (*Chapter 4*).

In several studies, PKC activity has been associated with regulation of cellular proliferation, suggesting that there could be a direct effect of inositol and PKC on the underlying cell proliferation defect in *curly tail* embryos. Effects of different isoforms on cell growth have been investigated by stable over-expression of individual PKC isoforms or through the use of PKC agonists that differentially activate specific members of the PKC family. Emerging evidence increasingly points to roles for PKCα, δ and ι in negative growth regulation and/or differentiation (Nakashima, 2002), and for PKC β, γ, and ε in positive control of cell growth (Yamamoto et al., 1998). Interestingly, different isoforms may have opposing effects in the same cell type. For example, over-expression of PKC βI in the R6 rat embryo fibroblast cell line resulted in enhanced growth (Suzuma et al., 2002), while over-expression of PKC α led to a marked inhibition of cell growth (Nakashima, 2002). It should also be emphasized that the actions of individual isoforms appear to be highly dependent on cellular background, and may differ between biological systems. For example, while over-expression of PKC βI in fibroblasts resulted in enhanced growth (Kuo et al., 1990), increased levels of this isoform in colon adenocarcinoma cells produced growth arrest and reduced tumorigenicity in nude mice (Yamamoto et al., 1998). Taken together, these findings suggest that the varying growth regulatory effects of PKC agonists in different systems may be the result of differential activation of individual members of the PKC family.

A full understanding of the function of PKC isoforms in control of the cell cycle under normal and pathological conditions requires clarification of the specific actions of these

molecules on cell cycle progression and on individual components of the cell cycle machinery. This is an emerging field and our current understanding of the molecular pathways is limited. However, accumulating evidence points to a role for member(s) of the PKC family in control of cell cycle progression at two sites: the G1 to S and the G2 to M transitions (Kampfer et al., 2001);(Thompson and Fields, 1996);(Yamamoto et al., 1998).

The aim of this chapter was to determine whether the protective effect of inositol on PNP closure in *ct/ct* embryos was mediated through correction of the proliferation defect in the hindgut endoderm.

5.2 RESULTS

Curly tail embryos were cultured in the presence of inositol, or PBS as a vehicle control, for 24 hours from E9.5, the period during which the neural tube is closing in the low spinal region of the mouse embryo. After culture, the extra-embryonic membranes were dissected away and each embryo was observed directly under a dissecting microscope. Crown-rump length and PNP length were measured and number of somites was noted. Any embryo which fell outside the 27-29 somite range was excluded. After the measurements were made, the embryo was cut into two parts at the level between somites 13 and 14. The rostral half was discarded and transverse histological sections of the posterior half were used to examine the neuroepithelium, notochord and hindgut endoderm by immunostaining to allow labelling indices to be determined in order to quantitate regional cell proliferation.

The population of dividing cells in the *curly tail* PNP was investigated in two ways: by immunostaining (i) for proliferating cell nuclear antigen (PCNA) and (ii) for phospho-histone H3. PCNA is expressed by proliferating cells and has a longer half-life than phospho-histone H3. Expression of PCNA is maintained through G1 and S phases of the cell cycle, labelling those cells about to enter or within the DNA synthetic phase. In contrast, phospho-histone H3 is detected only in cells that are currently in M-phase of the cell cycle.

5.2.1 PCNA analysis

PCNA-positive and total nuclei (visualised by DAPI staining) were counted within neural tube, notochord and gut endoderm at X 60 magnification (Fig. 5.1). The fraction of proliferating cells, as revealed by the proportion of cells in G1/S-phase, was calculated as the number of PCNA positive cells within a specific domain divided by the total number

of cells within the same domain. PNP length was determined by counting the number of serial sections between the first section with a clearly differentiated neural plate and the first section to show contact of the neural folds in the dorsal midline.

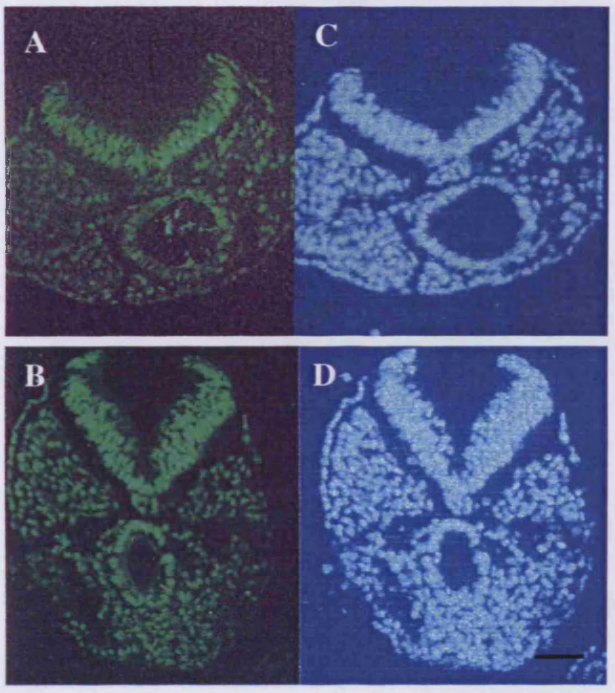

Figure 5.1 PCNA immunostaining in *curly tail* embryos after 24 hours culture from E8.5 to E9.5. **A**, **B**: immunohistochemistry for PCNA on transverse sections of caudal embryonic regions. Intensively green stained nuclei are those in S to G1 phase of the cell cycle. Section **A** is through the caudal part of the PNP, whereas section **B** is nearer the point of neural fold fusion **C**, **D**: DAPI staining, which labels all nuclei. Scale bar: 250 μm

Cell proliferation, is most rapid in neuroepithelium, less intense in hindgut endoderm and slowest in notochord (Fig. 5.2), as described previously (Copp et al., 1988c). No difference in PCNA labelling index, between inositol-treated and PBS-treated embryos was detected in the neuroepithelium or notochord. However, there was a significant increase in PCNA labelling index in the hindgut of inositol-treated embryos.

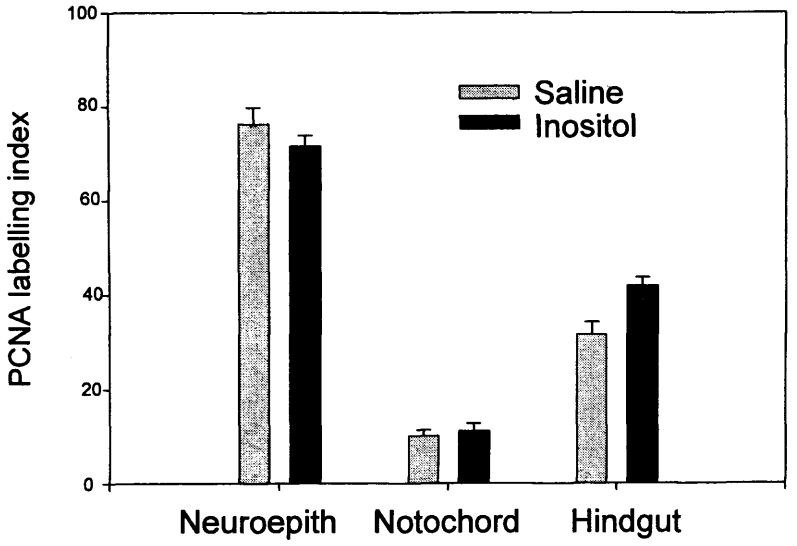

Figure 5.2 Inositol stimulates hindgut cell proliferation during NTD prevention. Cell proliferation was measured by PCNA labelling in tissues of the PNP region of cultured *curly tail* embryos a measure of cells in S-phase. Inositol significantly increased PCNA labelling index in the hindgut ($P<0.005$), whereas inositol has no significant effect on PCNA labelling in either neuroepithelium or notochord. Labelling index values are mean ± SEM of at least 10 embryos per treatment.

5.2.2 Phospho-histone 3 analysis

As an independent measure of cell proliferation marker, I also used phospho-histone H3 immunostaining in order to assess the proportion of cells in M-phase in the neuroepithelium, notochord and hindgut endoderm. Only a few cells were found to be labelled on each section (Fig. 5.3), in contrast to PCNA staining, reflecting the smaller proportion of cells in M-phase compared to G1/S phase.

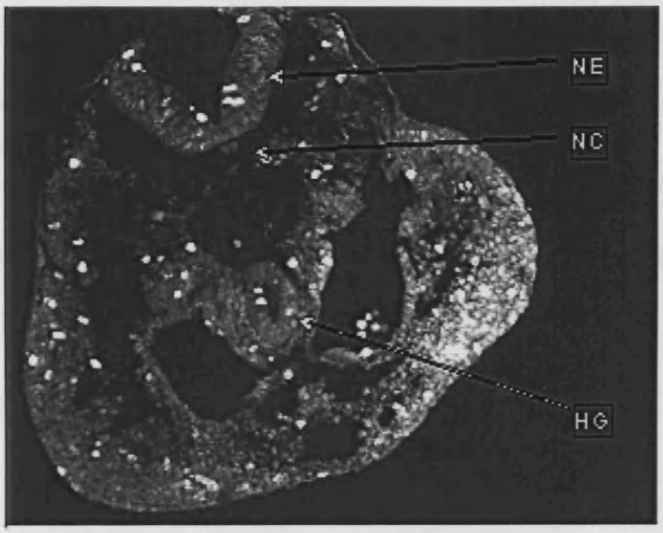

Figure 5.3 Phospho-histone H3-labelling in the PNP region of *curly tail* embryos after 24 hours culture from E8.5 to E9.5. Transverse section through the PNP, stained for phospho-histone H3 and photographed using epifluorescence plus Nomaski optics. Mitotic (H3-positive) nuclei appear as bright dots on the section. Note mitoses in neuroepithelium (NE) and hindgut (HG) but not in notochord (NC). Scale bar: 150 μm.

Inositol treatment caused a significant increase in the phospho-histone H3 labelling index in the hindgut (Fig. 5.4), suggesting a stimulatory effect on cell proliferation, as found by PCNA staining. In contrast, there was no significant effect of inositol treatment on phospho-histone H3-labelling in the neuroepithelium or notochord (Fig. 5.4). The increase in labeling of both a G1/S-phase and an M-phase marker strongly suggests that proliferation rate is indeed increased following inositol treatment, in association with prevention of PNP closure delay, and that this stimulation of cell proliferation specifically affects the hindgut epithelium.

A parallel set of cultures was performed to determine whether inhibition of a PKC isoform, PKC βI, that is required for prevention of NTDs (*Chapter 4*), is also essential for the effect of inositol on proliferation. As a control, another set of embryos were cultured in the presence of inositol plus the PKC ε inhibitor, that was found to be dispensable for

the inositol preventive effect (*Chapter 4*). Co-administration of the peptide inhibitor of PKC βI blocked the stimulatory effect of inositol on hindgut proliferation (Fig. 5.4), whereas the PKCε inhibitor had no effect. In the presence of inositol, neither inhibitor significantly altered proliferation in neuroepithelium or notochord. Hence, inositol overcomes the genetically-determined defect of cell proliferation in *curly tail* embryos, an effect that specifically requires activation of PKC ßI.

Figure 5.4 Cell proliferation was measured in tissues of the PNP region of cultured *curly tail* embryos using phospho-histone H3 as a measure of the proportion of cells in metaphase. Inositol significantly stimulates histone H3 labelling ($P<0.02$) in hindgut endoderm (hindgut 4th bar versus 1st bar), whereas inositol has no significant effect on histone H3 labelling in either neuroepithelium or notochord. In hindgut endoderm, inhibition of PKC ßI significantly reduces histone H3 labelling compared with inositol alone ($P<0.05$), whereas inhibition of PKCε has no significant effect ($P>0.05$). Blocking PKC ßI or ε has no significant effect on histone H3 labelling in neuroepithelium or notochord ($P>0.05$). No notochordal cells were positive for histone H3 in the presence of inositol and the PKC ßI inhibitor. Labelling indices are mean ± SEM of at least 10 embryos per treatment.

Figure 5.4

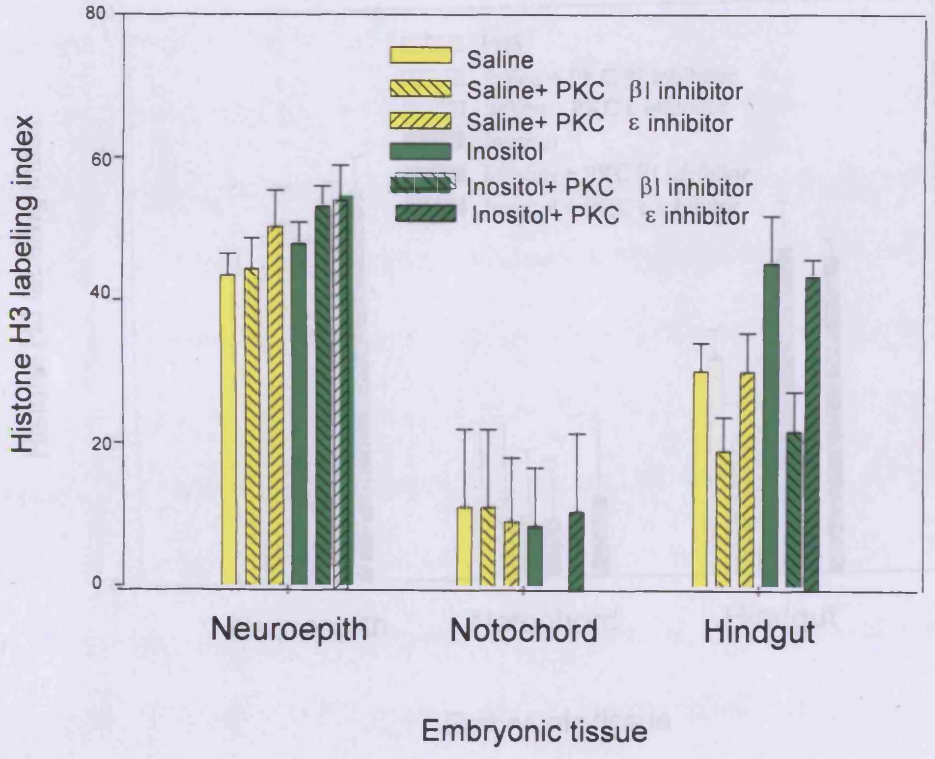
80
60
40
20
0
Histone H3 labeling index
Saline
Saline+ PKC βI inhibitor
Saline+ PKC ε inhibitor
Inositol
Inositol+ PKC βI inhibitor
Inositol+ PKC ε inhibitor
Neuroepith
Notochord
Hindgut
Embryonic tissue

5.3 DISCUSSION

In this chapter, I have demonstrated that inositol stimulates cell proliferation in the hindgut of *curly tail* embryos, reversing the imbalance of cell proliferation that is known to lead, via enhanced ventral curvature of the caudal region, to delay or failure of PNP closure (Copp et al., 1988c). Since the prevention of NTDs by inositol in *curly tail* mice requires specific PKC isoforms, it was predicted that these PKC isoforms would also be required for stimulation of the cell cycle in the embryonic hindgut. Indeed, I found that PKC ßI, which is required for correction of PNP closure, is also required for this stimulation of cell proliferation. S-phase entry/progression has been suggested to be defective in hindgut cells of *curly tail* embryos (Copp et al., 1988c), raising the possibility that activation of PKC ßI may reverse this defect, leading to 'rescue' of the mutant phenotype. Interestingly, inositol treatment of cells for 6 h resulted in nuclear translocation of PKC ßI as also observed for short-term exposure to TPA (see *Chapter 4*). This nuclear localization suggests that a role of PKC ßI in cell cycle regulation is plausible. However, PKC α also exhibits nuclear translocation in inositol-treated cells (both *curly tail* and non-mutant), but does not play an essential role in the prevention of NTDs, demonstrating that nuclear translocation *per se* is not sufficient to achieve the cell cycle regulation necessary for normalization of PNP closure.

PKC activation has previously been shown to regulate cell cycle progression in a wide variety of cell types (e.g., vascular endothelial cells (Kinsella et al., 1992), vascular smooth muscle cells (Suzuma et al., 2002), melanoma cells (Szalay et al., 2001), fibroblasts (Nakashima, 2002), keratinocytes (Suzuma et al., 2002), myeloid leukemia cells (Miyamoto et al., 2002), breast carcinoma cells (Kuo et al., 1990), and intestinal epithelial cells (Kuo et al., 1990). In particular, PKC ßI, the isoform required in prevention of *curly tail* defects, has been previously associated with increased cell cycle

entry. Its over-expression leads to increased proliferation of aortic endothelial cells, in contrast to PKC βII which has an inhibitory effect (Yamamoto et al., 1998). Similarly, proliferation of vascular smooth muscle cells is stimulated by PKC ßI, through increased S-phase entry, but inhibited by PKC ßII, through extension of S-phase (Yamamoto et al., 1998).

Furthermore, Aaltone et al (2006) in the study cell proliferation within transitional cell carcinoma, reported an increased PKC substrate phosphorylation which correlated with increased expression and nuclear localization of PKC βI in tumor samples and in cultures with increased PKC βI immunosignal. Moreover, they found that, in normal epithelium, a significant number of cells were negative for PKC βI nuclear localization, whereas in cancerous tissue, particularly in highly proliferative areas, nearly all nuclei were positive for immunosignal. Interestingly, in transitional cell carcinoma cultures, nuclear PKC βI appeared as a 65-kDa fragment, whereas in the cytoplasm, it was present as a full-size 79-kDa form, as demonstrated by La Porta et al. (La Porta, 1997) in a Western blotting study. There are earlier reports locating PKC-βI in the nucleus (Svensson et al., 2000); Raghunath et al. 2003), and it has been demonstrated that PKC-βI is transported to the nucleus and fragmented (Bastiaens and Jovin 1996). Others have shown a 65-kDa fragment for PKC βI in the membrane fraction of cells (al-Mazidi HA, 1998) and in whole-cell lysates (Pfaff et al. 1999; Redling et al. 2004). It is thus possible that PKC βI is fragmented during activation and that localization of the 65-kDa fragment in membranes (possibly nuclear membrane) is necessary for activation. Taken together, these reports confirm the likely involvement of PKC βI in cell cycle regulation, as also indicated by the findings presented in this thesis. In future work, it would be interesting to determine whether increased PKC substrate phosphorylation is correlated with PKC βI activity during inositol-mediated prevention, and whether there is a requirement for PKC βI

cleavage, in order to allow nuclear tranlocation and nuclear activity of PKC βI in *curly tail* embryos.

The possibility must also be considered that changes in PKC expression, as seen in this thesis, reflect changed activity of other cell signalling pathways affecting cell cycle progression. As an example, oncogenic Ras has been shown to up-regulate PKC α, c-myc oncogene induces increased PKC β expression, and wild-type p53 has been shown to suppress PKC γ expression (Barr et al. 1991; Delage et al. 1993; Zhan et al. 2005). Further studies would be needed to fully evaluate the role of such regulatory interactions during mouse neurulation.

The next step in studying the role of inositol in hindgut cell cycle regulation, would be to determine the effects of inositol treatment on phosphorylation of known PKC targets involved in proliferation, including the nuclear lamins and MARcKS (Aderem, 1992b). Specific isoforms of PKC regulate the transcriptional control of cyclin D1 (CCND1) expression, which plays a critical role in the progression of mammalian cells through the G1 phase of the cell cycle (Kampfer et al., 2001). G1 to S transition is a critical step because abnormalities in this step can enhance cell proliferation, genome instability, and tumor progression. However, the possibility that PKC βI, γ and ζ may stimulate cyclin D1 promoter activity in *curly tail* embryos remains to be investigated. Further studies might include the assessment of knockout mice lacking function of putative PKC targets, to determine whether double mutant combinations with *curly tail* would render the NTDs resistant to inositol-mediated prevention.

An interesting question that remains to be answered is why inositol stimulates PKC βI-dependent cell proliferation only in the hindgut endoderm and not in the neuroepithelium, which is an even more mitotically-active tissue than the hindgut. PKC βI, like all the PKC

isoforms studied, is expressed in all tissues of the caudal embryonic region (*Chapter 4*). Hence, selective PKC expression cannot explain the specific effect of inositol. It is possible that the sub-normal hindgut proliferation in *curly tail* embryos might reflect "available" capacity for a PKC βI-dependent response. Whereas non-mutant embryos have "maximal" hindgut proliferation and cannot be further stimulated. The same argument could apply to the neuroepithelium in *curly tail* embryos in which proliferation appears normal. This idea would predict that inositol would not stimulate enhanced proliferation in the hindgut of wild type embryos, a suggestion that could be addressed in future work.

Sections of *curly tail* mouse embryos at the stage just prior to PNP closure were recently analyzed by *in situ* hybridization for *Grhl3,* a compelling candidate for the *ct* gene. Specific expression in the hindgut endoderm was observed (Greene, unpublished data), raising the possibility that *Grhl3* expression may be required for an embryonic tissue to show a proliferative response to inositol. *Grhl3*$^{-/-}$ embryos do not respond to inositol treatment (Ting et al, 2003) in support of this idea. Currently, there is no information, however, on a possible molecular regulatory link between inositol/PKC βI, *Grhl3*, and the cell cycle machinery.

Last, Ting et al (2003) showed that *Grhl3*$^{-/-}$ embryos exhibit NTDs and growth retardation, particularly around the hindgut endoderm, results which are comparable to this chapter's finding in the *ct/ct* mice.

CHAPTER 6
GENERAL DISCUSSION

6. GENERAL DISCUSSION

Although some cases of human NTDs can be prevented by folic acid, there is increasing evidence that many cases do not respond. For instance, there was no major reduction in NTD frequency in the U.K. during the ten years after folic acid supplementation was introduced (Locksmith, 1998). The objective of this thesis was to investigate inositol as a possible treatment for folate-resistant NTDs, in order to prevent a larger proportion of human NTDs than is currently possible.

The specific aims of this theses were:

1. To use the *curly tail* mouse as a model of folate-resistant NTDs, in order to find the optimal dose and treatment method for maximal reduction of NTD frequency.
2. Determine the critical PKC isoformes that mediate the preventive effect of inositol in preventing folate-resistant NTDs, and determine the tissue-localisation of these PKC isoformes
3. Correlate inositol treatment/PKC activation with rates of cell proliferation in the caudal region of *curly tail* embryos, as their NTDs are being prevented.

The overall findings of this thesis are that exogenous inositol is able to prevent NTDs by stimulating specific PKC isoforms, and whose actively impinges upon the hindgut cell cycle in *curly tail* embryos to regulate spinal neurulation.

6.1 INOSITOL AND FOLATE-UNRESPONSIVE NTDS IN THE *CURLY TAIL* MUTANT.

Primary prevention of NTDs in humans became a reality when clinical trials demonstrated that folate-containing multivitamins (Smithells, 1998) and specifically folic acid (Wald, 1995) can reduce recurrence risk (a second NTD pregnancy in a family) and

perhaps reduce first occurrence of NTDs (Czeizel, 1995). Folate supplementation is underway by health advice in the UK, and by 'food fortification' in the USA (Simthells, 1998). Several major issues remain. First, little is known of the molecular basis of folate action in preventing NTDs. A genetic polymorphism in the methylene tetrahydrofolate reductase (MTHFR) gene is weakly related to NTD risk (Barber et al., 1999), but variants of other folate-related genes are not NTD-related. While several mouse models of NTD are folate-preventable (Barber, 1999), none result from mutation in folate-related genes. A second critical point is that a significant proportion of NTDs: around 30% in the MRC folate trial (Kirke, 1992), appear unresponsive to folic acid supplementation. The poor response to folate supplementation, with barely any decline in NTD frequency in the UK (Locksmith and Duff, 1998), and only a 19% decline in the USA (Kirke et al., 1992); (Honein et al., 2001), suggests adjunct therapies are needed to prevent folate-resistant NTDs.

While the mechanism of folic acid preventive action has not been studied in this thesis, new information has been gathered on the normalisation of neurulation, by inositol, in the folate-unresponsive NTDs of the *curly tail* mutant (Cogram et al., 2002; 2004). The thesis has shown that: (1) inositol is active in preventing these NTDs, with a greater potency of the D-*chiro*- than *myo*-inositol isoform; (2) inositol can prevent NTDs either via maternal administration or by a direct effect on the cultured embryo; (3) inositol stimulates PKC, an effect that is required for NTD prevention; (4) PKC isoforms $\beta 1$ and γ are required to mediate the inositol effect, whereas α, βII and all novel PKCs are dispensable; (5) inositol reverses the cell proliferation defect that was described previously in the hindgut of *curly tail* embryos (Copp et al., 1998); (6) the inositol effect is non-toxic during pregnancy, and not associated with an increase in other birth defects. In addition, (7) a case report of inositol usage in humans has been associated with a normal third pregnancy following

two consecutive NTDs while on folate therapy (Cavalli and Copp, 2002). It can be concluded, therefore, that inositol may offer a potential novel method for preventing human NTDs. As a result of these findings a pilot clinical trial is now in progress (Copp, Greene and others, unpublished). Hence this research, which began in a mouse genetic model, is being "translated" into clinical application.

6.2 *GRHL3, CT* AND INOSITOL PREVENTION

The effect of folate and inositol administration on pregnant *Grhl3*$^{+/-}$ females mated with *Grhl3*$^{+/-}$ males was studied by Ting et al (2003). Folate did not rescue spina bifida in *Grhl3*$^{-/-}$ embryos and, contrary to expectation neither did inositol (Ting et al., 2003). Hence, although the *Grhl3* gene seems very likely to be altered in *curly tail* mice, the *Grhl3* knockout appears inositol-resistant. Possible mechanisms for this difference in inositol responsiveness of *ct/ct* and *Grhl3*$^{-/-}$ mice could be related to the fact that *ct* is a hypomorphic allele of *Grhl3*, and therefore more easily normalised than the null *Grhl3* allele, or that the residual *Grhl3* function in *ct/ct* embryos enables inositol to exert its effect on hindgut cell proliferation, whereas complete loss of *Grhl3* renders the hindgut corresponsive to inositol (*Chapter 5*)

Interestingly, clones of *grh* mutant cells in the adult *Drosophila* epidermis have defects in pigmentation, cell polarity, and epidermal hair differentiation (Lee and Adler, 2004). Loss of *Grhl3* results in embryos with defective epidermal wound repair (Ting et al., 2005) suggesting that *Grhl3* may have other roles in epithelial fusion events. Furthermore, over-expression of *grh* in *Drosophila* embryos causes a failure in dorsal closure (Attardi, 1993), a widely studied epithelial fusion event that has many similarities to wound repair (Wood et al., 2002). Recent cellular and molecular studies have substantially increased our understanding of the elegant cascade of signalling events necessary for the wound

healing process (Frank, 2002). For example, several important biochemical mediators of cell migration and growth have been identified that are involved in tissue reformation (Frank, 2002).

Inositol receptor-mediated signal transduction can occur by various pathways to affect downstream targets which are ultimately involved in wound healing, planar cell polarity and cell proliferation. Activation of PKC stimulates the mitogen-activated protein kinase (MAPK) cascade leading to MAPK activation, and modulation of transcription factor activity. This can lead to changes in cell behaviour such as proliferation, as is seen in a variety of growth factor-mediated events of receptor tyrosine kinase stimulation (Liaw, 1995) Hence, stimulation of cell proliferation in curly tail embryos by inositol could act via this pathway. A prediction would be that intermediates in the MAPK pathway (e.g. ERK) would show increased phosphorylation after inositol stimulation. It is currently unknown how *Grhl3* might interact with such signalling pathways.

6.3 *CHIRO-* VS *MYO*-INOSITOL IN PREVENTING *CURLY TAIL* NTDs

The data presented in *Chapter 3* confirm previous observations supporting a role for inositol in neurulation, since administering inositol to *ct/ct* embryos reduces the incidence of spina bifida. In a prior study, relatively high doses of *myo*-inositol were required to give a protective effect (Greene and Copp, 1997a). However, here it has been shown that an alternative isomer, D-*chiro*-inositol, provides a similar protective effect at lower concentrations, indicating that it is more effective than *myo*-inositol at lowering the incidence of spinal neural tube defects. This observation has been shown in four independent experiments, involving three different routes of administration to the developing embryo. At present the reason for enhanced efficacy of D-*chiro*-inostitol is

not known. It is important to take into account the fact that *myo*-inositol converts to D-*chiro*-inositol *in vivo*, and since the D-*chiro*-form seems to be more effective, it would be very interesting to investigate the biosynthesis of D-*chiro*-inositol from *myo*-inositol *in curly* tail mice.

If it is to be used clinically, it is imperative that inositol is a safe treatment during pregnancy. It has been suggested that inositol treatment could stimulate uterine contractions during pregnancy (Colodny and Hoffman, 2000). The idea behind this suggestion is that oxytocin (a uterine stimulator) acts via activation of phospholipase C. However, although oxytocin is activated via the inositol phospholipid signalling pathway and can stimulate uterine contractions, there is no evidence to suggest that inositol supplementation has this effect. In the case report of a woman who took inositol in a third pregnancy, following two NTD pregnancies, there were no abnormal uterine contractions reported (Cavalli and Copp, 2002). Moreover, according to the data presented here (*Chapter 3*) there was no significant difference in pregnancy loss between the treated and the placebo groups of *curly tail* mice, suggesting that inositol is an effective and safe treatment, at least during mouse pregnancy.

6.4 INOSITOL ACTION IN NTDs IS MEDIATED VIA PKC

Using specific PKC inhibitors, both chemical and peptide in whole embryo culture, I showed in *Chapter 4* that the preventive effect of inositol is mediated via specific PKC isoforms. All PKC isoforms were detected, during mouse development from E9.5 to E17.5, in agreement with previous analysis of PKCs in E15–17 fetuses (Blackshear et al., 1996a). These findings contrast with a study of E10.5 embryos that detected PKCα, but not ßI, ßII, and ζ (Wilda et al., 2001). This difference may reflect the low abundance of

cPKCs on western blot, at early stages (E9.5–11.5) in particular (Cogram et al., 2004b), although all isoforms were clearly detectable in the PNP region by immunohistochemistry. Another member of the laboratory, Andrew Hynes, carried out the western blot analysis and found that each isoform exhibited a distinct distribution between sub-cellular fractions, which likely reflects the degree of activation. For instance, cPKCs were confined to the cytoplasmic fraction, suggesting minimal activation during undisturbed development, whereas aPKCs were present in membrane-associated and insoluble fractions throughout development, suggesting constitutive activation (Cogram et al., 2004b). This finding is consistent with a role for the cPKCs, ßI and γ, in mediating the preventive effect of inositol, since activation of these isoforms may be limiting in the absence of inositol, providing capacity for activation after treatment.

6.5 MOLECULAR BASIS OF THE REQUIREMENT FOR PKC AND PI3-KINASE

The normalizing effect of inositol on PNP closure was partially blocked by both the chemical inhibitor LY294002 and the peptide inhibitor specific for PKC ζ. LY294002 has activity against both PKC ζ and also the PI 3-kinase pathway, suggesting a possible role for the latter in the mechanism of inositol action. To test this idea, I performed preliminary experiments using the PI 3-kinase inhibitor wortmannin in whole embryo culture. Even at the low concentration of 0.1 μM, wortmannin proved extremely toxic to neurulation stage embryos, with all treated embryos dying during the culture period. Clearly, PI 3-kinase activity is essential for mouse embryonic development at this stage. The fact that LY294002 did not exhibit similar toxicity may indicate a more selective action, and the finding that specific inhibition of PKC ζ produced no general toxicity but a similar partial blockade of inositol-mediated prevention supports the idea that PKC ζ

and not the entire PI 3-kinase pathway was mainly affected in these studies.

6.6 IS PKC IMPLICATED IN THE MECHANISM OF NEURAL TUBE CLOSURE?

Several lines of evidence suggest that spinal neurulation *per se* does not depend on inositol and PKC activation and that defective closure in *curly tail* embryos is unlikely to result from an intrinsic deficiency in inositol or specific PKC isoforms. First, exposure of *curly tail* embryos to PKC inhibitors, in the absence of inositol, did not affect PNP closure. Second, uptake and incorporation of ^{3}H-inositol occurs similarly in cultured *curly tail* and non-mutant embryos, while inositol deficiency *in vitro* does not increase the penetrance of spinal NTDs in *curly tail* embryos (Copp et al., 1998) although the frequency of cranial NTDs is increased (Cockroft et al., 1992). Finally, mice with targeted inactivation of the genes encoding PKC, ß, γ and ζ do not exhibit neurulation defects (Erin, 2007).

6.7 CELLULAR ACTION OF INOSITOL

I propose that prevention of NTDs in *curly tail* mice by exogenous inositol operates via stimulation of the cell cycle in the embryonic hindgut, an effect that requires activation of specific PKC isoforms. I have shown in *Chapter 5* that cell proliferation, as judged by the percentage of cells positive for the S-phase marker PCNA, and the mitotic marker phospho-H3, is significantly increased in the hindgut endoderm of inositol-treated embryos, whereas proliferation in other tissues is not significantly affected. Hence, I have demonstrated that insoitol therapy, via PKC stimulation, corrects the cell behavioral defect that leads to spina bifida in the *curly tail* mouse (Copp et al., 1988c). Inositol is also reported to prevent NTDs in animal models of diabetes, whereas inositol deficiency causes cranial NTD, even in non-mutant mice (King, 2006). It remains to be determined

whether the protective action of inositol also involves stimulation of cell proliferation in these cases.

6.8 POSSIBLE INVOLVEMENT OF INS-DAG AND PKC IN CELL PROLIFERATION.

It is well known that many growth regulatory signals are directly or indirectly coupled to protein kinases intrinsic to, or associated with, the receptors for a variety of growth factors (Banan et al., 2004). These protein kinases have been subdivided into two major groups according to their ability to phosphorylate either serine or threonine residues of substrate proteins. Binding of growth factors to their surface receptors often leads to the activation of specific phospholipases (either by receptor-activated tyrosine phosphorylation or receptor coupling to GTP-binding proteins), which results in the elevation of intracellular calcium and diacylglycerol (DAG). It would be interesting in our system to measure levels of intracellular DAG in mutant *curly tail* and non-mutant mice. The purpose would be to understand the role of PKC subtypes in the regulation of cell proliferation in the hindgut endoderm of *curly tail* embryos, and to identify possible mechanisms by which inositol-DAG and PKC may contribute to the proliferation defect in *curly tail* mouse mutants.

The role of PKC in normal growth regulation is based on the idea that this enzyme family is the principal transducer for DAG that is generated upon activation of a phospholipase-linked cell surface receptor (Nishizuka, 1992). Intracellular levels of DAG have been considered a marker for the activation condition of PKC, since DAG initiates a broad range of cellular responses by activating PKC isoforms and other proteins (Nishizuka, 1992). One consequence of this regulation may be to modulate cell proliferation. Indeed, (Besson et al., 2004) demonstrated that PKC activity was an important factor regulating

cell proliferation and that a sustained increased in the cellular DAG and, PKC activity was required for cell cycle progression. Consequently, there is a possibility that normal hindgut cells have higher DAG levels and, therefore, a higher rate of proliferation compared with *curly tail* hindgut cells.

DAG binds to and activates PKC subtypes, together with acid phospholipids and Ca^{2+} (Nishizuka, 1992); (Dekker and Parker, 1994). Activation of PKC goes together with the tight association of the enzyme with membranes, a process referred to as 'translocation of PKC' (Anderson et. al. 1985; Wolf et al. 1985). Ca^{2+} -chelators promote the cytosolic localization of the cPKCs, whereas elevated Ca^{2+} levels encourage association of PKC with membranes. It is interesting to speculate that varying levels of Ca^{2+} may affect PKC translocation in *curly tail* cells and thus, affect cell proliferation.

6.9 PKC DOWNSTREAM TARGETS

In this thesis I have identified the PKC isoforms that mediate the preventive effect of inositol. The logical next step would be to identify proteins that may be phosphorylated by PKC during inositol action, for instance by comparing treated and untreated embryos. Below, I consider some possible PKC substrates, which are putative candidates to form part of the inositol-PKC preventive effect of inositol in *curly tail* embryos.

6.9.1 MAPK

Because of the possible link between *Grhl3* and MAPK, this would be the first candidate I would analyze. MAPK pathways are evolutionarily conserved kinase modules that link extracellular signals to the machinery that controls fundamental cellular processes such as growth, proliferation, differentiation, migration and apoptosis. There are two isoforms of MAPK, the p44 MAPK (Erk-1) and the p42 MAPK (Erk-2), which are expressed in most

cell types. The substrates of MAPK include nuclear transcription factors and non-nuclear substrates such as the protein, serine/threonine kinase p90sk and cytoskeletal proteins. EGF-induced nuclear transcriptional activation stimulates cell proliferation by initiating progression from G1 to S phase of the cell cycle. Another substrate of MAPK activation is phospholipase A_2 ($cPLA_2$) (Davis et al., 1994). $cPLA_2$ catalyzes the release of arachidonic acid from phospholipids in membranes and is one of the rate-limiting steps in the synthesis of prostaglandins. In cultured rabbit corneal endothelial cells, it was shown that the prostaglandin PGE_2 inhibits mitosis (Humblatt, 1994).

6.9.2 Myristoylated alanine-rich C kinase substrate

The major PKC substrate MARCKS may be of particular interest in relation to neural tube closure as the null mutant mouse displays exencephaly (Stumpo et al., 1995). Moreover, knockout of MARCKS family protein, MRP (also known as MARCKS-related protein, MacMARCK or F52) also causes NTDs, both spina bifida and exencephaly (Chen et al., 1996). The potential importance of these proteins is their involvement in cytoskeleton rearrangement and cell cycle.

6.9.3 Cyclins

Specific isoforms of PKC, such as βI and βII regulate the progression of cells through the G1 to S phases of the cell cycle. PKC is a potent activation of the transcriptional activity of the cyclin D1 promoter (Erin, 2007). PKC activation, leads to activation of *c-fos* and *c-jun*, which form AP-1 complexes and activate the cyclin D1 promoter. Expression of cyclin D1 then facilitates cell cycle progression from G1 to S phase and enhances proliferation. Activation of PKC also leads to activation of cyclin E expression, through mechanisms not fully understood. It could be interesting to determine if any of these

downstream PKC targets contribute to the enhancement of cell proliferation in inositol-treated *curly tail* mice.

6.9.4 Shuttle proteins

A considerable number of PKC substrates are localized in defined membrane compartments (Parker and Parkinson, 2001). It would be interesting, as a continuation of this thesis, to identify how these signals get into the nucleus to regulate gene expression, a mechanism that is unclear at present. The discovery of shuttle proteins capable of carrying information from the cytoplasm into the nucleus has improved the understanding on how growth factors regulate gene expression (Nigg, 1995). In the absence of stimuli, these shuttle proteins remain in the cytoplasm in the form of macromolecular complexes and translocate to the nucleus in response to cell stimulation, either because they are small enough to pass the nuclear membrane or because they carry special nuclear target sequences that facilitate nuclear uptake (Silver, 1990). The NFkappa β shuttle is especially interesting, as it appears to be regulated by PKC. The NFkappa β system is widespread in a variety of cell types and regulates many genes (Gilmore 1990). It consists of a heterotetradimer protein complex capable of interacting with a DNA regulatory sequence (the kβ sequence). NFkappa β is a transcriptional activator that participates in the induction of several genes, in particular those related to cell proliferation. NFkappa β is a possible PKC substrate whose translocation to the nucleus could be a possible rapid signalling pathway. It would be interesting to identify whether NFkappa β may be involved in the inositol-PKC protective effect in *curly tail*.

6.9.5 Lamins

Numerous studies indicate that gene transcription is regulated by the action of protein kinases in the nucleus. As described in *Chapter 4*, treatment of cells with TPA induces a

translocation of cytosolic PKC to nuclear fractions raising the possibility of that these isoforms are involved in nuclear function. Lamin B, a nuclear envelope protein, and topoisomerase I (Holaska et al., 2002) have been found to be substrates of PKC in vitro and be phsophorylated on serine or threonine in response of phorbol ester treatment of cells. Phosphorylation of lamin is escential for nuclear envelope disassembly during mitosis (Holaska et al., 2002) while phosphorylation of topoisomerase I relaxes positive DNA supercoiling, a crucial event for efficient gene transcription (Goss et al., 1994). There may be a role for nuclear PKCβI and γ in the regulation of cell growth via activation of nuclear lamins.

6.10 CONCLUSION AND PERSPECTIVES

Although there are still many unanswered questions about inositol lipid signaling, new techniques and tools are now available to study molecular cell physiology that should allow us to gain, in a relatively short time, a better understanding of their roles in the cell during the neurulation process. For example, in order to elucidate further the role of specific forms of PKC in modulating the expression of genes related to cellular growth control during neural development, it would be desirable to generate cell lines that stably produce elevated levels of a specific isoform of this enzyme. These cell lines would then provide a model system for studying cellular events occurring subsequent to activation of PKC γ and βI, by tumor promoters and other agents in an epithelial cell system.

Although there are also many unanswered questions about NTDs, this thesis work has established, a clear link between inositol lipid signaling and specific isoforms of PKC, PKC γ and βI, which together appear to integrate a complex network of signal transduction pathways. This PKC-related mechanism seems likely to control gene

expression and cell proliferation in the caudal region of inositol-treated *curly* embryos during rescue of NTDs.

7. REFERENCES

Abeliovich, A., Chen, C., Goda, Y., Silva, A.J., Stevens, C.F., Tonegawa, S., 1993a. Modified hippocampal long-term potentiation in PKCgamma mutant mice. Cell 75, 1253-1262.

Abeliovich, A., Paylor, R., Chen, C., Kim, J.J., Wehner, J.M., Tonegawa, S., 1993b. PKCgamma mutant mice exhibit mild deficits in spatial and contextual learning. Cell 75, 1263-1271.

Abramsky, L., Botting, B., Chapple, J., Stone, D., 1999. Has advice on periconceptional folate supplementation reduced neural-tube defects? Lancet 354, 998-999.

Aderem, A., 1992a. Signal transduction and the actin cytoskeleton: the roles of MARCKS and profilin. Trends Biochem.Sci. 17, 438-443.

Aderem, A., 1992b. The MARCKS brothers: a family of protein kinase C substrates. Cell 71, 713-716.

Adinolfi, M., Beck, S.E., Embury, S., Polani, P.E., Seller, M.J., 1976. Levels of alpha-fetoprotein in amniotic fluids of mice (curly tail) with neural tube defects. J.Med.Genet. 13, 511-513.

Adler, P.N., 2002. Planar signaling and morphogenesis in Drosophila. Developmental Cell 2, 525-535.

Akashi, M., Akazawa, S., Akazawa, M., Trocino, R., Hashimoto, M., Maeda, Y., Yamamoto, H., Kawasaki, E., Takino, H., Yokota, A., Nagataki, S., 1991. Effects of insulin and *myo*-inositol on embryo growth and development during early organogenesis in streptozocin-induced diabetic rats. Diabetes 40, 1574-1579.

al-Mazidi HA, K.L.F.D., 1998. The presence of an unusual PKC isozyme profile in rat liver cells., pp. 73-82.

Aley, K.O., Messing, R.O., Mochly-Rosen, D., Levine, J.D., 2000. Chronic hypersensitivity for inflammatory nociceptor sensitization mediated by the ε isozyme of protein kinase C. J.Neurosci. 20, 4680-4685.

Alvarez, I.S., Schoenwolf, G.C., 1992. Expansion of surface epithelium provides the major extrinsic force for bending of the neural plate. J.Exp.Zool. 261, 340-348.

Ang, S.-L., Rossant, J., 1994. *HNF*-3β is essential for node and notochord formation in mouse development. Cell 78, 561-574.

Antony, A.C., Hansen, D.K., 2000. Hypothesis: Folate-responsive neural tube defects and neurocristopathies. Teratology. 62, 42-50.

Arbuzova, A., Schmitz, A.A., Vergeres, G., 2002. Cross-talk unfolded: MARCKS proteins. Biochem.J 362, 1-12.

Asakai, R., Aoyama, Y., Fujimoto, T., 2002. Bisindolylmaleimide I and V inhibit necrosis induced by oxidative stress in a variety of cells including neurons. Neurosci.Res. 44, 297-304.

Asaoka, Y., Nakamura, S.-I., Yoshida, K., Nishizuka, Y., 1992. Protein kinase C, calcium and phospholipid degradation. Trends.Biochem.Sci. 17, 414-417.

Asplin, I., Galasko, G., Larner, J., 1993. *chiro*-Inositol deficiency and insulin resistance: a comparison of the *chiro*-inositol- and the *myo*-inositol-containing insulin mediators isolated from urine, hemodialysate, and muscle of control and type II diabetic subjects. Proc.Natl.Acad.Sci.USA 90, 5924-5928.

Atack, J.R., 1996. Inositol monophosphatase, the putative therapeutic target for lithium. Brain Res.Rev. 22, 183-190.

Auden, A., Caddy, J., Wilanowski, T., Ting, S.B., Cunningham, J.M., Jane, S.M., 2006. Spatial and temporal expression of the Grainyhead-like transcription factor family during murine development. Gene Expr.Patterns. 6, 964-970.

Axelrod, J.D., 2001. Unipolar membrane association of dishevelled mediates frizzled planar cell polarity signaling. Genes Dev. 15, 1182-1187.

Axelrod, J.D., Miller, J.R., Shulman, J.M., Moon, R.T., Perrimon, N., 1998. Differential recruitment of Dishevelled provides signaling specificity in the planar cell polarity and Wingless signaling pathways. Genes Dev. 12, 2610-2622.

Baker, L., Piddington, R., Goldman, A., Egler, J., Moehring, J., 1990. *Myo*-inositol and prostaglandins reverse the glucose inhibition of neural tube fusion in cultured mouse embryos. Diabetologia 33, 593-596.

Balogh, A., Csuka, O., Teplán, I., Kéri, G., 1995. Phosphatidylcholine could be the source of 1,2-DAG which activates protein kinase C in EGF-stimulated colon carcinoma cells (HT29). Cell.Signal. 7, 793-801.

Banan, A., Zhang, L.J., Farhadi, A., Fields, J.Z., Shaikh, M., Keshavarzian, A., 2004. PKC-β1 isoform activation is required for EGF-induced NF-kappaB inactivation and IkappaBα stabilization and protection of F-actin assembly and barrier function in enterocyte monolayers. Am.J.Physiol.Cell Physiol. 286, C723-C738.

Banker, G., 2003. Pars, PI 3-kinase, and the establishment of neuronal polarity. Cell 112, 4-5.

Bansal, V.S., Majerus, P.W., 1990. Phosphatidylinositol-derived precursors and signals. Annu.Rev.Cell Biol. 6, 41-67.

Barber, R.C., Lammer, E.J., Shaw, G.M., Greer, K.A., Finnell, R.H., 1999. The role of folate transport and metabolism in neural tube defect risk. Mol.Genet.Metab. 66, 1-9.

Bareggi, R., Grill, V., Zweyer, M., Narducci, P., Martelli, A.M., 1995. Distribution of the extended family of protein kinase C isoenzymes in fetal organs of mice: an immunohistochemical study. Cell Tissue Res. 280, 617-625.

Belmaker, R.H., Bersudsky, Y., Agam, G., Levine, J., Kofman, O., 1996. How does lithium work on manic depression? Clinical and psychological correlates of the inositol theory. Annu.Rev.Med. 47, 47-56.

Beltman, J., McCormick, F., Cook, S.J., 1996. The selective protein kinase C inhibitor, Ro-31-8220, inhibits mitogen-activated protein kinase phosphatase-1 (MKP-1)

expression, induces c-Jun expression, and activates Jun N-terminal kinase. J.Biol.Chem. 271, 27018-27024.

Berridge, M.J., 1987. Inositol trisphosphate and diacylglycerol: two interacting second messengers. Annu.Rev.Biochem. 56, 159-193.

Berridge, M.J., 1993. Inositol trisphosphate and calcium signalling. Nature 361, 315-325.

Berridge, M.J., 1995. Inositol trisphosphate and calcium signaling. Ann.NY Acad.Sci. 766, 31-43.

Besson, A., Gurian-West, M., Schmidt, A., Hall, A., Roberts, J.M., 2004. $p27^{Kip1}$ modulates cell migration through the regulation of RhoA activation. Genes Dev. 18, 862-876.

Blackshear, P.J., Lai, W.S., Tuttle, J.S., Stumpo, D.J., Kennington, E., Nairn, A.C., Sulik, K.K., 1996a. Developmental expression of MARCKS and protein kinase C in mice in relation to the exencephaly resulting from MARCKS deficiency. Dev.Brain Res. 96, 62-75.

Blackshear, P.J., Lai, W.S., Tuttle, J.S., Stumpo, D.J., Kennington, E., Nairn, A.C., Sulik, K.K., 1996b. Developmental expression of MARCKS and protein kinase C in mice in relation to the exencephaly resulting from MARCKS deficiency. Brain Res.Dev.Brain Res. 96, 62-75.

Blatter, B.M., Lafeber, A.B., Peters, P.W.J., Roeleveld, N., Verbeek, A.L.M., Gabreëls, F.J.M., 1997. Heterogeneity of spina bifida. Teratology. 55, 224-230.

Blobe, G.C., Stribling, S., Obeid, L.M., Hannun, Y.A., 1996. Protein kinase C isoenzymes: Regulation and function. Cancer Surv. 27, 213-248.

Botto, L.D., Mastroiacovo, P., 1998. Exploring gene-gene interactions in the etiology of neural tube defects. Clin.Genet 53, 456-459.

Boutros, M., Mlodzik, M., 1999. Dishevelled: at the crossroads of divergent intracellular signaling pathways. Mech.Dev. 83, 27-37.

Boutros, M., Paricio, N., Strutt, D.I., Mlodzik, M., 1998. Dishevelled activates JNK and discriminates between JNK pathways in planar polarity and wingless signaling. Cell 94, 109-118.

Brannon, M., Kimelman, D., 1996. Activation of *Siamois* by the *Wnt* pathway. Dev.Biol. 180, 344-347.

Braun, M.U., Mochly-Rosen, D., 2003. Opposing effects of δ- and zeta-protein kinase C isozymes on cardiac fibroblast proliferation: use of isozyme-selective inhibitors. J.Mol.Cell.Cardiol. 35, 895-903.

Brock, D.J.H., Sutcliffe, R.G., 1972. Early prenatal diagnosis of anencephaly. Lancet 2, 1252-1253.

Brook, F.A., Estibeiro, J.P., Copp, A.J., 1991a. Relationship between rate of embryonic development and the preponderance of cranial neural tube defects in females, p. 76.

Brook, F.A., Shum, A.S., van Straaten, H.W., Copp, A.J., 1991b. Curvature of the caudal region is responsible for failure of neural tube closure in the curly tail (ct) mouse embryo. Development 113, 671-678.

Buensuceso, C.S., Woodside, D., Huff, J.L., Plopper, G.E., O'Toole, T.E., 2001. The WD protein Rack1 mediates protein kinase C and integrin- dependent cell migration. J.Cell Sci. 114, 1691-1698.

Cadigan, K.M., Nusse, R., 1997. Wnt signaling: a common theme in animal development. Genes Dev. 11, 3286-3305.

Campbell, L.R., Dayton, D.H., Sohal, G.S., 1986. Neural tube defects: A review of human and animal studies on the etiology of neural tube defects. Teratology. 34, 171-187.

Campbell, S., Tsannatos, C., Pearce, J.M., 1984. The prenatal diagnosis of Joubert's syndrome of familial agenesis of the cerebellar vermis. Prenatal Diag. 4, 391-395.

Cantley, L.C., 2002. The phosphoinositide 3-kinase pathway. Science 296, 1655-1657.

Carmichael, S.L., Shaw, G.M., Schaffer, D.M., Laurent, C., Selvin, S., 2003. Dieting behaviors and risk of neural tube defects. Am.J.Epidemiol. 158, 1127-1131.

Carnac, G., Kodjabachian, L., Gurdon, J.B., Lemaire, P., 1996. The homeobox gene *Siamois* is a target of the Wnt dorsalisation pathway and triggers organiser activity in the absence of mesoderm. Development 122, 3055-3065.

Carter, C.O., 1974. Clues to the aetiology of neural tube malformations. Dev.Med.Child Neurol. 16 (Suppl.32), 3-15.

Casey, A.T.H., Kimmings, E.J., Kleinlugtebeld, A.D., Taylor, W.A.S., Harkness, W.F., Hayward, R.D., 1997. The long-term outlook for hydrocephalus in childhood - A ten-year cohort study of 155 patients. Pediatr.Neurosurg. 27, 63-70.

Castagna, M., Takai, Y., Kaibuchi, K., Sano, K., Kikkawa, U., Nishizuka, Y., 1982. Direct activation of calcium-activated, phospholipid-dependent protein kinase by tumor-promoting phorbol esters. J.Biol.Chem. 257, 7847-7851.

Catherine Chalmers, 2007. Genetically Ingeneered Mice, DeCordova Museum and Sculpture Park, Lincoln, MA, September 2, 2006 - January 7, 2007.

Cavalli, P., Copp, A.J., 2002. Inositol and folate-resistant neural tube defects. J.Med.Genet. 39, e5.

Chatkupt, S., Hol, F.A., Shugart, Y.Y., Geurds, M.P.A., Stenroos, E.S., Koenigsberger, M.R., Hamel, B.C.J., Johnson, W.G., Mariman, E.C.M., 1995. Absence of linkage between familial neural tube defects and PAX3 gene. J.Med.Genet. 32, 200-204.

Chen, C.H., Von Kessler, D.P., Park, W.J., Beachy, P.A., 1999. Nuclear trafficking of cubitus interruptus in the transcriptional regulation of hedgehog target gene expression. Cell 98, 305-316.

Chen, J., Chang, S., Duncan, S.A., Okano, H.J., Fishell, G., Aderem, A., 1996. Disruption of the MacMARCKS gene prevents cranial neural tube closure and results in anencephaly. Proc.Natl.Acad.Sci.USA 93, 6275-6279.

Chen, L., Hahn, H., Wu, G.Y., Chen, C.H., Liron, T., Schechtman, D., Cavallaro, G., Banci, L., Guo, Y.R., Bolli, R., Dorn, G.W., II, Mochly-Rosen, D., 2001. Opposing cardioprotective actions and parallel hypertrophic effects of delta PKC and epsilon PKC. Proc.Natl.Acad.Sci.USA 98, 11114-11119.

Chen, W.-H., Morriss-Kay, G.M., Copp, A.J., 1994. Prevention of spinal neural tube defects in the curly tail mouse mutant by a specific effect of retinoic acid. Dev.Dyn. 199, 93-102.

Chiang, C., Litingtung, Y., Lee, E., Young, K.E., Corden, J.L., Westphal, H., Beachy, P.A., 1996. Cyclopia and defective axial patterning in mice lacking *Sonic hedgehog* gene function. Nature 383, 407-413.

Chou, M.M., Hou, W., Johnson, J., Graham, L.K., Lee, M.H., Chen, C.S., Newton, A.C., Schaffhausen, B.S., Toker, A., 1998. Regulation of protein kinase C zeta by PI 3-kinase and PDK-1. Curr.Biol. 8, 1069-1077.

Christian, J.L., Gavin, B.J., McMahon, A.P., Moon, R.T., 1991. Isolation of cDNAs partially encoding four Xenopus Wnt-1/int-1-related proteins and characterization of their transient expression during embryonic development. Dev.Biol. 143, 230-234.

Cockroft, D.L., 1990. Dissection and culture of postimplantation embryos, in: A.J. Copp, D.L. Cockroft (Eds.), Postimplantation Mammalian Embryos: A Practical Approach. IRL Press, Oxford, pp. 15-40.

Cockroft, D.L., Brook, F.A., Copp, A.J., 1992. Inositol deficiency increases the susceptibility to neural tube defects of genetically predisposed (curly tail) mouse embryos in vitro. Teratology. 45, 223-232.

Coelho, C.N.D., Weber, J.A., Klein, N.W., Daniels, W.G., Hoagland, T.A., 1989. Whole rat embryos require methionine for neural tube closure when cultured on cow serum. J.Nutr. 119, 1716-1725.

Cogram, P., Hynes, A., Dunlevy, L.P., Greene, N.D., Copp, A.J., 2004a. Specific isoforms of protein kinase C are essential for prevention of folate-resistant neural tube defects by inositol. Hum.Mol.Genet. 13, 7-14.

Cohen, M.M., Jr., Shiota, K., 2002. Teratogenesis of holoprosencephaly. Am.J.Med.Genet. 109, 1-15.

Colas, J.F., Schoenwolf, G.C., 2001. Towards a cellular and molecular understanding of neurulation. Dev.Dyn. 221, 117-145.

Copp, A., Cogram, P., Fleming, A., Gerrelli, D., Henderson, D., Hynes, A., Kolatsi-Joannou, M., Murdoch, J., Ybot-Gonzalez, P., 1999. Neurulation and neural tube closure defects, in: R.S. Tuan, C.W. Lo (Eds.), Developmental Biology Protocols, Volume 1. Humana Press Inc, Totowa, New Jersey, pp. 135-160.

Copp, A.J., 1985. Relationship between timing of posterior neuropore closure and development of spinal neural tube defects in mutant (curly tail) and normal mouse embryos in culture. J.Embryol.Exp.Morphol. 88, 39-54.

Copp, A.J., Bernfield, M., 1988a. Accumulation of basement membrane-associated hyaluronate is reduced in the posterior neuropore region of mutant (curly tail) mouse embryos developing spinal neural tube defects. Dev.Biol. 130, 583-590.

Copp, A.J., Bernfield, M., 1988b. Glycosaminoglycans vary in accumulation along the neuraxis during spinal neurulation in the mouse embryo. Dev.Biol. 130, 573-582.

Copp, A.J., Bernfield, M., 1994. Etiology and pathogenesis of human neural tube defects: Insights from mouse models. Curr.Opin.Pediatr. 6, 624-631.

Copp, A.J., Brook, F.A., 1989. Does lumbosacral spina bifida arise by failure of neural folding or by defective canalisation? J.Med.Genet. 26, 160-166.

Copp, A.J., Brook, F.A., Estibeiro, J.P., Shum, A.S.W., Cockroft, D.L., 1990. The embryonic development of mammalian neural tube defects. Prog.Neurobiol. 35, 363-403.

Copp, A.J., Brook, F.A., Roberts, H.J., 1988a. A cell-type-specific abnormality of cell proliferation in mutant (curly tail) mouse embryos developing spinal neural tube defects. Development 104, 285-295.

Copp, A.J., Crolla, J.A., Brook, F.A., 1988c. Prevention of spinal neural tube defects in the mouse embryo by growth retardation during neurulation. Development 104, 297-303.

Copp, A.J., Estibeiro, J.P., Brook, F.A., Downs, K.M., 1992. Exogenous transferrin is taken up and localized by the neurulation-stage mouse embryo in vitro. Dev.Biol. 153, 312-323.

Copp, A.J., Fleming, A., Greene, N.D.E., 1998. Embryonic mechanisms underlying the prevention of neural tube defects by vitamins. Ment.Retard.Dev.Disabil.Res.Rev. 4, 264-268.

Copp, A.J., Greene, N.D.E., Murdoch, J.N., 2003. The genetic basis of mammalian neurulation. Nat.Rev.Genet. 4, 784-793.

Copp, A.J., Seller, M.J., Polani, P.E., 1982. Neural tube development in mutant (curly tail) and normal mouse embryos: the timing of posterior neuropore closure in vivo and in vitro. J.Embryol.Exp.Morphol. 69, 151-167.

Costanzo, R., Watterson, R.L., Schoenwolf, G.C., 1982. Evidence that secondary neurulation occurs autonomously in the chick embryo. J.Exp.Zool. 219, 233-240.

Criley, B.B., 1969. Analysis of the embryonic sources and mechanisms of development of posterior levels of chick neural tubes. J.Morph. 128, 465-501.

Curtin, J.A., Quint, E., Tsipouri, V., Arkell, R.M., Cattanach, B., Copp, A.J., Fisher, E.M., Nolan, P.M., Steel, K.P., Brown, S.D.M., Gray, I.C., Murdoch, J.N., 2003. Mutation of *Celsr1* disrupts planar polarity of inner ear hair cells and causes severe neural tube defects in the mouse. Curr.Biol. 13, 1-20.

Czeizel, A.E., 1995. Congenital abnormalities are preventable. Epidemiology 6, 205-207.

Czeizel, A.E., Dudás, I., 1992. Prevention of the first occurrence of neural-tube defects by periconceptional vitamin supplementation. N.Engl.J.Med. 327, 1832-1835.

Davidson, L.A., Keller, R.E., 1999. Neural tube closure in *Xenopus* laevis involves medial migration, directed protrusive activity, cell intercalation and convergent extension. Development 126, 4547-4556.

Davis, S., Gale, N.W., Aldrich, T.H., Maisonpierre, P.C., Lhotak, V., Pawson, T., Goldfarb, M., Yancopoulos, G.D., 1994. Ligands for EPH-related receptor tyrosine kinases that require membrane attachment or clustering for activity. Science 266, 816-819.

Dekker, L.V., Parker, P.J., 1994. Protein kinase C, a question of specificity. Trends.Biochem.Sci. 19, 73-77.

Derossi, D., Joliot, A.H., Chassaing, G., Prochiantz, A., 1994. The third helix of the antennapedia homeodomain translocates through biological membranes. J.Biol.Chem. 269, 10444-10450.

Disatnik, M.H., Boutet, S.C., Lee, C.H., Mochly-Rosen, D., Rando, T.A., 2002. Sequential activation of individual PKC isozymes in integrin-mediated muscle cell spreading: a role for MARCKS in an integrin signaling pathway. J.Cell Sci. 115, 2151-2163.

Divecha, N., Irvine, R.F., 1995. Phospholipid signaling. Cell 80, 269-278.

Djiane, A., Riou, J.F., Umbhauer, M., Boucaut, J.C., Shi, D.L., 2000. Role of *frizzled 7* in the regulation of convergent extension movements during gastrulation in *Xenopus laevis*. Development 127, 3091-3100.

Dorn, G.W., Souroujon, M.C., Liron, T., Chen, C.H., Gray, M.O., Zhou, H.Z., Csukai, M., Wu, G., Lorenz, J.N., Mochly-Rosen, D., 1999. Sustained in vivo cardiac protection by a rationally designed peptide that causes epsilon protein kinase C translocation. Proc.Natl.Acad.Sci.USA 96, 12798-12803.

Dutil, E.M., Toker, A., Newton, A.C., 1998. Regulation of conventional protein kinase C isozymes by phosphoinositide-dependent kinase 1 (PDK-1). Curr.Biol. 8, 1366-1375.

Edmonds, L.D., James, L.M., 1993. Temporal trends in the birth prevalence of selected congenital malforamtions in the Birth Defects Monitoring Progam/Commission on Professional and Hospital Activities, 1979-1989. Teratology. 48, 647-649.

Embury, S., Seller, M.J., Adinolfi, M., Polani, P.E., 1979. Neural tube defects in curly-tail mice. I. Incidence and expression. Proc.R.Soc.Lond.B 206, 85-94.

Estibeiro, J.P., Copp, A.J., 1990. A possible interaction between retarded splotch and curly tail, p. 245.

Fan, H., Oro, A.E., Scott, M.P., Khavari, P.A., 1997. Induction of basal cell carcinoma features in transgenic human skin expressing Sonic Hedgehog. Nature Med. 3, 788-792.

Fleming, A., Copp, A.J., 2000. A genetic risk factor for mouse neural tube defects: defining the embryonic basis. Hum.Mol.Genet. 9, 575-581.

Flynn, T.J., Friedman, L., Black, T.N., Klein, N.W., 1987. Methionine and iron as growth factors for rat embryos cultured in canine serum. J.Exp.Zool. 244, 319-324.

Geelen, J.A.G., Langman, J., 1979. Ultrastructural observations on closure of the neural tube in the mouse. Anat.Embryol. 156, 73-88.

Glanville, N.T., Cook, H.W., 1992. Folic acid and prevention of neural tube defects. Can.Med.Assoc.J. 146, 39.

Gofflot, F., Hall, M., Morriss-Kay, G.M., 1998. Genetic patterning of the posterior neuropore region of curly tail mouse embryos: deficiency of Wnt5a expression. Int.J.Dev.Biol. 42, 637-644.

Golden, J.A., Chernoff, G.F., 1993. Intermittent pattern of neural tube closure in two strains of mice. Teratology. 47, 73-80.

Golden, J.A., Chernoff, G.F., 1995. Multiple sites of anterior neural tube closure in humans: Evidence from anterior neural tube defects (anencephaly). Pediatrics 95, 506-510.

Goodrich, L.V., Milenkovic, L., Higgins, K.M., Scott, M.P., 1997. Altered neural cell fates and medulloblastoma in mouse *patched* mutants. Science 277, 1109-1113.

Goss, V.L., Hocevar, B.A., Thompson, L.J., Stratton, C.A., Burns, D.J., Fields, A.P., 1994. Identification of nuclear beta II protein kinase C as a mitotic lamin kinase. J.Biol.Chem. 269, 19074-19080.

Greene, N.D.E., Copp, A.J., 1997a. Inositol prevents folate-resistant neural tube defects in the mouse. Nature Med. 3, 60-66.

Greene, N.D.E., Copp, A.J., 1997b. Inositol prevents folate-resistant neural tube defects in the mouse . Nature Med. 3, 60-66.

Greene, N.D.E., Gerrelli, D., Van Straaten, H.W.M., Copp, A.J., 1998. Abnormalities of floor plate, notochord and somite differentiation in the *loop-tail* (*Lp*) mouse: a model of severe neural tube defects. Mech.Dev. 73, 59-72.

Haigo, S.L., Hildebrand, J.D., Harland, R.M., Wallingford, J.B., 2003. Shroom induces apical constriction and is required for hingepoint formation during neural tube closure. Curr.Biol 13, 2125-2137.

Hamblet, N.S., Lijam, N., Ruiz-Lozano, P., Wang, J., Yang, Y., Luo, Z., Mei, L., Chien, K.R., Sussman, D.J., Wynshaw-Boris, A., 2002. Dishevelled 2 is essential for cardiac outflow tract development, somite segmentation and neural tube closure. Development 129, 5827-5838.

Harris, M.J., Juriloff, D.M., 2007c. Mouse mutants with neural tube closure defects and their role in understanding human neural tube defects. Birth Defects Res.A Clin Mol.Teratol. 79, 187-210.

Harris, M.J., Juriloff, D.M., 2007a. Mouse mutants with neural tube closure defects and their role in understanding human neural tube defects. Birth Defects Res.A Clin Mol.Teratol. 79, 187-210.

Harris, M.J., Juriloff, D.M., 2007b. Mouse mutants with neural tube closure defects and their role in understanding human neural tube defects. Birth Defects Res.A Clin Mol.Teratol. 79, 187-210.

Harris, R.A., McQuilkin, S.J., Paylor, R., Abeliovich, A., Tonegawa, S., Wehner, J.M., 1995. Mutant mice lacking the gamma isoform of protein kinase C show decreased behavioral actions of ethanol and altered function of gamma-aminobutyrate type A receptors. Proc.Natl.Acad.Sci.USA 92, 3658-3662.

Heid, M.K., Bills, N.D., Hinrichs, S.H., Clifford, A.J., 1992. Folate deficiency alone does not produce neural tube defects in mice. J.Nutr. 122, 888-894.

Heidenreich, K.A., Zeppelin, T., Robinson, L.J., 1993. Insulin and insulin-like growth factor I induce c-fos expression in postmitotic neurons by a protein kinase C-dependent pathway. J.Biol.Chem. 268, 14663-14670.

Heisenberg, C.P., Tada, M., Rauch, G.J., Saúde, L., Concha, M.L., Geisler, R., Stemple, D.L., Smith, J.C., Wilson, S.W., 2000. Silberblick/Wnt11 mediates convergent extension movements during zebrafish gastrulation. Nature 405, 76-81.

Hildebrand, J.D., Soriano, P., 1999. Shroom, a PDZ domain-containing actin-binding protein, is required for neural tube morphogenesis in mice. Cell 99, 485-497.

Hinchliffe, K., Irvine, R., 1997. Signal transduction - Inositol lipid pathways turn turtle. Nature 390, 123-124.

Hirai, T., Chida, K., 2003. Protein kinase Czeta (PKCzeta): Activation mechanisms and cellular functions. J.Biochem.(Tokyo) 133, 1-7.

Hol, F.A., Hamel, B.C.J., Geurds, M.P.A., Mullaart, R.A., Barr, F.G., Macina, R.A., Mariman, E.C.M., 1995. A frameshift mutation in the gene for PAX3 in a girl with spina bifida and mild signs of Waardenburg syndrome. J.Med.Genet. 32, 52-56.

Holaska, J.M., Wilson, K.L., Mansharamani, M., 2002. The nuclear envelope, lamins and nuclear assembly. Curr.Opin.Cell Biol. 14, 357-364.

Honein, M.A., Paulozzi, L.J., Mathews, T.J., Erickson, J.D., Wong, L.Y.C., 2001. Impact of folic acid fortification of the US food supply on the occurrence of neural tube defects. JAMA 285, 2981-2986.

Hoyle, C., Henderson, D.J., Matthews, D.J., Copp, A.J., 1996. Transferrin and its receptor in the development of genetically-determined neural tube defects in the mouse embryo. Dev.Dyn. 207, 35-46.

Huang, Y., Roelink, H., McKnight, G.S., 2002. Protein kinase A deficiency causes axially localized neural tube defects in mice. J.Biol.Chem. 277, 19889-19896.

Hug, H., Sarre, T.F., 1993. Protein kinase C isoenzymes: divergence in signal transduction? Biochem.J. 291, 329-343.

Hui, C., Joyner, A.L., 1993. A mouse model of Greig cephalopolysyndactyly syndrome: The *extra-toes*^{J} mutation contains an intragenic deletion of the *Gli3* gene. Nature Genet. 3, 241-246.

Hunter, T., 1995. Protein kinases and phosphatases: The yin and yang of protein phosphorylation and signaling. Cell 80, 225-236.

Jacobson, A.G., Tam, P.P.L., 1982. Cephalic neurulation in the mouse embryo analyzed by SEM and morphometry. Anat.Rec. 203, 375-396.

Jaken, S., Parker, P.J., 2000. Protein kinase C binding partners. BioEssays 22, 245-254.

Johnson, J.A., Gray, M.O., Chen, C.H., Mochly-Rosen, D., 1996. A protein kinase C translocation inhibitor as an isozyme-selective antagonist of cardiac function. J.Biol.Chem. 271, 24962-24966.

Joosten, P.H., Hol, F.A., van Beersum, S.E., Peters, H., Hamel, B.C., Afink, G.B., Van Zoelen, E.J., Mariman, E.C., 1998. Altered regulation of platelet-derived growth factor receptor-alpha gene-transcription in vitro by spina bifida-associated mutant Pax1 proteins. Proc.Natl.Acad.Sci.U.S.A 95, 14459-14463.

Juriloff, D.M., Gunn, T.M., Harris, M.J., Mah, D.G., Wu, M.K., Dewell, S.L., 2001. Multifactorial genetics of exencephaly in SELH/Bc mice. Teratology. 64, 189-200.

Juriloff, D.M., Harris, M.J., 2000. Mouse models for neural tube closure defects. Hum.Mol.Genet. 9, 993-1000.

Juriloff, D.M., Harris, M.J., Tom, C., MacDonald, K.B., 1991. Normal mouse strains differ in the site of initiation of closure of the cranial neural tube. Teratology. 44, 225-233.

Justice, M.J., 2000. Capitalizing on large-scale mouse mutagenesis screens. Nat Rev.Genet. 1, 109-115.

Justice, M.J., Noveroske, J.K., Weber, J.S., Zheng, B.H., Bradley, A., 1999. Mouse ENU mutagenesis. Hum.Mol.Genet. 8, 1955-1963.

Kampfer, S., Windegger, M., Hochholdinger, F., Schwaiger, W., Pestell, R.G., Baier, G., Grunicke, H.H., Uberall, F., 2001. Protein kinase C isoforms involved in the transcriptional activation of cyclin D1 by transforming Ha-Ras. J.Biol.Chem. 276, 42834-42842.

Karfunkel, P., 1974. The mechanisms of neural tube formation. Int.Rev.Cytol. 38, 245-271.

Kauffman, S.L., 1968. Lengthening of the generation cycle during embryonic differentiation of the mouse neural tube. Exp.Cell Res. 49, 420-424.

Keller, R., 2002. Shaping the vertebrate body plan by polarized embryonic cell movements. Science 298, 1950-1954.

Keller, R., Shih, J., Sater, A.K., Moreno, C., 1992. Planar induction of convergence and extension of the neural plate by the organizer of *Xenopus*. Dev.Dyn. 193, 218-234.

Khandelwal, M., Reece, E.A., Wu, Y.K., Borenstein, M., 1998. Dietary myo-inositol therapy in hyperglycemia-induced embryopathy. Teratology. 57, 79-84.

Kibar, Z., Vogan, K.J., Groulx, N., Justice, M.J., Underhill, D.A., Gros, P., 2001. *Ltap*, a mammalian homolog of *Drosophila Strabismus/Van Gogh*, is altered in the mouse neural tube mutant Loop-tail. Nature Genet. 28, 251-255.

Kim, M.S., Lim, W.K., Cha, J.G., An, N.H., Yoo, S.J., Park, J.H., Kim, H.M., Lee, Y.M., 2001. The activation of PI 3-K and PKC zeta in PMA-induced differentiation of HL-60 cells. Cancer Lett. 171, 79-85.

Kinsella, J.L., Grant, D.S., Weeks, B.S., Kleinman, H.K., 1992. Protein kinase C regulates endothelial cell tube formation on basement membrane matrix, Matrigel. Exp.Cell Res. 199, 56-62.

Kirke, P.N., Daly, L.E., Elwood, J.H., 1992. A randomised trial of low dose folic acid to prevent neural tube defects. Arch.Dis.Child. 67, 1442-1446.

Koleske, A.J., Gifford, A.M., Scott, M.L., Nee, M., Bronson, R.T., Miczek, K.A., Baltimore, D., 1998. Essential roles for the Abl and Arg tyrosine kinases in neurulation. Neuron 21, 1259-1272.

Kubow, S., Yaylayan, V., Mandeville, S., 1993. Protection by acetylsalicylic acid against hyperglycemia-induced glycation and neural tube defects in cultured early somite mouse embryos. Diabetes Res. 22, 145-158.

Kühl, M., Sheldahl, L.C., Park, M., Miller, J.R., Moon, R.T., 2000. The Wnt/Ca^{2+} pathway - a new vertebrate Wnt signaling pathway takes shape. Trends Genet. 16, 279-283.

Kuo, J.F., Shoji, M., Kiss, Z., Girard, P.R., Deli, E., Oishi, K., Vogler, W.R., 1990. Protein kinase C in cell growth and differentiation. Adv.Exp.Med.Biol. 255, 9-20.

Langman, J., Guerrant, R.L., Freeman, B.G., 1967. Behaviour of neuro-epithelial cells during closure of the neural tube. J.Comp.Neurol. 127, 399-412.

Larner, J., 2001. D-chiro-inositol in insulin action and insulin resistance - Old-fashioned biochemistry still at work. IUBMB Life 51, 139-148.

Lee, H., Adler, P.N., 2004. The grainy head transcription factor is essential for the function of the frizzled pathway in the Drosophila wing. Mech.Dev. 121, 37-49.

Lemire, R.J., 1988. Neural tube defects. JAMA 259, 558-562.

Levine, J., Aviram, A., Holan, A., Ring, A., Barak, Y., Belmaker, R.H., 1997. Inositol treatment of autism. J.Neural Transm. 104, 307-310.

Limpach, A., Dalton, M., Miles, R., Gadson, P., 2000. Homocysteine inhibits retinoic acid synthesis: A mechanism for homocysteine-induced congenital defects. Exp.Cell Res. 260, 166-174.

Liu, Y.H., Kundu, R., Wu, L., Luo, W., Ignelzi, M.A., Jr., Snead, M.L., Maxson, R.E., Jr., 1995. Premature suture closure and ectopic cranial bone in mice expressing *Msx2* transgenes in the developing skull. Proc.Natl.Acad.Sci.USA 92, 6137-6141.

Locksmith, G.J., Duff, P., 1998. Preventing neural tube defects: The importance of periconceptional folic acid supplements. Obstet.Gynecol. 91, 1027-1034.

MacDonald, K.B., Juriloff, D.M., Harris, M.J., 1989. Developmental study of neural tube closure in a mouse stock with a high incidence of exencephaly. Teratology. 39, 195-213.

Mace, K.A., Pearson, J.C., McGinnis, W., 2005. An epidermal barrier wound repair pathway in *Drosophila* is mediated by *grainy head*. Science 308, 381-385.

Mackay, K., Mochly-Rosen, D., 2001. Localization, anchoring, and functions of protein kinase C isozymes in the heart. J.Mol.Cell.Cardiol. 33, 1301-1307.

Majerus, P.W., 1992. Inositol phosphate biochemistry. Annu.Rev.Biochem. 61, 225-250.

Marigo, V., Johnson, R.L., Vortkamp, A., Tabin, C.J., 1996. Sonic hedgehog differentially regulates expression of *GLI* and *GLI3* during limb development. Dev.Biol. 180, 273-283.

Martin, J.V., Nagele, R.G., Lee, H., 1994. Temporal changes in intracellular free calcium levels in the developing neuroepithelium during neurulation in the chick. Comp.Biochem.Physiol.[A] 107A, 655-659.

Martiny-Baron, G., Kazanietz, M.G., Mischak, H., Blumberg, P.M., Kochs, G., Hug, H., Marme, D., Schachtele, C., 1993. Selective inhibition of protein kinase C isozymes by the indolocarbazole Go 6976. J.Biol.Chem. 268, 9194-9197.

Mathur, A., Vallano, M.L., 2000. 2,2',3,3',4,4'-Hexahydroxy-1,1'-biphenyl-6,6'-dimethanol dimethyl ether (HBDDE)-induced neuronal apoptosis independent of classical protein kinase C alpha or gamma inhibition. Biochem.Pharmacol. 60, 809-815.

Matise, M.P., Epstein, D.J., Park, H.L., Platt, K.A., Joyner, A.L., 1998. Gli2 is required for induction of floor plate and adjacent cells, but not most ventral neurons in the mouse central nervous system. Development 125, 2759-2770.

Medina, A., Reintsch, W., Steinbeisser, H., 2000. *Xenopus frizzled 7* can act in canonical and non-canonical Wnt signaling pathways: implications on early patterning and morphogenesis. Mech.Dev. 92, 227-237.

Medina, A., Steinbeisser, H., 2000. Interaction of frizzled 7 and dishevelled in *Xenopus*. Dev.Dyn. 218, 671-680.

Milenkovic, L., Goodrich, L.V., Higgins, K.M., Scott, M.P., 1999. Mouse *patched1* controls body size determination and limb patterning. Development 126, 4431-4440.

Miller, J.W., Nadeau, M.R., Smith, J., Smith, D., Selhub, J., 1994. Folate-deficiency-induced homocysteinaemia in rats: disruption of S-adenosylmethionine's co-ordinate regulation of homocysteine metabolism. Biochem.J 298 (Pt 2), 415-419.

Mitchell, K.J., Pinson, K.I., Kelly, O.G., Brennan, J., Zupicich, L., Scherz, P., Leighton, P.A., Goodrich, L.V., Lu, X.W., Avery, B.J., Tate, P., Dill, K., Pangilinan, E., Wakenight, P., Tessier-Lavigne, M., Skarnes, W.C., 2001. Functional analysis of secreted and transmembrane proteins critical to mouse development. Nature Genet. 28, 241-249.

Miyamoto, A., Nakayama, K., Imaki, H., Hirose, S., Jiang, Y., Abe, M., Tsukiyama, T., Nagahama, H., Ohno, S., Hatakeyama, S., Nakayama, K.I., 2002. Increased proliferation of B cells and auto-immunity in mice lacking protein kinase C delta. Nature 416, 865-869.

Mlodzik, M., 2002. Planar cell polarization: do the same mechanisms regulate Drosophila tissue polarity and vertebrate gastrulation? Trends Genet. 18, 564-571.

Mochly-Rosen, D., Kauvar, L.M., 2000. Pharmacological regulation of network kinetics by protein kinase C localization. Semin.Immunol. 12, 55-61.

Mooij, P.N., Thomas, C.M., Doesburg, W.H., Eskes, T.K., 1993. The effects of periconceptional folic acid and vitamin supplementation on maternal folate levels and on neurulating hamster embryos in vivo. Int.J.Vitam.Nutr.Res. 63, 212-216.

Moran, D., Rice, R.W., 1975. An ultrastructural examination of the role of cell membrane surface coat material during neurulation. J.Cell Biol. 64, 172-181.

Morris-Wiman, J., Brinkley, L.L., 1990. Changes in mesenchymal cell and hyaluronate distribution correlate with in vivo elevation of the mouse mesencephalic neural folds. Anat.Rec. 226, 383-395.

Morriss, G.M., Solursh, M., 1978. The role of primary mesenchyme in normal and abnormal morphogenesis of mammalian neural folds. Zoon 6, 33-38.

Morriss-Kay, G., Wood, H., Chen, W.-H., 1994. Normal neurulation in mammals. Ciba.Found.Symp. 181, 51-63.

Morriss-Kay, G.M., 1981. Growth and development of pattern in the cranial neural epithelium of rat embryos during neurulation. J.Embryol.Exp.Morphol. 65 (Suppl.), 225-241.

Morriss-Kay, G.M., Tuckett, F., 1985. The role of microfilaments in cranial neurulation in rat embryos: effects of short-term exposure to cytochalasin D. J.Embryol.Exp.Morphol. 88, 333-348.

Motoyama, J., Liu, J., Mo, R., Ding, Q., Post, M., Hui, C.C., 1998. Essential function of Gli2 and Gli3 in the formation of lung, trachea and oesophagus. Nature Genet. 20, 54-57.

Murdoch, J.N., Doudney, K., Paternotte, C., Copp, A.J., Stanier, P., 2001. Severe neural tube defects in the *loop-tail* mouse result from mutation of *Lpp1*, a novel gene involved in floor plate specification. Hum.Mol.Genet. 10, 2593-2601.

Murdoch, J.N., Henderson, D.J., Doudney, K., Gaston-Massuet, C., Phillips, H.M., Paternotte, C., Arkell, R., Stanier, P., Copp, A.J., 2003. Disruption of *scribble* (*Scrb1*) causes severe neural tube defects in the *circletail* mouse. Hum.Mol.Genet. 12, 87-98.

Nagele, R.G., Lee, H., 1980. Studies on the mechanisms of neurulation in the chick: microfilament-mediated changes in cell shape during uplifting of neural folds. J.Exp.Zool. 213, 391-398.

Nakashima, S., 2002. Protein kinase Ca (PKCa): Regulation and biological function. J.Biochem.(Tokyo) 132, 669-675.

Nakhost, A., Kabir, N., Forscher, P., Sossin, W.S., 2002. Protein kinase C isoforms are translocated to microtubules in neurons. J.Biol.Chem. 277, 40633-40639.

Nestler, J.E., Jakubowicz, D.J., Reamer, P., Gunn, R.D., Allan, G., 1999. Ovulatory and metabolic effects of D-*chiro*-inositol in the polycystic ovary syndrome. N.Engl.J.Med. 340, 1314-1320.

Nigg, E.A., 1995. Cyclin-dependent protein kinases: Key regulators of the eukaryotic cell cycle. BioEssays 17, 471-480.

Nikawa, J., Tsukagoshi, Y., Yamashita, S., 1991. Isolation and characterization of two distinct myo-inositol transporter genes of Saccharomyces cerevisiae. J.Biol.Chem. 266, 11184-11191.

Nishizuka, Y., 1986. Studies and perspectives of protein kinase C. Science 233, 305-312.

Nishizuka, Y., 1988. The molecular heterogeneity of protein kinase C and its implications for cellular regulation. Nature 334, 661-665.

Nishizuka, Y., 1992. Intracellular signalling by hydrolysis of phospholipids and activation of protein kinase C. Science 158, 607-613.

Nolan, P.M., Peters, J., Strivens, M., Rogers, D., Hagan, J., Spurr, N., Gray, I.C., Vizor, L., Brooker, D., Whitehill, E., Washbourne, R., Hough, T., Greenaway, S., Hewitt, M., Liu, X.H., McCormack, S., Pickford, K., Selley, R., Wells, C., Tymowska-Lalanne, Z., Roby, P., Glenister, P., Thornton, C., Thaung, C., 2000. A systematic, genome-wide, phenotype-driven mutagenesis programme for gene function studies in the mouse. Nature Genet. 25, 440-443.

O'Rahilly, R., Müller, F., 2002. The two sites of fusion of the neural folds and the two neuropores in the human embryo. Teratology. 65, 162-170.

O'Shea, K.S., Kaufman, M.H., 1980. Phospholipase C induced neural tube defects in the mouse embryo. Experientia 36, 1217-1219.

Ortmeyer, H.K., Huang, L.C., Zhang, L., Hansen, B.C., Larner, J., 1993. Chiroinositol deficiency and insulin resistance. II. Acute effects of D-chiroinositol administration in streptozotocin- diabetic rats, normal rats given a glucose load, and spontaneously insulin-resistant rhesus monkeys. Endocrinology 132, 646-651.

Pak, Y., Huang, L.C., Lilley, K.J., Larner, J., 1992. In vivo conversion of [3H]myoinositol to [3H]chiroinositol in rat tissues. J.Biol.Chem. 267, 16904-16910.

Pak, Y., Larner, J., 1992. Identification and characterization of chiroinositol-containing phospholipids from bovine liver. Biochem.Biophys.Res.Commun. 184, 1042-1047.

Pak, Y., Paule, C.R., Bao, Y.D., Huang, L.C., Larner, J., 1993. Insulin stimulates the biosynthesis of chiro-inositol-containing phospholipids in a rat fibroblast line expressing the human insulin receptor. Proc.Natl.Acad.Sci.USA 90, 7759-7763.

Pandur, P., LΣsche, M., Eisenberg, L.M., Khl, M., 2002. Wnt-11 activation of a non-canonical Wnt signalling pathway is required for cardiogenesis. Nature 418, 636-641.

Parekh, D.B., Ziegler, W., Parker, P.J., 2000. Multiple pathways control protein kinase C phosphorylation. EMBO J 19, 496-503.

Park, H.L., Bai, C., Platt, K.A., Matise, M.P., Beeghly, A., Hui, C.C., Nakashima, M., Joyner, A.L., 2000. Mouse *Gli1* mutants are viable but have defects in SHH signaling in combination with a *Gli2* mutation. Development 127, 1593-1605.

Parker, P.J., 1995. Intracellular signalling. PI 3-kinase puts GTP on the Rac. Curr.Biol. 5, 577-579.

Parker, P.J., Murray-Rust, J., 2004. PKC at a glance. J.Cell Sci. 117, 131-132.

Parker, P.J., Parkinson, S.J., 2001. AGC protein kinase phosphorylation and protein kinase C. Biochem.Soc.Trans. 29, 860-863.

Peeters, M.C., Schutte, B., Lenders, M.H., Hekking, J.W., Drukker, J., van Straaten, H.W., 1998. Role of differential cell proliferation in the tail bud in aberrant mouse neurulation. Dev.Dyn. 211, 382-389.

Rauch, G.J., Hammerschmidt, M., Blader, P., Schauerte, K.E., Strähle, U., Ingham, P.W., McMahon, A.P., Haffter, P., 1997. *WNT5* is required for tail formation in the zebrafish embryo. Cold Spring Harbor Symp.Quant.Biol. 62, 227-234.

Rodgers, E.E., Theibert, A.B., 2002. Functions of PI 3-kinase in development of the nervous system. Int.J.Dev.Neurosci. 20, 187-197.

Ron, D., Mochly-Rosen, D., 1995. An autoregulatory region in protein kinase C: the pseudoanchoring site. Proc.Natl.Acad.Sci.USA 492-496.

Rousset, R., Wharton, D.A., Jr., Zimmermann, G., Scott, M.P., 2002. Zinc-dependent interaction between dishevelled and the *Drosophila* Wnt antagonist naked cuticle. J.Biol.Chem. 277, 49019-49026.

Ruiz i Altaba, A., 1999. The works of GLI and the power of hedgehog. Nat.Cell Biol. 1, E147-E148.

Sadler, T.W., 1978. Distribution of surface coat material on fusing neural folds of mouse embryos during neurulation. Anat.Rec. 191, 345-350.

Sadler, T.W., Greenberg, D., Coughlin, P., Lessard, J.L., 1982. Actin distribution patterns in the mouse neural tube during neurulation. Science 215, 172-174.

Sardet, C., Counillon, L., Franchi, A., Pouyssegur, J., 1990. Growth factors induce phosphorylation of the Na^+/H^+ antiporter, glycoprotein of 110 kD. Science 247, 723-726.

Schoenwolf, G.C., 1984. Histological and ultrastructural studies of secondary neurulation of mouse embryos. Am.J.Anat. 169, 361-374.

Schoenwolf, G.C., 1985. Shaping and bending of the avian neuroepithelium: morphometric analyses. Dev.Biol. 109, 127-139.

Seller, M.J., 1981. Recurrence risks for neural tube defects in a genetic counselling clinic population. J.Med.Genet. 18, 245-248.

Seller, M.J., Embury, S., Polani, P.E., Adinolfi, M., 1979. Neural tube defects in curly-tail mice. II. Effect of maternal administration of vitamin A. Proc.R.Soc.Lond.B 206, 95-107.

Sheldahl, L.C., Park, M., Malbon, C.C., Moon, R.T., 1999. Protein kinase C is differentially stimulated by Wnt and Frizzled homologs in a G-protein-dependent manner. Curr.Biol. 9, 695-698.

Shum, A.S.W., Copp, A.J., 1996. Regional differences in morphogenesis of the neuroepithelium suggest multiple mechanisms of spinal neurulation in the mouse. Anat.Embryol. 194, 65-73.

Silver, L.M., 1990. At the crossroads of developmental genetics: The cloning of the classical mouse *T* locus. BioEssays 12, 377-380.

Skarnes, W.C., Auerbach, B.A., Joyner, A.L., 1992. A gene trap approach in mouse embryonic stem cells: The *lacZ* reporter is activated by splicing, reflects endogenous gene expression, and is mutagenic in mice. Genes Dev. 6, 903-918.

Slusarski, D.C., Corces, V.G., Moon, R.T., 1997. Interaction of Wnt and a frizzled homologue triggers G-protein- linked phosphatidylinositol signalling. Nature 390, 410-413.

Smith, J.L., Schoenwolf, G.C., 1987. Cell cycle and neuroepithelial cell shape during bending of the chick neural plate. Anat.Rec. 218, 196-206.

Smith, J.L., Schoenwolf, G.C., 1988. Role of cell-cycle in regulating neuroepithelial cell shape during bending of the chick neural plate. Cell Tissue Res. 252, 491-500.

Smith, J.L., Schoenwolf, G.C., 1997. Neurulation: coming to closure. Trends Neurosci. 20, 510-517.

Smith, J.L., Schoenwolf, G.C., Quan, J., 1994. Quantitative analyses of neuroepithelial cell shapes during bending of the mouse neural plate. J.Comp.Neurol. 342, 144-151.

Smithells, D., 1998. Dominant gene probably caused some of defects ascribed to thalidomide. Br.Med.J. 316, 149.

Solursh, M., Morriss, G.M., 1977. Glycosaminoglycan synthesis in rat embryos during the formation of the primary mesenchyme and neural folds. Dev.Biol. 57, 75-86.

Sporle, R., Gunther, T., Struwe, M., Schughart, K., 1996. Severe defects in the formation of epaxial musculature in open brain (opb) mutant mouse embryos. Development 122, 79-86.

Standaert, M.L., Galloway, L., Karnam, P., Bandyopadhyay, G., Moscat, J., Farese, R.V., 1997. Protein kinase C-zeta as a downstream effector of phosphatidylinositol 3-kinase during insulin stimulation in rat adipocytes - Potential role in glucose transport. J.Biol.Chem. 272, 30075-30082.

Stark, G., 1977. Spina Bifida: Problems and Management. Blackwell Scientific Publications, Oxford.

Stebbins, L., Mochly-Rosen, D., 2001. Binding specficity of RACK1 resides in the V5 region of βII protein kinase C. J.Biol.Chem. 276, 29644-29650.

Stegmann, K., Boecker, J., Kosan, C., Ermert, A., Kunz, J., Koch, M.C., 1999. Human transcription factor SLUG: mutation analysis in patients with neural tube defects and identification of a missense mutation (D119E) in the Slug subfamily-defining region. Mutat.Res. 406, 63-69.

Stegmann, K., Boecker, J., Richter, B., Capra, V., Finnell, R.H., Ngo, E.T.K.N., Strehl, E., Ermert, A., Koch, M.C., 2001. A screen for mutations in human homologues of mice exencephaly genes *Tfap2α* and *Msx2* in patients with neural tube defects. Teratology. 63, 167-175.

Stumpo, D.J., Bock, C.B., Tuttle, J.S., Blackshear, P.J., 1995a. MARCKS deficiency in mice leads to abnormal brain development and perinatal death. Proc.Natl.Acad.Sci.U.S.A 92, 944-948.

Stumpo, D.J., Bock, C.B., Tuttle, J.S., Blackshear, P.J., 1995b. MARCKS deficiency in mice leads to abnormal brain development and perinatal death. Proc.Natl.Acad.Sci.USA 92, 944-948.

Suzuma, K., Takahara, N., Suzuma, I., Isshiki, K., Ueki, K., Leitges, M., Aiello, L.P., King, G.L., 2002. Characterization of protein kinase C b isoform's action on retinoblastoma protein phosphorylation, vascular endothelial growth factor-induced endothelial cell proliferation, and retinal neovascularization. Proc.Natl.Acad.Sci.USA 99, 721-726.

Svensson, E.C., Huggins, G.S., Lin, H., Clendenin, C., Jiang, F., Tufts, R., Dardik, F.B., Leiden, J.M., 2000. A syndrome of tricuspid atresia in mice with a targeted mutation of the gene encoding Fog-2. Nature Genet. 25, 353-356.

Szalay, J., Bruno, P., Bhati, R., Adjodha, J., Schueler, D., Summerville, V., Vazeos, R., 2001. Associations of PKC isoforms with the cytoskeleton of B16F10 melanoma cells. J Histochem.Cytochem. 49, 49-66.

Tabin, C.J., McMahon, A., 1997. Recent advances in Hedgehog signalling. Trends Cell Biol. 7, 442-446.

Theodore, L., Derossi, D., Chassaing, G., Llirbat, B., Kubes, M., Jordan, P., Chneiweiss, H., Godement, P., Prochiantz, A., 1995. Intraneuronal delivery of protein kinase C pseudosubstrate leads to growth cone collapse. J.Neurosci. 15, 7158-7167.

Thompson, L.J., Fields, A.P., 1996. Beta II protein kinase C is required for the G2/M phase transition of cell cycle. J.Biol.Chem. 271, 15045-15053.

Ting, S.B., Caddy, J., Hislop, N., Wilanowski, T., Auden, A., Zhao, L.L., Ellis, S., Kaur, P., Uchida, Y., Holleran, W.M., Elias, P.M., Cunningham, J.M., Jane, S.M., 2005. A homolog of Drosophila grainy head is essential for epidermal integrity in mice. Science 308, 411-413.

Ting, S.B., Wilanowski, T., Auden, A., Hall, M., Voss, A.K., Thomas, T., Parekh, V., Cunningham, J.M., Jane, S.M., 2003. Inositol- and folate-resistant neural tube defects in mice lacking the epithelial-specific factor Grhl-3. Nature Med. 9, 1513-1519.

Toullec, D., Pianetti, P., Coste, H., Bellevergue, P., Grand Perret, T., Ajakane, M., Baudet, V., Boissin, P., Boursier, E., Loriolle, F., et al., 1991. The bisindolylmaleimide GF 109203X is a potent and selective inhibitor of protein kinase C. J.Biol.Chem. 266, 15771-15781.

Tran, P., Hiou-Tim, F., Frosst, P., Lussier-Cacan, S., Bagley, P., Selhub, J., Bottiglieri, T., Rozen, R., 2002. The curly-tail (ct) mouse, an animal model of neural tube defects,

displays altered homocysteine metabolism without folate responsiveness or a defect in Mthfr. Mol.Genet.Metab 76, 297-304.

Van Allen, M.I., Kalousek, D.K., Chernoff, G.F., Juriloff, D., Harris, M., McGillivray, B.C., Yong, S.-L., Langlois, S., MacLeod, P.M., Chitayat, D., Friedman, J.M., Wilson, R.D., McFadden, D., Pantzar, J., Ritchie, S., Hall, J.G., 1993. Evidence for multi-site closure of the neural tube in humans. Am.J.Med.Genet. 47, 723-743.

Van der Put, N.M.J., Steegers-Theunissen, R.P.M., Frosst, P., Trijbels, F.J.M., Eskes, T.K.A.B., Van den Heuvel, L.P., Mariman, E.C.M., Den Heyer, M., Rozen, R., Blom, H.J., 1995. Mutated methylenetetrahydrofolate reductase as a risk factor for spina bifida. Lancet 346, 1070-1071.

van Straaten, H.W., Copp, A.J., 2001. Curly tail: a 50-year history of the mouse spina bifida model. Anat.Embryol.(Berl) 203, 225-237.

van Straaten, H.W., Hekking, J.W., Copp, A.J., Bernfield, M., 1992. Deceleration and acceleration in the rate of posterior neuropore closure during neurulation in the curly tail (ct) mouse embryo. Anat.Embryol.(Berl) 185, 169-174.

Van Straaten, H.W.M., Copp, A.J., 2001. Curly tail: a 50-year history of the mouse spina bifida model. Anat.Embryol. 203, 225-237.

Van Straaten, H.W.M., Hekking, J.W.M., Consten, C., Copp, A.J., 1993. Intrinsic and extrinsic factors in the mechanism of neurulation: effect of curvature of the body axis on closure of the posterior neuropore. Development. 117, 1163-1172.

VanAerts, L.A.G.J.M., Blom, H.J., Deabreu, R.A., Trijbels, F.J.M., Eskes, T.K.A.B., Peereboom-Stegeman, J.H.J.C., Noordhoek, J., 1994. Prevention of neural tube defects by and toxicity of L-homocysteine in cultured postimplantation rat embryos. Teratology. 50, 348-360.

Vlahos, C.J., Matter, W.F., Hui, K.Y., Brown, R.F., 1994. A specific inhibitor of phosphatidylinositol 3-kinase, 2-(4- morpholinyl)-8-phenyl-4H-1-benzopyran-4-one (LY294002). J.Biol.Chem. 269, 5241-5248.

Wald, D.S., Bishop, L., Wald, N.J., Law, M., Hennessy, E., Weir, D., McPartlin, J., Scott, J., 2001. Randomized trial of folic acid supplementation and serum homocysteine levels. Arch.Intern.Med. 161, 695-700.

Wald, N., Sneddon, J., Densem, J., Frost, C., Stone, R., MRC Vitamin Study Res Group, 1991. Prevention of neural tube defects: Results of the Medical Research Council Vitamin Study. Lancet 338, 131-137.

Wald, N.J., 1995. Folic acid and the prevention of neural tube defects: The need for public health action. Bibl.Nutr.Dieta 52, 56-65.

Wald, N.J., Cuckle, H., Brock, J.H., Peto, R., Polani, P.E., Woodford, F.P., 1977. Maternal serum-alpha-fetoprotein measurement in antenatal screening for anencephaly and spina bifida in early pregnancy. Report of U.K. collaborative study on alpha-fetoprotein in relation to neural-tube defects. Lancet 1, 1323-1332.

Wallingford, J.B., Harland, R.M., 2002. Neural tube closure requires Dishevelled-dependent convergent extension of the midline. Development 129, 5815-5825.

Wallingford, J.B., Rowning, B.A., Vogeli, K.M., Rothbächer, U., Fraser, S.E., Harland, R.M., 2000. Dishevelled controls cell polarity during *Xenopus* gastrulation. Nature 405, 81-85.

Wechsler-Reya, R.J., Scott, M.P., 1999. Control of neuronal precursor proliferation in the cerebellum by Sonic Hedgehog. Neuron 22, 103-114.

Wetsel, W.C., Khan, W.A., Merchenthaler, I., Rivera, H., Halpern, A.E., Phung, H.M., Negro Vilar, A., Hannun, Y.A., 1992. Tissue and cellular distribution of the extended family of protein kinase C isoenzymes. J.Cell Biol. 117, 121-133.

Whittaker, J., Dix, K.M., 1979. Double staining technique for rat skeletons in teratological studies. Lab.Anim. 13, 309-310.

Wilda, M., Ghaffari-Tabrizi, N., Reisert, I., Utermann, G., Baier, G., Hameister, H., 2001. Protein kinase C isoenzyme: selective expression pattern of protein kinase C-θ during mouse development. Mech.Dev. 103, 197-200.

Wilson, D.B., 1974. Proliferation in the neural tube of the splotch (Sp) mutant mouse. J.Comp.Neurol. 154, 249-256.

Wilson, D.B., Center, E.M., 1974. The neural cell cycle in the loop-tail (*Lp*) mutant mouse. J.Embryol.Exp.Morphol. 32, 697-705.

Wilson, J.G., 1965. Methods for administering agents and detecting malformations in experimental animals, in: J.G. Wilson, J. Warkany (Eds.), Teratology: Principles and Techniques. University of Chicago Press, Chicago, Illinois, pp. 262-277.

Wood, W., Jacinto, A., Grose, R., Woolner, S., Gale, J., Wilson, C., Martin, P., 2002. Wound healing recapitulates morphogenesis in Drosophila embryos. Nat.Cell Biol. 4, 907-912.

Wu, G.Y., Toyokawa, T., Hahn, H., Dorn, G.W., II, 2000. ε Protein kinase C in pathological myocardial hypertrophy - Analysis by combined transgenic expression of translocation modifiers and $G\alpha_q$. J.Biol.Chem. 275, 29927-29930.

Wu, M., Chen, D.F., Sasaoka, T., Tonegawa, S., 1996. Neural tube defects and abnormal brain development in F52- deficient mice. Proc.Natl.Acad.Sci.USA 93, 2110-2115.

Xu, W.M., Baribault, H., Adamson, E.D., 1998. Vinculin knockout results in heart and brain defects during embryonic development. Development 125, 327-337.

Yamamoto, M., Acevedo-Duncan, M., Chalfant, C.E., Patel, N.A., Watson, J.E., Cooper, D.R., 1998. The roles of protein kinase C beta I and beta II in vascular smooth muscle cell proliferation. Exp Cell Res. 240, 349-358.

Yamanaka, H., Moriguchi, T., Masuyama, N., Kusakabe, M., Hanafusa, H., Takada, R., Takada, S., Nishida, E., 2002. JNK functions in the non-canonical Wnt pathway to regulate convergent extension movements in vertebrates. EMBO Rep. 3, 69-75.

Yang-Snyder, J., Miller, J.R., Brown, J.D., Lai, C.J., Moon, R.T., 1996. A *frizzled* homolog functions in a vertebrate *Wnt* signaling pathway. Curr.Biol. 6, 1302-1306.

Ybot-Gonzalez, P., Cogram, P., Gerrelli, D., Copp, A.J., 2002. Sonic hedgehog and the molecular regulation of neural tube closure. Development 129, 2507-2517.

Ybot-Gonzalez, P., Copp, A.J., 1999. Bending of the neural plate during mouse spinal neurulation is independent of actin microfilaments. Dev.Dyn. 215, 273-283.

Ybot-Gonzalez, P., Gaston-Massuet, C., Girdler, G., Klingensmith, J., Arkell, R., Greene, N.D., Copp, A.J., 2007a. Neural plate morphogenesis during mouse neurulation is regulated by antagonism of BMP signalling.

Ybot-Gonzalez, P., Savery, D., Gerrelli, D., Signore, M., Mitchell, C.E., Faux, C.H., Greene, N.D., Copp, A.J., 2007b. Convergent extension, planar-cell-polarity signalling and initiation of mouse neural tube closure. Development 134, 789-799.

Zhao, Q., Behringer, R.R., De Crombrugghe, B., 1996. Prenatal folic acid treatment suppresses acrania and meroanencephaly in mice mutant for the *Cart1* homeobox gene. Nature Genet. 13, 275-283.

Ziegler, W.H., Parekh, D.B., Le Good, J.A., Whelan, R.D., Kelly, J.J., Frech, M., Hemmings, B.A., Parker, P.J., 1999. Rapamycin-sensitive phosphorylation of PKC on a carboxy-terminal site by an atypical PKC complex. Curr.Biol. 9, 522-529.

8. PUBLICATIONS

Cogram, P., Tesh, S., Tesh, J., Wade, A., Allan, G., Greene, N.D.E., Copp, A.J., 2002. D-*chiro*-inositol is more effective than *myo*-inositol in preventing folate-resistant mouse neural tube defects. Hum.Reprod. 17, 2451-2458.

Cogram, P., Hynes, A., Dunlevy, L.P., Greene, N.D., Copp, A.J., 2004a. Specific isoforms of protein kinase C are essential for prevention of folate-resistant neural tube defects by inositol. Hum.Mol.Genet. 13, 7-14.

Human Reproduction Vol.17, No.9 pp. 2451–2458, 2002

D-*chiro*-inositol is more effective than *myo*-inositol in preventing folate-resistant mouse neural tube defects

Patricia Cogram[1], Sheila Tesh[2], John Tesh[2], Angie Wade[3], Geoffrey Allan[4], Nicholas D.E.Greene[1] and Andrew J.Copp[1,5]

[1]Neural Development Unit, Institute of Child Health, University College London, [2]Tesh Consultants International, Sweffling, Saxmundham, Suffolk, [3]Centre for Paediatric Epidemiology and Biostatistics, Institute of Child Health, University College London, UK and [4]Insmed Incorporated, Richmond, VA, USA

[5]To whom correspondence should be addressed at: Neural Development Unit, Institute of Child Health, 30 Guilford Street, London, WC1N 1EH, UK. E-mail: a.copp@ich.ucl.ac.uk

BACKGROUND: Among mouse genetic mutants that develop neural tube defects (NTDs), some respond to folic acid administration during early pregnancy, whereas NTDs in other mutants are not prevented. This parallels human NTDs, in which up to 30% of cases may be resistant to folic acid. Most spina bifida cases in the folic acid-resistant 'curly tail' mouse can be prevented by treatment with inositol early in embryonic development. Here, the effectiveness and safety during pregnancy of two isomers, *myo*- and D-*chiro*-inositol, in preventing mouse NTDs was compared. METHODS AND RESULTS: Inositol was administered either directly to embryos *in vitro*, or to pregnant females by s.c. or oral routes. Although D-*chiro*- and *myo*-inositol both reduced the frequency of spina bifida in curly tail mice by all routes of administration, D-*chiro*-inositol consistently exhibited the more potent effect, reducing spina bifida by 73–86% *in utero* compared with a 53–56% reduction with *myo*-inositol. Pathological analysis revealed no association of either *myo*- or D-*chiro*-inositol with reduced litter size or fetal malformation. CONCLUSIONS: D-*chiro*-inositol offers a safe and effective method for preventing folic acid-resistant NTDs in the curly tail mouse. This raises the possibility of using inositol as an adjunct therapy to folic acid for prevention of NTDs in humans.

Keywords: embryo culture/malformations/pregnancy/spina bifida/teratogen

Introduction

Folic acid supplementation during early pregnancy can prevent a proportion of neural tube defects (NTDs) (Wald *et al.*, 1991; Czeizel and Dudás, 1992; Berry *et al.*, 1999), whereas other cases of NTD appear resistant to folic acid. In the randomized controlled trial of the Medical Research Council, UK (Wald *et al.*, 1991), 28% of NTD cases recurred despite supplementation with 4 mg folic acid per day. Moreover, the recent introduction of folic acid fortification of bread flour in the USA resulted in only a 19% decline in the prevalence of NTDs (Honein *et al.*, 2001). While these findings may indicate the need for increased levels of folic acid supplementation, they are also consistent with a proportion of NTDs exhibiting resistance to exogenous folic acid.

Mouse genetic models also indicate the existence of folate-resistant NTDs. Mutant strains including 'splotch', 'crooked tail' and the 'Cart1' knockout exhibit NTDs that can be prevented by folic acid treatment during early pregnancy (Fleming and Copp, 1998; Zhao *et al.*, 1996; Carter *et al.*, 1999), whereas folic acid is ineffective in preventing NTDs in the mutant strains 'curly tail', 'axial defects' and the 'ephrin-A5' knockout (Essien and Wannberg, 1993; Seller, 1994; Holmberg *et al.*, 2000).

Previously, it was demonstrated that a proportion of the folate-resistant NTDs in curly tail mice can be prevented by treating pregnant females, or embryos *in vitro*, with *myo*-inositol (Greene and Copp, 1997). These findings were consistent with earlier work showing that deficiency of *myo*-inositol in the culture medium of rat and mouse embryos caused a high incidence of cranial NTDs (Cockroft, 1988; Cockroft *et al.*, 1992), and that NTDs developing in rat embryos cultured under diabetic conditions could be ameliorated by supplementation with *myo*-inositol (Baker *et al.*, 1990; Hashimoto *et al.*, 1990). Together, these findings suggest inositol as a potential therapeutic option for prevention of folate-resistant NTDs.

Here, the analysis of inositol as a primary therapeutic agent in preventing mouse NTDs has been extended. The study was intended to serve as a preliminary to a human clinical therapeutic trial. It was shown that inositol could prevent NTDs both *in vitro* and following administration to pregnant curly tail females, either by s.c. or oral routes. A detailed pathological

SPECIAL NOTE

ITEM SCANNED AS SUPPLIED
PAGINATION IS AS SEEN

Human Reproduction Vol.17, No.9 pp. 2451–2458, 2002

D-*chiro*-inositol is more effective than *myo*-inositol in preventing folate-resistant mouse neural tube defects

Patricia Cogram[1], Sheila Tesh[2], John Tesh[2], Angie Wade[3], Geoffrey Allan[4], Nicholas D.E.Greene[1] and Andrew J.Copp[1,5]

[1]Neural Development Unit, Institute of Child Health, University College London, [2]Tesh Consultants International, Sweffling, Saxmundham, Suffolk, [3]Centre for Paediatric Epidemiology and Biostatistics, Institute of Child Health, University College London, UK and [4]Insmed Incorporated, Richmond, VA, USA

[5]To whom correspondence should be addressed at: Neural Development Unit, Institute of Child Health, 30 Guilford Street, London, WC1N 1EH, UK. E-mail: a.copp@ich.ucl.ac.uk

BACKGROUND: Among mouse genetic mutants that develop neural tube defects (NTDs), some respond to folic acid administration during early pregnancy, whereas NTDs in other mutants are not prevented. This parallels human NTDs, in which up to 30% of cases may be resistant to folic acid. Most spina bifida cases in the folic acid-resistant 'curly tail' mouse can be prevented by treatment with inositol early in embryonic development. Here, the effectiveness and safety during pregnancy of two isomers, *myo*- and D-*chiro*-inositol, in preventing mouse NTDs was compared. METHODS AND RESULTS: Inositol was administered either directly to embryos *in vitro*, or to pregnant females by s.c. or oral routes. Although D-*chiro*- and *myo*-inositol both reduced the frequency of spina bifida in curly tail mice by all routes of administration, D-*chiro*-inositol consistently exhibited the more potent effect, reducing spina bifida by 73–86% *in utero* compared with a 53–56% reduction with *myo*-inositol. Pathological analysis revealed no association of either *myo*- or D-*chiro*-inositol with reduced litter size or fetal malformation. CONCLUSIONS: D-*chiro*-inositol offers a safe and effective method for preventing folic acid-resistant NTDs in the curly tail mouse. This raises the possibility of using inositol as an adjunct therapy to folic acid for prevention of NTDs in humans.

Keywords: embryo culture/malformations/pregnancy/spina bifida/teratogen

Introduction

Folic acid supplementation during early pregnancy can prevent a proportion of neural tube defects (NTDs) (Wald *et al.*, 1991; Czeizel and Dudás, 1992; Berry *et al.*, 1999), whereas other cases of NTD appear resistant to folic acid. In the randomized controlled trial of the Medical Research Council, UK (Wald *et al.*, 1991), 28% of NTD cases recurred despite supplementation with 4 mg folic acid per day. Moreover, the recent introduction of folic acid fortification of bread flour in the USA resulted in only a 19% decline in the prevalence of NTDs (Honein *et al.*, 2001). While these findings may indicate the need for increased levels of folic acid supplementation, they are also consistent with a proportion of NTDs exhibiting resistance to exogenous folic acid.

Mouse genetic models also indicate the existence of folate-resistant NTDs. Mutant strains including 'splotch', 'crooked tail' and the 'Cartl' knockout exhibit NTDs that can be prevented by folic acid treatment during early pregnancy (Fleming and Copp, 1998; Zhao *et al.*, 1996; Carter *et al.*, 1999), whereas folic acid is ineffective in preventing NTDs in the mutant strains 'curly tail', 'axial defects' and the 'ephrin-A5' knockout (Essien and Wannberg, 1993; Seller, 1994; Holmberg *et al.*, 2000).

Previously, it was demonstrated that a proportion of the folate-resistant NTDs in curly tail mice can be prevented by treating pregnant females, or embryos *in vitro*, with *myo*-inositol (Greene and Copp, 1997). These findings were consistent with earlier work showing that deficiency of *myo*-inositol in the culture medium of rat and mouse embryos caused a high incidence of cranial NTDs (Cockroft, 1988; Cockroft *et al.*, 1992), and that NTDs developing in rat embryos cultured under diabetic conditions could be ameliorated by supplementation with *myo*-inositol (Baker *et al.*, 1990; Hashimoto *et al.*, 1990). Together, these findings suggest inositol as a potential therapeutic option for prevention of folate-resistant NTDs.

Here, the analysis of inositol as a primary therapeutic agent in preventing mouse NTDs has been extended. The study was intended to serve as a preliminary to a human clinical therapeutic trial. It was shown that inositol could prevent NTDs both *in vitro* and following administration to pregnant curly tail females, either by s.c. or oral routes. A detailed pathological

analysis revealed no significant adverse effects of inositol therapy on mouse fetuses. Moreover, the effectiveness of *myo*-inositol was compared with that of D-*chiro*-inositol, a closely related enantiomer that differs in the orientation of the carbon-two hydroxyl group (C2-OH) relative to the plane of the six carbon ring.

Materials and methods

Mice

Curly tail mice are maintained as a homozygous, random-bred stock in which NTDs develop in ~60% of individuals (Van Straaten and Copp, 2001). Experimental litters were generated by timed matings, and the day of finding a copulation plug was designated embryonic day (E) 0.5.

In-vitro inositol treatment

E9.5 embryos (17–19 somite stage) were cultured for 24 h at 38°C in whole rat serum, as described previously (Copp *et al.*, 1999). At 30 min after the start of culture, *myo*-inositol (Sigma, UK) or D-*chiro*-inositol (Insmed, VA, USA) was added to the medium (62.5 μl of inositol stock per ml rat serum) to a final concentration of 5, 10, 20 or 50 μg/ml inositol. Control cultures received an equal volume of phosphate-buffered saline (PBS). Following culture, embryos were scored for: (i) posterior neuropore length (the distance from the rostral end of the posterior neuropore to the tip of the tail bud); (ii) crown–rump length; and (iii) somite number.

In-utero inositol treatment

For s.c. administration, osmotic mini-pumps (capacity 100 μl, delivery rate 1 μl/h; model 1003D, Alzet) were filled with solutions of 30, 75 or 150 mg/ml inositol (delivering 29, 72 and 144 μg inositol/g body weight per day respectively for a 25 g mouse), or PBS as a control. Mini-pumps were incubated in sterile PBS at 37°C for 4 h and then implanted s.c. on the back of pregnant mice at E8.5. General anaesthesia was induced by an i.p. injection of 0.01 ml/g body weight of a solution comprising 10% Hypnovel® (midazolam 5 mg/ml) and 25% Hypnorm® (fentanyl citrate 0.315 mg/ml, fluanisone 10 mg/ml) in sterile distilled water. For oral administration, pregnant mice were gavaged with 0.5 ml inositol solution in PBS twice daily intervals from E8.5 to E10.5 (six doses in total; 800 μg/g body weight per day).

Analysis of fetuses following inositol treatment in utero

Pregnant females were killed at E18.5, and the total number of implantations, classified as viable fetuses or resorptions, was recorded. Fetuses were dissected from the uterus and inspected immediately for the presence of open lumbo-sacral spina bifida and tail flexion defects: the primary manifestations of the curly tail genetic defect (Gruneberg, 1954; Van Straaten and Copp, 2001). A randomly selected sample of fetuses was fixed in Bouin's fluid and subjected to detailed internal pathological analysis by free-hand serial sectioning (Wilson, 1965). Other fetuses were fixed in 95% ethanol and processed for skeletal examination (Whittaker and Dix, 1979).

Statistical data analysis

Continuous variables (somite number, crown–rump length, posterior neuropore length, litter size) were compared between treatment groups using analysis of variance or Kruskal–Wallis test. Ordinal regression was used to quantify further the effects of treatment and dosage on posterior neuropore length. Fisher's exact or χ^2-tests were used to compare phenotype frequencies between groups. To evaluate possible litter effects, multilevel ordinal logistic models were fitted to the data in Table III (MLwiN v1.10.0006) (Goldstein, 1995). Logistic regression was used to determine whether the number of resorptions *in utero* was linked to dose and/or treatment.

Results

D-chiro-inositol is more effective than myo-inositol in normalizing neural tube closure in embryo culture

Curly tail embryos were cultured in the presence of inositol for 24 h from E9.5, the period during which the neural tube is closing at the posterior neuropore of the mouse embryo. In curly tail embryos, neuropore closure is delayed or fails to be completed, leading to the development of tail flexion defects and spina bifida, respectively (Figure 1A–C) (Copp, 1985). Posterior neuropore length at E10–10.5 is positively correlated with the likelihood that an embryo will progress to develop a spinal NTD (Copp, 1985; Van Straaten *et al.*, 1992).

Both *myo*- and D-*chiro*-inositol exhibited a dose-dependent normalization of posterior neuropore length in embryo culture, as judged by the reduction in neuropore length observed in embryos treated with higher inositol doses (Table I; Figure 2A). Strikingly, D-*chiro*-inositol significantly reduced neuropore length at dose levels of both 20 and 50 μg/ml, whereas a comparable effect was seen with *myo*-inositol only at 50 μg/ml. Embryos exposed to 20 μg/ml *myo*-inositol (or 5–10 μg/ml D-*chiro*-inositol) exhibited neuropore lengths that were not different from PBS-treated controls.

Neither myo- nor D-chiro-inositol affect the rate of embryonic growth in embryo culture

In the experimental design, embryos in the different treatment groups were matched for somite number before culture, in order to avoid differences in developmental outcome (neuropore length) that might arise from comparing embryos of different stages. Following culture, all groups exhibited mean somite numbers in the range 30–31, with no difference between treatments (Table I). Moreover, no significant difference was found in crown–rump length of embryos treated with either *myo*- or D-*chiro*-inositol compared with PBS-treated controls (Table I), suggesting that the effect of inositol is specific to the closing posterior neuropore, and not mediated via alteration of embryonic growth.

D-chiro-inositol is more effective than myo-inositol in preventing NTDs in utero

Next, the effectiveness of s.c. and oral routes of inositol administration in preventing NTDs in curly tail litters was evaluated. Using surgically implanted osmotic mini-pumps to administer inositol at a constant rate over a period of 72 h of pregnancy, encompassing the stages of neural tube closure, a dose-dependent effect of both *myo*- and D-*chiro*-inositol was observed. At 29 μg/g body weight per day, neither *myo*- nor D-*chiro*-inositol significantly affected the frequency of fetuses with spina bifida (Figure 2B), whereas at dose levels of 72 and 144 μg/g body weight per day, both inositols reduced the frequency of spina bifida compared with PBS-treated pregnancies (Figure 2B). At these higher dose levels, inositol

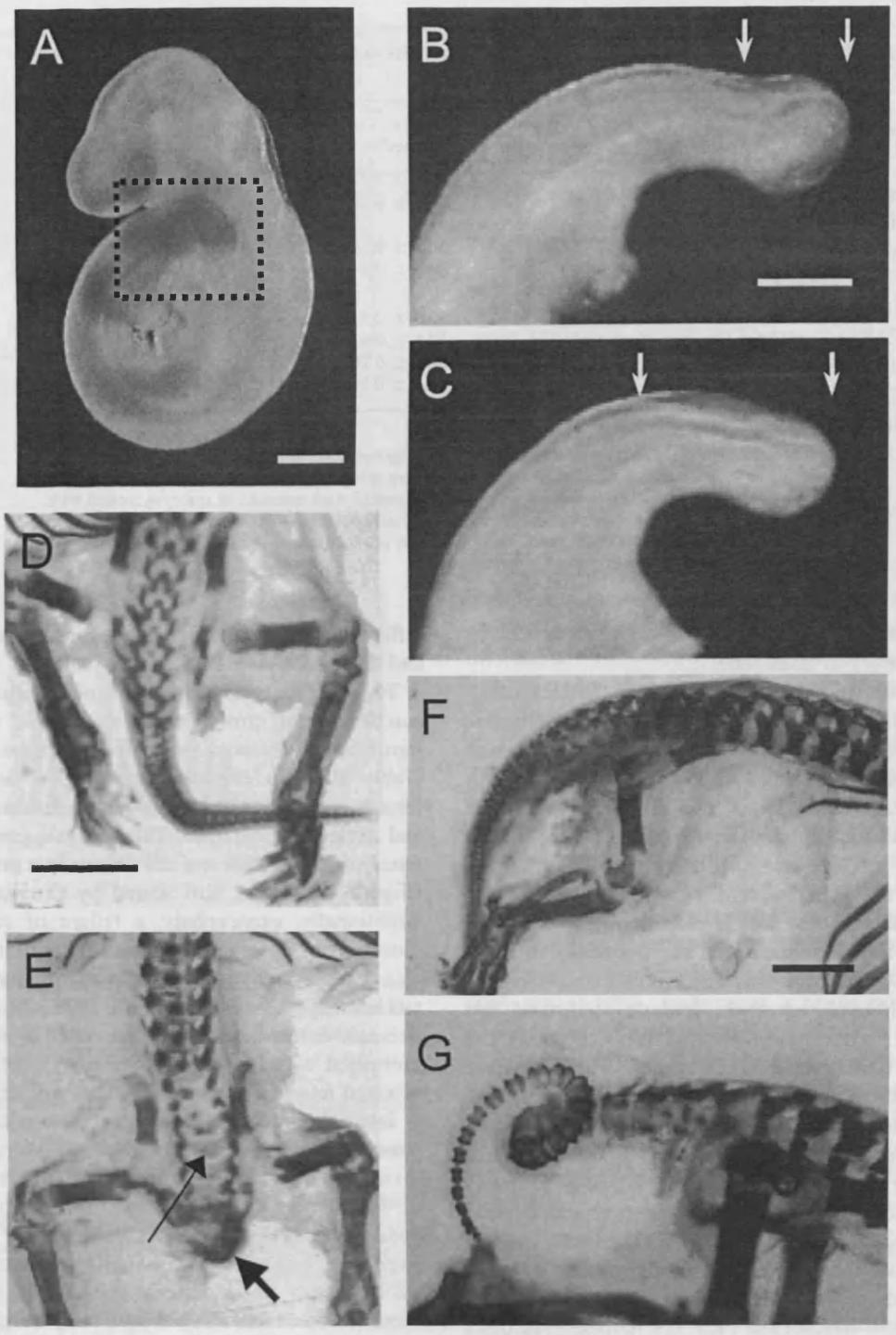

Figure 1. (**A**) Curly tail embryo after 24 h culture from E9.5 to E10.5. The box indicates the posterior neuropore region. (**B**,**C**) Higher magnification of the caudal region of cultured curly tail embryos. The posterior neuropore, a region of open neural folds, occupies the dorsal part of the caudal region, between the arrows in (**B**) and (**C**). Embryos with a large neuropore (**C**) develop spina bifida and/or a tail flexion defect, whereas embryos with a small neuropore (**B**) complete neural tube closure normally. (**D–G**) Skeletal preparations of E18.5 curly tail fetuses in dorsal view (**D**,**E**: rostral to the top) or right lateral view (**F**,**G**: rostral to the right). Compared with the normal fetus in (**D**), the fetus with spina bifida (**E**) exhibits vertebral pedicles widely spaced apart and absent neural arches in the low lumbar/sacral region (long arrow in **E**). The tail (short arrow in **E**) is enclosed in a skin sac and appears reduced in length owing to deformation and fusion of caudal vertebrae. The tail flexion defect (**G**) comprises a 360° curl of the tail, compared with the normal fetus which exhibits a straight tail (**F**). Scale bars: **A** = 0.5 mm; **B**,**C** = 0.2 mm; **D**,**E** = 2 mm; **F**,**G** = 2 mm.

caused a significant shift towards the mild end of the NTD phenotype spectrum, with fewer fetuses having spina bifida and more appearing normal (Table II). As with the in-vitro study, D-*chiro*-inositol appeared most effective, causing a 73–83% decrease in spina bifida frequency relative to PBS controls, at both 72 and 144 μg/g body weight per day.

Table I. Comparison of growth and developmental parameters in curly tail embryos cultured in the presence of *myo*- and D-*chiro*-inositol

Treatment	Conc. μg/ml	No. of embryos	Somite number[a]	Crown–rump length[a]	PNP length[a]
PBS	–	16	30.3 ± 0.15	3.56 ± 0.10	0.59 ± 0.13
Myo-inositol					
	20	16	30.5 ± 0.12	3.50 ± 0.12	0.62 ± 0.06
	50	16	30.5 ± 0.14	3.57 ± 0.07	0.06 ± 0.03*
D-*chiro*-inositol					
	5	15	30.6 ± 0.13	3.50 ± 0.10	0.62 ± 0.11
	10	15	30.5 ± 0.13	3.39 ± 0.10	0.55 ± 0.11
	20	18	30.6 ± 0.16	3.55 ± 0.10	0.09 ± 0.11*
	50	15	30.3 ± 0.16	3.49 ± 0.08	0.07 ± 0.03*

[a]Values are mean ± SEM.
Statistical analysis: somite number and crown–rump length do not differ significantly, whereas posterior neuropore (PNP) length varies significantly between treatment groups ($P < 0.0001$). Ordinal regression analysis indicates that PNP length is significantly reduced (marked with asterisk) in embryos treated with *myo*-inositol (50 μg/ml) and D-*chiro*-inositol (20 and 50 μg/ml) compared with those exposed to phosphate-buffered saline (PBS) alone ($P < 0.05$), whereas PNP length in other inositol-treated groups does not differ significantly from the PBS control group.

Myo-inositol produced a consistent 54–56% reduction in spina bifida frequency (Figure 2B).

Inositol was administered orally to pregnant females, using a twice-daily dosing regime, from E8.5 to E10.5, that delivered 800 μg/g body weight per day, equivalent to the i.p. dose used in a previous study (Greene and Copp, 1997). As with s.c. administration, a marked reduction was detected in the frequency of spina bifida among the offspring of mice treated with either *myo*- or D-*chiro*-inositol (Figure 2B), and a significant shift in the distribution of fetuses between the three phenotype categories (Table II). D-*chiro*-inositol was most effective, causing a 86% reduction in the frequency of spina bifida, while a 53% reduction was observed for *myo*-inositol.

An ordinal multilevel regression analysis confirmed that fetuses treated s.c. with D-*chiro*-inositol ($P < 0.0005$) and *myo*-inositol ($P < 0.002$) were significantly less likely to have spina bifida than those treated with PBS. In the oral dosing study, fetuses treated with D-*chiro*-inositol were less likely to have spina bifida than PBS-treated controls ($P < 0.01$), whereas the trend towards reduced spina bifida frequency in litters treated with *myo*-inositol did not reach statistical significance.

A further investigation was made to determine whether clustering of fetuses of particular phenotypes within litters may have affected the outcome of the comparison between *myo*-inositol, D-*chiro*-inositol and PBS. The multilevel analysis (which took into account the potential non-independence of fetuses within litters) showed that the difference between treatment groups is unaffected when possible litter effects are taken into account.

No evidence of an adverse effect of inositol on pregnancy success or fetal outcome

One possible explanation for a decrease in spina bifida frequency following maternal inositol administration could be an increase in loss of affected fetuses during pregnancy. When both resorption rate and litter size were examined in pregnancies receiving either s.c. or oral inositol, no significant difference was found between pregnancies treated with inositol and those receiving PBS alone (Table III).

To identify any adverse effects of inositol treatment on fetal outcome, fetal crown–rump length was measured, but no significant differences were found between treatment groups (Table III). An extensive pathological analysis of treated fetuses was performed using both free-hand serial sectioning and skeletal preparation. This analysis confirmed the occurrence of spina bifida and tail defects in a proportion of fetuses (Figure 1D–G), as also scored by external fetal inspection. Additionally, exencephaly, a failure of cranial neural tube closure, was observed in a small proportion of fetuses (Table IV). Exencephaly is a recognized, infrequent defect in curly tail homozygotes (Embury *et al.*, 1979). No overall increase or decrease in this defect was observed in inositol-treated fetuses compared with PBS controls, although the low frequency of affected fetuses may have obscured any treatment effect.

Internal and skeletal examination revealed almost no major structural defects, apart from NTDs (Table IV). For instance, no major malformations of the heart, lungs, kidney, gut, limbs or skeleton were identified. Of the morphological changes observed in the analysis, most were minor (e.g. small additional liver lobe) and the great majority occurred as frequently in PBS controls as in fetuses treated with inositol. D-*chiro*-inositol-treated fetuses (144 μg/g body weight per day) showed a somewhat elevated frequency of enlargement of the renal pelvis/ureter, rudimentary ribs on the seventh cervical vertebra and occurrence of anomalous cervical vertebrae (Table IV), although these trends were not statistically significant. Anomalous cervical vertebrae was associated with exencephaly in several litters, suggesting that cervical anomalies may form part of the spectrum of vertebral column defects present in the curly tail mouse.

Discussion

In the present study, the ability of exogenous inositol to prevent spinal NTDs in the folate-resistant curly tail mouse genetic

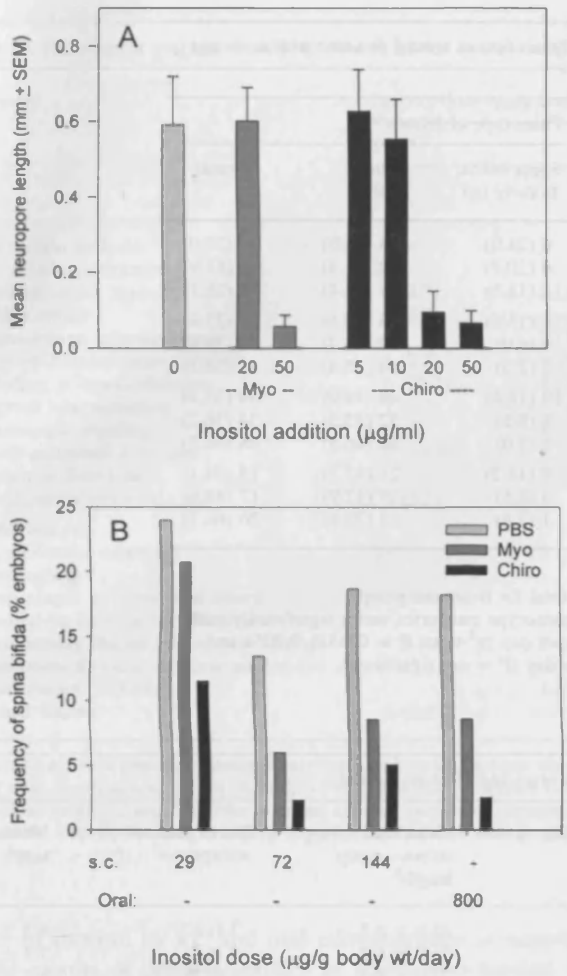

Figure 2. (**A**) Exposure of curly tail embryos in culture to *myo*- (dark grey bars) or D-*chiro*-inositol (black bars) causes a dose-dependent reduction in posterior neuropore length. Embryos treated with phosphate-buffered saline (PBS) (light grey bar; $n = 16$), 20 μg/ml *myo*-inositol ($n = 16$), or 5–10 μg/ml D-*chiro*-inositol ($n = 15$ in each group) all exhibit mean neuropore lengths of ~0.6 mm, evidence of delayed posterior neuropore closure. Treatment with 50 μg/ml *myo*-inositol ($n = 16$) or 20–50 μg/ml D-*chiro*-inositol ($n = 18$ and 15 respectively) significantly reduced ($P < 0.05$) mean neuropore length to values typical of non-mutant embryos at this somite stage. (**B**) Administration of *myo*- or D-*chiro*-inositol to pregnant curly tail females by slow release from s.c. implanted minipumps reduces the frequency of spina bifida at doses of 72 and 144 μg/g body weight per day, but not at 29 μg/g body weight per day. A similar preventive effect of inositol is seen with oral dosing at 800 μg/g body weight per day. For results of statistical analysis, see text.

model was evaluated. Maternal inositol administration significantly reduced the frequency of spina bifida in curly tail mice and normalized closure of the posterior neuropore in whole cultured embryos. A striking finding was the increased potency of D-*chiro*-inositol compared with *myo*-inositol—two closely related enantiomers that differ only in the orientation of the carbon-two hydroxyl group (C2-OH) relative to the plane of the six carbon ring. At identical dosage levels, s.c. administered D-*chiro*-inositol caused a consistently greater reduction in frequency of spina bifida than *myo*-inositol. Moreover, *in vitro*, D-*chiro*-inositol was effective in normalizing neural tube closure at a concentration at which *myo*-inositol had no effect.

Reasons for the differing potency of myo- and D-chiro-inositol in preventing NTD

It was shown previously that the protective effect of *myo*-inositol is mediated via the phosphoinositide cycle (Greene and Copp, 1997), which generates the second messengers inositol triphosphate and diacylglycerol (DAG) (Majerus, 1992). Among the downstream events of this signalling pathway, activation of protein kinase C (PKC) by DAG appears critical for normalization of neuropore closure in curly tail embryos. For instance, activation of PKC by phorbol esters mimics the effect of inositol supplementation, whereas PKC inhibitors abrogate the protective effect (Greene and Copp, 1997).

It is possible that D-*chiro*-inositol also acts through a PKC-dependent pathway, in which case the greater preventive effect of D-*chiro*-inositol may result from its differential incorporation and metabolism within the phosphoinositide cycle. Insulin stimulation of rat fibroblasts expressing the human insulin receptor leads to a significant increase in the incorporation of D-*chiro*-inositol into phospholipids, whereas the effect on *myo*-inositol incorporation is only marginal (Pak *et al.*, 1993). Moreover, D-*chiro*-inositol induces a much larger reduction in plasma glucose level in rats rendered diabetic by streptozotocin administration compared with exogenous *myo*-inositol (Ortmeyer *et al.*, 1993). In humans, D-*chiro*-inositol can increase the action of insulin in patients with polycystic ovarian syndrome, improving ovulatory function, reducing blood pressure, and decreasing blood androgen and triglyceride concentrations (Nestler *et al.*, 1999). These findings suggest an inherently greater potency or bioactivity of D-*chiro*-inositol than *myo*-inositol, perhaps as a result of incorporation into different phosphatidylinositol species (Pak and Larner, 1992). It is striking, however, that these differences of in-vivo potency are maintained in the face of the demonstrated interconversion of the two inositol isomers (Pak *et al.*, 1992). Perhaps the rate of interconversion is too low to obscure the inherently greater potency of D-*chiro*-inositol in short-term effects on embryonic development.

How does inositol normalize neural tube closure in curly tail mice?

Although the causative gene responsible for the curly tail defect is unknown (Van Straaten and Copp, 2001), the primary cellular abnormality leading to the development of spina bifida has been identified as a reduced rate of cell proliferation in the hindgut endoderm and notochord (Copp *et al.*, 1988). The resultant growth imbalance between dorsal and ventral tissues causes excessive ventral curvature of the caudal embryonic region, which mechanically opposes closure of the posterior neuropore (Brook *et al.*, 1991). Exogenous inositol treatment may correct the underlying cell proliferation defect in curly tail embryos. In support of this idea, inositol metabolism is known to be intimately involved with cell cycle progression in a variety of cell types. For instance, a nuclear polyphosphoinositide cycle exists in which phosphatidylinositol-specific

Table II. Frequency of neural tube and tail defects among curly tail fetuses treated *in utero* with *myo*- and D-*chiro*-inositol

Dose route	Treatment	Inositol dose[a]	No. of fetuses	Phenotype of fetuses[b,c]		
				Spina bifida ± curly tail	Curly tail	Normal
s.c.	PBS	–	25	6 (24.0)	14 (56.0)	5 (20.0)
	myo	29	29	6 (20.7)	12 (41.4)	11 (37.9)
	D-*chiro*	29	26	3 (11.5)	17 (65.4)	6 (23.1)
	PBS	–	104	14 (13.5)	63 (60.6)	27 (25.9)
	myo	72	67	4 (6.0)	37 (55.2)	26 (38.8)
	D-*chiro*	72	86	2 (2.3)	39 (45.4)	45 (52.3)
	PBS	–	102	19 (18.6)	49 (48.0)	34 (33.3)
	myo	144	94	8 (8.5)	52 (55.3)	34 (36.2)
	D-*chiro*	144	99	5 (5.0)	46 (46.5)	48 (48.5)
Oral	PBS	–	44	8 (18.2)	21 (47.7)	15 (34.1)
	myo	800	35	3 (8.6)	15 (42.9)	17 (48.6)
	D-*chiro*	800	39	1 (2.6)	12 (30.8)	26 (66.7)

[a]μg inositol/g body weight per day.
[b]Phenotype frequencies expressed as number of fetuses (% of total for treatment group).
[c]Statistical analysis: distribution of embryos among the three phenotype categories varies significantly with treatment group at 72, 144 and 800 μg inositol/g body weight per day (χ^2-tests, P = 0.0005, 0.0051 and 0.026 respectively) but not at 29 μg inositol/g body weight per day (P = not significant).
PBS = phosphate-buffered saline.

Table III. Survival of embryos and fetuses among curly tail litters treated *in utero* with *myo*- and D-*chiro*-inositol

Dose route	Treatment	Inositol dose[a]	No. of litters	No. of viable fetuses	Mean fetal crown—rump length[b]	No. of uterine resorptions[c]	Mean litter size[a]
s.c.	PBS	–	4	25	22.3 ± 0.3	3 (10.7)	6.3 ± 1.0
	myo	29	4	29	21.8 ± 0.3	2 (6.5)	7.3 ± 1.8
	D-*chiro*	29	3	26	22.0 ± 0.3	1 (3.7)	8.7 ± 1.8
	PBS	–	12	104	21.4 ± 0.6	10 (8.8)	8.7 ± 0.5
	myo	72	8	67	21.9 ± 0.2	7 (9.5)	8.4 ± 0.8
	D-*chiro*	72	12	86	21.8 ± 0.2	8 (8.5)	7.2 ± 0.9
	PBS	–	12	102	20.9 ± 0.3	9 (8.1)	8.5 ± 0.8
	myo	144	12	94	21.4 ± 0.5	9 (8.7)	7.8 ± 0.4
	D-*chiro*	144	14	99	21.6 ± 0.4	6 (5.7)	7.1 ± 0.8
Oral	PBS	–	7	44	22.3 ± 0.4	5 (10.2)	6.3 ± 0.4
	myo	800	6	35	22.0 ± 0.3	3 (7.9)	5.8 ± 0.5
	D-*chiro*	800	6	39	21.7 ± 0.2	3 (7.1)	6.5 ± 1.1

[a]μg inositol/g body weight per day.
[b]Crown–rump length (mm; mean ± SEM) measured on a subset of fetuses (n = 6–9 per group). Values do not differ significantly between treatments or dose levels.
[c]Values in parentheses are resorptions as % of total number of implantations (i.e. viable fetuses + resorptions). Logistic regression analysis: the proportion of resorptions does not differ significantly between *myo*-inositol and PBS litters, between D-*chiro*-inositol and PBS litters, or between inositol dose levels.
[d]Litter size (mean no. of viable fetuses per litter ± SEM) does not vary significantly with treatment group or inositol dose level. Although not statistically significant, litters treated with oral inositol contain an average of 1.6 (95% confidence intervals: 0.4–2.8) fewer fetuses than litters treated with s.c. inositol.

phospholipase C generates elevated levels of nuclear DAG specifically during G_2 phase of the cell cycle (Sun *et al.*, 1997). This DAG production is required for the G_2/M transition, perhaps by attracting specific activated PKC isozymes to the nucleus, where they are stabilized by binding to nuclear proteins including lamins A, B and C. The elevation of DAG levels is transient, as DAG is rapidly converted to phosphatidic acid by nuclear DAG kinases, enzymes that are also induced by growth-promoting agents (Martelli *et al.*, 2000). It is possible that inositol treatment of curly tail embryos stimulates this nuclear DAG cycle leading, via the activation of specific PKC isozymes, to the increased proliferation of hindgut and notochordal cells, so normalizing neural tube closure.

Relevance of the findings for clinical application of inositol therapy

In order for these experimental findings to be translated into a clinical application, inositol supplementation must be not only effective in preventing NTDs, but also safe for use during human pregnancy. The current demonstration of a protective

Table IV. Pathological analysis of curly tail fetuses treated *in utero* with *myo*- and D-*chiro*-inositol[a]

Pathology	Inositol dose (μg/g body weight per day)					
	PBS[b]		*myo*		D-*chiro*	
	72	144	72	144	72	144
Serial section analysis						
No. of fetuses examined	27	17	11	21	24	19
Exencephaly ± open eye	1 (3.7)	2 (11.8)	–	2 (9.5)	–	1 (5.3)
Hydrocephaly	1 (3.7)	–	–	1 (4.8)	–	1 (5.3)
Haemorrhage in/around brain	–	2 (11.8)	–	2 (9.5)	–	1 (5.3)
Microphthalmia/macrophthalmia	1 (3.7)	1 (5.9)	–	–	–	–
Bleeding in thorax/abdomen	6 (22.2)	4 (23.6)	2 (18.2)	–	2 (8.4)	1 (5.3)
Thyroid lobe reduction	1 (3.7)	–	–	1 (4.8)	–	–
Intrahepatic bleeding	–	1 (5.9)	1 (9.1)	1 (4.8)	–	–
Small additional liver lobe	9 (33.3)	4 (23.5)	6 (54.5)	4 (19.0)	6 (25.0)	4 (21.1)
Fissure in liver lobe	–	2 (11.8)	1 (9.1)	–	–	1 (5.3)
Renal pelvis/ureter enlarged	1 (3.7)	–	–	–	1 (4.2)	3 (15.8)[c]
Skeletal analysis						
No. of fetuses examined	29	18	16	18	22	21
Exencephaly	–	–	–	2 (11.1)	–	2 (9.5)
Bony plaque in frontonasal suture	1 (3.4)	–	1 (6.3)	–	–	1 (4.8)
Anomalous cervical vertebra(e)	–	–	–	–	1 (5.6)	4 (19.0)[c]
Rudimentary ribs on 7th cervical vertebra	4 (13.8)	2 (11.1)	1 (6.3)	3 (16.7)	1 (4.5)	7 (33.3)[c]
Anomalous thoracic vertebrae and/or ribs	–	–	–	–	–	2 (2.5)[c]
Rudimentary 14th ribs	–	1 (5.6)	–	1 (5.6)	–	1 (4.8)
Sternal fusions	1 (3.4)	–	–	–	–	2 (9.5)

[a]Summary of most prevalent findings only are listed. A single fetus may have more than one morphological finding. Values are number of fetuses with defect (% of total for treatment group). A dash (–) indicates that no fetuses exhibited that finding.
[b]PBS dose levels 72 and 144 refer to saline controls performed contemporaneously with the stated dose levels of *myo*- and D-*chiro*-inositol.
[c]Proportion with defect does not differ significantly between fetuses treated with D-*chiro*-inositol and PBS controls (144 μg/g body weight per day; Fisher's exact test; $P > 0.05$).

effect of inositol by s.c. and oral administration is supported by the results of previous studies in which *myo*-inositol was injected i.p. (Greene and Copp, 1997). Further support for the effectiveness of oral supplementation with *myo*-inositol comes from the finding of a reduction in the incidence of diabetes-induced abnormalities in rats by oral administration of *myo*-inositol (Khandelwal *et al.*, 1998). The efficacy of inositol in preventing human NTDs has not yet been tested in a clinical trial. Nevertheless, a recent case study has documented inositol supplementation in association with a normal outcome in the third pregnancy of a woman who had two previous consecutive NTD pregnancies despite taking 4 mg folic acid throughout the periconceptional period (Cavalli and Copp, 2002). The empirical recurrence risk of NTD following two previous affected fetuses is ~1 in 9 (Seller, 1981), so the association of inositol therapy with normal pregnancy outcome in this case may have been a chance association. A larger study of pregnancies at risk of 'folate-resistant' NTDs is needed, to test the idea that inositol may be as effective in humans as in mice.

With regard to the safety of inositol therapy during pregnancy, the present pathological study revealed no major defects, apart from NTDs, and no increase in the frequency of embryonic or fetal loss *in utero* in inositol-treated mice. The present study was limited, however, and in particular the effects of inositol administration during the periconceptional period—when inositol would be taken during a clinical trial—were not assessed. The reproductive toxicology of D-*chiro*-inositol has been the subject of studies in rats and rabbits, with more extensive administration at doses up to 2000 mg/kg per day, and no adverse effects on mating, fertility or embryo/fetal development have been found (Insmed Inc., data on file). There is much less information available on the safety of inositol therapy in human pregnancy. In the case of the mother who took inositol in her third pregnancy following two apparently 'folate-resistant' NTD pregnancies, a dose of 0.5 g inositol per day was used, with no known side-effects for either mother or baby (Cavalli and Copp, 2002). In particular, there was no evidence of abnormal uterine contractions, such as have been suggested as a possible adverse effect of inositol therapy (Colodny and Hoffman, 1998). *Myo*-inositol has also been tested in adults for prevention of depression, panic disorder and obsessive compulsive disorder (Benjamin *et al.*, 1995; Levine *et al.*, 1995; Fux *et al.*, 1996) and in children for treatment of autism (Levine *et al.*, 1997). No significant side-effects were reported in these studies, which employed relatively high inositol doses of up to 18 g per day in adults and 200 mg/kg in children.

In conclusion, D-*chiro*-inositol has been shown to be highly effective in preventing folate-resistant mouse NTDs. A clinical trial could next evaluate the effectiveness of peri-conceptional inositol supplementation, as an adjunct to folic acid therapy, in preventing human NTDs. If folate-resistant NTDs can be prevented, in addition to those cases already prevented by folic acid, this could lead to a significant further reduction in the frequency of this birth defect.

Acknowledgements

The authors thank Katie Gardner for valuable technical assistance. This study was supported by Wellbeing, Insmed Incorporated and the Wellcome Trust.

References

Baker, L., Piddington, R., Goldman, A., Egler, J. and Moehring, J. (1990) *Myo*-inositol and prostaglandins reverse the glucose inhibition of neural tube fusion in cultured mouse embryos. *Diabetologia*, **33**, 593–596.

Benjamin, J., Levine, J., Fux, M., Aviv, A., Levy, D. and Belmaker, R.H. (1995) Double-blind, placebo-controlled, crossover trial of inositol treatment for panic disorder. *Am. J. Psychiatry*, **152**, 1084–1086.

Berry, R.J., Li, Z., Erickson, J.D., Li, S., Moore, C.A., Wang, H., Mulinare, J., Zhao, P., Wong, L.Y.C., Gindler, J. *et al.* (1999) Prevention of neural-tube defects with folic acid in China. *N. Engl. J. Med.*, **341**, 1485–1490.

Brook, F.A., Shum, A.S.W., Van Straaten, H.W.M. and Copp, A.J. (1991) Curvature of the caudal region is responsible for failure of neural tube closure in the curly tail (ct) mouse embryo. *Development*, **113**, 671–678.

Carter, M., Ulrich, S., Oofuji, Y., Williams, D.A. and Ross, M.E. (1999) *Crooked tail* (*Cd*) models human folate-responsive neural tube defects. *Hum. Mol. Genet.*, **8**, 2199–2204.

Cavalli, P. and Copp, A.J. (2002) Inositol and folate-resistant neural tube defects. *J. Med. Genet.*, **39**, e5.

Cockroft, D.L. (1988) Changes with gestational age in the nutritional requirements of postimplantation rat embryos in culture. *Teratology*, **38**, 281–290.

Cockroft, D.L., Brook, F.A. and Copp, A.J. (1992) Inositol deficiency increases the susceptibility to neural tube defects of genetically predisposed (curly tail) mouse embryos *in vitro*. *Teratology*, **45**, 223–232.

Colodny, L. and Hoffman, R.L. (1998) Inositol—clinical applications for exogenous use. *Altern. Med. Rev.*, **3**, 432–447.

Copp, A.J. (1985) Relationship between timing of posterior neuropore closure and development of spinal neural tube defects in mutant (curly tail) and normal mouse embryos in culture. *J. Embryol. Exp. Morphol.*, **88**, 39–54.

Copp, A.J., Brook, F.A. and Roberts, H.J. (1988) A cell-type-specific abnormality of cell proliferation in mutant (curly tail) mouse embryos developing spinal neural tube defects. *Development*, **104**, 285–295.

Copp, A., Cogram, P., Fleming, A., Gerrelli, D., Henderson, D., Hynes, A., Kolatsi-Joannou, M., Murdoch, J. and Ybot-Gonzalez, P. (1999) Neurulation and neural tube closure defects. In Tuan, R.S. and Lo, C.W. (eds), *Methods in Molecular Biology, Vol. 136: Developmental Biology Protocols, Vol II.* Humana Press Inc., Totowa, NJ, pp. 135–160.

Czeizel, A.E. and Dudás, I. (1992) Prevention of the first occurrence of neural-tube defects by periconceptional vitamin supplementation. *N. Engl. J. Med.*, **327**, 1832–1835.

Embury, S., Seller, M.J., Adinolfi, M. and Polani, P.E. (1979) Neural tube defects in curly-tail mice. I. Incidence and expression. *Proc. R. Soc. Lond. B*, **206**, 85–94.

Essien, F.B. and Wannberg, S.L. (1993) Methionine but not folinic acid or vitamin B-12 alters the frequency of neural tube defects in *Axd* mutant mice. *J. Nutr.*, **123**, 27–34.

Fleming, A. and Copp, A.J. (1998) Embryonic folate metabolism and mouse neural tube defects. *Science*, **280**, 2107–2109.

Fux, M., Levine, J., Aviv, A. and Belmaker, R.H. (1996) Inositol treatment of obsessive-compulsive disorder. *Am. J. Psychiatry*, **153**, 1219–1221.

Goldstein, H. (1995) *Multilevel Statistical Models. Kendall's Library of Statistics 3*. Edward Arnold, London.

Greene, N.D.E. and Copp, A.J. (1997) Inositol prevents folate-resistant neural tube defects in the mouse. *Nature Med.*, **3**, 60–66.

Gruneberg, H. (1954) Genetical studies on the skeleton of the mouse. VIII. Curly tail. *J. Genet.*, **52**, 52–67.

Hashimoto, M., Akazawa, S., Akazawa, M., Akashi, M., Yamamoto, H., Maeda, Y., Yamaguchi, Y., Yamasaki, H., Tahara, D., Nakanishi, T. *et al.* (1990) Effects of hyperglycaemia on sorbitol and *myo*-inositol contents of cultured embryos: treatment with aldose reductase inhibitor and *myo*-inositol supplementation. *Diabetologia*, **33**, 597–602.

Holmberg, J., Clarke, D.L. and Frisén, J. (2000) Regulation of repulsion versus adhesion by different splice forms of an Eph receptor. *Nature*, **408**, 203–206.

Honein, M.A., Paulozzi, L.J., Mathews, T.J., Erickson, J.D. and Wong, L.Y.C. (2001) Impact of folic acid fortification of the US food supply on the occurrence of neural tube defects. *JAMA*, **285**, 2981–2986.

Khandelwal, M., Reece, E.A., Wu, Y.K. and Borenstein, M. (1998) Dietary myo-inositol therapy in hyperglycemia-induced embryopathy. *Teratology*, **57**, 79–84.

Levine, J., Barak, Y., Gonzalves, M., Szor, H., Elizur, A., Kofman, O. and Belmaker, R.H. (1995) Double-blind, controlled trial of inositol treatment of depression. *Am. J. Psychiatry*, **152**, 792–794.

Levine, J., Aviram, A., Holan, A., Ring, A., Barak, Y. and Belmaker, R.H. (1997) Inositol treatment of autism. *J. Neural Transm.*, **104**, 307–310.

Majerus, P.W. (1992) Inositol phosphate biochemistry. *Annu. Rev. Biochem.*, **61**, 225–250.

Martelli, A.M., Tabellini, G., Bortul, R., Manzoli, L., Bareggi, R., Baldini, G., Grill, V., Zweyer, M., Narducci, P. and Cocco, L. (2000) Enhanced nuclear diacylglycerol kinase activity in response to a mitogenic stimulation of quiescent Swiss 3T3 cells with insulin-like growth factor I. *Cancer Res.*, **60**, 815–821.

Nestler, J.E., Jakubowicz, D.J., Reamer, P., Gunn, R.D. and Allan, G. (1999) Ovulatory and metabolic effects of D-*chiro*-inositol in the polycystic ovary syndrome. *N. Engl. J. Med.*, **340**, 1314–1320.

Ortmeyer, H.K., Huang, L.C., Zhang, L., Hansen, B.C. and Larner, J. (1993) Chiroinositol deficiency and insulin resistance. II. Acute effects of D-chiroinositol administration in streptozotocin- diabetic rats, normal rats given a glucose load, and spontaneously insulin-resistant rhesus monkeys. *Endocrinology*, **132**, 646–651.

Pak, Y. and Larner, J. (1992) Identification and characterization of chiroinositol-containing phospholipids from bovine liver. *Biochem. Biophys. Res. Commun.*, **184**, 1042–1047.

Pak, Y., Huang, L.C., Lilley, K.J. and Larner, J. (1992) *In vivo* conversion of [3H]myoinositol to [3H]chiroinositol in rat tissues. *J. Biol. Chem.*, **267**, 16904–16910.

Pak, Y., Paule, C.R., Bao, Y.D., Huang, L.C. and Larner, J. (1993) Insulin stimulates the biosynthesis of chiro-inositol-containing phospholipids in a rat fibroblast line expressing the human insulin receptor. *Proc. Natl Acad. Sci. USA*, **90**, 7759–7763.

Seller, M.J. (1981) Recurrence risks for neural tube defects in a genetic counselling clinic population. *J. Med. Genet.*, **18**, 245–248.

Seller, M.J. (1994) Vitamins, folic acid and the cause and prevention of neural tube defects. In Bock, G. and Marsh, J. (eds), *Neural Tube Defects (Ciba Foundation Symposium 181)*. John Wiley & Sons, Chichester, pp. 161–173.

Sun, B., Murray, N.R. and Fields, A.P. (1997) A role for nuclear phosphatidylinositol-specific phospholipase C in the G2/M phase transition. *J. Biol. Chem.*, **272**, 26313–26317.

Van Straaten, H.W.M. and Copp, A.J. (2001) Curly tail: a 50-year history of the mouse spinal bifida model. *Anat. Embryol.*, **203**, 225–237.

Van Straaten, H.W.M., Hekking, J.W.M., Copp, A.J. and Bernfield, M. (1992) Deceleration and acceleration in the rate of posterior neuropore closure during neurulation in the curly tail (ct) mouse embryo. *Anat. Embryol.*, **185**, 169–174.

Wald, N., Sneddon, J., Densem, J., Frost, C., Stone, R. and MRC Vitamin Study Research Group (1991) Prevention of neural tube defects: Results of the Medical Research Council Vitamin Study. *Lancet*, **338**, 131–137.

Whittaker, J. and Dix, K.M. (1979) Double staining technique for rat skeletons in teratological studies. *Lab. Anim.*, **13**, 309–310.

Wilson, J.G. (1965) Methods for administering agents and detecting malformations in experimental animals. In Wilson, J.G. and Warkany, J. (eds), *Teratology: Principles and Techniques*. University of Chicago Press, Chicago, IL, USA, pp. 262–277.

Zhao, Q., Behringer, R.R. and De Crombrugghe, B. (1996) Prenatal folic acid treatment suppresses acrania and meroanencephaly in mice mutant for the *Cart1* homeobox gene. *Nature Genet.*, **13**, 275–283.

Submitted on February 25, 2002; accepted on May 10, 2002

SPECIAL NOTE

ITEM SCANNED AS SUPPLIED
PAGINATION IS AS SEEN

Human Molecular Genetics, 2004, Vol. 13, No. 1 7–14
DOI: 10.1093/hmg/ddh003
Advance Access published on November 12, 2003

Specific isoforms of protein kinase C are essential for prevention of folate-resistant neural tube defects by inositol

Patricia Cogram, Andrew Hynes[†], Louisa P.E. Dunlevy, Nicholas D.E. Greene and Andrew J. Copp*

[1]Neural Development Unit, Institute of Child Health, University College London, London WC1N 1EH, UK

Received July 8, 2003; Revised and Accepted October 27, 2003

A proportion of neural tube defects (NTDs) can be prevented by maternal folic acid supplementation, although some cases are unresponsive. The *curly tail* mutant mouse provides a model of folate-resistant NTDs, in which defects can be prevented by inositol therapy in early pregnancy. Hence, inositol represents a possible novel adjunct therapy to prevent human NTDs. The present study investigated the molecular mechanism by which inositol prevents mouse NTDs. Activation of protein kinase C (PKC) is known to be essential, and we examined neurulation-stage embryos for PKC expression and applied PKC inhibitors to *curly tail* embryos developing in culture. Although all known PKC isoforms were detected in the closing neural tube, use of chemical PKC inhibitors identified a particular requirement for 'conventional' PKC isoforms. Peptide inhibitors offer selective inhibition of individual PKCs, and we demonstrated isoform-specific inhibition of PKC in embryonic cell cultures. Application of peptide inhibitors to neurulation-stage embryos revealed an absolute dependence on the activity of PKCβI and γ for prevention of NTDs by inositol, and partial dependence on PKCζ, whereas other PKCs (α, βII δ, and ε) were dispensable. To investigate the cellular action of inositol and PKCs in NTD prevention, we examined cell proliferation in *curly tail* embryos. Defective proliferation of hindgut cells is a key component of the pathogenic sequence leading to NTDs in *curly tail*. Hindgut cell proliferation was stimulated specifically by inositol, an effect that required activation of PKCβI. Our findings reveal an essential role of specific PKC isoforms in mediating the prevention of mouse NTDs by inositol.

INTRODUCTION

Neural tube defects (NTDs) are common, severe birth defects with a multifactorial aetiology involving both genetic and environmental factors. In a proportion of cases, NTDs can be prevented by maternal peri-conceptional supplementation with folic acid (1,2). Around 30% of NTDs appear unresponsive to folic acid, however, and there is currently no preventive therapy available for these 'folate-resistant' defects. A large number of mouse genetic mutants exhibit NTDs and, as in humans, some of these are responsive to folic acid treatment whereas others are not (3,4). Mice homozygous for the *curly tail* mutation develop spina bifida that exhibits many similarities to the corresponding human NTD (5). NTDs in *curly tail* mice are folate-resistant (6), but we showed that the majority of NTDs in *curly tail* mice can be prevented by both *myo*-inositol and its D-*chiro*- enantiomer, either administered to pregnant females or directly to embryos *in vitro* (7,8). Our findings raise the possibility of developing a novel clinical therapy based on inositol. The recent observation that inositol therapy is well tolerated during human pregnancy at high risk of NTD recurrence (9), encourages progress towards a clinical trial of inositol.

The mechanism of action of inositol in preventing NTDs in *curly tail* mice involves activation of PKC, a family of serine/threonine kinases (7). The effect of inositol can be mimicked by brief treatment of embryos with TPA (12-O-tetradecanoyl-phorbol-13-acetate), an agonist of PKC. Moreover, the effect of inositol is blocked by co-administration of a broad-spectrum chemical inhibitor of PKC (7). At least 10 isoforms of PKC are known, grouped according to their dependence on diacylglycerol (DAG) and Ca^{2+} for activation (10). Conventional PKCs

*To whom correspondence should be addressed at: Neural Development Unit, Institute of Child Health, 30 Guilford Street, London WC1N 1EH, UK. Tel: +44 2078298893; Fax: +44 2078314366; Email: a.copp@ich.ucl.ac.uk
[†]Present address:
Etiologics Limited, Harwell, Oxfordshire OX11 0RD, UK.

(cPKCs; α, βI, βII, γ) require DAG and Ca^{2+}, novel PKCs (nPKCs; δ, ε, η, θ) are DAG-sensitive but Ca^{2+}-insensitive, and atypical PKCs (aPKCs; ζ, λ and the related PKCμ) are activated by neither DAG or Ca^{2+} (10).

To elucidate the molecular mechanism by which inositol normalizes neural tube closure, we determined which of the PKC isoforms mediate this effect. All known PKC isoforms could be detected during mouse neural tube closure, but culture of intact *curly tail* embryos in the presence of isoform-specific PKC inhibitors identified PKCβI and γ as essential for the normalizing action of inositol. Other PKC isoforms were not required. At the cellular level, inositol treatment was found to correct the deficit of cell proliferation that underlies NTD development in *curly tail* embryos (11), an effect that is blocked by inhibition of PKCβI. Moreover, treatment of cultured cells with either the PKC activator TPA or inositol itself, could induce translocation of PKC isoforms, including PKCβI and γ to the nucleus. We conclude that PKCβI and γ are essential components of the molecular mechanism underlying the preventive effect of inositol on mouse NTDs.

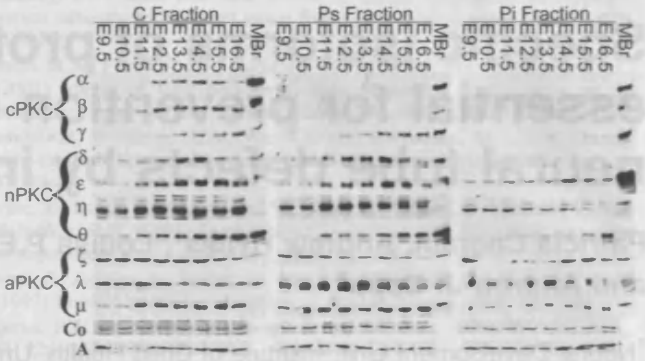

Figure 1. Developmental regulation of PKC isoform expression in mouse embryos from E9.5 to E16.5. Sub-cellular protein fractions of whole embryo homogenates were western blotted using isoform-specific anti-PKC antibodies. PKC isoforms exhibit varying patterns of developmental regulation ranging from limited expression in only the C fraction, at only the most advanced developmental stages (PKCα and β) to constitutive expression in all three fractions, throughout the developmental period studied (PKCη, ζ, λ and μ). Abbreviations: A, β-actin control; C, cytoplasmic fraction; Co, Coomassie Blue stained loading control; MBr, mouse brain standard; Ps, soluble pelleted fraction (membrane associated); Pi, insoluble pelleted fraction. Experiment performed on two occasions with same result.

RESULTS

PKC isoform expression during mouse embryogenesis

In order to identify the isoforms that might play a role in prevention of NTD, we initially determined which PKC isoforms are expressed in mouse embryos undergoing organogenesis (E9.5 to E16.5). Western blot analysis of cytoplasmic (C), membrane-associated (Ps) and insoluble (Pi) fractions of embryonic cell extracts indicated the degree to which PKC isoforms are activated (i.e. associated with membrane or insoluble cellular compartments). All PKC isoforms could be detected, but their relative abundance varied with stage and cellular fraction (Fig. 1). cPKCs (α, β, γ) were weak or undetectable in the cytoplasmic fraction at E9.5 and E10.5, although expression increased from E11.5 onwards. Among the cPKCs, only PKCγ was present in the Ps fraction from E11.5 and in the Pi fraction at the latest stages. nPKCs (δ, ε, θ, η) were expressed throughout the developmental period in both C and Ps fractions, whereas expression in the Pi fraction was more variable. aPKCs (λ, ζ and the related PKCμ) were abundant from E9.5 onwards in all cellular fractions, with a fairly constant level of expression. All PKC isoforms were also detected in mutant *curly tail* embryos with no consistent differences in abundance compared with non-mutant CD1 mice (data not shown). Hence, the DAG-responsive cPKCs and nPKCs, which are likely to mediate the normalizing effect of inositol (6), exhibit evidence of stage-dependent activation unlike the aPKCs which appear ubiquitous and constitutively activated, as also described in other systems (12).

Western blot analysis was insufficiently sensitive to detect PKC isoform expression in specific embryonic regions, such as the posterior neuropore (PNP), the site of spinal neurulation (13). We performed immunohistochemistry on histological sections through the PNP region, and detected expression of PKCs α, βI, βII, γ and ε in the closing neural tube, hindgut, notochord and presomitic mesoderm, at both E9.5 and E10.5 (Fig. 2). We conclude that although cPKCs, in particular, are variably expressed in whole neurulation-stage embryos by immunoblotting, they can be detected in all tissues of the PNP region by immunohistochemistry and, therefore, are candidates for a role in mediating the preventive effect of inositol on NTDs. Immunostaining was not carried out for the remaining isoforms as they were clearly detectable by western blot (Fig. 1).

Chemical PKC inhibitors block the protective effect of inositol on NTDs

We used PKC inhibitors to block the effect of inositol on neural tube closure. *Curly tail* embryos were cultured from E9.5 to E10.5, and the length of unclosed neural folds at the PNP was then measured to indicate predisposition to spina bifida (13). Embryos exposed to PBS (vehicle) alone had enlarged PNPs (Fig. 3A), reflecting the *in vivo* development of spinal NTDs by 50–60% of *curly tail* embryos (5), whereas treatment with *myo*-inositol decreased PNP length significantly (first grey bar, Fig. 3A), to a value characteristic of normally developing embryos (5). Hence, inositol normalizes PNP closure *in vitro*, confirming previous findings (7,8). *Curly tail* embryos were exposed in culture to chemical inhibitors that block different combinations of PKC isoforms. Bisindolylmaleimide I (BisI) inhibits PKCα, βI, βII, γ and ε (14), Go6976 inhibits solely cPKCs (15), HBDDE inhibits PKCα and γ *in vitro* (16) and LY294002 is an inhibitor of phosphatidylinositol-3-kinase (17), an activator of PKCζ (18). When added alone, none of the inhibitors significantly altered PNP length (white bars, Fig. 3A). Moreover, BisV, an inactive control, did not prevent the reduction in PNP length caused by co-administration of inositol (second grey bar, Fig. 3A). In contrast, BisI, Go6976, HBDDE and LY294002 all partially blocked the normalizing effect of inositol, such that PNP length was reduced to a significantly lesser degree than in the presence of inositol alone (black bars, Fig. 3A). Hence, use of chemical inhibitors highlights the

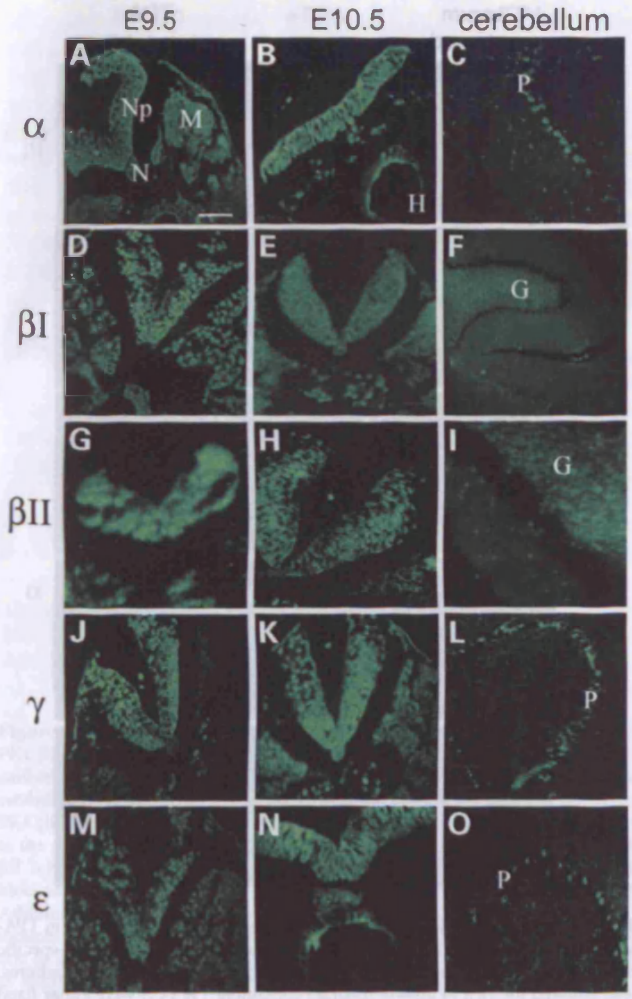

Figure 2. Ubiquitous expression of PKC isoforms during mouse spinal neurulation, detected by immunohistochemistry. Transverse histological sections through the posterior neuropore region of *curly tail* mouse embryos at E9.5 (**A**, **D**, **G**, **J**, **M**) and E10.5 (**B**, **E**, **H**, **K**, **N**) stained with antibodies specific for PKCα, βI, βII, γ and ε. All PKCs exhibit ubiquitous expression in the neural plate, notochord, hindgut and presomitic mesoderm of the posterior neuropore region. Sections of adult mouse cerebellum (**C**, **F**, **I**, **L**, **O**) provide a positive control for the isoform-specific PKC antibodies: anti-PKCα, γ and ε stain only Purkinje cells, whereas anti-PKCβI and βII stain only granule cells, as described previously for the rat cerebellum (46). Abbreviations: G, granule cells; H, hindgut; M, presomitic mesoderm; N, notochord; Np, neural plate; P, Purkinje cells. Scale bar represents 20 μm.

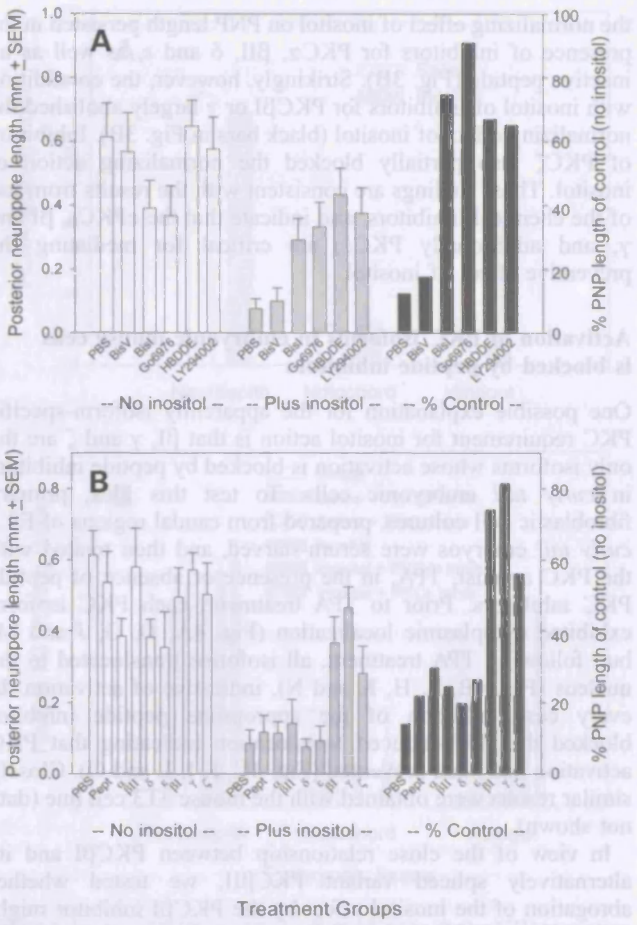

Figure 3. Normalization of spinal neural tube closure by inositol in *curly tail* embryos is abrogated by inhibition of specific PKC isoforms. (**A**) Chemical and (**B**) isoform-specific peptide PKC inhibitors were applied to *curly tail* mouse embryos cultured from E9.5 for 24 h, followed by measurement of posterior neuropore (PNP) length, an indicator of predisposition to spinal NTD (13). White bars: PNP length of embryos exposed to PKC inhibitors in the absence of inositol; grey bars: PNP length of embryos exposed to PKC inhibitors in the presence of inositol; black bars: PNP length in the presence of PKC inhibitor plus inositol as a % of the value in the presence of PKC inhibitor alone (right axis). (**A**) Inositol significantly reduces PNP length in the absence of inhibitor (PBS; $P < 0.001$) and in the presence of inactive BisV ($P < 0.002$), whereas the inositol effect is abrogated in the presence of chemical inhibitors BisI, Go6976, HBDDE and LY294002 ($P > 0.05$). (**B**) Inositol significantly reduces PNP length in the absence of inhibitor (PBS; $P < 0.001$) and in the presence of inactive peptide (Pept) or peptide inhibitors to PKC α, βII, δ ($P < 0.005$) and ε ($P < 0.05$), whereas the inositol effect is abrogated by inhibitors to PKCβI, γ and ζ ($P > 0.05$). There is no effect on PNP length of either chemical or peptide inhibitors in the absence of inositol (analysis of variance, $P > 0.05$).

potential importance of PKCα, β, γ, ε and ζ in mediating NTD prevention by inositol.

Peptide inhibitors identify a critical role for PKCβI, γ and ζ in the inositol effect

Because of the relatively broad spectrum activity of chemical PKC inhibitors, we next applied isoform-specific peptide PKC inhibitors to cultured *curly tail* embryos, to more precisely define the PKC isoform requirement for the inositol effect. Each peptide inhibitor was designed to the amino acid sequence corresponding to the isoform-specific RACK (receptor for activated C kinase) binding site on PKC. Inhibitors of this type prevent PKC translocation and/or activation in an isoform-specific manner (19,20). Peptide inhibitors were coupled to a sequence derived from the *Drosophila* Antennapedia homeodomain, ensuring cell permeability.

As with the chemical inhibitors, peptide PKC inhibitors alone had no significant effect on PNP length. Moreover,

the normalizing effect of inositol on PNP length persisted in the presence of inhibitors for PKCα, βII, δ and ε, as well as an inactive peptide (Fig. 3B). Strikingly, however, the co-addition with inositol of inhibitors for PKCβI or γ largely abolished the normalizing effect of inositol (black bars in Fig. 3B). Inhibition of PKCζ also partially blocked the normalizing action of inositol. These findings are consistent with the results from use of the chemical inhibitors, and indicate that the cPKCs, βI and γ, and additionally PKCζ, are critical for mediating the preventive effect of inositol.

Activation of PKC isoforms in embryonic mouse cells is blocked by peptide inhibitors

One possible explanation for the apparently isoform-specific PKC requirement for inositol action is that βI, γ and ζ are the only isoforms whose activation is blocked by peptide inhibitors in *curly tail* embryonic cells. To test this idea, primary fibroblastic cell cultures, prepared from caudal regions of E9.5 *curly tail* embryos were serum-starved, and then treated with the PKC agonist, TPA, in the presence or absence of peptide PKC inhibitors. Prior to TPA treatment, each PKC isoform exhibited cytoplasmic localization (Fig. 4A, D, G, J and M) but, following TPA treatment, all isoforms translocated to the nucleus (Fig. 4B, E, H, K and N), indicative of activation. In every case, addition of the appropriate peptide inhibitor blocked this TPA-induced translocation indicating that PKC activation had been prevented (Fig. 4C, F, I, L and O). Closely similar results were obtained with the mouse 3T3 cell line (data not shown).

In view of the close relationship between PKCβI and its alternatively spliced variant PKCβII, we tested whether abrogation of the inositol effect by the PKCβI inhibitor might have resulted from antagonism of both PKCβI and βII activation. PKCβI translocated to the nucleus following TPA stimulation, and this translocation was blocked by the βI inhibitor, but not by the βII inhibitor (Fig. 5A–C). Conversely, translocation of PKCβII was blocked by the βII inhibitor but not the βI inhibitor (Fig. 5D–F). This finding confirms that the peptide inhibitors of PKCβI and βII are indeed isoform-specific and suggests separate roles for these splice variants. We conclude that the requirement for specific PKC isoforms is unlikely to reflect differential activity of the peptide inhibitors, but may reflect a difference in participation of PKC isoforms in the action of inositol in preventing mouse NTDs.

To determine whether the PKC stimulation observed after TPA treatment also follows inositol administration, we studied PKC localization after inositol treatment. Inositol treatment was capable of inducing the translocation of PKCα from the cytoplasm, as in serum-starved cells, to the nucleus (Fig. 5G and H). Similarly, PKCβI and γ, isoforms whose activity is essential for prevention of NTD, were also found to exhibit nuclear localization in inositol-treated but not in untreated cells (data not shown). No difference in the localization of PKCζ could be detected after 6 h inositol treatment (50 μg/ml), but we cannot rule out the possibility that PKCζ is activated at a different dose or at a different time point. This observation suggests that PKCα, βI and γ can be activated by inositol treatment. However, PKCα is not required for prevention of NTD whereas PKCβI and γ are essential.

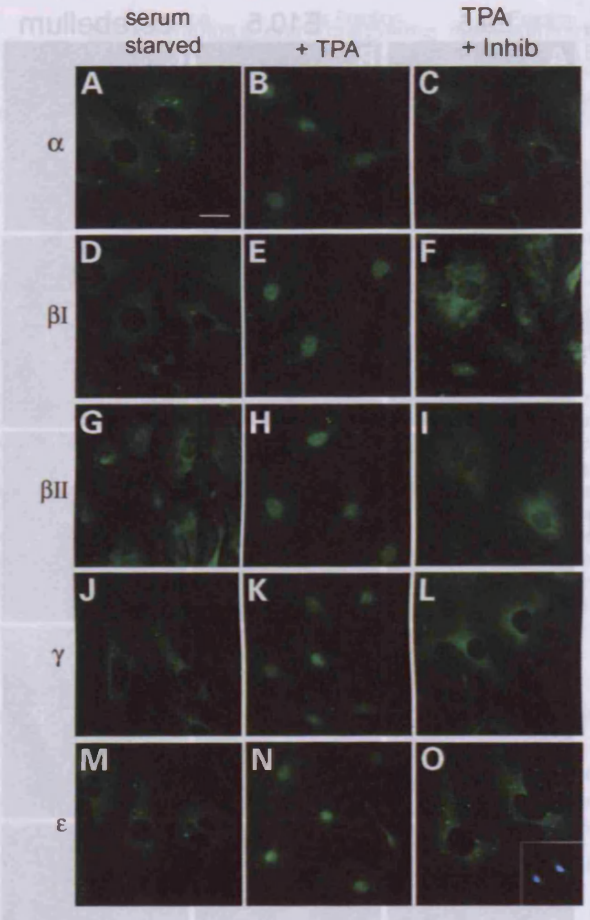

Figure 4. Inhibition of PKC isoform translocation by peptide inhibitors in TPA-treated mouse embryonic cells. Immunocytochemistry using isoform-specific antibodies to PKC (as in Fig. 2) in *curly tail* primary embryonic cell cultures. Cells cultured for 18 h in growth medium containing 1% FCS were either fixed with no additional treatment ('serum starved'; **A**, **D**, **G**, **J**, **M**), exposed to 100 μM TPA for 10 min prior to fixation (+TPA; **B**, **E**, **H**, **K**, **N**), or exposed to 1 mM isoform-specific PKC inhibitor for 20 min and to TPA for 10 min prior to fixation (TPA + Inhib; **C**, **F**, **I**, **L**, **O**). PKCs are uniformly located in the cytoplasm of serum starved cells whereas a 10 min treatment with TPA induces translocation to the nucleus in all cases. Pre-treatment with isoform-specific PKC inhibitors prevents TPA-induced translocation and all PKC isoforms exhibit cytoplasmic staining. Inset in (O) shows same field stained with DAPI to demonstrate nuclei. Scale bar represents 20 μm.

Embryonic cell proliferation is stimulated by inositol, in a PKCβI-sensitive manner

Delayed closure of the PNP in *curly tail* embryos results from a reduced rate of cell proliferation, specifically in the embryonic hindgut, within the caudal region (3,11,21,22). The resulting proliferation imbalance causes ventral curvature of the caudal region, counteracting the apposition of the neural folds, and leading to spina bifida (23,24). The effect of inositol on cell proliferation was examined by immunohistochemistry for PCNA (proliferating cell nuclear antigen) and phospho-histone H3, markers of S-phase and M-phase of the cell cycle respectively. A significant stimulatory effect of inositol on

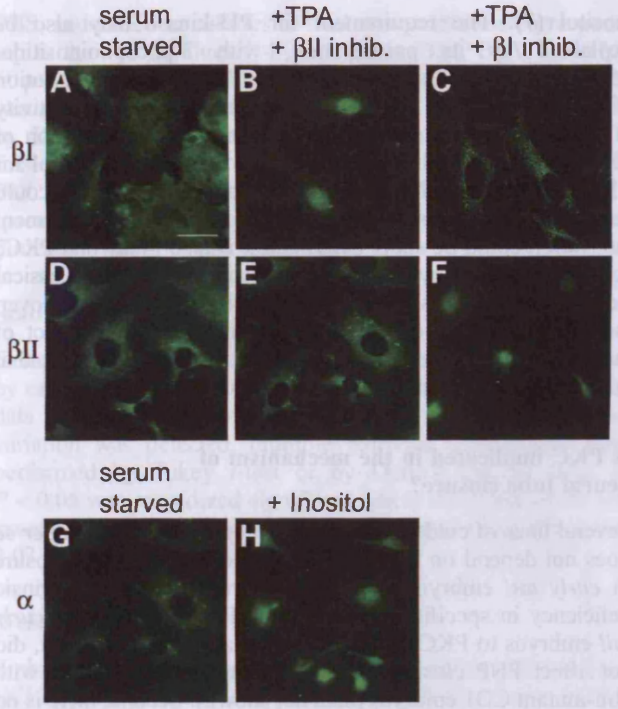

Figure 5. Inositol stimulates PKC translocation, whereas peptide inhibitors to PKCβI and βII exhibit isoform-specificity in blocking translocation. PKC isoforms were localized by immunocytochemistry on primary cell cultures established from *curly tail* mouse embryos. Serum starved cells exhibit PKCβI and βII immunoreactivity in the cytoplasm. TPA-induced translocation to the nucleus of PKCβI can be blocked by the βI inhibitor (**C**) but not by the βII inhibitor (**B**). Conversely, translocation to the nucleus of PKCβII can be blocked by the inhibitor to βII (**E**) but not by the inhibitor to βI (**F**). Addition of 50 μg/ml *myo*-inositol to serum starved cells 6 h prior to fixation induces translocation of PKCα to the nucleus (**H**) whereas PKCα is cytoplasmic in untreated cells (**G**). This effect of inositol is not unique to *curly tail* cells as similar results were obtained in 3T3 cells. Scale bar represents 20 μm.

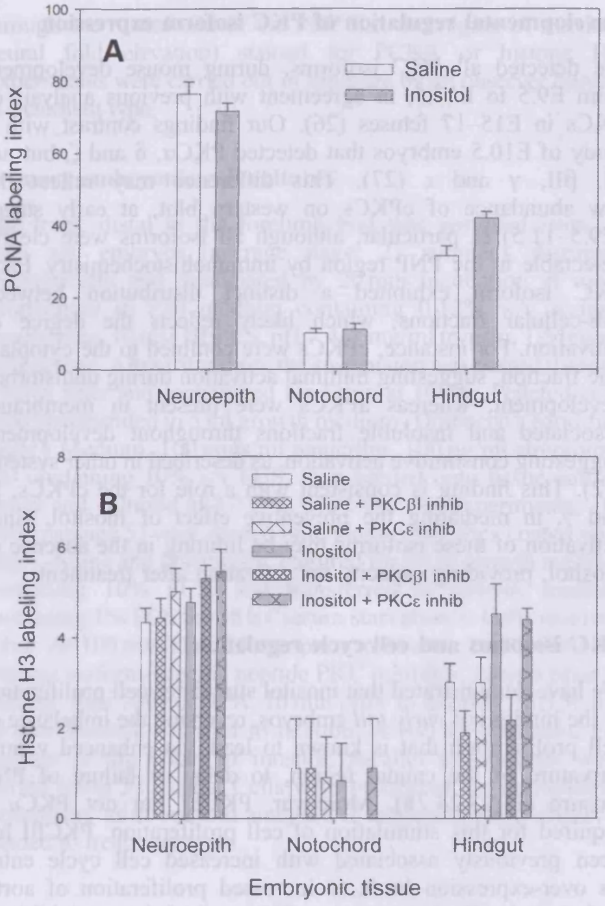

Figure 6. Inositol stimulates hindgut cell proliferation during NTD prevention, an effect requiring activation of PKCβI but not PKCε. Cell proliferation was measured in tissues of the posterior neuropore region of cultured *curly tail* embryos by (**A**) PCNA labelling, a measure of cells in S-phase and (**B**) phospho-histone H3 labelling, a marker of mitotic cells. Cell proliferation is most rapid in neuroepithelium, less intense in hindgut endoderm and slowest in notochord, as described previously (11). Inositol significantly stimulates PCNA labelling ($P < 0.005$) and histone H3 labelling ($P < 0.02$) in hindgut endoderm, whereas inositol has no significant effect on PCNA or histone H3 labelling in either neuroepithelium or notochord ($P > 0.05$). In hindgut endoderm, inhibition of PKCβI significantly reduces histone H3 labelling compared with inositol alone ($P < 0.05$), whereas inhibition of PKCε has no significant effect ($P > 0.05$). Blocking PKCβI or ε has no significant effect on histone H3 labelling in neuroepithelium or notochord ($P > 0.05$). No cells were positive for histone H3 in the presence of inositol and the PKCβI inhibitor (Fig. 6B, notochord data, bar 5). Labelling indices are mean ± SEM of at least 10 embryos per treatment.

the percentage of PCNA-positive (Fig. 6A) and histone H3-positive (Fig. 6B) cells was detected in the hindgut, whereas inositol treatment had no effect on either proliferation marker in the neuroepithelium or notochord (Fig. 6A and B). Co-administration of the PKCβI peptide inhibitor blocked the stimulatory effect of inositol on hindgut proliferation, whereas the PKCε inhibitor had no effect. Neither inhibitor significantly altered proliferation in neuroepithelium or notochord. Hence, inositol overcomes the genetically-determined defect of cell proliferation in *curly tail* embryos, an effect that requires activation of PKCβI.

DISCUSSION

Inositol normalizes neural tube closure in the spinal region of *curly tail* mouse embryos destined to develop spina bifida (7), whereas folic acid has no preventive effect (6). Brief treatment with the PKC agonist TPA mimics the inositol effect, whereas the PKC inhibitor BisI abrogates inositol-mediated prevention (7). Here, we used other chemical PKC inhibitors, with reportedly narrower spectra of action, and showed that these are also able to block the inositol effect. However, the precise specificity of chemical PKC inhibitors may vary between cell types. For example, HBDDE is specific for PKCα and γ *in vitro* (16), but acts on other molecular targets in cerebellar granule neurons (25). This prompted the use of peptide PKC inhibitors which were able to block the translocation of specific PKC isoforms. Isoform-by-isoform analysis using these inhibitors revealed a requirement for PKCβI, γ and ζ, but not other PKCs in the normalization of neural tube closure in *curly tail* embryos.

Developmental regulation of PKC isoform expression

We detected all PKC isoforms, during mouse development from E9.5 to E17.5, in agreement with previous analysis of PKCs in E15–17 fetuses (26). Our findings contrast with a study of E10.5 embryos that detected PKCα, δ and ζ, but not βI, βII, γ and ε (27). This difference may reflect the low abundance of cPKCs on western blot, at early stages (E9.5–11.5) in particular, although all isoforms were clearly detectable in the PNP region by immunohistochemistry. Each PKC isoform exhibited a distinct distribution between sub-cellular fractions, which likely reflects the degree of activation. For instance, cPKCs were confined to the cytoplasmic fraction, suggesting minimal activation during undisturbed development, whereas aPKCs were present in membrane-associated and insoluble fractions throughout development, suggesting constitutive activation, as described in other systems (12). This finding is consistent with a role for the cPKCs, βI and γ, in mediating the preventive effect of inositol, since activation of these isoforms may be limiting in the absence of inositol, providing capacity for activation after treatment.

PKC isoforms and cell cycle regulation

We have demonstrated that inositol stimulates cell proliferation in the hindgut of *curly tail* embryos, reversing the imbalance of cell proliferation that is known to lead, via enhanced ventral curvature of the caudal region, to delay or failure of PNP closure (11,23,24,28). Moreover, PKCβI but not PKCε is required for this stimulation of cell proliferation. PKCβI has been previously associated with increased cell cycle entry. Its over-expression leads to increased proliferation of aortic endothelial cells, in contrast to PKCα which has an inhibitory effect (29). Similarly, proliferation of vascular smooth muscle cells is stimulated by PKCβI, through increased S-phase entry, but inhibited by PKCβII, through extension of S-phase (30). S-phase entry/progression has been suggested to be defective in hindgut cells of *curly tail* embryos (11), raising the possibility that activation of PKCβI may reverse this defect, leading to 'rescue' of the mutant phenotype. Interestingly, inositol treatment of cells for 6 h resulted in nuclear translocation of PKCβI and γ in some cells, as observed for short-term exposure to TPA. This nuclear localization suggests that a role of PKCβI in cell cycle regulation is plausible. PKCα also exhibits nuclear translocation in inositol-treated cells (both *curly tail* and non-mutant), but does not play an essential role in the prevention of NTD.

Molecular basis of the requirement for PKCζ and PI3-kinase

The normalizing effect of inositol on PNP closure was partially blocked by inhibition of PKCζ or PI3-kinase. The requirement for PKCζ may reflect a role in regulating other PKC isoforms (31). PKCζ is activated downstream of PI3-kinase (18), whose activity in turn depends on availability of phosphatidylinositol species. Hence, inositol administration may activate both PI3-kinase and PKCζ, by increasing flux through intracellular phosphoinositide metabolism. Indeed, inhibition of the inositol phosphate cycle by lithium blocks the preventive effect of inositol (7). The requirement for PI3-kinase may also be explained by its participation, with 3-phosphoinositide-dependent protein kinase-1 (PDK1) (32), in phosphorylation of the T-loop of the kinase domain, a requirement for activity of PKCs (33). Although we detected nuclear translocation of PKCα, βI and γ following treatment of cells with inositol for 6 h, altered localization of PKCζ was not detected. This could be simply due to suboptimal dose or period of treatment (activation could be short-lived), but it is also likely that PKCζ activation occurs by a different mechanism to the classical isoforms as PKCζ is not diacylglycerol-responsive. Moreover, the partial requirement for PKCζ in the protective effect of inositol may reflect a permissive role for PKCζ activity that does not involve translocation to the nucleus.

Is PKC implicated in the mechanism of neural tube closure?

Several lines of evidence suggest that spinal neurulation *per se* does not depend on PKC activation and that defective closure in *curly tail* embryos is unlikely to result from an intrinsic deficiency in specific PKC isoforms. First, exposure of *curly tail* embryos to PKC inhibitors, in the absence of inositol, did not affect PNP closure. Similar findings were obtained with non-mutant CD1 embryos (data not shown). Second, there is no difference in abundance of PKC isoforms between affected and unaffected *curly tail* embryos (data not shown). Third, uptake and incorporation of ^{3}H-inositol occurs similarly in cultured *curly tail* and non-mutant embryos, while inositol deficiency *in vitro* does not increase the penetrance of spinal NTDs in *curly tail* embryos (7). Finally, mice with targeted inactivation of the genes encoding PKCα, β, γ, δ, ε and ζ do not exhibit neurulation defects (34–39). We suggest, therefore, that prevention of NTDs in *curly tail* mice by exogenous inositol operates via stimulation of the cell cycle in the embryonic hindgut, an effect that requires activation of specific PKC isoforms. Inositol is also reported to prevent NTDs in animal models of diabetes (40), whereas inositol deficiency causes cranial NTD, even in non-mutant mice (41). It remains to be determined whether the protective action of inositol also involves stimulation of cell proliferation in these cases.

MATERIALS AND METHODS

Mouse strains and embryo culture

Curly tail mice were maintained as described (5). Non-mutant random-bred CD1 mice were purchased from Charles River, UK. Mice were paired overnight and females checked for copulation plugs the following morning, designated embryonic day (E) 0.5. Embryos were explanted at E9.5 and those with 17–19 somites were cultured for 24 h in rat serum (6). Embryos were randomly allocated to treatment groups to minimize the effect of litter-to-litter variation. Cultures were supplemented with 1% (v/v) additions of phosphate buffered saline (PBS) or *myo*-inositol (50 μg/ml, final concentration). PKC inhibitors were added as 1% (v/v) additions. Bisindolylmaleimide (Bis) I and V, Go6976, HBDDE and LY294002 (all from Calbiochem) were diluted in minimal volumes of DMSO, further diluted in

PBS, and added to cultures at final concentrations corresponding to their IC_{50} values (14–17): 10 μM (BisI, BisV, Go6976), 50 μM (HBDDE) or 1.4 μM (LY294002). DMSO diluted in PBS was added to control cultures. Peptide PKC inhibitors (supplied by Dr D. Mochly-Rosen) were added to embryo cultures to final concentrations of 1 μM: PKCαC2-4, PKCβIV5-3, PKCβIIV5-3, PKCγC2-4, PKCδV1-1; PKCεV1-2 and PKCζ (pseudosubstrate region) (19,42–45). An Antennapedia peptide dimer served as an inactive control.

Statistical analysis

Comparison of multiple experimental groups was carried out by one way analysis of variance or by Kruskal–Wallis test (for data that were not normally distributed). Where significant variation was detected, multiple pairwise comparisons were performed by Tukey *t*-test or by Dunn's test. A value of $P < 0.05$ was considered significant where the power of the test exceeded 0.8. Statistical tests were computed using SigmaStat 2.03 software.

Western blot of PKC isoforms

Embryos were homogenized in ice cold buffer (60 mM Tris/HCl, pH 7.5, 0.25 M sucrose, 10 mM EGTA, 5 mM EDTA, 500 μM leupeptin, 1 mM PMSF, 0.1 U/ml aprotinin, 1 mM dithiothreitol, 100 μM sodium vanadate, 50 μM sodium fluoride) and prepared as sub-cellular fractions: centrifugation at 100 000*g* for 30 min yielded a supernatant (C fraction). The pellet was resuspended in homogenization buffer containing 1% Triton X-100, and spun at 40 000*g* for 15 min., yielding a second supernatant (Ps-fraction) and a pellet (Pi-fraction). Samples were western blotted with mouse monoclonal IgGs for specific PKC isoforms (Transduction Laboratories), diluted as: α, 1 : 1000; β, 1 : 250; γ, 1 : 5000; δ, 1 : 500; ε, 1 : 1000; ι/λ, 1 : 250; μ, 1 : 250; θ, 1 : 250; ζ, 1 : 1000, or rabbit polyclonal anti-PKC η (1 : 2000; Sigma). Constant protein loading was confirmed in parallel blots probed with rabbit anti-β-actin (1 : 5000; Sigma). Blots were exposed to horseradish peroxidase-linked rabbit secondary antibodies and visualized by ECL detection system (Amersham Bioscience). Positive controls were C-fraction from adult male CD1 mouse brain or spleen.

Immunohistochemistry

E9.5–10.5 embryos were fixed in 4% paraformaldehyde (PFA), embedded in paraffin wax and sectioned at 6 μm. Sections were re-fixed in 4% PFA then exposed to rabbit IgG primary antibodies to PKCα, βI, βII, γ or ε (1 : 200; Santa Cruz Biotechnology), anti-PCNA (1 : 100; Santa Cruz Biotechnology) or anti-phosphohistone H3 (1 : 100; Upstate Biotechnology). After washing in PBS, 0.1% BSA, 0.05% Triton X-100, sections were exposed to FITC-linked secondary antibodies (1 : 40; Jackson Immuno Research). Controls included non-specific rabbit IgG [R&D Systems, 1 : 100 dilution in 10% foetal calf serum (FCS) in PBS] in place of primary antibody or pre-absorption of primary antibody with blocking peptides. Both yielded no signal. Labelling indices (number of labelled cells/total cell number × 100) were obtained from alternate transverse sections through the rostral end of the PNP (i.e. the region of maximal neural fold elevation) stained for PCNA or histone H3. Experiments were carried out in triplicate by an observer blinded to treatment type.

Primary embryonic cell cultures

The trunk distal to the forelimb bud was removed from 15 *curly tail* embryos (average stage: 27 somites), disrupted mechanically and dissociated by 20 min incubation at room temperature in F10 medium containing 0.12% w/v sodium bicarbonate, 10 mM HEPES, pH 7.4, 1 mg/ml trypsin, 1.5 mg/ml collagenase. After trituration, the suspension was passed through a Nitex filter and centrifuged for 5 min at 1000*g*. Pelleted cells were resuspended in 5 ml growth medium (Dulbecco's Modified Eagle's Medium, 100 units/ml penicillin, 100 μg/ml streptomycin) containing 10% v/v FCS, then seeded onto tissue culture dishes and cultured at 37°C in 5% CO_2. For experiments, 10^4 cells (passage 5) were seeded onto glass cover slips coated with poly-L-lysine and fibronectin, cultured for 5 h in growth medium containing 10% FCS, and transferred to growth medium containing 1% FCS for 18 h ('serum starvation'). Cells received either: (i) 100 mM TPA, 10 min prior to fixation in 4% PFA; (ii) 100 mM isoform-specific peptide PKC inhibitor, 20 min prior to fixation, then 100 mM TPA, 10 min prior to fixation; (iii) 50 μg/ml *myo*-inositol, 6 h prior to fixation; or (iv) no treatment. For analysis of the effect of inositol, parallel experiments were carried using 3T3 cells. Cells were processed for immunohistochemistry as above and analysed in triplicate by an observer blinded to treatment type.

ACKNOWLEDGEMENTS

We thank Dr Peter Parker and Dr Radu Aricescu for advice and assistance during the study, and Dr Daria Mochly-Rosen for generously providing the PKC peptide inhibitors. This work was supported by the Wellcome Trust, Wellbeing and Birth Defects Foundation.

REFERENCES

1. Wald, N., Sneddon, J., Densem, J., Frost, C., Stone, R. and the MRC Vitamin Study Res Group (1991) Prevention of neural tube defects: results of the Medical Research Council Vitamin Study. *Lancet*, **338**, 131–137.
2. Czeizel, A.E. and Dudás, I. (1992) Prevention of the first occurrence of neural-tube defects by periconceptional vitamin supplementation. *N. Engl. J. Med.*, **327**, 1832–1835.
3. Copp, A.J. and Greene, N.D.E. (2000) Neural tube defects: prevention by folic acid and other vitamins. *Indian J. Pediatr.*, **67**, 915–921.
4. Greene, N.D.E. and Copp, A.J. (2002) In Massaro, E.J. and Rogers, J.M. (eds). *Folate and Human Development*. Humana Press Inc, Totowa, New Jersey, pp. 1–26.
5. Van Straaten, H.W.M. and Copp, A.J. (2001) Curly tail: a 50-year history of the mouse spina bifida model. *Anat. Embryol.*, **203**, 225–237.
6. Seller, M.J. (1994) In Bock, G. and Marsh, J. (eds). *Neural Tube Defects* (Ciba Foundation Symposium 181). John Wiley and Sons, Chichester, pp. 161–173.
7. Greene, N.D.E. and Copp, A.J. (1997) Inositol prevents folate-resistant neural tube defects in the mouse. *Nature Med.*, **3**, 60–66.
8. Cogram, P., Tesh, S., Tesh, J., Wade, A., Allan, G., Greene, N.D.E. and Copp, A.J. (2002) D-*chiro*-inositol is more effective than *myo*-inositol in preventing folate-resistant mouse neural tube defects. *Hum. Reprod.*, **17**, 2451–2458.

9. Cavalli, P. and Copp, A.J. (2002) Inositol and folate-resistant neural tube defects. *J. Med. Genet.*, **39**, e5.
10. Mellor, H. and Parker, P.J. (1998) The extended protein kinase C superfamily. *Biochem. J.*, **332**, 281–292.
11. Copp, A.J., Brook, F.A. and Roberts, H.J. (1988) A cell-type-specific abnormality of cell proliferation in mutant (curly tail) mouse embryos developing spinal neural tube defects. *Development*, **104**, 285–295.
12. Liyanage, M., Frith, D., Livneh, E. and Stabel, S. (1992) Protein kinase C group B members PKC-delta, -epsilon, -zeta and PKC-L(eta). Comparison of properties of recombinant proteins *in vitro* and *in vivo*. *Biochem. J.*, **283**, 781–787.
13. Copp, A.J. (1985) Relationship between timing of posterior neuropore closure and development of spinal neural tube defects in mutant (curly tail) and normal mouse embryos in culture. *J. Embryol. Exp. Morphol.*, **88**, 39–54.
14. Toullec, D., Pianetti, P., Coste, H., Bellevergue, P., Grand Perret, T., Ajakane, M., Baudet, V., Boissin, P., Boursier, E., Loriolle, F. *et al.* (1991) The bisindolylmaleimide GF 109203X is a potent and selective inhibitor of protein kinase C. *J. Biol. Chem.*, **266**, 15771–15781.
15. Martiny-Baron, G., Kazanietz, M.G., Mischak, H., Blumberg, P.M., Kochs, G., Hug, H., Marme, D. and Schachtele, C. (1993) Selective inhibition of protein kinase C isozymes by the indolocarbazole Go 6976. *J. Biol.Chem.*, **268**, 9194–9197.
16. Kashiwada, Y., Huang, L., Ballas, L.M., Jiang, J.B., Janzen, W.P. and Lee, K.H. (1994) New hexahydroxybiphenyl derivatives as inhibitors of protein kinase C. *J. Med. Chem.*, **37**, 195–200.
17. Vlahos, C.J., Matter, W.F., Hui, K.Y. and Brown, R.F. (1994) A specific inhibitor of phosphatidylinositol 3-kinase, 2-(4- morpholinyl)-8-phenyl-4H-1-benzopyran-4-one (LY294002). *J. Biol. Chem.*, **269**, 5241–5248.
18. Standaert, M.L., Galloway, L., Karnam, P., Bandyopadhyay, G., Moscat, J. and Farese, R.V. (1997) Protein kinase C-zeta as a downstream effector of phosphatidylinositol 3-kinase during insulin stimulation in rat adipocytes—Potential role in glucose transport. *J. Biol. Chem.*, **272**, 30075–30082.
19. Ron, D., Luo, J. and Mochly-Rosen, D. (1995) C2 region-derived peptides inhibit translocation and function of beta protein kinase C *in vivo*. *J. Biol. Chem.*, **270**, 24180–24187.
20. Johnson, J.A., Gray, M.O., Chen, C.H. and Mochly-Rosen, D. (1996) A protein kinase C translocation inhibitor as an isozyme-selective antagonist of cardiac function. *J. Biol. Chem.*, **271**, 24962–24966.
21. Peeters, M.C.E., Schutte, B., Lenders, M.H.J.N., Hekking, J.W.M., Drukker, J. and Van Straaten, H.W.M. (1998) Role of differential cell proliferation in the tail bud in aberrant mouse neurulation. *Dev. Dyn.*, **211**, 382–389.
22. Copp, A.J., Crolla, J.A. and Brook, F.A. (1988) Prevention of spinal neural tube defects in the mouse embryo by growth retardation during neurulation. *Development.*, **104**, 297–303.
23. Brook, F.A., Shum, A.S.W., Van Straaten, H.W.M. and Copp, A.J. (1991) Curvature of the caudal region is responsible for failure of neural tube closure in the curly tail (ct) mouse embryo. *Development.*, **113**, 671–678.
24. Peeters, M.C.E., Shum, A.S.W., Hekking, J.W.M., Copp, A.J. and Van Straaten, H.W.M. (1996) Relationship between altered axial curvature and neural tube closure in normal and mutant (*curly tail*) mouse embryos. *Anat. Embryol.*, **193**, 123–130.
25. Mathur, A. and Vallano, M.L. (2000) 2,2′,3,3′,4,4′-Hexahydroxy-1, 1′-biphenyl-6,6′-dimethanol dimethyl ether (HBDDE)-induced neuronal apoptosis independent of classical protein kinase C alpha or gamma inhibition. *Biochem. Pharmacol.*, **60**, 809–815.
26. Bareggi, R., Grill, V., Zweyer, M., Narducci, P. and Martelli, A.M. (1995) Distribution of the extended family of protein kinase C isoenzymes in fetal organs of mice: an immunohistochemical study. *Cell Tissue Res.*, **280**, 617–625.
27. Blackshear, P.J., Lai, W.S., Tuttle, J.S., Stumpo, D.J., Kennington, E., Nairn, A.C. and Sulik, K.K. (1996) Developmental expression of MARCKS and protein kinase C in mice in relation to the exencephaly resulting from MARCKS deficiency. *Dev. Brain Res.*, **96**, 62–75.
28. Van Straaten, H.W.M., Hekking, J.W.M., Consten, C. and Copp, A.J. (1993) Intrinsic and extrinsic factors in the mechanism of neurulation: effect of curvature of the body axis on closure of the posterior neuropore. *Development.*, **117**, 1163–1172.
29. Rosales, O.R., Isales, C.M. and Bhargava, J. (1998) Overexpression of protein kinase C alpha and beta1 has distinct effects on bovine aortic endothelial cell growth. *Cell Signal.*, **10**, 589–597.
30. Yamamoto, M., Acevedo-Duncan, M., Chalfant, C.E., Patel, N.A., Watson, J.E. and Cooper, D.R. (1998) The roles of protein kinase C beta I and beta II in vascular smooth muscle cell proliferation. *Exp. Cell Res.*, **240**, 349–358.
31. Ziegler, W.H., Parekh, D.B., Le Good, J.A., Whelan, R.D., Kelly, J.J., Frech, M., Hemmings, B.A. and Parker, P.J. (1999) Rapamycin-sensitive phosphorylation of PKC on a carboxy-terminal site by an atypical PKC complex. *Curr. Biol.*, **9**, 522–529.
32. Le Good, J.A., Ziegler, W.H., Parekh, D.B., Alessi, D.R., Cohen, P. and Parker, P.J. (1998) Protein kinase C isotypes controlled by phosphoinositide 3-kinase through the protein kinase PDK1. *Science*, **281**, 2042–2045.
33. Chan, T.O., Rittenhouse, S.E. and Tsichlis, P.N. (1999) AKT/PKB and other D3 phosphoinositide-regulated kinases: kinase activation by phosphoinositide-dependent phosphorylation. *Annu. Rev. Biochem.*, **68**, 965–1014.
34. Leitges, M., Plomann, M., Standaert, M.L., Bandyopadhyay, G., Sajan, M.P., Kanoh, Y. and Farese, R.V. (2002) Knockout of PKCα enhances insulin signaling through PI3K. *Mol. Endocrinol.*, **16**, 847–858.
35. Leitges, M., Schmedt, C., Guinamard, R., Davoust, J., Schaal, S., Stabel, S. and Tarakhovsky, A. (1996) Immunodeficiency in protein kinase c beta-deficient mice. *Science*, **273**, 788–791.
36. Abeliovich, A., Chen, C., Goda, Y., Silva, A.J., Stevens, C.F. and Tonegawa, S. (1993) Modified hippocampal long-term potentiation in PKCgamma- mutant mice. *Cell*, **75**, 1253–1262.
37. Miyamoto, A., Nakayama, K., Imaki, H., Hirose, S., Jiang, Y., Abe, M., Tsukiyama, T., Nagahama, H., Ohno, S., Hatakeyama, S. and Nakayama, K.I. (2002) Increased proliferation of B cells and auto-immunity in mice lacking protein kinase Cδ. *Nature*, **416**, 865–869.
38. Khasar, S.G., Lin, Y.H., Martin, A., Dadgar, J., McMahon, T., Wang, D., Hundle, B., Aley, K.O., Isenberg, W., McCarter, G. *et al.* (1999) A novel nociceptor signaling pathway revealed in protein kinase C ε mutant mice. *Neuron*, **24**, 253–260.
39. Leitges, M., Sanz, L., Martin, P., Duran, A., Braun, U., Garcia, J.F., Camacho, F., Diaz-Meco, M.T., Rennert, P.D. and Moscat, J. (2001) Targeted disruption of the zeta PKC gene results in the impairment of the NF-kappaB pathway. *Mol. Cell*, **8**, 771–780.
40. Reece, E.A., Khandelwal, M., Wu, Y.K. and Borenstein, M. (1997) Dietary intake of *myo*-inositol and neural tube defects in offspring of diabetic rats. *Am. J. Obstet. Gynecol.*, **176**, 536–539.
41. Cockroft, D.L., Brook, F.A. and Copp, A.J. (1992) Inositol deficiency increases the susceptibility to neural tube defects of genetically predisposed (curly tail) mouse embryos *in vitro*. *Teratology.*, **45**, 223–232.
42. Stebbins, L. and Mochly-Rosen, D. (2001) Binding specificity for RACK1 resides in the V5 region of beta II protein kinase C. *J. Biol. Chem.*, **276**, 29644–29650.
43. Gray, M.O., Karliner, J.S. and Mochly-Rosen, D. (1997) A selective ε-protein kinase C antagonist inhibits protection of cardiac myocytes from hypoxia-induced cell death. *J. Biol. Chem.*, **272**, 30945–30951.
44. Laudanna, C., Mochly-Rosen, D., Liron, T., Constantin, G. and Butcher, E.C. (1998) Evidence of zeta protein kinase C involvement in polymorphonuclear neutrophil integrin-dependent adhesion and chemotaxis. *J. Biol. Chem.*, **273**, 30306–30315.
45. Chen, L., Hahn, H., Wu, G.Y., Chen, C.H., Liron, T., Schechtman, D., Cavallaro, G., Banci, L., Guo, Y.R., Bolli, R. *et al.* (2001) Opposing cardioprotective actions and parallel hypertrophic effects of dPKC and +PKC. *Proc. Natl Acad. Sci. USA*, **98**, 11114–11119.
46. Wetsel, W.C., Khan, W.A., Merchenthaler, I., Rivera, H., Halpern, A.E., Phung, H.M., Negro Vilar, A. and Hannun, Y.A. (1992) Tissue and cellular distribution of the extended family of protein kinase C isoenzymes. *J. Cell Biol.*, **117**, 121–133.